

**Technical Memorandum:
Delta Risk Management Strategy (DRMS) Phase 1**

**Topical Area
Seismology
Draft 2**

Prepared by:
URS Corporation/Jack R. Benjamin & Associates, Inc.

Prepared for:
Department of Water Resources

June 15, 2007



June 15, 2007

Mr. Ralph R. Svetich, P.E.
Delta Risk Management Strategy Project Manager
Department of Water Resources
Division of Flood Management
Delta-Suisun Marsh Office
901 P Street, Suite 313A
Post Office Box 942836
Sacramento, CA 94236-0001

**Subject: Delta Risk Management Strategy
Phase 1 Draft 2 Technical Memorandum - Seismology**

Dear Mr. Svetich,

Please find herewith a copy of the subject technical memorandum. Members of the Steering Committee's Technical Advisory Committee and agency staff have reviewed the draft technical memorandum, and this second draft addresses their comments.

This document was prepared by Ivan Wong and Patricia Thomas (URS Corporation), Jeff Unruh (William Lettis & Associates), and Kathryn Hanson and Bob Youngs (Geomatrix Consulting, Inc.). Internal peer review was provided in accordance with URS' quality assurance program, as outlined in the (DRMS) project management plan.

Sincerely,

URS Corporation

Jack R. Benjamin & Associates, Inc.

Said Salah-Mars, Ph.D., P.E.
URS Engineering Division Manager
DRMS Project Manager
1333 Broadway Ave, Suite 800
Oakland, CA 94612
Ph. 510-874-3051
Fax: 510-874-3268

Martin W. McCann, Jr., Ph.D.
President JBA
DRMS Technical Manager
530 Oak Grove Ave., Suite 202
Menlo Park, CA 94025
Ph. 650-473-9955

Topical Area: Seismology

Preamble

The Delta Risk Management Strategy (DRMS) project was authorized by DWR to perform a risk analysis of the Delta and Suisun Marsh (Phase 1) and to develop a set of improvement strategies to manage those risks (Phase 2) in response to Assembly Bill 1200 (Laird, Chaptered, September 2005). The Technical Memorandum (TM), is one of 12 TMs (2 topics are presented in one TM: hydrodynamics and water management) prepared for topical areas for Phase 1 of the DRMS project. The topical areas covered in the Phase 1 Risk Analysis include:

1. Geomorphology of the Delta and Suisun Marsh
2. Subsidence of the Delta and Suisun Marsh
3. Seismic Hazards of the Delta and Suisun Marsh
4. Global Warming Effects in the Delta and Suisun Marsh
5. Flood Hazard of the Delta and Suisun Marsh
6. Wind Wave Action of the Delta and Suisun Marsh
7. Levee Vulnerability of the Delta and Suisun Marsh
8. Emergency Response and Repair of the Delta and Suisun Marsh Levees
9. Hydrodynamics of the Delta and Suisun Marsh
10. Water Management and Operation of the Delta and Suisun Marsh
11. Ecological Impacts of the Delta and Suisun Marsh
12. Impact to Infrastructure of the Delta and Suisun Marsh
13. Economic Impacts of the Delta and Suisun Marsh

Note that the Hydrodynamics and Water Quality topical area was combined with the Water Management and Operations topical area because they needed to be considered together in developing the model of levee breach water impacts for the risk analysis. The resulting team is the Water Analysis Module (WAM) Team and this TM is the Water Analysis Module TM.

The work product described in these TMs will be used to develop the integrated risk analysis of the Delta and Suisun Marsh. The results of the integrated risk analysis will be presented in a technical report referred to as:

14. Risk Analysis – Report

The first draft of this report was made available to the DRMS Steering Committee in April 2007.

Assembly Bill 1200 amends Section 139.2 of the Water Code, to read, “The department shall evaluate the potential impacts on water supplies derived from the Sacramento-San Joaquin Delta based on 50-, 100-, and 200-year projections for each of the following possible impacts on the delta:

1. Subsidence.
2. Earthquakes.
3. Floods.
4. Changes in precipitation, temperature, and ocean levels.
5. A combination of the impacts specified in paragraphs (1) to (4) inclusive.”

Topical Area: Seismology

In addition, Section 139.4 was amended to read: (a) The Department and the Department of Fish and Game shall determine the principal options for the delta. (b) The Department shall evaluate and comparatively rate each option determined in subdivision (a) for its ability to do the following:

1. Prevent the disruption of water supplies derived from the Sacramento-San Joaquin Delta.
2. Improve the quality of drinking water supplies derived from the delta.
3. Reduce the amount of salts contained in delta water and delivered to, and often retained in, our agricultural areas.
4. Maintain Delta water quality for Delta users.
5. Assist in preserving Delta lands.
6. Protect water rights of the “area of origin” and protect the environments of the Sacramento- San Joaquin river systems.
7. Protect highways, utility facilities, and other infrastructure located within the delta.
8. Preserve, protect, and improve Delta levees....”

In meeting the requirements of AB 1200, the DRMS project is divided into two parts. Phase 1 involves the development and implementation of a risk analysis to evaluate the impacts to the Delta of various stressing events. In Phase 2 of the project, risk reduction and risk management strategies for long-term management of the Delta will be developed.

Definitions and Assumptions

During the Phase 1 study, the DRMS project team developed various predictive models of future stressing events and their consequences. These events and their consequences have been estimated using engineering and scientific tools readily available or based on a broad and current consensus among practitioners. Such events include the likely occurrence of future earthquakes of varying magnitude in the region, future rates of subsidence given continued farming practices, the likely magnitude and frequency of storm events, the potential effects of global warming (sea level rise, climate change, and temperature change) and their effects on the environment. Using the current state of knowledge, estimates of the likelihood of these events occurring can be made for the 50-, 100-, and 200-year projections with some confidence.

While estimating the likelihood of stressing events can generally be done using current technologies, estimating the consequences of these stressing events at future times is somewhat more difficult. Obviously, over the next 50, 100, and 200 years, the Delta will undergo changes that will affect what impact the stressing events will have. To assess those consequences, some assumptions about the future “look” of the Delta must be established.

To address the challenge of predicting impacts under changing conditions, DRMS adopted the approach of evaluating impacts absent changes in the Delta as a baseline.

Topical Area: Seismology

This approach is referred to as the “business-as-usual” (BAU) scenario. Defining a business-as-usual Delta is required, since one of the objectives of this work is to estimate whether ‘business-as-usual’ is sustainable for the foreseeable future. Obviously changes from this baseline condition can occur; however, as a basis of comparison for risks and risk reduction measures, the BAU scenario serves as a consistent standard rather than as a “prediction of the future” and relies on existing agreements, policies, and practices to the extent possible.

In some cases, there are instances where procedures and policies may not exist to define standard emergency response procedure during a major (unprecedented) stressing event in the Delta or restoration guidelines after such a major event. In these cases, prioritization of action will be based on: (1) existing and expected future response resources, and (2) highest value recovery/restoration given available resources.

This study relies solely on available data. Because of the limited time to complete this work, no investigation or research were to be conducted to supplement the state of knowledge.

Perspective

The analysis results presented in this technical memorandum do not represent the full estimate of risk for the topic presented herein. The subject and results are expressed whenever possible in probabilistic terms to characterize the uncertainties and the random nature of the parameters that control the subject under consideration. The results are the expression of either the probable outcome of the hazards (earthquake, floods, climate change, subsidence, wind waves, and sunny day failures) or the conditional probability of the subject outcome (levee failures, emergency response, water management, hydrodynamic response of the Delta and Suisun Marsh, ecosystem response, and economic impacts) given the stressing events.

A full characterization of risk is presented in the Risk Analysis Report. In that report, the integration of the probable initiating events, the conditional probable response of the Delta levee system, and the expected probable consequences are integrated in the risk analysis module to develop a complete assessment of risk to the Delta and Suisun Marsh.

Consequently, the subject areas of the technical memoranda should be viewed as pieces contributing to the total risk, and their outcomes represent the input to the risk analysis module.

Table of Contents

1.0	Introduction.....	1
1.1	Products	2
1.2	Scope of Work.....	2
1.3	Uncertainty	4
1.4	Assumptions, Constraints, and Limitations.....	4
2.0	Methodology	4
3.0	Seismic Source Inputs to Analysis.....	6
3.1	Seismic Source Model for Time-Independent Hazard	7
3.1.1	Faults.....	7
3.1.2	Model Discrepancy	17
3.1.3	Background Seismicity	18
3.1.4	Cascadia Subduction Zone	18
3.2	WGCEP Model for Time-Dependent Hazard	19
3.2.1	Inputs to the Hazard Program	20
4.0	Attenuation Relations	21
5.0	Time-Dependent PSHA Results.....	22
5.1	Comparison With Time-Independent Hazard.....	24
5.2	Other Sensitivity Analyses	24
5.3	Comparison With USGS National Hazard Maps	25
6.0	Ground Shaking Hazard Maps.....	25
7.0	References.....	25

Tables

1	Bay Area Time-Independent Seismic Source Parameters
2	Bay Area Time-Dependent Seismic Source Parameters
3	Mean Expert Weights for Probability Models Applied to the SFBR Fault Systems (Table 5.5, WGCEP, 2003)
4	Empirical Model Factors
5	Ground Motions for Return Periods of 100 to 2,500 Years in 2005
6a	Controlling Seismic Sources at a Return Period of 100 Years in 2005
6b	Controlling Seismic Sources at a Return Period of 2,500 Years in 2005

Topical Area: Seismology

Figures

- 1 Active Faults and Historical Seismicity of San Francisco Bay Region ($M \geq 3.0$), 1800 – 2006
- 2 Active Faults of the San Francisco Bay Region
- 3a Active Faults in the Site Region
- 3b Contemporary Seismicity (1966 to 2006) in the Site Region
- 4 Time-Dependent Probabilities for the San Andreas Rupture Scenarios for 2005
- 5 Time-Dependent Probabilities for the San Andreas Rupture Scenarios for 2050
- 6 Time-Dependent Probabilities for the San Andreas Rupture Scenarios for 2100
- 7 Time-Dependent Probabilities for the San Andreas Rupture Scenarios for 2200
- 8 Illustration of Magnitude Probability Density Function for Time-Dependent Sources
- 9 Magnitude Probability Density Function for the Mt. Diablo Fault
- 10 Cumulative Annual Recurrence Curve for the Mt. Diablo Fault
- 11 Cumulative Annual Recurrence Curve for the San Andreas Fault
- 12 Cumulative Annual Recurrence Curve for the Hayward-Rodger's Creek Fault
- 13 Cumulative Annual Recurrence Curve for the Concord-Green Valley Fault
- 14 Cumulative Annual Recurrence Curve for the Calaveras Fault
- 15 Cumulative Annual Recurrence Curve for the Greenville Fault
- 16 Cumulative Annual Recurrence Curve for the San Gregorio Fault
- 17 Magnitude Probability Density Function for the San Andreas Fault from WGCEP (2003)
- 18 Magnitude Probability Density Functions for the San Andreas Rupture Sources
- 19 Time-Dependent Seismic Hazard Curves for Mean Peak Horizontal Acceleration for Clifton Court for 2005
- 20 Time-Dependent Seismic Hazard Curves for Mean Peak Horizontal Acceleration for Delta Cross Channel for 2005
- 21 Time-Dependent Seismic Hazard Curves for Mean Peak Horizontal Acceleration for Montezuma Slough for 2005
- 22 Time-Dependent Seismic Hazard Curves for Mean Peak Horizontal Acceleration for Sacramento for 2005
- 23 Time-Dependent Seismic Hazard Curves for Mean Peak Horizontal Acceleration for Sherman Island for 2005
- 24 Time-Dependent Seismic Hazard Curves for Mean Peak Horizontal Acceleration for Stockton for 2005

Topical Area: Seismology

- 25 Time-Dependent Seismic Hazard Curves for 1.0 Sec Horizontal Spectral Acceleration for Clifton Court for 2005
- 26 Time-Dependent Seismic Hazard Curves for 1.0 Sec Horizontal Spectral Acceleration for Delta Cross Channel for 2005
- 27 Time-Dependent Seismic Hazard Curves for 1.0 Sec Horizontal Spectral Acceleration for Montezuma Slough for 2005
- 28 Time-Dependent Seismic Hazard Curves for 1.0 Sec Horizontal Spectral Acceleration for Sacramento for 2005
- 29 Time-Dependent Seismic Hazard Curves for 1.0 Sec Horizontal Spectral Acceleration for Sherman Island for 2005
- 30 Time-Dependent Seismic Hazard Curves for 1.0 Sec Horizontal Spectral Acceleration for Stockton for 2005
- 31 Seismic Source Contributions to Mean Peak Horizontal Acceleration Time-Dependent Hazard for Clifton Court for 2005
- 32 Seismic Source Contributions to Mean Peak Horizontal Acceleration Time-Dependent Hazard for Delta Cross Channel for 2005
- 33 Seismic Source Contributions to Mean Peak Horizontal Acceleration Time-Dependent Hazard for Montezuma Slough for 2005
- 34 Seismic Source Contributions to Mean Peak Horizontal Acceleration Time-Dependent Hazard for Sacramento for 2005
- 35 Seismic Source Contributions to Mean Peak Horizontal Acceleration Time-Dependent Hazard for Sherman Island for 2005
- 36 Seismic Source Contributions to Mean Peak Horizontal Acceleration Time-Dependent Hazard for Stockton for 2005
- 37 Seismic Source Contributions to 1.0 Sec Horizontal Spectral Acceleration Time-Dependent Hazard for Clifton Court for 2005
- 38 Seismic Source Contributions to 1.0 Sec Horizontal Spectral Acceleration Time-Dependent Hazard for Delta Cross Channel for 2005
- 39 Seismic Source Contributions to 1.0 Sec Horizontal Spectral Acceleration Time-Dependent Hazard for Montezuma Slough for 2005
- 40 Seismic Source Contributions to 1.0 Sec Horizontal Spectral Acceleration Time-Dependent Hazard for Sacramento for 2005
- 41 Seismic Source Contributions to 1.0 Sec Horizontal Spectral Acceleration Time-Dependent Hazard for Sherman Island for 2005
- 42 Seismic Source Contributions to 1.0 Sec Horizontal Spectral Acceleration Time-Dependent Hazard for Stockton for 2005
- 43 Seismic Source Contributions to Mean Peak Horizontal Acceleration Time-Dependent Hazard for Clifton Court for 2200
- 44 Seismic Source Contributions to Mean Peak Horizontal Acceleration Time-Dependent Hazard for Delta Cross Channel for 2200
- 45 Seismic Source Contributions to Mean Peak Horizontal Acceleration Time-Dependent Hazard at Montezuma Slough for 2200

Topical Area: Seismology

- 46 Seismic Source Contributions to Mean Peak Horizontal Acceleration Time-Dependent Hazard for Sacramento for 2200
- 47 Seismic Source Contributions to Mean Peak Horizontal Acceleration Time-Dependent Hazard for Sherman Island for 2200
- 48 Seismic Source Contributions to Mean Peak Horizontal Acceleration Time-Dependent Hazard for Stockton for 2200
- 49 Seismic Source Contributions to 1.0 Sec Horizontal Spectral Acceleration Time-Dependent Hazard for Clifton Court for 2200
- 50 Seismic Source Contributions to 1.0 Sec Horizontal Spectral Acceleration Time-Dependent Hazard for Delta Cross Channel for 2200
- 51 Seismic Source Contributions to 1.0 Sec Horizontal Spectral Acceleration Time-Dependent Hazard for Montezuma Slough for 2200
- 52 Seismic Source Contributions to 1.0 Sec Horizontal Spectral Acceleration Time-Dependent Hazard for Sacramento for 2200
- 53 Seismic Source Contributions to 1.0 Sec Horizontal Spectral Acceleration Time-Dependent Hazard for Sherman Island for 2200
- 54 Seismic Source Contributions to 1.0 Sec Horizontal Spectral Acceleration Time-Dependent Hazard for Stockton for 2200
- 55 Magnitude and Distance Contributions to the Mean Peak Horizontal Acceleration Hazard for Clifton Court for 2005
- 56 Magnitude and Distance Contributions to the Mean Peak Horizontal Acceleration Hazard for Delta Cross Channel for 2005
- 57 Magnitude and Distance Contributions to the Mean Peak Horizontal Acceleration Hazard for Montezuma Slough for 2005
- 58 Magnitude and Distance Contributions to the Mean Peak Horizontal Acceleration Hazard for Sacramento for 2005
- 59 Magnitude and Distance Contributions to the Mean Peak Horizontal Acceleration Hazard for Sherman Island for 2005
- 60 Magnitude and Distance Contributions to the Mean Peak Horizontal Acceleration Hazard for Stockton for 2005
- 61 Magnitude and Distance Contributions to the 1.0 Sec Horizontal Spectral Acceleration Hazard for Clifton Court for 2005
- 62 Magnitude and Distance Contributions to the 1.0 Sec Horizontal Spectral Acceleration Hazard for Delta Cross Channel for 2005
- 63 Magnitude and Distance Contributions to the 1.0 Sec Horizontal Spectral Acceleration Hazard for Montezuma Slough for 2005
- 64 Magnitude and Distance Contributions to the 1.0 Sec Horizontal Spectral Acceleration Hazard for Sacramento for 2005
- 65 Magnitude and Distance Contributions to the 1.0 Sec Horizontal Spectral Acceleration Hazard for Sherman Island for 2005
- 66 Magnitude and Distance Contributions to the 1.0 Sec Horizontal Spectral Acceleration Hazard for Stockton for 2005

Topical Area: Seismology

- 67 Sensitivity of Mean Peak Horizontal Acceleration Time-Dependent Hazard to Attenuation Relationships for Clifton Court for 2005
- 68 Sensitivity of Mean Peak Horizontal Acceleration Time-Dependent Hazard to Attenuation Relationships for Delta Cross Channel for 2005
- 69 Sensitivity of Mean Peak Horizontal Acceleration Time-Dependent Hazard to Attenuation Relationships for Montezuma Slough for 2005
- 70 Sensitivity of Mean Peak Horizontal Acceleration Time-Dependent Hazard to Attenuation Relationships for Sacramento for 2005
- 71 Sensitivity of Mean Peak Horizontal Acceleration Time-Dependent Hazard to Attenuation Relationships for Sherman Island for 2005
- 72 Sensitivity of Mean Peak Horizontal Acceleration Time-Dependent Hazard to Attenuation Relationships for Stockton for 2005
- 73 Sensitivity of 1.0 Sec Spectral Horizontal Acceleration Time-Dependent Hazard to Attenuation Relationships for Clifton Court for 2005
- 74 Sensitivity of 1.0 Sec Spectral Horizontal Acceleration Time-Dependent Hazard to Attenuation Relationships for Delta Cross Channel for 2005
- 75 Sensitivity of 1.0 Sec Spectral Horizontal Acceleration Time-Dependent Hazard to Attenuation Relationships for Montezuma Slough for 2005
- 76 Sensitivity of 1.0 Sec Spectral Horizontal Acceleration Time-Dependent Hazard to Attenuation Relationships for Sacramento for 2005
- 77 Sensitivity of 1.0 Sec Spectral Horizontal Acceleration Time-Dependent Hazard to Attenuation Relationships for Sherman Island for 2005
- 78 Sensitivity of 1.0 Sec Spectral Horizontal Acceleration Time-Dependent Hazard to Attenuation Relationships for Stockton for 2005
- 79 Sensitivity of Cascadia Subduction Zone 1.0 Sec Horizontal Acceleration Hazard to Subduction Attenuation Relationships for Sacramento for 2005
- 80 1.0 Sec Spectral Acceleration Hazard for Sacramento for 2005: Effect of Truncating Sigma for Cascadia Subduction Zone
- 81 Mean Peak Horizontal Acceleration Hazard for Clifton Court for 2005, 2050, 2100 and 2200
- 82 Mean Peak Horizontal Acceleration Hazard for Delta Cross Channel for 2005, 2050, 2100 and 2200
- 83 Mean Peak Horizontal Acceleration Hazard for Montezuma Slough for 2005, 2050, 2100 and 2200
- 84 Mean Peak Horizontal Acceleration Hazard for Sacramento for 2005, 2050, 2100 and 2200
- 85 Mean Peak Horizontal Acceleration Hazard for Sherman Island for 2005, 2050, 2100 and 2200
- 86 Mean Peak Horizontal Acceleration Hazard for Stockton for 2005, 2050, 2100 and 2200
- 87 Horizontal Spectral Acceleration Hazard at 1.0 Sec for Clifton Court for 2005, 2050, 2100 and 2200

Topical Area: Seismology

- 88 Horizontal Spectral Acceleration Hazard at 1.0 Sec for Delta Cross Channel for 2005, 2050, 2100 and 2200
- 89 Horizontal Spectral Acceleration Hazard at 1.0 Sec for Montezuma Slough for 2005, 2050, 2100 and 2200
- 90 Horizontal Spectral Acceleration Hazard at 1.0 Sec for Sacramento for 2005, 2050, 2100 and 2200
- 91 Horizontal Spectral Acceleration Hazard at 1.0 Sec for Sherman Island for 2005, 2050, 2100 and 2200
- 92 Horizontal Spectral Acceleration Hazard at 1.0 Sec for Stockton for 2005, 2050, 2100 and 2200
- 93 Mean Peak Horizontal Acceleration Hazard for Time-Dependent and Poisson Models for Clifton Court for 2005
- 94 Mean Peak Horizontal Acceleration Hazard for Time-Dependent and Poisson Models for Delta Cross Channel for 2005
- 95 Mean Peak Horizontal Acceleration Hazard for Time-Dependent and Poisson Models for Montezuma Slough for 2005
- 96 Mean Peak Horizontal Acceleration Hazard for Time-Dependent and Poisson Models for Sacramento for 2005
- 97 Mean Peak Horizontal Acceleration Hazard for Time-Dependent and Poisson Models for Sherman Island for 2005
- 98 Mean Peak Horizontal Acceleration Hazard for Time-Dependent and Poisson Models for Stockton for 2005
- 99 1.0 Sec Horizontal Spectral Acceleration Hazard for Time-Dependent and Poisson Models for Clifton Court for 2005
- 100 1.0 Sec Horizontal Spectral Acceleration Hazard for Time-Dependent and Poisson Models for Delta Cross Channel for 2005
- 101 1.0 Sec Horizontal Spectral Acceleration Hazard for Time-Dependent and Poisson Models for Montezuma Slough for 2005
- 102 1.0 Sec Horizontal Spectral Acceleration Hazard for Time-Dependent and Poisson Models for Sacramento for 2005
- 103 1.0 Sec Horizontal Spectral Acceleration Hazard for Time-Dependent and Poisson Models for Sherman Island for 2005
- 104 1.0 Sec Horizontal Spectral Acceleration Hazard for Time-Dependent and Poisson Models for Stockton for 2005
- 105 Sensitivity of Mean Peak Horizontal Acceleration Hazard to Delta Fault Sources for Clifton Court for 2005
- 106 Sensitivity of Mean Peak Horizontal Acceleration Hazard to Delta Fault Sources for Delta Cross Channel for 2005
- 107 Sensitivity of Mean Peak Horizontal Acceleration Hazard to Delta Fault Sources for Montezuma Slough for 2005
- 108 Sensitivity of Mean Peak Horizontal Acceleration Hazard to Delta Fault Sources for Sacramento for 2005

Topical Area: Seismology

- 109 Sensitivity of Mean Peak Horizontal Acceleration Hazard to Delta Fault Sources for Sherman Island for 2005
- 110 Sensitivity of Mean Peak Horizontal Acceleration Hazard to Delta Fault Sources for Stockton for 2005
- 111 Comparison of Historical Seismicity Recurrence (1800-2006) With PSHA Model Recurrence
- 112 PGA Hazard for a 100-Year Return Period
- 113 PGA Hazard for a 500-Year Return Period
- 114 1 Second Hazard for a 100-Year Return Period
- 115 1 Second Hazard for a 500-Year Return Period

Appendices

- A Potential Deformation of the Base of Holocene Delta Peat by the Midland Fault

1.0 Introduction

The effects of earthquakes may be the most significant natural hazard that can impact the Delta levees (Figure 1). As part of the Delta Risk Management Strategy (DRMS) Project, this technical memorandum (TM) describes an evaluation of the ground shaking hazard that will be input into an analysis of the risk of failure of the Delta levees under present as well as foreseeable future conditions. In this memorandum, we describe the approach, methodology, inputs, and the hazard results in terms of the probabilities of the levels and character of earthquake ground shaking events that will contribute to the risk of levee failure in the Delta.

The general approach of performing a probabilistic seismic hazard analysis (PSHA) is standard practice in the engineering seismology/earthquake engineering community (McGuire, 2004). The PSHA methodology to be used in this study allows for the explicit consideration of epistemic uncertainties and inclusion of the range of possible interpretations of components in the seismic hazard model, including seismic source characterization and ground motion estimation. Uncertainties in models and parameters are incorporated into the hazard analysis through the use of logic trees.

A key assumption of the standard PSHA model is that earthquake occurrences can be modeled as a Poisson process. The occurrence of ground motions at the site in excess of a specified level is also a Poisson process, if (1) the occurrence of earthquakes is a Poisson process, and (2) the probability that any one event will result in ground motions at the site in excess of a specified level is independent of the occurrence of other events.

In a departure from standard PSHAs, which assume a time-independent Poissonian process, time-dependent hazard was calculated for the major Bay Area faults using the range of models that were considered by the Working Group on California Earthquake Probabilities (WGCEP, 2003). Note the models considered by WGCEP (2003) are not 100% time-dependent (see Section 3.2). Also the hazard from the other Bay area faults is time-independent. From hereon, what we refer to as “time-dependent hazard” in this study also contains a large “time-independent” component. The seismic hazard is calculated at selected times over the next 200 years.

Based on the results of the WGCEP (2003), there is an increasing probability of a large ($M \geq 6.7$) earthquake occurring in the San Francisco Bay region in the period 2002 to 2031. The estimated probability in 2002 was 62% and this value will increase with time. Inclusion of time-dependent earthquake occurrence probabilities in a PSHA has been done in the past (e.g., the PSHA recently completed for evaluation of the BART system) and have been incorporated into this PSHA. Hence in this study, time-dependent hazard is calculated and provided as input into the risk analysis. We have also calculated the time-independent hazard in the Delta solely for the purposes of comparison.

What is needed from the PSHA are the time-dependent probabilities of occurrence of all plausible earthquake events (defined by their locations, magnitudes, and ground motions). These have been used to develop estimates of risk (defined as the annual probability of seismically-induced levee failure) at selected times over the next 200 years (URS/JBA, 2007). The seismic hazard results are defined for a stiff soil condition. The site response analysis to characterize ground shaking at the top of the peat is presented in

Topical Area: Seismology

URS/JBA (2007). The products of the PSHA also include hazard maps of the Delta that are described herein.

1.1 Products

The products developed in this study include:

1. The annual probabilities of occurrence at selected times over the next 200 years (e.g., 2005, 2050, etc.) of plausible earthquake events, characterized by their location, magnitude, and ground motion amplitude, for all seismic sources that could impact the Delta have been defined.
2. The likelihood of multiple/simultaneous levee failures during individual scenario earthquakes needs to be estimated and thus the correlation in ground motions that occurs during an event needs to be accounted for in the risk analysis. A possible approach to track these correlations was to incorporate elements of PSHA code into the risk calculations code. Ground motions for each of the earthquake events (item 1) at each of the levee reach locations have been estimated and given these ground motions, the probability of levee failure has been computed within the risk calculations code. This is described in URS/JBA (2007).
3. Time-dependent seismic hazard results are computed at six sites in the Delta in the years of 2005, 2050, 2100, and 2200 (Figures 2 and 3a). The results include: fractile hazard curves for all ground motion measures the 5th, 15th, 50th (median), 85th, and 95th percentiles, and the mean; M-D (magnitude-distance) deaggregated hazard results for all ground motion measures for 0.01, 0.001, 0.002 and 0.0004 annual probabilities of exceedance; and mean hazard curves for each seismic source for each ground motion measure.
4. Time-dependent probabilistic ground shaking hazard maps for 100 and 500 year return periods have been developed for the Delta area as defined in Figures 2 and 3a. The maps are for peak horizontal acceleration and 1.0 sec horizontal spectral accelerations, and a stiff soil site condition.

1.2 Scope of Work

This study's approach is consistent with the guidelines for a Level 2 analysis using the TI approach as defined by the Senior Seismic Hazard Analysis Committee (SSHAC, 1997). In SSHAC terminology, the TI or Technical Integrator is defined as: "a single entity (individual, team, company, etc.) that is responsible for ultimately developing the composite representation of the informed technical community (herein called the community distribution) for source and ground motion characterization issues. This could involve deriving information relevant to an issue from the open literature or through discussions with experts." In a Level 2 analysis, the TI interacts with proponents and resource experts to identify issues and interpretations and estimates the community distribution. This Level 2 study was further enhanced by peer review by representatives of the U.S. Geological Survey (USGS) and the California Geological Survey (CGS).

Topical Area: Seismology

The TI in this study is the DRMS Seismic Hazards Topical Area Team (SHTAT) consisting of:

- Ivan Wong, URS Corporation Task Leader;
- Patricia Thomas, URS Corporation;
- Jeff Unruh, Lettis & Associates, Inc.;
- Kathryn Hanson, Geomatrix Consultants, Inc.;
- Bob Youngs, Geomatrix Consultants, Inc.;
- Kevin Coppersmith, Coppersmith Consulting; and
- Walter Silva, Pacific Engineering & Analysis;

The PSHA calculations were performed by URS with assistance from Bob Youngs and Norm Abrahamson. The following was our detailed scope of work.

Task 1 Review and Revision of the Seismic Source Model

The URS seismic source model for the greater San Francisco region was used as a “strawman” to review and revise to produce the final DRMS model for the PSHA calculations. A subgroup of the SHTAT (Unruh, Hanson, and Wong) reviewed, evaluated, revised, and updated the seismic source model based on the most recent research. Characterization of the major faults was adopted from WGCEP (2003).

Task 2 Selection of Attenuation Relationships

Ground motion attenuation relationships were evaluated, selected, and weighted by a subgroup of the SHTAT (Youngs, Silva, and Wong).

Task 3 PSHA Calculations for Defining Earthquake Events and for Hazard at Specific Sites

Based on Tasks 1 and 2, PSHA calculations were performed for multiple sites throughout the study region. The results identified plausible earthquake events, defined by their location, magnitude, and ground motion. In addition, time-dependent and time-independent hazard results were calculated for six selected sites (Figures 2 and 3a). Final hazard results consisted of those products described above.

Task 4 Final Report and Review

This Final Technical Memorandum describes and summarizes the methodology and results of this study. The report has been reviewed by the USGS and CGS and we have attempted to address as many of their comments as possible given time constraints imposed by the project schedule.

An additional task not contained in the original scope of work was the development of hazard maps of the Delta for selected return periods.

1.3 Uncertainty

The most recent PSHA studies distinguish between two types of uncertainty, namely epistemic uncertainty and aleatory variability. Aleatory variability (sometimes called randomness) is probabilistic variability that results from natural physical processes. The size, location, and time of the next earthquake on a fault and the details of the ground motion are examples of quantities considered aleatory. In current practice, these quantities cannot be predicted, even with the collection of additional data. Thus, the aleatory component of uncertainty is irreducible. The second category of uncertainty is epistemic, which results from imperfect knowledge about the process of earthquake generation and the assessment of their effects. An example of epistemic uncertainty is the shape of the magnitude distribution for a given seismic source. In principle, this uncertainty can be reduced with advances in knowledge and the collection of additional data.

These two types of uncertainty are treated differently in advanced PSHA studies. Integration is carried out over aleatory variabilities to get a single hazard curve, whereas epistemic uncertainties are expressed by incorporating multiple hypotheses, models, or parameter values. These multiple interpretations are each assigned a weight and propagated through the analysis, resulting in a suite of hazard curves and their associated weights. Results are presented as curves showing statistical summaries (e.g., mean, median, fractiles) of the exceedance probability for each ground motion amplitude. The mean and median hazard curves convey the central tendency of the calculated exceedance probabilities. The separation among fractile curves conveys the net effect of epistemic uncertainty about the source characteristics and ground motion prediction on the calculated exceedance.

1.4 Assumptions, Constraints, and Limitations

As described in SSHAC (1997), the model of randomness (aleatory variability) of earthquake behavior underlies virtually all PSHAs. A model is a mathematical representation of a conceptual model that is based on established scientific and engineering principles and from which the approximate behavior of a system, process, or phenomenon can be calculated within determinable limits of uncertainty. A limitation of models is they only approximate the behavior of a physical process and cannot capture its every detail. There are also uncertainties in the parameters that are required by the model, which are generally due to the availability and uncertainties of data. The components of the aleatory model are in simplistic terms those that (1) characterize the seismicity in the vicinity of a site and (2) represent the predicted ground motion effect at a site given an earthquake of specified magnitude occurring at a given distance. SSHAC (1997) endorses this model for all but “certain uncommon cases where the available information may permit or require specific deviations.” As with any effective presentation of nature, the model represents a compromise between complexity, availability of information, and sensitivity of the results (SSHAC, 1997).

2.0 Methodology

A PSHA is an evaluation of the ground motion that will be exceeded at a specified annual frequency or probability. The inputs to a PSHA are the same as those used in a

Topical Area: Seismology

deterministic analysis of ground motion hazard plus the assessment of the frequency of occurrence of the earthquakes. The following steps taken in a PSHA are somewhat similar to a deterministic analysis:

- Identify all seismic sources that can generate strong ground shaking at the site.
- Characterize each seismic source in terms of location, geometry, sense of slip, maximum magnitude, and earthquake occurrence rates for all magnitudes of significance to the site hazard (typically moment magnitude [M] ≥ 5).
- Select ground motion attenuation relationships appropriate for the seismic sources, seismotectonic setting, and site conditions.
- Calculate the probabilistic hazard using a qualified computer program. The hazard can be expressed in terms of seismic hazard curves and a Uniform Hazard Spectrum (UHS).

The traditional PSHA approach is based on the model developed principally by Cornell (1968). The occurrence of earthquakes on a fault is assumed to be a Poisson process. The Poisson model is widely used and is a reasonable assumption in regions where data are sufficient to provide only an estimate of average recurrence rate (Cornell, 1968). When there are sufficient data to permit a time-dependent estimate of the occurrence of earthquakes, the probability of exceeding a given value can be modeled as an equivalent Poisson process in which a variable average recurrence rate is assumed.

The probability that a ground motion parameter “ Z ” exceeds a specified value “ z ” in a time period “ t ” is given by:

$$p(Z > z) = 1 - e^{-v(z) \cdot t} \quad (1)$$

where $v(z)$ is the annual mean number (or rate) of events in which Z exceeds z . It should be noted that the assumption of a Poisson process for the number of events is not critical. This is because the mean number of events in time t , $v(z) \cdot t$, can be shown to be a close upper bound on the probability $p(Z > z)$ for small probabilities (less than 0.10) that generally are of interest for engineering applications. The annual mean number of events is obtained by summing the contributions from all sources, that is:

$$v(z) = \sum_n v_n(z) \quad (2)$$

where $v_n(z)$ is the annual mean number (or rate) of events on source n for which Z exceeds z at the site. The parameter $v_n(z)$ is given by the expression:

$$v_n(z) = \sum_i \sum_j \beta_n(m_i) \cdot p(R=r_j|m_i) \cdot p(Z > z|m_i, r_j) \quad (3)$$

where:

$\beta_n(m_i)$ = annual mean rate of recurrence of earthquakes of magnitude increment m_i on source n ;

Topical Area: Seismology

$p(R=r_j|m_i)$ = probability that given the occurrence of an earthquake of magnitude m_i on source n , r_j is the closest distance increment from the rupture surface to the site;

$p(Z > z|m_i, r_j)$ = probability that given an earthquake of magnitude m_i at a distance of r_j , the ground motion exceeds the specified level z .

The calculations were made using the computer program HAZ38 developed by Norm Abrahamson. An earlier version of this program HAZ36 was validated as part of PG&E's submittal to the NRC and the new features resulting in HAZ38 were validated as part of ongoing URS work for the U.S. Department of Energy.

3.0 Seismic Source Inputs to Analysis

Seismic source characterization is concerned with three fundamental elements: (1) the identification location and geometry of significant sources of earthquakes; (2) the maximum size of the earthquakes associated with these sources; and (3) the rate at which they occur. In this study, the dates of past earthquakes on specific faults are also required in addition to the frequency of occurrence. The source parameters for the significant faults in the site region (Figure 2) are characterized for input into the hazard analyses. Both areal source zones and Gaussian smoothing of the historical seismicity are used in the PSHA to account for the hazard from background earthquakes.

The guiding philosophy for characterizing seismic sources in this study is the following. The fundamental seismic source characterization came from the work done by the USGS Working Group on Northern California Earthquake Potential (WGNCEP, 1996), the USGS Working Group on California Earthquake Probabilities (WGCEP, 2003) and the CGS's seismic source model used in the USGS National Hazard Maps (Cao et al., 2003). This characterization was updated and revised based on recent research. Also, additional and more detailed characterization of potential seismic sources in the Delta and the western margin of the Great Valley are included (Figure 2), in order to fully capture the range of assessments that might affect the Delta region.

Uncertainties in the seismic source parameters were incorporated into the PSHA using a logic tree approach. In this procedure, values of the source parameters are represented by the branches of logic trees with weights that define the distribution of values. In general, three values for each parameter were weighted and used in the analysis. Statistical analyses by Keefer and Bodily (1983) indicate that a three-point distribution of 5th, 50th, and 95th percentiles weighted 0.185, 0.63, and 0.185 (rounded to 0.2, 0.6, and 0.2), respectively, is the best discrete approximation of a continuous distribution. Alternatively, they found that the 10th, 50th, and 90th percentiles weighted 0.3, 0.4, and 0.3, respectively, can be used when limited available data make it difficult to determine the extreme tails (i.e., the 5th and 95th percentiles) of a distribution. Note that the weights associated with the percentiles are not equivalent to probabilities for these values, but rather are weights assigned to define the distribution. We generally applied these guidelines in developing distributions for seismic source parameters with continuous distributions (e.g., M_{max} , fault dip, slip rate or recurrence) unless the available data suggested otherwise. Estimating the 5th, 95th, or even 50th percentiles is typically challenging and involves subjective judgment given limited available data.

Topical Area: Seismology

In their analyses to estimate earthquake probabilities along the major faults in the San Francisco Bay Area, the WGCEP (2003) used several models including non-Poissonian models that are time-dependent, i.e., they account for the size and time of the last earthquake. In this study, the probabilities of occurrence for all significant and plausible earthquake scenarios for each seismic source at specified times over the next 200 years are required for the risk analysis. This requirement mandates heavy reliance on the results of WGCEP (2003). For many seismic sources, insufficient information exists to estimate time-dependent probabilities of occurrence and they were treated in a Poissonian manner (Section 3.1). We have incorporated the time-dependent behavior of the major faults using the WGCEP (2003) fault characterization (Section 3.2).

The basic inputs required for the PSHA and the risk analysis are the seismic source model and the ground motion attenuation relations or more accurately ground motion predictive equations. We describe these inputs in the following.

3.1 Seismic Source Model for Time-Independent Hazard

The following describes the time-independent seismic source model. Table 1 describes the model and specifically the bases for the characterization of each seismic source.

3.1.1 Faults

Based on reviews of published and unpublished data, a model of the active and potentially active seismogenic faults has been developed for the greater San Francisco Bay region (Figure 2; Table 1). Each seismic source has been characterized using the latest geologic, seismological, and paleoseismic data and the currently accepted models of fault behavior. The major study recently completed by the WGCEP (2003) entitled “Earthquake Probabilities in the San Francisco Bay Region: 2002-2031” describes and summarizes the current understanding of the major faults in the San Francisco Bay area. We have adopted their seismic source model for the San Andreas, Hayward/Rodgers Creek, Calaveras, Concord/Green Valley, San Gregorio, Greenville, and Mt. Diablo thrust faults in our analyses. The characterization of the Calaveras fault has been slightly modified by WLA and URS. The characterizations of other faults such as the Sargent and Foothill thrust belt are based to a large extent on the CGS model (Cao et al., 2003) and other available studies.

Of particular significance to the study are the blind faults beneath the Delta and the Western Tracy and Vernalis faults, part of the Coast Ranges-Sierran Block boundary zone (CRSB; Wong et al., 1988) (Figure 2). The seismogenic potential of the Midland fault, which transects beneath much of the Delta area and other sources of crustal deformation beneath the Delta have been characterized (Sections 3.1.1.1 and 3.1.1.2).

Magnitudes not adopted from WGCEP (2003) or Cao et al. (2003) were computed using the rupture area relationships of Wells and Coppersmith (1994) and Hanks and Bakun (2002) and the rupture length relationship of Wells and Coppersmith (1994). The relationships are equally weighted. The latter was only used for $M \geq 7.0$.

Uncertainties in determining recurrence models can significantly impact the hazard analysis. We considered the truncated exponential, maximum-magnitude, and characteristic recurrence models, with various weights depending on the source geometry

Topical Area: Seismology

and type of rupture model. For faults we have weighted the characteristic and maximum magnitude models 0.7 and 0.3, respectively. The weighting of these recurrence models, recurrence intervals for the major faults from WGCEP (2003), and slip rates have been critically reviewed and adopted for use in the PSHA.

To address the uncertainty in segmentation models, a “floating earthquake” was used in the PSHA for some seismic sources. A floating earthquake is an event of some specified maximum magnitude distribution whose rupture length is less than the total length of the fault. The event is not associated with a specific segment and is thus allowed to “float” along the length of the fault. The maximum magnitude is based on the observations of the rupture behavior of other faults. The WGCEP (2003) also employed a floating earthquake approach.

Fault Creep (Aseismic Slip) and the R Factor

Some faults or sections of faults are thought to move in a continuous aseismic manner, i.e., they slip without generating large earthquakes. The San Juan Bautista segment of the San Andreas fault is the best example of a creeping fault segment. Fault creep has been documented along portions of the Hayward, Calaveras, San Andreas, and Concord faults in the San Francisco Bay region. However, fault creep is still poorly understood. The primary indicator of the presence of aseismic slip at depth is the observation of surficial fault creep (e.g., Galehouse, 1995). If surficial fault creep is not observed, there is little reason to suspect that it is a significant fault attribute at seismogenic depths. If surficial fault creep is observed, aseismic slip may extend to seismogenic depths beneath that section of that fault and can account for a significant portion of the slip rate available for earthquake generation (WGCEP, 2003).

WGCEP (2003) accounted for aseismic slip through a seismic slip factor R that varies from 0, where all slip rate is accounted for by aseismic slip, to 1.0, where all of the slip rate is accounted for by earthquakes. Regional tectonic models based on geodetic observations collected in the San Francisco Bay region in the last few decades are the primary basis for determining the R values. The R values affect the maximum magnitude of each fault by reducing the rupture area used to calculate magnitudes. The incorporation of the R values in the PSHA was evaluated and adopted by the SHTAT.

3.1.1.1 Delta Seismic Sources

The following describes the characterization of the four Delta seismic sources considered in the PSHA and that are not included in either the CGS (Cao et al., 2003) or WGNCEP (2005) models: Northern Midland zone, Southern Midland fault, Thornton Arch Zone, and Source Montezuma Hills Source Zone (Figure 3a). As is the case for many “blind” faults, the characterization of the Delta seismic sources is highly uncertain because of the very limited amount of data. What is known about these sources has come from subsurface seismic data. Despite these limitations, we have developed characterizations of these seismic sources with their associated uncertainties.

Midland Fault

The Midland fault is an approximately north-striking, west-dipping fault underlying the central Delta region that accommodated extension and subsidence in the early Tertiary

Topical Area: Seismology

Sacramento Valley forearc basin (Krug et al., 1992). As shown on the California State geologic map, the fault is at least 60 km long (Wagner et al., 1981). The Midland fault is not exposed at the surface and is known primarily from natural gas exploration in the greater Delta region. Proprietary seismic reflection profiles indicate that the dip of the fault is relatively steep at shallow depths and decreases with depth, suggesting a downward-flattening or listric geometry. Although the Midland fault is commonly shown as a single buried trace on state maps along its entire length (Wagner et al., 1981; Jennings, 1994), subsurface mapping by the California Division of Oil and Gas (1982) and Krug et al. (1992) indicate the fault breaks into a series of northwest-striking splays north of the town of Rio Vista that exhibit a right-stepping, *en echelon* pattern. The northwest-striking splays of the fault are associated with a series of active and abandoned gas fields in the Sacramento Valley between the towns of Rio Vista and Woodland (California Division of Oil and Gas, 1982).

Based on analysis of seismic reflection data, Weber-Band (1998) documented late Cenozoic reactivation of the Midland fault to accommodate net horizontal crustal shortening. Reverse reactivation of the fault is clearly shown by antiformal folding of shallow reflectors up-dip of the fault tip on a seismic reflection profile that was published as the cover of Volume MP-41, "Structural Geology of the Sacramento Basin," for the 1992 Annual Meeting of the Pacific Section, Society of Economic Paleontologists and Mineralogists (Cherven and Edmondson, eds., 1992). Weber-Band (1998) interpreted that the Montezuma Hills, an anomalous low-lying set of hills along the western margin of the Delta capped by a dissected Pleistocene surface, were uplifted in the hanging wall of the Midland fault. Inspection of topographic maps of the Sacramento Valley between Rio Vista and Woodland reveals numerous low hills that are anomalous and locally associated with the northwest-striking splays of the northern Midland fault (e.g., "Dixon Ridge" near the town of Dixon; "Plainfield Ridge" west of the city of Davis).

Previous Source Characterization. The Thrust Fault Subgroup (1999) developed estimates of slip rate for the Midland fault based on reverse offset of Quaternary strata inferred from interpretation of seismic reflection data. Weber-Band (1998) used a two-way time to depth conversion to estimate about 243 m of vertical reverse separation on the late Cenozoic U1 unconformity due to late Cenozoic reverse slip on the Midland fault. From a survey of the available stratigraphic literature, Weber-Band (1998) adopted a provisional age of 1.0 ± 0.5 Ma for the U1 unconformity in the vicinity of the Montezuma Hills. Based on a review of supplemental data, the Thrust Fault Subgroup of Working Group 1999 concluded that the full range in possible ages for the U1 unconformity is $1.5 \text{ Ma} \pm 1.0 \text{ Ma}$. From consideration of a range in fault dip and the age of the U1 unconformity, the Thrust Fault Subgroup (1999) adopted the following range of weighted values for the long-term average reverse slip rate on the Midland fault:

Midland Fault Slip Rate (mm/yr) (Reverse Displacement)

0.1	(0.2)
0.15	(0.6)
0.5	(0.2)

In developing estimates of maximum earthquake magnitude for the Midland fault, the Thrust Fault Subgroup (1999) considered several scenarios:

Topical Area: Seismology

- 1) Cumulative reverse slip on the Midland fault during repeated earthquakes has uplifted the modern Montezuma Hills as a tectonic-geomorphic feature in the hanging wall, according to the kinematic model of Weber-Band (1998). The maximum north-south extent of uplifted Plio-Pleistocene Montezuma Formation in the Montezuma Hills is about 20 km, implying that ruptures of comparable length or greater may have occurred on the Midland fault;
- 2) Smaller segments (i.e., 10-15 km) have ruptured. If so, then it is possible that the Midland fault may have been the source of the 1889 **M** 6 Antioch area earthquake;
- 3) The full length of the Midland fault mapped in the subsurface is greater than 60 km (Wagner et al., 1981). It is possible that a large part (i.e., about 30 km or more) of the full length of the fault ruptures in large, infrequent events.

Based on these scenarios, the Thrust Fault Subgroup (1999) adopted a weighted range of earthquake magnitudes consistent with subsurface rupture lengths corresponding to 10, 20, and 30 km (per Wells and Coppersmith, 1994):

<u>Midland Fault Maximum Earthquake (M)</u>	
6	(0.3)
6.25	(0.4)
6.5	(0.3)

The Thrust Fault Subgroup (1999) placed the highest weight on the central value because this corresponds to an approximately 20-km-long subsurface rupture length from empirical relations in Wells and Coppersmith (1994), and this is consistent with the model for uplift of the approximately 20-km-long Montezuma hills by repeated earthquakes on the Midland fault (Weber-Band, 1998).

New Observations. As part of our literature review and survey of expert opinion for the DRMS project, we met with Dr. Janine Weber and Mr. Scott Hector, both of whom have expert knowledge of the geology of the Delta. Dr. Weber shared proprietary seismic reflection data from the Delta region that provided additional confirmation of reverse reactivation of the Midland fault in the area east of the town of Rio Vista and discussed her analysis of the subsurface structure of the Montezuma hills. Mr. Hector also let us examine proprietary reflection data (CGG seismic line 804) that confirmed late Cenozoic reverse reactivation of the Midland fault on Twitchell Island between Seven Mile Slough and the San Joaquin River (Figure 3a), and he showed us detailed structure contour maps he prepared from analysis and correlation of borehole data that illustrate the style of deformation along and adjacent to the Midland fault. In particular, Mr. Hector mapped a complexly faulted structure along the Midland fault in the Rio Vista Gas Unit that he interpreted as a zone of localized shortening in a restraining bend associated with right-lateral displacement along the Midland fault.

Additionally, we compared existing mapping of the Midland fault by the California Division of Oil and Gas (1982) with subsurface data on the elevation of the base of Holocene peat in the Delta region provided by the CDWR. Our analysis of these data, described in Appendix A, reveals systematic west-side-up anomalies in the base of peat across the Midland fault in Webb Tract, Franks Tract and Holland Tract. If it is assumed

Topical Area: Seismology

these anomalies are due to Holocene movement on the Midland fault, then the implied vertical separation rate is about 0.3 to 0.6 mm/yr (Appendix A), which is comparable to the reverse slip rate of 0.1 to 0.5 mm/yr for the Midland fault estimated by the Thrust Fault Subgroup (1999) of the WGNCEP (1996).

Characterization of the Midland Fault. Based on the change in character of the Midland fault at about the latitude of Rio Vista (Krug et al., 1992), we separate it into two distinct sources (Table 1; Figure 3a):

- 1) The Southern Midland fault, which we characterize as a single, potentially seismogenic fault; and
- 2) The Northern Midland zone, which we characterize as an areal source zone to encompass the numerous right-stepping northwest-striking splays of the Midland fault.

We follow the previous work of the Thrust Fault Subgroup (1999) in assigning a high probability of activity to both reaches of the Midland fault. The work of Weber-Band (1998) documents evidence for Quaternary activity of the southern Midland fault, and cross-sections of the base of peat across splays of the fault provide evidence for possible Holocene activity. The anomalous hilly topography of the southern Sacramento Valley in the Northern Midland zone is most simply explained by reactivation of splays of the northern Midland fault zone. For example, the north-northwest-trending Plainfield Ridge west of the town of Davis is a low rise above the flat valley floor that is associated with a northern splay of the Midland fault in the vicinity of the Fairfield Knolls gas field (Krug et al., 1992; California Division of Oil and Gas, 1982). An abandoned channel of east-draining Putah Creek is incised and has cut multiple terraces across Plainfield Ridge, but is less incised and has cut fewer or no terraces both upstream and downstream of the ridge. These geomorphic relations are consistent with uplift of Plainfield Ridge by reactivation of an underlying splay of the Midland fault.

Based on geodetic data that indicate dextral shear associated with Pacific-Sierran plate motion extends into the western part of the Delta region (Prescott et al., 2001), and the subsurface mapping of S. Hector (personal communication, 2006) that suggests possible right-lateral motion on the Midland fault, we interpret that net slip on the Southern Midland fault is probably oblique, with components of dextral and reverse displacement. We modify the weighted range of slip rates for the Midland fault developed by the Thrust Fault Subgroup (1999) to account for a component of right-lateral motion as follows:

Slip Rate (mm/yr), Southern Midland Fault (Right-Reverse Displacement)

0.1 (0.3)

0.5 (0.4)

1.0 (0.3)

We assume that slip on the Southern Midland fault passes northward and is distributed across the multiple splays in the Northern Midland Zone. We therefore adopt the same weighted slip rate values for the Northern Midland Zone as for the Southern Midland fault (Table 1).

For the Southern Midland fault, we consider two scenarios for evaluating earthquake magnitude: (1) unsegmented rupture of the entire length of the fault (**M** 6.6, from

Topical Area: Seismology

regressions on rupture parameters and earthquake magnitude); and (2) Rupture of only part of the fault in a single event, with the same weighted range of floating earthquake magnitudes centered on **M** 6.25 as adopted by the Thrust Fault Subgroup (1999) (Table 1). We place higher weight on the floating earthquake model because geomorphic expression of activity is not uniform along the entire mapped length of the fault.

For the Northern Midland Zone, we consider a floating earthquake model only and adopt the same weighted range of magnitudes as for the floating earthquake on the Southern Midland fault (Table 1). We specify N30°W as the preferred orientation of modeled fault planes within Northern Midland zone, consistent with orientations of the northern splays of the Midland fault mapped by the California Division of Oil and Gas (1982) and Krug et al. (1992).

Thornton Arch Source Zone

We define the Thornton Arch source zone to encompass the possibility that a buried structure in the vicinity of the Thornton and West-Thornton-Walnut Grove gas fields is an active fault (Figure 3a). The motivation for this is the observation that the Mokelumne River does not continue along a straight course across the Delta from the point where it exits the western Sierran foothills, but rather it appears to be deflected to the north in an anomalous loop north and west of the town of Thornton (E. Helley, personal communication, 1999). The deflection of the Mokelumne River occurs around the “Thornton arch”, an antiformal structure that comprises the Thornton and West-Thornton-Walnut Grove gas fields (California Division of Oil and Gas, 1982). Available data on the structure of the gas fields are limited to structure contour maps on Eocene stratigraphic markers and cross sections developed from bore hole data (California Division of Oil and Gas, 1982). The “Thornton Arch” is a roughly east-west-trending antiformal closure in Eocene and older strata. The California Division of Oil and Gas (1982) has interpreted the presence of several north-northwest-striking faults in the gas fields from analysis of borehole data, but it is not clear how these structures are related to the development of the fold.

Based primarily on the possibility that the northward deflection of the Mokelumne River is due to localized Quaternary uplift of a blind structure, we defined a source zone to encompass the Thornton Arch and associated faults as potential causative structures. We assign a low probability of activity to the Thornton Arch zone as an independent source of earthquakes ($P(a) = 0.2$) (Table 1). We assume that the primary causative fault(s) for the deformation have an approximately east-west strike similar to the trend of the antiformal. We assume that earthquake magnitudes are limited by the relatively small dimensions of the Thornton Arch source zone and structures encompassed therein, and adopt a range of maximum magnitudes with a weighted mean of **M** 6.25 (Table 1). Given the lack of geomorphic expression of surface deformation within the Thornton Arch source zone other than the possible deflection of the Mokelumne River, we infer that deformation rates must be very low, and adopt a weighted range of slip rates centered on a mean of 0.10 mm/yr.

Montezuma Hills Source Zone

We define the Montezuma Hills source zone to encompass our uncertainty about whether Quaternary uplift of the Montezuma Hills is due exclusively or even primarily to west-

Topical Area: Seismology

side-up motion on the Midland fault. The motivation for this is a structural geologic interpretation by Dr. Janine Band of a grid of proprietary seismic reflection lines that cross the Montezuma Hills. Dr. Band identified a seismic marker that she correlated with the U1 unconformity ($1.5 \text{ Ma} \pm 1.0 \text{ Ma}$; see discussion above). Structure contours on the depth of the U1 marker (in two-way time) show the marker is at its highest elevation in the southern Montezuma Hills about 10 km west of the Midland fault, and the marker slopes toward the north-northeast in the subsurface (Janine Band, personal communication, 2006). If it is assumed the U1 marker was originally subhorizontal, then the relief on this feature as expressed in Dr. Band's interpretation suggests that maximum uplift has occurred well to the west of the Midland fault, and that the hanging wall block is tilted toward the northeast. These observations are contrary to our expectations about deformation associated with simple block uplift and folding in the hanging wall of the west-dipping Midland fault, and suggests that a different mechanism may be responsible for uplift of the Montezuma Hills. Other faults have been mapped in the subsurface of southern Montezuma Hills (e.g., Sherman Island fault system; California Division of Oil and Gas, 1982). These structures were active in late Cretaceous-early Tertiary time (Krug et al., 1992), but to date have not been studied for evidence of Quaternary reactivation.

Given these observations, we defined a source zone to encompass possible undetected active structures that may be responsible for the uplift of the Montezuma Hills. We extend the zone southward along the general trend of the Sherman Island fault system in the subsurface (Figure 3a). We assign a probability of activity $P(a)$ of 0.5 to the Montezuma Hills zone as an independent source of earthquakes (Table 1). Our preferred orientation of modeled fault planes within the Montezuma Hills zone is $N20^\circ W$, which is approximately parallel to the general strike of the Sherman Island fault zone in the subsurface (California Division of Oil and Gas, 1982). We assume that earthquake magnitudes will be limited by the NW-SE dimensions of the zone, and thus adopt a range of maximum magnitudes with a weighted mean of M 6.25 (Table 1). Our preferred range (0.05 to 0.5 mm/yr) and weighting of slip rates reflects our interpretation that tectonic activity in the Montezuma Hills, if independent of the Midland fault, may be related to transfer of slip from the Vernalis and West Tracy faults to the Pittsburg-Kirby Hills fault zone.

Dips of the Delta Fault

In general, there are few direct observations documenting the dip of known and suspected active faults in the Delta study region. We assume that faults along the northwestern margin of the San Joaquin Valley and in the Delta region have moderate to steep dips because the surface traces are relatively straight and cut across, rather than follow, topography. Also, GPS geodesy indicates that the dominant style of deformation in this region is distributed dextral shear (Prescott et al., 2001; d'Alessio et al., 2005), which we assume is most likely to be accommodated by steeply dipping to subvertical strike-slip faults. For example, the Pittsburg-Kirby Hills fault zone is a steeply east-dipping fault in the western Delta region that is associated with strike-slip seismicity (Parsons et al., 2002). In the case of the Midway fault, slickenside lineations observed in trench exposures indicate dominantly horizontal, strike-slip motion (Bieber, 2002). Based on these observations, we assume that most active faults in the Delta region and northwestern Sacramento Valley have moderately steep dips (i.e., about 70°), reflecting

Topical Area: Seismology

dominantly strike-slip deformation with local components of reverse vertical separation (Table 1).

Seismicity of the Delta

Contemporary seismicity in the Delta has exhibited a low-level pattern of scattered small magnitude events since 1966, when adequate seismographic coverage came into existence (Figure 3b). There is no apparent correlation of seismicity with any of the Delta seismic sources, which is not an unusual observation for buried faults. No $M \geq 4.0$ events have occurred in the past 40 years in the Delta (Figure 3b). Similarly, no $M \geq 5.0$ earthquakes have occurred in the Delta in historical times (Figure 1). The absence of significant seismicity in the Delta does not necessarily indicate the absence of seismogenic structures. The neighboring CRSB boundary zone has been for the most part, not seismically active and yet the occurrence of large earthquakes ($M > 6$) such as the 1892 Vacaville-Winters and 1983 Coalinga events are testimony to the seismogenic potential of buried faults (Wong et al., 1988).

3.1.1.2 CRSB Boundary Zone

The following describes the elements of the CRSB that have been characterized as part of this study: West Tracy, Vernalis, Black Butte, and Midway faults.

West Tracy Fault

The West Tracy fault strikes northwest-southeast and is mapped for a total distance of about 34 km along the eastern flank of the northern Diablo Range between Corral Hollow south of Tracy and the town of Byron (Figure 3a). The fault has no documented surface trace on small-scale geologic maps published by the State of California (Rogers, 1966; Wagner et al., 1991), and is known primarily from analysis of proprietary borehole data and seismic reflection data acquired for oil and gas exploration (Sterling, 1992). The West Tracy fault is well imaged as a moderately to steeply west-dipping fault on seismic reflection lines (R. Sterling, written communication, 2006; J. Weber-Band, personal communication, 2006). The reflection data provide clear evidence for west-side-up reverse displacement on the fault, including offset of reflectors associated with Cretaceous marine strata at depth and monoclinical folding above the fault tip (Sterling, 1992; R. Sterling, written communication, 2006). The fault dies out as a discernable feature in the upper 1 to 2 seconds depth two-way time on seismic time sections, and fold displacement can be traced above the fault tip to the shallowest reflectors imaged in the data. Angular unconformities are present in the shallow reflectors that indicate progressive uplift and fold deformation has occurred during deposition of the youngest imaged strata. The folded shallow reflectors project updip to exposures of northeast-dipping deposits along the eastern Diablo Range front mapped as "Pliocene-Pleistocene gravels" by Crane (1995b; Brentwood 7.5 minute quadrangle). The "Plio-Pleistocene gravels" unconformably overlie more steeply dipping strata mapped by Crane (1995b) as Miocene Neroly Formation. Geologic mapping at 1:250,000 scale by the State of California (Rogers, 1966) shows a contact between older and younger Quaternary deposits that follows the buried trace of the West Tracy fault. The older deposits are preferentially associated with the hanging wall of the fault, consistent with Quaternary uplift. We interpret these map relations as prima facie evidence for Quaternary uplift and fault-propagation folding above the West Tracy fault.

Topical Area: Seismology

Very limited data are available to estimate the rate of slip and recent behavior of the West Tracy fault. In addition to the reverse separation expressed in reflection profiles, we infer a component of right-lateral slip on the West Tracy fault given its northwest strike sub-parallel to regional Pacific-Sierran plate motion, and the fact that it is parallel to the Black Butte-Midway faults, which exhibit evidence for dextral-reverse oblique slip. We assume that the slip rate of the West Tracy fault is less than that of the Midway/Black Butte fault zone because it lies farther to the east, consistent with geodetic data that document eastward decreasing rates of dextral motion across the Pacific-Sierran plate boundary (Prescott et al., 2001; d'Alessio et al., 2005). A lower bound of 0.07 mm/yr on the slip rate (Table 1) is estimated based on total vertical separation of about 800 ft (244 m) of a basal Miocene unconformity across the fault as reported by Sterling (1992) and an assumed duration of deformation (active during the past ~3.5 Ma). We arbitrarily assume that the maximum slip rate on the West Tracy fault (0.5 mm/yr) is 50% of the maximum slip rate on the Midway/Black Butte fault zone (1.0 mm/yr), based on the more easterly location of the fault within the plate boundary and its relatively more subdued geomorphic expression.

Vernalis Fault

The Vernalis fault is an approximately northwest-striking, moderately to steeply west-dipping fault in the subsurface of the western San Joaquin Valley, about 9 to 12 km east of the physiographic front of the Diablo Range (Figure 3a). The Vernalis fault extends for a minimum of 31 km between Tracy and the town of Patterson to the southeast (Sterling, 1992). Exploration geologists who have examined proprietary subsurface data suggest that the fault may continue an unknown distance south of Patterson, so the full length of the fault is poorly known (Scott Hector, personal communication, 2006).

The Vernalis fault is known primarily from analysis of proprietary borehole data and seismic reflection data acquired for oil and gas exploration (Sterling, 1992; S. Hector, personal communication, 2006). Subsurface relations imaged in the reflection data suggest the fault is a subvertical to steeply west-dipping structure that has accommodated west-side-up separation (Sterling, 1992). Interpreted reflection profiles published by Sterling (1992) show reverse separation of a Miocene unconformity across the Vernalis fault. The fault appears to die out above the offset unconformity and below the earth's surface, but folding of the layered reflectors can be traced above the tip of the fault to the top of the seismic record section. Sterling (1992) describes stratigraphic and structural relationships imaged by seismic reflection data indicating "movement as recently as late Pliocene."

A small-scale map in Sterling (1992) shows the northern end of the Vernalis fault curving to the west and terminating against the southern end of the West Tracy fault. This pattern may represent a link between the two faults and transfer of slip. Sterling (1992) originally inferred a component of left-lateral motion on the Vernalis fault, but now feels it is more likely that there is a component of right-lateral motion (R. Sterling, written communication, 2006), which is consistent with the current tectonic regime and geodetic data indicating measurable NW dextral shear extending to the western margin of the Central Valley at the latitude of the Delta (Prescott et al., 2001; d'Alessio I., 2005).

Topical Area: Seismology

We infer Quaternary activity of the Vernalis fault based on the systematic occurrence of older Quaternary deposits on the upthrown hanging wall block. Geologic maps of the 2° San Jose (Rogers, 1966) and San Francisco-San Jose quadrangles (Wagner et al., 1991) published by the State of California show Pleistocene fluvial deposits on the upthrown western side of the fault, and generally younger basin deposits on the downthrown side. The contact between the older and younger deposits closely follows the buried fault trace in the subsurface. The Vernalis fault also may exert control on local stream and drainage patterns. For example, the course of the San Joaquin River closely follows the buried trace of the fault for a minimum of 35 km between Patterson and Tracy, and the stream is confined to the inferred downthrown eastern block. This pattern continues north and west of Tracy, where the Vernalis fault turns more toward the west and streams like Tom Paine slough and Old River are confined to the downthrown block and appear to be deflected parallel to fault strike. These geomorphic relations are consistent with late Quaternary west-up motion on the fault, expressed as uplift of the hanging wall block and local fault-propagation folding above the fault tip.

Given the possible link between the structures, we assume the slip rate on the Vernalis fault is comparable to the estimated rate for the West Tracy fault (0.07 to 0.5 mm/yr; Table 1). We adopt a range of weighted magnitudes centered on a mean magnitude of **M** 6.5, encompassing the possibility of rupture of all or part of the fault in a single event.

Black Butte and Midway Faults

The Black Butte fault is a northwest-striking, moderately to steeply west-dipping Quaternary fault along the physiographic boundary between the northern Diablo Range and northwestern San Joaquin Valley, located approximately 10 km southeast of the city of Tracy (Figure 3a). Sowers et al. (1992) documented about 180 m of west-side-up displacement of an early to middle Quaternary pediment surface across the Black Butte fault in the vicinity of Corral Hollow. Although these geomorphic and structural relations provide evidence for Quaternary activity on the fault, there is significant uncertainty in the age of the deformed surface, as well as the correlation of the pediment across the fault. Given the northwest strike of the fault and recent geodetic studies that suggest moderate rates of NW-directed dextral shear extend out to the eastern margins of the Pacific-Sierran plate boundary at the latitude of the San Francisco Bay area (d'Alessio et al., 2005), we believe it is likely the Black Butte fault accommodates a component of dextral motion in addition to the observed reverse displacement.

The late Cenozoic Midway fault strikes northwest and is separated from the northwest end of the Black Butte fault by a left *en echelon* step across a small west-northwest-trending anticline that deforms Miocene-Pliocene strata (Crane, 1995a; Midway 7.5 minute quadrangle). Geologic mapping by Crane (1995a) documents about 800 m of apparent right-lateral offset of an unconformable contact between Cretaceous and Miocene strata across the Midway fault in the SW 1/4 of section 19, T.2S., R.4E. Paleoseismic trenching investigations of the Midway fault conducted in 2004 by Geocon, Inc. documented late Pleistocene surface rupture on the fault (David Bieber, Geocon, Inc., personal communication, 2007). Slickensides on the exposed fault plane indicate dominantly subhorizontal displacement (Bieber, personal communication, 2007). Based on analysis of stereo aerial photography, Bieber (2002) interpreted geomorphic features along the fault to indicate left-lateral displacement. This interpretation is contrary to the

Topical Area: Seismology

dextral offset of the Miocene-Cretaceous contact mapped by Crane (1995a), but it is possible that the apparent dextral offset could have been created by differential uplift of the eastern block of the fault.

Based on these data and observations, we conclude the Midway fault is an active structure that primarily accommodates strike-slip displacement. Bieber's (2002) interpretation that the Midway fault is a left-lateral structure is intriguing; if this is correct, then the fault is a kinematic anomaly within the dextral Pacific-Sierran plate boundary. Alternatively, if the Midway fault is a right-lateral structure, then the small anticline separating the Black Butte and Midway faults is a restraining bend or stepover connecting the two structures.

Based on the preponderance of evidence, we characterize the Black Butte and Midway faults as a single structure that accommodates dextral-reverse displacement. We estimate a range in slip rate for the Black Butte fault from the inferred displacement of the pediment and middle to early Pleistocene age estimates (Sowers et al., 1992), and an inferred horizontal to vertical (H:V) ratio for the components of slip. If it is assumed that the offset pediment ranges in age from about 300 ka to 1 Ma, then the corresponding range in long-term average vertical separation rate is about 0.2 to 0.6 mm/yr (Table 1). With an assumed $\leq 3:1$ ratio of strike-slip to dip-slip displacement, the implied rate of net oblique slip is less than 0.6-1.8 mm/yr. For the Midway fault, we estimate a long-term average rate of dextral offset of about 0.2 mm/yr based on 800 m of late Cenozoic right-separation and an assumed duration of deformation (active during the past ~ 3.5 Ma). We assume the activity rate on the two faults is comparable, and thus discount the upper end of the range in the estimated slip rate on the Black Butte fault in favor of a range that better overlaps the slip rate estimates of both structures (i.e., 0.1 to 1.0 mm/yr; Table 1). For maximum magnitude, we adopt a floating earthquake model with a weighted range of magnitudes that favors rupture of all or most of the combined length of the Black Butte and Midway faults (Table 1).

3.1.2 Model Discrepancy

A significant unresolved issue in the San Francisco Bay region revolves around the distribution of slip on major strands of the San Andreas system east of the Hayward fault, and the discrepancy between geologic and geodetic estimates of slip rate. The integrated slip rate in the model in this study of the major strike-slip faults east of the Hayward fault is lower north of the Sacramento River (about 7.5 mm/yr) than south of the Sacramento River (about 10.5 mm/yr). Although the 3.5 mm/yr discrepancy falls within the uncertainty in the geologic slip rate estimates, we acknowledge that it could be due to higher rates adopted for eastern strands of the San Andreas system south of the Sacramento River in our model (i.e., Greenville fault and Delta faults). The higher slip rate on the Greenville fault in our model relative to the WGCEP (2003) characterization (4 mm/yr vs. 2 mm/yr) could account for about 2 mm/yr of the discrepancy. The Delta faults in the our model have low slip rates (less than or equal to about 1 mm/yr) but generally lie south of the Sacramento River and thus potentially contribute to the apparent 3.5 mm/yr discrepancy.

We also suggest the alternative hypothesis that the discrepancy reflects a systematic underestimate of slip rates north of the Sacramento River in our model. Models of GPS

Topical Area: Seismology

data in Prescott et al. (2001) and d'Alessio et al. (2005) consistently place higher slip rates on the eastern strands of the San Andreas system than those adopted by the WGCEP (2003). For example, kinematic models of GPS data find preferred slip rates on the Green Valley fault of about 7 mm/yr or more (Prescott et al., 2001; d'Alessio et al., 2005), compared to the mean centered average about 6 mm/yr in the WGCEP (2003) model. The GPS model of d'Alessio et al. (2005) has a preferred slip rate of 4 mm/yr on the West Napa fault, which is higher than the upper bound of 3 mm/yr in our model. Increasing slightly the slip rates in our model for the West Napa and Green Valley faults would be permissible within the constraints of the GPS data, and would reconcile the apparent dextral slip deficit north of the Sacramento River. Note that by increasing the slip rate on the Greenville fault to about 4 ± 2 mm/yr, our model is more consistent with modeled slip rates of about 5 mm/yr on this structure from analysis of GPS data (d'Allesio et al., 2005).

To summarize, we acknowledge the discrepancy in our model, and believe it reflects a deficiency in the existing data and models accounting for the distribution of slip among faults of the eastern San Andreas system. Although the discrepancy is present in the mean-centered slip rate estimates in our model, the discrepancy is encompassed within the uncertainty expressed by the modeled ranges in slip rates.

3.1.3 Background Seismicity

To account for the hazard from background (floating or random) earthquakes in the PSHA that are not associated with known or mapped faults, regional seismic source zones were used. In most of the western U.S., the maximum magnitude of earthquakes not associated with known faults usually ranges from **M** 6 to 6½. Repeated events larger than these magnitudes generally produce recognizable fault-or-fold related features at the earth's surface (e.g., dePolo, 1994). An example of a background earthquake is the 1986 **M** 5.7 Mt. Lewis earthquake that occurred east of San Jose.

Earthquake recurrence estimates of the background seismicity in each seismic source zone are required. The site region was divided into two regional seismic source zones: the Coast Ranges and Central Valley. The recurrence parameters for the Coast Ranges source zone were adopted from Youngs et al. (1992). They calculated values for background earthquakes based on the historical seismicity record after removing earthquakes within 10-km-wide corridors along each of the major faults. The recurrence values for the Central Valley zone were estimated by URS as part of this study. The maximum earthquake for the source zones is **M** 6.5 ± 0.3 .

3.1.4 Cascadia Subduction Zone

Because of the large long-period ground motions that can be generated by very large (**M** > 8) earthquakes on the Cascadia subduction zone (CSZ) in northwestern California, we have included it in the PSHA. The CSZ defines the plate boundary between the overriding North America plate and the underlying Gorda plate. In this study, we have adopted the model of the megathrust from Wong and Dober (2007). Maximum magnitudes were **M** $9 \pm \frac{1}{2}$ and recurrence intervals of 450 ± 150 years.

The maximum depth of the megathrust (defines the easternmost extent) was varied at 12 km, 20 km, and 25 km weighted 0.4, 0.5, and 0.1, respectively. The depths are based on

Topical Area: Seismology

the model proposed by Wang et al. (2003), which shows the megathrust locked zone offshore of northernmost California and the transition zone only extending to a depth of about 15 km. Rupture of the megathrust will initiate in the locked zone and may extend into the transition zone (Hyndmann et al., 1993; 1995). How far rupture will extend into the transition zone is highly uncertain. One possible indicator of the eastern extent is the maximum depth of the overlying crustal seismicity. Ruff and Kanamori (1983) have observed in other subduction zones that the maximum depth of the crustal seismicity coincided with the downdip edge of historical megathrust ruptures. An examination of crustal seismicity extending to a depth of about 20 km suggests that megathrust rupture would extend downdip along the Gorda plate to this depth in northwestern California.

3.2 WGCEP Model for Time-Dependent Hazard

The time-dependent hazard calculations are based on WGCEP (2003). The source characterization and the time-dependent earthquake probability models were used

directly with computer codes obtained from the USGS to obtain rates of characteristic events for the seven major faults in the San Francisco Bay Area considered by WGCEP (2003): San Andreas, Hayward/Rodger's Creek, Calaveras, Concord/Green Valley, San Gregorio, Greenville, and Mt. Diablo referred to as the SFBR model faults. All other faults considered in the hazard analysis were modeled only with a time-independent probability model due to the lack of data to characterize time dependence for these faults (Section 3.1).

The SFBR model consists of many rupture sources (i.e., a single fault segment or combination of two or more adjacent segments that produce an earthquake). For instance, the Greenville source has three rupture sources (southern segment (GS), northern segment (GN), and unsegmented (GS+GN). A rupture scenario is a combination of rupture sources that describe complete failure of the entire fault, i.e., for the Greenville fault there are three scenarios: GN and GS rupture independently, GN+GS, and a floating rupture along GN+GS. Fault rupture models are the weighted combinations of the fault-rupture scenarios. These weights were determined by each expert considering what would be the frequency (percentage) of each rupture scenario if the entire length of the fault failed completely 100 times. These weights are adjusted slightly to account for moment balancing. The rupture scenarios and adjusted model weights provide the long term mean rate of occurrence of each rupture source for each of the characterized faults. The WGCEP (2003) approach described above differs from the logic tree characterization used in typical time-independent hazard analyses (Section 3.1). Rupture scenarios in the WGCEP (2003) model are treated as an aleatory variable. The experts were asked to consider the distribution of the rupture scenarios for each fault. Logic trees characterize rupture scenarios as epistemic uncertainty, with each rupture scenario given a weight representing the expert's estimation of how likely it is the actual rupture scenario. The rupture sources and their characteristics are shown in Table 2.

The time-dependent hazard is calculated using the range of earthquake probability models that were considered by WGCEP (2003). WGCEP (2003) considered five probability models that take into account various degrees of physics, date of last rupture, recent seismicity rates, and slip in the 1906 earthquake. One of the models in the suite is

Topical Area: Seismology

the Poisson model, which yields time-independent probabilities. Therefore, the results using the WGCEP (2003) model are not 100% time-dependent. The five probability models (Poisson, Empirical, Brownian Passage Time (BPT), BPT-step, and Time-Predictable) are alternative methods for calculating earthquake probabilities. WGCEP (2003) applied weights to these five models for each of the seven major faults it considered (see Table 3). The five probability models and their weights along with the source characterization were used to compute the rates of characteristic events on each rupture source, which would then be used in the hazard analysis. Rupture probabilities were calculated for 1-year exposure windows using starting dates of 2005, 2055, 2105, and 2205. The following modifications to the WGCEP (2003) inputs were made.

The program for computing the time-predictable probabilities for the San Andreas rupture scenarios was obtained from Dr. William Ellsworth, USGS. The inputs to this program were modified to change the exposure time to 1 year and to compute results for the four starting times. Figures 4 through 7 show the program output plots for each case.

The Empirical Model of Reasenberg et al. (2003) was used to obtain the scale factors to modify the long term rate. WGCEP (2003) used Reasenberg et al. (2003) models A through F and assigned weights of 0.1, 0.5, and 0.4 to the minimum, average, and maximum scale factor, respectively. Using the values for models A through D listed in the WGCEP (2003) Table 5.1 and scaling the linear models E and F from WGCEP (2003) Figure 5.6, the values listed in Table 4 were obtained.

The only modifications made for the Poisson, BPT and BPT-step model inputs were to change the exposure time to 1 year and to compute results for the four starting times.

3.2.1 Inputs to the Hazard Program

The mean, 5th and 95th rates of characteristic events for each rupture source provided from the WGCEP (2003) model were used as input to the hazard code, along with the source geometries, characteristic magnitudes and shape of the magnitude distributions. The hazard code requires the activity rate of all events above the minimum magnitude and the rate of characteristic events. This activity rate is used along with the normalized magnitude probability density function (pdf) to describe the rate of all size magnitudes events on the rupture source. The activity rates were calculated by scaling up the normalized magnitude pdf such that the rate of characteristic events matched the rate provided by the WGCEP (2003) model. This process is illustrated in Figures 8 through 10. Figure 8 shows the magnitude pdf used in the WGCEP (2003) and the hazard code. The characteristic event is defined by a normal distribution truncated at the upper and lower ends at $2 \times \sigma$, where σ is 0.12 magnitude units. A portion of the moment rate of the fault is accounted for with an exponential tail of smaller events, defined by a b-value. WGCEP (2003) used a mean value of 6% of moment rate in the exponential tail, along with branches that used 4% and 8% with lower weights. For simplicity, a single value of 6% of the moment rate was applied to the exponential tail in the hazard analyses.

Figure 9 shows the normalized magnitude pdf used in the hazard code for the Mt. Diablo fault. Note this normalized distribution is actually constructed from a suite of normalized magnitude pdfs, as characteristic magnitude, fault width, and rate of characteristic events are defined as three point distributions. The portion of the rate of events in the characteristic range for the Mt. Diablo fault is 0.56. This factor is used along with the

Topical Area: Seismology

rates of characteristic events to compute the activity rate for all events above the minimum magnitude. The resulting annual recurrence curve for the Mt. Diablo fault is shown on Figure 9 for the case of 100% Poisson. The WGCEP (2003) model was run for the case of 100% Poisson in order to compare the recurrence curves from the hazard code with the 100% Poisson recurrence curves provided by WGCEP (2003). This comparison for the Mt. Diablo fault is shown on Figure 10. The rate of characteristic events and the activity rate used in the hazard program for all rupture sources and years are shown in Table 2.

The cumulative annual recurrence curves (WGCEP [2003] model and hazard code model) for the other major SFR faults are shown on Figures 11 through 16. Note the curves do not match in the region of the exponential tails. This mismatch is due to differences in the construction of the magnitude pdf's. The WGCEP (2003) magnitude pdf's are constructed with two discrete parts, a normal distribution for the characteristic events truncated at ± 2 sigma (0.24 magnitude units), and an exponential tail defined by a b-value and 4 to 8 percent (6% mean) of the total moment. The threshold magnitude is the magnitude at which the exponential tail is truncated at the upper end. Threshold magnitudes are defined for each fault, not rupture source. Each threshold magnitude is defined as 0.24 magnitude units less than the minimum mean characteristic magnitude of all rupture sources of the fault. (See Chapter 4, pages 12-14 of WGCEP [2003] for further details.) For rupture sources with characteristic magnitudes larger than this threshold magnitude plus 0.24, there is a gap in the magnitude pdf. The moment that would be accounted for from these missing magnitudes is put into the tail, causing the exponential tail to be shifted up. In the hazard program we constructed magnitude pdf's for each rupture source with exponential tails that are truncated at 2 sigma below the characteristic magnitude of that source, eliminating any gaps. Figures 17 and 18 illustrate this issue for the San Andreas Fault.

Figure 17 shows the normalized magnitude pdf for the San Andreas Fault; note the length of the exponential tail. Figure 18 shows the individual magnitude pdf's for all rupture sources of the San Andreas. These curves are from the hazard program, so there are no gaps in magnitude. Also shown on Figure 17 is the threshold magnitude used to construct the exponential tail portion for the WGCEP (2003) model. For all sources except the Santa Cruz segment of the San Andreas fault and the floating earthquake, there is a gap in the WGCEP (2003) model.

For this reason, the threshold magnitudes defined by WGCEP (2003) were not maintained for the hazard analysis. The hazard analysis model contains fewer small magnitude events than the WGCEP (2003) (Figure 11). This difference is acceptable because these small magnitude events on the major SFR faults do not contribute to the hazard in the Delta region. In addition, WGCEP (2003) did not compute hazard, rather only rupture probabilities and focused on $M > 6.7$.

4.0 Attenuation Relations

To characterize the attenuation of ground motions in the PSHA, empirical attenuation relationships appropriate for the western U.S., particularly coastal California were used. All relationships provide the attenuation of peak ground acceleration and response spectral acceleration (5% damping).

Topical Area: Seismology

New attenuation relations developed as part of the Next Generation of Attenuation (NGA) Project sponsored by the Pacific Earthquake Engineering Research (PEER) Center Lifelines Program have been released to the public. Two members of the SHTAT, Drs. Silva and Youngs are co-authors of two of the four relationships. These new attenuation relationships have a substantially better scientific basis than current relationships because they are developed through the efforts of five selected attenuation relationship developer teams working in a highly interactive process with other researchers who have: (a) developed an expanded and improved database of strong ground motion recordings and supporting information on the causative earthquakes, the source-to-site travel path characteristics, and the site and structure conditions at ground motion recording stations; (b) conducted research to provide improved understanding of the effects of various parameters and effects on ground motions that are used to constrain attenuation models; and (c) developed improved statistical methods to develop attenuation relationships including uncertainty quantification. Review of the NGA relationships indicate that, in general, ground motions particularly at short-periods (e.g., peak acceleration) are significantly reduced particularly for very large magnitudes ($M \geq 7.5$) compared to current relationships.

At the time of performing the PSHA for input into the risk analysis, only the relationships by Chiou and Youngs, Campbell and Bozorgnia, and Boore and Atkinson are available (see PEER NGA web site) and these were used in the PSHA. The relationships were reviewed and weighted equally in the PSHA. Intra-event and inter-event aleatory uncertainties for each attenuation relationship are required for the risk analysis.

We have attempted to include 3D basin effects in the PSHA through the use of the NGA relationships. However, only one of the NGA models, Campbell and Bozorgnia, addresses basin effects through their use of the basin depth parameter $Z_{2.5}$, depth to a velocity of 2.5 km/sec. The basin depth beneath the Delta ($Z_{2.5}$) was assumed to be 5 km based on Brocher (2005). Quantifying 3D basin effects as recommended by the USGS/CGS would require an extensive research effort well beyond the scope of this study. More importantly, the response of the levees appears to be sensitive to ground motions out to a period of only 1 sec and so longer period motions (> 1 sec) where deep basin effects such as beneath the Delta would be most pronounced are probably not that significant to the Delta levees.

For the CSZ megathrust, the relationships by Youngs et al. (1997), Atkinson and Boore (2003), and Gregor et al. (written communication, 2007) were used with equal weights.

A geologic site condition needs to be defined where the hazard will be calculated. Often this has been parameterized as a generic condition such as rock or soil or more recently the average shear-wave velocity (V_S) in the top 30 m (V_{S30}) of a site. In this analysis, the hazard will be defined for a stiff soil site condition characterized by an average V_{S30} of 1,000 ft/sec (URS/JBA, 2007). The fragility estimates for the levees are referenced to these ground motions. All of the NGA relationships use V_{S30} as an input.

5.0 Time-Dependent PSHA Results

The results of the time-dependent PSHA of the six locations in the Delta are presented in terms of ground motion as a function of annual exceedance probability. This probability

Topical Area: Seismology

is the reciprocal of the average return period. Figures 19 to 24 show the mean, median, 5th, 15th, 85th, and 95th percentile hazard curves for peak horizontal acceleration (PGA) for 2005 at the six sites. The 1.0 sec horizontal spectral acceleration (SA) hazard is shown on Figures 25 to 30. These fractiles indicate the range of epistemic uncertainties about the mean hazard. At a return period of 2,500 years, there is a factor of about two difference between the 5th and 95th percentile values at the Montezuma Slough (Figure 27). The probabilistic PGA and 1.0 sec horizontal SA are listed in Table 5 for return periods of 100, 200, 500, and 2,500 years for the year 2005. At all return periods, the ground motions decrease from west to east due to increasing distance from the San Andreas fault system. At 100 years, the PGA values range from 0.12 g in Sacramento, which is the most eastern site on the edge of the Delta faults to 0.27 g at Montezuma Slough. The latter site is located adjacent to the Pittsburg-Kirby Hills fault.

The contributions of the various seismic sources to the mean PGA hazard in 2005 are shown on Figures 31 to 36. The controlling seismic source varies from site to site but the Southern Midland fault and Northern Midland zone are major contributors to several sites within the Delta at return periods of 100 and 2,500 years. At long-period ground motions, e.g., 1.0 sec SA, and a return period of 100 years, the faults of the San Andreas fault system are major contributors. At 2,500 years, the Southern Midland and the CSZ are contributing significantly to the hazard in 2005 (Figures 37 to 42).

The deaggregated seismic source hazard curves for 2200 are shown for the six sites in Figures 43 to 48 for PGA and Figures 49 to 54 for 1.0 sec SA. The results are similar at PGA but at 1.0 sec SA, the San Andreas fault becomes a major contributor due to its potential to generate 1906-type ruptures. Results for 2050 and 2100 are not shown because they lie between the 2005 and 2100 hazard results.

Figures 55 to 66 illustrate the contributions by events for four return periods when we deaggregate the mean PGA hazard and 1.0 sec horizontal SA hazard by magnitude and distance bins in 2005. At the 500-year return period, the PGA hazard is from moderate to large earthquakes within a distance of 50 km in the M 5.75 to 7.25 range (Figures 55 to 66). For Sacramento and Stockton, the PGA hazard is relatively low and more distant events are contributing. At long period ground motions, > 1.0 sec SA, the contribution from $M \sim 8.0$ San Andreas earthquakes and in particular the CSZ is quite apparent (Figures 61 to 66) (see following discussion).

The largest source of uncertainty in hazard results are usually from the attenuation relationships. Figures 67 to 78 show the sensitivity to choice of crustal attenuation relationships for PGA and 1.0 sec SA in 2005. Each hazard curve shown is calculated using only a single relationship, i.e., assigned a weight of 1.0. At PGA, the relationships give similar results. At 1.0 sec, Campbell and Bozorgnia (PEER website) relationship gives higher hazard because of the effect of the basin parameter. The other two relationships do not parameterize for basin effects. The PGA and 1.0 sec SA values for a 2,500-year return period for the four years are listed in Table 5.

Figure 79 illustrates the sensitivity of the hazard from the CSZ megathrust to the choice of subduction attenuation relationship for 1.0 second SA for Sacramento in 2005. Each hazard curve shown is calculated using only a single relationship, i.e., assigned a weight of 1.0. At 1.0 second SA, Gregor et al. (2006) gives a significantly higher hazard than

Topical Area: Seismology

Youngs et al. (1997) and Atkinson and Boore (2003). In the hazard analysis these relationships are weighted equally. Figure 80 shows the effect on the CSZ and a total mean 1.0 sec SA hazard to the level of truncation of sigma in the attenuation relationships for Sacramento in 2005. The decrease in hazard for longer return periods (greater than 2000 years) indicates that the 1.0 sec SA hazard is controlled largely by high sigma events. In the hazard analysis, sigma was truncated for all crustal and subduction attenuation relationships at three. The use of Gregor et al. (2006) and the large values of sigma defined by all three subduction zone attenuation relationships lead to the CSZ becoming a major contributor to the hazard in Sacramento and Stockton at 1.0 sec for return periods greater than 2000 years.,

Figures 81 to 86 show the time-dependent PGA hazard in 2005, 2050, 2100, and 2200 for the six sites. The results indicate that the hazard is not sensitive to the time-dependent characterization of the major faults considered by the WGCEP (2003) because the hazard is controlled by the nearby Delta faults (Table 5). The 1.0 sec SA shows slightly increasing hazard with increasing years due to the influence of the San Andreas fault (Figures 87 to 92).

5.1 Comparison With Time-Independent Hazard

Figures 93 to 104 show the time-dependent hazard compared to the time-independent (Poissonian) hazard for both PGA and 1.0 sec SA. In general, the hazard is quite similar due to the small influence of the faults with the time-dependent recurrence (e.g., San Andreas, Hayward, etc.). The time-independent is slightly higher for some sites, e.g., Sacramento (Figure 96) due to the influence of the Greenville fault, which gives a higher hazard due to the higher slip rate in the time-independent model, i.e., 4 mm/yr compared to 2 mm/yr in the time-dependent model (WGCEP, 2003).

5.2 Other Sensitivity Analyses

As reflected in the PSHA results (Tables 6a and 6b) and recognized in the USGS/CGS review, the Delta faults are significant contributors to the hazard in the Delta. Given the very large uncertainties in their characterization based on sparse data (Section 3.1.1.1), we have examined their impact on the hazard by carrying out the PSHA with and without the Delta faults. The results are shown in Figures 105 to 110 for PGA. For Clifton Court, Delta Cross Channel, and Sherman Island, the differences are significant at return periods longer than a few hundred years. However, at shorter return periods (e.g., 100 years), which may be the return periods of greatest interest, the difference in hazard is small at all the sites in the Delta (Figures 105 to 110).

In their review of this study, the USGS and CGS also identified several other seismic sources that they believed should be addressed in the PSHA. These sources included faults within the Sierran Foothills, the Sierra Nevada Front fault system, and CRSB zone faults north and south of the Delta. Based on limited sensitivity analyses, none of these seismic sources can generate large enough earthquakes at a significant enough rate that they will contribute to the seismic hazard in the Delta. Two other seismic sources, the Cascadia subduction zone and the 1857 section of the southern San Andreas fault, were included in the PSHA as recommended by the USGS/CGS (see previous discussion).

Topical Area: Seismology

In Figure 111, the historical seismicity recurrence for the San Francisco Bay region (1800-2006) including the Delta is compared with the total recurrence from all seismic sources in the PSHA model including faults and background seismicity. The comparison is good at **M** 5 to 6 but the model recurrence is higher than the historical rate up to **M** 7.5. The curves agree for 1906. Thus our model predicts more moderate sized earthquakes (**M** 6 to 7) than contained in the historical record. This higher model bias is typically observed in PSHA studies due to the incompleteness of the historical seismicity record. The PSHA seismic source model is derived from the longer term paleoseismic record, which captures several seismic cycles of earthquake activity in the San Francisco Bay region in contrast to the short historical record that samples only a portion of the regional seismic cycle. Alternatively, the higher weight given to the characteristic recurrence model in the PSHA would also result in too many moderate-sized events.

5.3 Comparison With USGS National Hazard Maps

In the 2002 version of the USGS National Hazard Maps, which are the basis for the International Building Code, Frankel et al. (2002) have estimated probabilistic ground motions for the U.S. for the exceedance probabilities of 2%, 5%, and 10% in 50 years (return periods of 2500, 1000, and 500 years, respectively). The maps are for a firm rock site condition (NEHRP site class B/C) so a direct comparison with the firm soil results of this study is not possible. The USGS values for a 500-year return period range from about 0.14 g to 0.40 g. The firm soil values in this study range from about 0.20 g to 0.50 g (Table 5). Thus the difference can be attributed to site amplification of the soil versus the USGS firm rock ground motions.

6.0 Ground Shaking Hazard Maps

Based on the PSHA, we have produced ground shaking hazard maps for PGA and 1.0 sec SA for return periods of 100 and 500 years. The same site condition of firm soil was assumed. Exceptions in the PSHA for the maps included (1) the use of an unreleased NGA version of the Abrahamson and Silva attenuation relationship in addition to the three other NGA relationships; (2) an updated version (April 2007) of Boore and Atkinson was also used; (3) the weights for the subduction zone megathrust were revised to: Youngs et al. (1997), 0.5; Atkinson and Boore (2003), 0.25; and Gregor (written communication, 2006), 0.25 based on consultation with Mark Peterson, USGS; and finally (4) the basin factor in Campbell and Bozorgnia was not used because of the significantly different ground motions it provides relative to the other attenuation relationship. The maps are shown on Figures 112 to 115. As expected, the hazard decreases from west to east at these short return periods. An important point is that these maps are for a uniform site condition so site response effects are not apparent on these maps.

7.0 References

Anderson, L.W. and Piety, L.A., 2001, Geologic seismic source characterization of the San Luis-O'Neill area, eastern Diablo Range, California for B.F. Sisk and O'Neill Forebay dams, San Luis Unit, Central Valley Project, California: U.S. Bureau of Reclamation, Seismotectonic Report 2001-2, 76 p.

Topical Area: Seismology

- Angell, M.A., Hanson, K.L., and Crampton, T., 1997, Characterization of Quaternary contractional deformation adjacent to the San Andreas fault, Palo Alto, California: Final Report submitted to the U.S. Geological Survey, National Earthquake Hazards Reduction Program, Award No. 1434-95-G-2586.
- Atwater, B.F., 1982, Geologic maps of the Sacramento-San Joaquin Delta, California: U.S. Geological Survey Miscellaneous Field Studies Map - U.S. Geological Survey: MF-1401, 21 sheets.
- Atkinson, G.M., and Boore, D.M., 2003, Empirical ground-motion relations for subduction zone earthquakes and their applications to Cascadia and other regions: Bulletin of the Seismological Society of America, v. 93, p. 1703-1729.
- Aydin, A., 1982, The East Bay hills, a compressional domain resulting from interaction between the Calaveras and Hayward-Rogers Creek faults, *in* Hart, E.W., Hirschfeld, S.E., and Schulz, S.S. (eds.), Proceedings, Conference on Earthquake Hazards in the Eastern San Francisco Bay Area: California Division of Mines and Geology Special Publication 62, p. 11-21.
- Bieber, D.W., 2002, The Midway fault, a left-lateral fault in a right-lateral world (abs): Association of Engineering Geologists News, v. 45, p. 56, Poster Session, AEG Annual Convention, Reno, Nevada, September 2002.
- Brocher, T.M., 2005, A regional view of urban sedimentary basins in northern California based on oil industry compressional-wave velocity and density logs: Bulletin of the Seismological Society of America, v. 95, p. 2093-2114.
- Bullard, T.F., Hanson, K.L., and Abramson-Ward, H.F., 2004, Quaternary Investigations to Evaluate Seismic Source Characteristics of the Frontal Thrust Belt, Palo Alto region, California: Final Report to U.S. Geological Survey, National Earthquake Hazards Reduction Program, Awards 01HQGR0015 and 01HQCR0016.
- Bürgmann, R., Arrowsmith, R., Dumitru, T., and McLaughlin, R., 1994, Rise and fall of the Southern Santa Cruz Mountains, California, from fission tracks, geomorphology, and geodesy: Journal of Geophysical Research, v. 99, p. 20181-20202.
- California Division of Oil and Gas (CDOG), 1982, Oil and gas fields, Northern California: Volume 3 of Publication TR10, State of California.
- Cao, T., Bryant, W.A., Rowshandel, B., Branum, D., Wills, C.J., 2003, The revised 2002 California probabilistic seismic hazard maps, June 2003: California Geological Survey, http://www.consrv.ca.gov/CGS/rghm/psha/fault_parameters/pdf/2002_CA_Hazard_Maps.pdf.
- Carpenter, D.W., Ramirez, A.L., and Wagoner, J., 1980, Status report on the geology of the Lawrence Livermore Laboratory site and adjacent areas: Lawrence Livermore National Laboratories, UCLR-53065, v. 2.
- Carpenter, D.W., Sweeney, J.J., Kasameyer, P.W., Burkhard, N.R., Knauss, K.G., and Shlemon, R.J., 1984, Geology of the Lawrence Livermore National Laboratory site and adjacent areas: Lawrence Livermore National Laboratory UCRL-53316, 150 p.

Topical Area: Seismology

- CDWR, 1979, Re-evaluation of seismic hazards for Clifton Court Forebay, Bethany Dams and Reservoir, Patterson Reservoir, Del Valle Dam and Lake Del Valle: State of California, Department of Water Resources, Sacramento, CA.
- Cherven, V.B. and Edmondson, W.F. (eds.), 1992, Structural Geology of the Sacramento Basin: Annual Meeting, Pacific Section, Society of Economic Paleontologists and Mineralogists, Volume MP-41.
- Clahan, K.B., Wagner, D., Bezore, S., Saucedo, G., and Gutierrez, C., 2005, New geologic mapping of the northern San Francisco Bay region: Implications and findings for Quaternary faulting: U.S. Geological Survey National Earthquake Research Program, Northern California Earthquake Hazards, Research Summaries, FY2005, 2p.
- Cornell, C. A., 1968, Engineering seismic risk analysis: Bulletin of the Seismological Society of America, v. 58, p. 1583-1606.
- Crane, R.C., 1995a, Geologic map of the Midway 7.5 minute quadrangle.
- Crane, R.C., 1995b, Geologic map of the Brentwood 7.5 minute quadrangle.
- d'Allesio, M.A., Johanson, I.A., Bürgmann, R., Schmidt, D.A., and Murray, M.H., 2005, Slicing up the San Francisco Bay Area: Block kinematics and fault slip rates from GPS-derived surface velocities: Journal of Geophysical Research 110, doi:10.1029/2004JB003496, 19 p.
- dePolo, C. M., 1994, The maximum background earthquake for the Basin and Range Province, western North America: Bulletin of the Seismological Society of America, v. 84, p. 466-472.
- Dibblee, T.W., 1980, A preliminary geologic map of the Livermore Quadrangle, Alameda and Contra Costa counties, California: U.S. Geological Survey Open-File Report 80-533b, scale 1:24,000.
- Dibblee, T.W., Jr., 1981b, A preliminary map of the Mendenhall Springs Quadrangle, Alameda County, California: U.S. Geological Survey Open-File Report 81-235, scale 1:24,000.
- Drexler, J Z, Verosub, K L, Delusina, I, de Fontaine, C S, Lunning, N, Wong, S, 2006, Project REPEAT: Rates and Evolution of Peat Accretion through Time in the Sacramento- San Joaquin Delta, California: Eos Trans. AGU, 87(52), Fall Meet. Suppl., Abstract PP51A-1125.
- Fenton, C.H. and Hitchcock, C.S., 2001, Recent geomorphic and paleoseismic investigations of thrust faults in Santa Clara Valley, California, *in* Ferriz, H., and Anderson, R. (eds.), Engineering Geology Practice in Northern California: California Division of Mines and Geology Bulletin 210, p. 71-89.
- Frankel, A., 1995, Mapping seismic hazard in the central and eastern United States, Seismological Research Letters, v. 66, p. 8-21.
- Frankel, A., Peterson, M., Mueller, C., Haller, K., Wheeler, R., Leyendecker, E., Wesson, R., Harmsen, S., Cramer, C., Perkins, D., and Rukstales, K., 2002, Documentation

Topical Area: Seismology

- for the 2002 update of the national seismic hazard maps: U.S. Geological Survey Open-File Report 02-420, 33 p.
- Galehouse, J.S., 1995, Theodolite measurements of creep rates on San Francisco Bay region faults, U.S. Geological Survey Open-file Report 95-210.
- Graymer, R.W., Bryant, W., McCabe, C.A., Hecker, S., and Prentice, C.S., 2006, Map of Quaternary-active faults in the San Francisco Bay region: U. S. Geological Survey Scientific Investigations Map 2919, one sheet, scale 1:275,000.
- Hanks, T.C. and Bakun, W.H., 2002, A bilinear source-scaling model for M-log A observations of continental earthquakes: Bulletin of the Seismological Society of America, v. 92, p. 1841-1846.
- Hanson, K.L. and Wesling, J.R., 2006, Mapping of the West Napa fault zone for input into the Northern California Quaternary fault database: USGS NEHRP Northern California Earthquake Hazards Research Summaries FY2005: 3rd Annual Northern California Earthquake Hazards Workshop, January 18-19, 2006, Workshop Report, p. 38-39.
- Hanson, K.L. and Wesling, J.R., 2007, Mapping of the West Napa fault zone for input into the Northern California Quaternary fault database: USGS NEHRP Northern California Earthquake Hazards Research Summaries FY2006: 3rd Annual Northern California Earthquake Hazards Workshop, January 18-19, 2007, Workshop Report, 2 p.
- Harland Tait & Associates, 1994, Fault and limited geotechnical investigation North Fairfield Site, Fairfield, California: unpublished report submitted to the City of Fairfield.
- Hart, E.W., 1980, Calaveras and Verona faults (Dublin Quadrangle): California Division of Mines and Geology Fault Evaluation Report FER-108.
- Hart, E.W., 1981a, Las Positas fault, south branch: California Division of Mines and Geology Fault Evaluation Report FER-112.
- Hart, E.W., 1981b, Pleasanton and related faults (Dublin Quadrangle vicinity): California Division of Mines and Geology Fault Evaluation Report FER-109.
- Haugerud, R.A. and Ellen, S.D., 1990, Coseismic ground deformation along the northeast margin of the Santa Cruz Mountains, *in* Schwartz, D.P. and Ponti, D.J. (eds.), Field guide to neotectonics of the San Andreas fault system, Santa Cruz Mountains, in light of the 1989 Loma Prieta earthquake: U.S. Geological Survey Open File Report 90-274, p. 32-38.
- Herd, D.G. and Brabb, E.E., 1980, Faults at the General Electric test reactor site, Vallecitos Nuclear Center, Pleasanton, California: A summary review of their geometry, age of last movement, recurrence, origin, and tectonic setting and the age of the Livermore Gravels: U. S. Geological Survey Administrative Report, 77 p.

Topical Area: Seismology

- Hitchcock, C.S. and Kelson, K.I., 1999, Growth of late Quaternary folds in southwest Santa Clara Valley, San Francisco Bay area, Implications of triggered slip for seismic hazard and earthquake recurrence: *Geology*, v. 27, no. 5, p. 391-394.
- Hyndmann, R.D. and Wang, K., 1993, Thermal constraints on the zone of major thrust earthquake failure: The Cascadia subduction zone: *Journal of Geophysical Research*, v. 98, p. 2039-2060.
- Hyndman, R.D. and Wang, K., 1995, The rupture zone of Cascadia great earthquakes from current deformation and the thermal regime: *Journal of Geophysical Research*, v. 100, p. 22, 133-22, 154.
- Jahns, R.H. and Harding, R.C., 1982, Evaluation of the inferred Verona fault in the Vallecitos Valley, California (abs.), in *Proceedings, Conference on Earthquake Hazards in the Eastern San Francisco Bay Area, California*, E.W. Hart, S.E. Hirschfeld, and S.S. Schulz (eds.): California Division of Mines Geological Special Publication 62, 185 p.
- Jennings, C.W., 1994, Fault activity map of California and adjacent areas: California Department of Conservation, Division of Mines and Geology, Geologic Data Map No. 6, scale 1:750,000.
- Keefer, D.I. and Bodily, S.E., 1983, Three-point approximations for continuous random variables: *Management Science*, v. 26, p. 595-609.
- Kelson, K.I., Baldwin, J.N., and Brankman, C.M., 2003, Late Holocene Displacement of the Central Calaveras Fault, Furtado Ranch Site, Gilroy, CA: Final Technical Report, U.S. Geological Survey, Award 01-HQ-GR00124, p. 1-38.
- Kennedy, D.G., Caskey, J., Hitchcock, C.S., Kelson, K.I., Thompson, S.C., Rubin, R.S., Connelly, S.F., Borchardt, G., Bullard, T.F., Hanson, K.L., AbramsonWard, H., Angell, M.M., and Wesling, J. R., 2005, Seismic Hazard of the Front Range Thrust Faults, Santa Cruz Mountains, Field trip guidebook and volume prepared for the Joint Meeting of the Cordilleran Section, GSA and Pacific Section, AAPG, April 29-May 1, 2005, San Jose, California.
- Krug, E.H., Cherven, V.B., Hatten, C.W., and Roth, J.C., 1992, Subsurface structure in the Montezuma Hills, southwestern Sacramento basin, *in* Cherven, V.B., and Edmondson, W.F. (eds.), *Structural Geology of the Sacramento Basin: Volume MP-41, Annual Meeting, Pacific Section, Society of Economic Paleontologists and Mineralogists*, p. 41-60.
- McGuire, R.K., 2004, Seismic hazard and risk analysis: EERI Monograph MNO-10, Earthquake Engineering Research Institute.
- O'Connell, D.R.H., Unruh, J.R. and Block, L.V., 2001, Source characterization and ground-motion modeling of the 1892 Vacaville-Winters earthquake sequence, California: *Bulletin of the Seismological Society of America*, v. 91, p. 1,471-1,497.
- Prescott, W.H. and Burford, R.O., 1976, Slip on the Sargent fault: *Seismological Society of America Bulletin*, v. 66, p. 1013-1016.

Topical Area: Seismology

- Prescott, W.H., Savage, J.C., Svarc, J.L., and Manaker, D., 2001, Deformation across the Pacific-North American plate boundary near San Francisco, California: *Journal of Geophysical Research*, v. 106, p. 6673-6682.
- Reasenber, P.A., Hanks, T.C., and Bakun, W.H., 2003, An empirical model for earthquake probabilities in the San Francisco Bay region, California, 2002-3031: v. to be submitted.
- Rogers, T.H., 1966, San Jose sheet, geologic map of California: California Division of Mines and Geology 2° sheet, 1:250,000 scale.
- Ruff, L. and Kanamori, H., 1983, Seismic coupling and uncoupling at subduction zones: *Tectonophysics*, v. 99, p. 99-117.
- Savy, J.B. and Foxall, W., 2002, Lawrence Livermore National Laboratory site seismic safety program: Summary of findings: UCRL-LR-53674 Rev. 2.
- Sawyer, T.L. and Unruh, J.R., 2002a, Paleoseismic investigation of the Holocene slip rate on the Greenville fault, eastern San Francisco Bay area, California: final technical report submitted to the U.S. Geological Survey, Award No. 00HQGR005.
- Sawyer, T.L. and Unruh, J.R., 2002b, Holocene slip rate constraints for the northern Greenville fault, eastern San Francisco Bay area, California: implications for the Mt. Diablo restraining stepover model: *EOS (Transactions, American Geophysical Union)*, v.83, Fall Meeting supplement, p. F1300
- Schlemon, R. J., and E. L. Begg. 1973, Late Quaternary evolution of the Sacramento-San Joaquin Delta, California: *Proc. Ninth Congress of the International Union for Quaternary Research 1973*:259-266.
- Senior Seismic Hazard Analysis Committee (SSHAC), 1997, Recommendations for probabilistic seismic hazard analysis-guidance on uncertainty and use of experts: U.S. Nuclear Regulatory Commission NUREG/CR-6327, variously paginated.
- Sims, J.D., Fox, K.F., Jr., Bartow, J.A., and Helley, E.J., 1973, Preliminary geologic map of Solano County and parts of Napa, Contra Costa, Marin, and Yolo counties, California: U.S. Geological Survey Miscellaneous Field Investigations Map MF-484, 5 shts.
- Sowers, J.M., Noller, J.S., and Unruh, J.R., 1992, Quaternary deformation and blind-thrust faulting on the east flank of the Diablo Range near Tracy, California, *in* Borchardt, Glenn, and others (eds.), *Proceedings of the Second Conference on Earthquake Hazards in the Eastern San Francisco Bay Area*: California Department of Conservation, Division of Mines and Geology Special Publication 113, p. 377-383.
- Sterling, R., 1992, Intersection of the Stockton and Vernalis faults, southern Sacramento Valley, California, *in* Chervon, V.B., and Edmondson, W.F. (eds.), *Structural Geology of the Sacramento Basin*: American Association of Petroleum Geologists Miscellaneous Publication 41, Pacific Section, p. 143-151.
- Thrust Fault Subgroup 1999, Report to the Working Group on Northern California Earthquake Probabilities, 15 p. plus tables.

Topical Area: Seismology

- Unruh, J.R. and Hector, S.T., 1999, Subsurface characterization of the Potrero-Ryer Island thrust system, western Sacramento-San Joaquin Delta, northern California, William Lettis and Associates, Inc., Final Technical Report, U.S. Geological Survey, National Earthquake hazards Reduction Program Award No. 1434-HQ-96-GR-02724, 32 p.
- Unruh, J.R. and Kelson, K.I., 2002, Critical evaluation of the northern termination of the Calaveras fault, eastern San Francisco Bay area, California, U.S. Geological Survey National Earthquake Hazard Reduction Program: Final Technical Report Award No. 00-HQ-GR-0082, 77 p.
- Unruh, J.R., and Sawyer, T.L., 1997, Assessment of blind seismogenic sources, Livermore Valley, eastern San Francisco Bay region: Final Technical Report, USGS NEHRP Award 1434-95-G-2611, 95 p.
- URS/JBA (URS Corporation/Jack R. Benjamin & Associates, Inc.), 2007, Delta Risk Management Strategy, Phase 2: Risk Analysis Technical Memorandum.
- Wagner, D.L., Jennings, C.W., Bedrossian, T.L., and Bortugno, E.J., 1981, Geologic map of the Sacramento Quadrangle: California Division of Mines and Geology Regional Geologic Map Series, 1:250,000 scale.
- Wagner, D.L., Bortugno, E.J., and McJunkin, R.D., 1991, Geologic map of the San Francisco-San Jose quadrangle: California Division of Mines and Geology, Regional Geologic Map Series, 1:250,000 scale.
- Wang, K., Wells, R., Mazzotti, S., Hyndman, R.D., Sagiya, T., 2003, A revised dislocation model of the Cascadia subduction zone: *Journal of Geophysical Research*, v. 108, p. ETG 9-1 – 9-13.
- Weber-Band, J., 1998, Neotectonics of the Sacramento-San Joaquin Delta area, east-central Coast Ranges, California: unpublished Ph.D., University of California, Berkeley, 216 p.
- Wells, D.L. and Coppersmith, K.J., 1994, New empirical relationships among magnitude, rupture length, rupture width, rupture area, and surface displacement: *Bulletin of the Seismological Society of America*, v. 84, p. 974-1002.
- Wong, I.G., Ely, R.W., and Kollman, A.C., 1988, Contemporary seismicity and tectonics of the northern and central Coast Ranges-Sierran block boundary zone, California: *Journal of Geophysical Research*, v. 93, p. 7813-7833.
- Wong, I. and Dober, M., 2007, Screening/scoping level probabilistic seismic hazard analysis for Buckhorn Dam, California, unpublished report prepared for U.S. Bureau of Reclamation by URS Corporation.
- Working Group for California Earthquake Probabilities (WGCEP), 2003, Earthquake probabilities in the San Francisco Bay area: 2002-2031: U.S. Geological Survey Open-File Report 03-214.
- Working Group on Northern California Earthquake Potential (WGNCEP), 1996, Database of potential sources for earthquakes larger than magnitude 6 in northern California: U.S. Geological Survey Open-File Report 96-705, 53 p.

Topical Area: Seismology

Youngs, R.R., Chiou, S.-J, Silva, W.J., and Humphrey, J.R., 1997, Strong ground motion attenuation relationships for subduction zone earthquakes, *Seismological Research Letters*, v. 68, p. 58-73.

Youngs, R.R, Coppersmith, K.J., Taylor, C.L., Power, M.S., Di Silvestro, L.A., Angell, M.L., Hall, N.T., Wesling, J.R., and Mualchin, L., 1992, A comprehensive seismic hazard model for the San Francisco Bay Region, *in* Proceedings of the Second Conference on Earthquake Hazards in the Eastern San Francisco Bay Area, Borchardt, G., Hirschfeld, S.E., Lienkaemper, J.J., McClellan, P., Williams, P.L. and Wong, I.G. (eds.), California Division of Mines and Geology Special Publication 113, p. 431-441.

Tables

Table 1. Bay Area Time-Independent Seismic Source Parameters

Fault Name	Probability of Activity ¹	Rupture Scenario ²	Segment Name	Rupture Length ³	Width ⁴	Dip ⁵	Direction of Dip ⁶	Sense of Slip ⁷	Magnitude ⁸	Slip Rate ⁹	Notes
San Andreas (Northern and Central)	1.0	Unsegmented (0.5)	1906	473	13 ± 3	90	N/A	SS	7.9	24 ± 3	Characterization based on WGCEP (2003). Unsegmented rupture scenario is a repeat of the 1906 M 7.9 San Francisco earthquake.
		Two Segments (0.2)	Offshore + North Coast	326	11 ± 2	90	N/A	SS	7.7	24 ± 3	
			Peninsula + Santa Cruz Mountains	147	13 ± 2	90	N/A	SS	7.4	17 ± 4	
		Three Segments (0.1)	Offshore + North Coast	326	11 ± 2	90	N/A	SS	7.7	24 ± 3	
			Peninsula	85	13 ± 2	90	N/A	SS	7.2	17 ± 4	
			Santa Cruz Mountains	62	15 ± 2	90	N/A	SS	7.0	17 ± 4	
		Floating Earthquake (0.2)	N/A	N/A	13 ± 3	90	N/A	SS	6.9	24 ± 3	
Calaveras	1.0	Unsegmented (0.05)	Northern + Central + Southern Calaveras	123	11 ± 2	90	N/A	SS	6.9	4 (0.2) 6 (0.4) 15 (0.3) 20 (0.1)	Characterization of WGCEP (2003) modified by recent paleoseismic data of Kelson (written communication, 2006).
		Two Segments (0.05)	Northern Calaveras	45	13 ± 2	90	N/A	SS	6.8	6 ± 2	
			South + Central Calaveras	78	11 ± 2	90	N/A	SS	6.4	15 ± 3	
		Three Segments (0.3)	Northern Calaveras	45	13 ± 2	90	N/A	SS	6.8	6 ± 2	
			Central Calaveras	59	11 ± 2	90	N/A	SS	6.2	15 ± 3	
			Southern Calaveras	19	11 ± 2	90	N/A	SS	5.8	15 ± 3	
		Segment + Floating Earthquake (0.5)	Northern Calaveras	45	13 ± 2	90	N/A	SS	6.8	6 ± 2	
			Floating Earthquake on Central + South Calaveras	N/A	11 ± 2	90	N/A	SS	6.2	15 ± 3	
		Floating Earthquake (0.1)	N/A	N/A	11 ± 2	90	N/A	SS	6.2	4 (0.2) 6 (0.4) 15 (0.3) 20 (0.1)	
		Concord – Green Valley	1.0	Unsegmented (0.35)	N/A	56	14 ± 2	90	N/A	SS	
Three Segments (0.1)	Concord			20	16 ± 2	90	N/A	SS	6.25	4 ± 2	
	Southern Green Valley			22	14 ± 2	90	N/A	SS	6.25	5 ± 3	
	Northern Green Valley			14	14 ± 2	90	N/A	SS	6.0	5 ± 3	
Two Segments (0.15)	Concord			20	16 ± 2	90	N/A	SS	6.25	4 ± 2	
	Green Valley			36	14 ± 2	90	N/A	SS	6.5	5 ± 3	
Two Segments (0.15)	Concord + Southern Green Valley			42	14 ± 2	90	N/A	SS	6.6	5 ± 3	
	Northern Green Valley			14	14 ± 2	90	N/A	SS	6.0	5 ± 3	
Floating Earthquake (0.25)	N/A	N/A	14 ± 2	90	N/A	SS	6.2	5 ± 3			

Table 1. Bay Area Time-Independent Seismic Source Parameters

Fault Name	Probability of Activity ¹	Rupture Scenario ²	Segment Name	Rupture Length ³	Width ⁴	Dip ⁵	Direction of Dip ⁶	Sense of Slip ⁷	Magnitude ⁸	Slip Rate ⁹	Notes
Greenville	1.0	Unsegmented (0.4)	N/A	58	15 ± 3	90	N/A	SS	6.9	2 (0.2) 4 (0.6) 6 (0.2)	Sawyer and Unruh (2002a) conducted a paleoseismic investigation to evaluate the Holocene slip rate of the dextral Greenville fault at a site near Laughlin Road in northeastern Livermore Valley. Two channel-fill units and a large paleo-channel exposed in fault-parallel trenches were right-laterally offset 17 to 25 m along the Greenville fault. Initial age constraints for these offset features based on 6 AMS radiocarbon dates on pedogenic calcium carbonate suggested a limiting minimum age range of 4.1 to 8.5 ka. Based on these data, Sawyer and Unruh (2002a, 2002b) developed a preliminary estimate of 4.1 ± 1.8 mm/yr for the Holocene right-lateral slip rate on Greenville fault. Subsequent exposure dating of the faulted channel-fill deposits in 2004-2005 by Glen Berger of the Desert Research Institute confirmed their mid-Holocene age (G. Berger, written communication, 2005), which supports the 4.1 ± 1.8 mm/yr slip rate estimate reported in Sawyer and Unruh (2002a, 2002b).
		Floating (0.6)	N/A	N/A	15 ± 3	90	N/A	SS	6.5	2 (0.2) 4 (0.6) 6 (0.2)	
Hayward – Rodgers Creek	1.0	Unsegmented (0.05)	Hayward + Rodgers Creek	151	12 ± 2	90	N/A	SS	7.3	9 ± 2	Characterization based on WGCEP (2003) model.
		Two Segment (A) (0.1)	North Hayward + Rodgers Creek	98	12 ± 2	90	N/A	SS	7.1	9 ± 2	
			Southern Hayward	53	12 ± 2	90	N/A	SS	6.7	9 ± 2	
		Two Segment (B) (0.3)	Rodgers Creek	63	12 ± 2	90	N/A	SS	7.0	9 ± 2	
			Hayward	88	12 ± 2	90	N/A	SS	6.9	9 ± 2	
		Three Segment (0.5)	Rodgers Creek	63	12 ± 2	90	N/A	SS	7.0	9 ± 2	
			North Hayward	35	12 ± 2	90	N/A	SS	6.5	9 ± 2	
Floating Earthquake (0.05)	N/A	N/A	12 ± 2	90	N/A	SS	6.9	9 ± 2			
Mt Diablo	1.0	Unsegmented (0.5)	N/A	31	17 ± 2	30 (0.2) 45 (0.6) 50 (0.2)	NE	R	6.7	1 (0.2) 3 (0.6) 5 (0.2)	Characterization from Unruh (2006). Fault tip inferred to approach within 5 km (0.5) to 1 km (0.5) of the surface based on restorable cross section, and on map-scale relationships between surface faults and fold axis.
		Segmented (0.5)	Mt. Diablo North	12	17 ± 2	30 (0.2) 45 (0.6) 50 (0.2)	NE	R	6.3	1 (0.2) 3 (0.6) 5 (0.2)	North: Fault tip inferred to approach within 4 km (0.5) to 2 km (0.5) of the surface based on model in restorable cross section.
			Mt. Diablo South	19	17 ± 2	30 (0.2) 45 (0.6) 50 (0.2)	NE	R	6.6	1 (0.2) 3 (0.6) 5 (0.2)	South: Fault tip inferred to approach within 5 km (0.5) to 1 km (0.5) of the surface based on model in restorable cross section, and map-scale relationships between surface faults and fold axis.
San Gregorio	1.0	Unsegmented (0.35)	Northern + Southern San Gregorio	176	13 ± 2	90	N/A	SS	7.5	1 (0.1) 3 (0.4) 7 (0.4) 10 (0.1)	Characterization based on WGCEP (2003) model.
		Segmented (0.35)	Northern San Gregorio	110	13 ± 2	90	N/A	SS	7.2	7 ± 3	
			Southern San Gregorio	66	12 ± 2	90	N/A	SS	7.0	3 ± 2	

Table 1. Bay Area Time-Independent Seismic Source Parameters

Fault Name	Probability of Activity ¹	Rupture Scenario ²	Segment Name	Rupture Length ³	Width ⁴	Dip ⁵	Direction of Dip ⁶	Sense of Slip ⁷	Magnitude ⁸	Slip Rate ⁹	Notes
		Floating Earthquake (0.3)	N/A	N/A	13 ± 2	90	N/A	SS	6.9	1 (0.1) 3 (0.4) 7 (0.4) 10 (0.1)	
Briones (zone)	1.0	N/A	N/A	23	15 ± 3	90	N/A	SS	6.5	0.5 (0.2) 1.0 (0.6) 2.0 (0.2)	<p>A geomorphically well-defined fault in the Briones source zone is parallel to and spatially associated with the NNW-trending alignment of epicenters in the Briones earthquake swarm (Unruh and Kelson, 2002). We interpret both the seismicity and the association of a mapped fault with seismicity as evidence for Holocene activity of the Briones zone. Unruh and Kelson (2002) describe tectonic-geomorphic evidence for late Quaternary activity on other faults within the Briones source zone.</p> <p>The slip rate was estimated from dextral offset of late Cenozoic structures and stratigraphic units across faults in the northern East Bay hills. Based on offset stratigraphic contacts in the northern East Bay Hills, Unruh and Kelson (2002) estimated about 5 km of post-late Neogene dextral slip on the Lafayette-Reliez Valley fault zone, which implies a long-term average slip rate of ≥ 1 mm/yr over the past 5 Ma. The upper end in the range in slip rates adopted for this study (3.0 mm/yr) encompasses the possibility that the Briones zone comprises a system of faults that transfers slip to the West Napa fault (maximum slip rate = 3.0 mm/yr).</p>
Collayomi	1.0	Unsegmented (1.0)	N/A	29	10	90	N/A	SS	6.5	0.6 ± 0.3	Cao <i>et al.</i> (2003)
Cordelia	1.0	Unsegmented (1.0)	N/A	19	15 ± 3	90	N/A	SS	6.6	0.05 (0.4) 0.6 (0.5) 1.0 (0.1)	Characterization based on paleoseismic data from Harlan Tait & Associates (1994).
CRSB North of Delta	1.0	Multisegment (0.1)	Mysterious Ridge	35	13 ± 2	25 ± 5	W	R	6.7	1.0 (0.7) 3.5 (0.3)	Characterization revised from Working Group on California Earthquake Potential (1996) using data from O'Connell <i>et al.</i> (2001). Fault tip of Mysterious Ridge, Trout Creek, and Gordon Valley at depths of 7, 9, and 8 km, respectively. Segment lengths have an uncertainty of ± 5 km.
			Trout Creek + Gordon Valley	38	13 ± 2	25 ± 10	W	R	6.8	0.5 (0.3) 1.25 (0.6) 2.0 (0.1)	
		Segmented (0.9)	Mysterious Ridge	35	13 ± 2	25 ± 5	W	R	6.7	1.0 (0.7) 3.5 (0.3)	
			Trout Creek	20	13 ± 2	20 ± 5	W	R	6.5	0.5 (0.3) 1.25 (0.6) 2.0 (0.1)	
			Gordon Valley	18	13 ± 2	30 ± 5	W	R	6.4	0.5 (0.3) 1.25 (0.6) 2.0 (0.1)	
Cull Canyon-Lafayette-Reliz Valley	1.0	Unsegmented (1.0)	N/A	25	12 ± 3	90°	N/A	SS	6.6	0.5 (0.2) 1.0 (0.6) 3.0 (0.2)	Characterization from Unruh and Kelson (2002) and Unruh (2006).

Table 1. Bay Area Time-Independent Seismic Source Parameters

Fault Name	Probability of Activity ¹	Rupture Scenario ²	Segment Name	Rupture Length ³	Width ⁴	Dip ⁵	Direction of Dip ⁶	Sense of Slip ⁷	Magnitude ⁸	Slip Rate ⁹	Notes
Foothill Thrust System	0.6	Floating Earthquake (1.0)	N/A	N/A	15 ± 3	60	SW	R	6.25 (0.3) 6.5 (0.3) 6.75 (0.3) 7.0 (0.1)	0.2 (0.2) 0.5 (0.6) 0.8 (0.2)	Simplified characterization based on WGCEP (2003) subgroup and recent studies as summarized in Kennedy <i>et al.</i> (2005).. Incorporates Berrocal, Shannon-MonteVista, Stanford, and Cascade faults. Although there is clear evidence of Holocene and latest Pleistocene fold deformation along this fault zone (Hitchcock and Kelson, 1999; Bullard <i>et al.</i> , 2004), the fault is assigned a Probability of Activity of 0.6 to address the uncertainty as to whether the fault is an independent seismic source capable of generating moderate to large magnitude earthquakes. The seismogenic potential of the range front thrust faults is not well known. Aseismic slip (Bürgmann <i>et al.</i> , 1994) and coseismic slip during large magnitude events on the San Andreas fault system fault, such as occurred during the 1989 Loma Prieta earthquake (Haugerud and Ellen, 1990) may account for some or all of the local San Andreas fault-normal contraction, precluding the need for independent large magnitude events on the compressive structures. (Angell <i>et al.</i> , 1997; Hitchcock and Kelson, 1999).
Hunting Creek-Berryessa	1.0	Unsegmented (1.0)	N/A	60	12	90	N/A	SS	6.9	6 ± 3	Cao <i>et al.</i> (2003)
Las Trampas	0.5	Unsegmented	N/A	12	14 ± 3	45° 60° 75°	SW	R	6.2	0.5 (0.2) 1.0 (0.6) 3.0 (0.2)	Characterization from Unruh and Kelson (2002) and Unruh (personal communication, 2006).
Los Medanos Fold and Thrust Belt	1.0	Unsegmented (0.2)	N/A	15	17 ± 2	30 (0.2) 45 (0.2) 60 (0.6)	NE	R	6.5	0.3 (0.3) 0.5 (0.4) 0.7 (0.3)	Characterization based on Unruh and Hector (1999) and the Thrust Fault Subgroup of the 1999 Working Group. Roe thrust: fault tip inferred to lie between 0 km and 1 km depth based on analysis of gas well data.
		Segmented (0.8)	Roe Island	5	5 ± 2	30 (0.2) 45 (0.2) 60 (0.6)	NE	R	5.8	0.3 (0.3) 0.5 (0.4) 0.7 (0.3)	Roe thrust: fault tip inferred to lie between 0 km and 1 km depth based on analysis of gas well data.
			Los Medanos	10	10 ± 2	30 (0.2) 45 (0.6) 60 (0.2)	NE	R	6.0	0.3 (0.3) 0.5 (0.4) 0.7 (0.3)	Los Medanos thrust: fault tip inferred to lie between 1 km and 2 km depth based on analysis of gas well data and construction of geologic cross sections.
Maacama-Garberville	1.0	Unsegmented (1.0)	N/A	182	12	90	N/A	SS	7.4	9.0 ± 2.0	Cao <i>et al.</i> (2003)
Midway/ Black Butte	1.0	Floating Earthquake (1.0)	N/A	31	15 ± 3	70 ± 10	W	RO	6.25 (0.2) 6.5 (0.4) 6.75 (0.4)	0.1 (0.3) 0.5 (0.4) 1.0 (0.3)	The Black Butte fault is a documented late Quaternary-active reverse (oblique?) fault (Sowers <i>et al.</i> , 1992) that appears to be related to the late Cenozoic dextral Midway fault by a short left-restraining bend. Limited data are available on slip rate and rupture behavior. The slip rate estimate is based on uplift of middle to early Pleistocene pediment surface across the Black Butte fault (Sowers <i>et al.</i> , 1992) and an inferred H:V ratio for the components of slip of ≤ 3:1.
Monterey Bay-Tularcitos	1.0	Unsegmented (1.0)	N/A	84	14	90	N/A	SS	7.1	0.5 ± 0.4	Cao <i>et al.</i> (2003)

Table 1. Bay Area Time-Independent Seismic Source Parameters

Fault Name	Probability of Activity ¹	Rupture Scenario ²	Segment Name	Rupture Length ³	Width ⁴	Dip ⁵	Direction of Dip ⁶	Sense of Slip ⁷	Magnitude ⁸	Slip Rate ⁹	Notes
Montezuma Hills (zone)	0.5	Floating Earthquake (1.0)	N/A	N/A	15 ± 5	70	W	RO	6.0 (0.3) 6.25 (0.4) 6.5 (0.3)	0.05 (0.3) 0.25 (0.4) 0.5 (0.3)	The Montezuma Hills source zone is considered as a possible independent source of seismicity based on the following: 1) the topographic and structural gradient of the hills is to the northeast, which is contrary to what would be expected if the hills were being uplifted in the hanging wall of the Midland fault; 2) the topography dies out west of the subsurface trace of the Midland fault, rather than extending up to the fault; 3) the Montezuma hills are spatially associated with the Antioch and Sherman Island faults, as well as some anomalous topography near the town of Oakley south of the Sacramento River. Alternatively, the uplift of this region is secondary tectonic deformation related to movement in the hanging wall of the Midland fault or transfer of slip from the Vernalis/West Tracy faults to the Pittsburg/Kirby Hills fault zone. Preferred orientation of modeled fault planes within zone (N20°W).
Mt Oso	0.7	Unsegmented (1.0)	N/A	25	15 ± 2	30 (0.3) 45 (0.4) 60 (0.3)	NE	R	6.9	0.5 (0.2) 1.5 (0.6) 2.5 (0.2)	Inferred thrust fault occupying the contractional stepover between the Ortigalita and Greenville faults. NE-dipping rupture geometry inferred from the SW-vergence of the Mt. Oso anticline and analogy to Mt. Diablo thrust (J. Unruh, Wm. Lettis and Associates, <i>Pers. Comm.</i> , 2006). Fault tip at 5 km depth. The estimate of slip rate is based entirely on the assumption that dextral slip on the Ortigalita fault steps west (left) across Mt. Oso anticline to the southern Greenville fault, i.e., the slip rate on the inferred Mt. Oso thrust fault is a function of the slip rate on the Ortigalita fault. To date, the only observations that support Quaternary activity of the Mt. Oso fault are geomorphic relations documented by Hart (1981) and Unruh and Sawyer (1998) that tectonic-geomorphic expression of the Greenville fault increases significantly north of the western end of the Mt. Oso anticline.
Northern Midland (zone)	1.0	Floating Earthquake (1.0)	N/A	N/A	15 ± 5	70	W	RO	6.0 (0.3) 6.25 (0.4) 6.5 (0.3)	0.1 (0.3) 0.5 (0.4) 1.0 (0.3)	Preferred orientation of modeled fault planes within zone (N30°W). North of Rio Vista, published data from gas exploration indicate that the Midland fault breaks into a zone of right-stepping en echelon fault traces. Anomalous, apparently uplifted Quaternary topography that appears to be associated with the stepover regions may be related to recent movement on a system of underlying oblique reverse faults in this zone. Tips of faults are inferred by CDOG (1982) to extend above the base of the Tertiary Markley Formation to depths of about 1.5 km, and possibly shallower. Minimum fault depth not constrained by data in CDOG (1982).

Table 1. Bay Area Time-Independent Seismic Source Parameters

Fault Name	Probability of Activity ¹	Rupture Scenario ²	Segment Name	Rupture Length ³	Width ⁴	Dip ⁵	Direction of Dip ⁶	Sense of Slip ⁷	Magnitude ⁸	Slip Rate ⁹	Notes
Orestimba	1.0	Unsegmented (1.0)	N/A	60	Tip 1 (0.5) 3 (0.5) Base 15 ± 3	30° (0.2) 45° (0.6) 60° (0.2)	W	R	6.7	0.2 (0.2) 0.4 (0.6) 0.6 (0.2)	Characterization based on Anderson and Piety (2001). Segment of Coast Range/Sierran block boundary(CRSB) (also referred to as the Coast Range/Central Valley fault system.). Anderson and Piety (2001) assign steeper dips (20 to 30°) to the Orestimba fault than considered in the CGS source model (Cao <i>et al.</i> , 2003). The Thrust Subgroup of the 1999 Working Group, that provided input to WGCEP (2003), suggested a range of dip between 25° (similar to the Coalinga thrust fault) and 60° (predicted by Coulomb failure criteria).The steepness of the range along these segments from between approximately 36.5°N to 38°N suggests that the dip of the underlying structures is probably at the higher end of this range. Anderson and Piety (2001) provide estimates for the uplift rate along several segments based on the elevation of uplifted early (?) to middle Pleistocene pediment surfaces and late Pleistocene fluvial terraces (Sowars <i>et al.</i> , 1992). These uplift rates are converted into slip rates using the range of fault dips assigned to each segment.
Ortigalita	1.0	Segmented (0.3)	Northern Ortigalita	40	15 ± 3	90	N/A	SS	6.9	0.5 (0.15) 1.0 (0.35) 2.0 (0.35) 2.5 (0.15)	Characterization revised from Cao <i>et al.</i> (2003) using recent mapping and paleoseismic data from Anderson and Piety (2001) to modify the lengths and slip rates for the north and south segments of the fault. They estimate a slip rate of 1.0-2.0 mm/yr for the northern section based on abundant geomorphic evidence for probable latest Pleistocene and Holocene displacement and, paleoseismic trench investigations that indicate that Quaternary deposits estimated to be between 10 ka and 25 ka, are right laterally offset between about 13 and 25 m by the Cottonwood Arm segment of the Ortigalita fault. They note the southern segment appears much less active and accordingly, they assign a lower slip rate of 0.2 to 1.0 mm/yr to this segment.
			Southern Ortigalita	60	15 ± 3	90	N/A	SS	7.1	0.2 (0.2) 0.6 (0.6) 1.0 (0.2)	
		Segmented + Floating Earthquake (0.7)	Northern Ortigalita	40	15 ± 3	90	N/A	SS	6.9	0.5 (0.15) 1.0 (0.35) 2.0 (0.35) 2.5 (0.15)	
			Floating Earthquake on Southern Ortigalita	60	15 ± 3	90	N/A	SS	6.6	0.2 (0.2) 0.6 (0.6) 1.0 (0.2)	
Pittsburgh-Kirby Hills	1.0	Unsegmented (0.4)	N/A	24	20 ± 5	80 ± 10	E	SS	6.7	0.3 (0.4) 0.5 (0.4) 0.7 (0.2)	Characterization from the Thrust Fault Subgroup of the 1999 Working Group.
		Floating Earthquake (0.6)	N/A	N/A	20 ± 5	80 ± 10	E	SS	6.3	0.3 (0.4) 0.5 (0.4) 0.7 (0.2)	
Potrero Hills	0.7	Unsegmented (1.0)	N/A	9	9 ± 2	40 ± 10	SW	R	5.75 (0.3) 6.0 (0.6) 6.25 (0.1)	0.1 (0.2) 0.3 (0.6) 0.6 (0.2)	Characterization based on Unruh and Hector (1999). Fault tip inferred to lie between 0 km and 1 km depth based on analysis of gas well data and construction of geologic cross sections. The fault is assigned a Probability of Activity of (0.7) based on geomorphic and physiographic evidence that slip is being transferred from the active Pittsburgh Kirby Hills fault to Wragg Canyon and Hunting Creek-Berryessa fault zones to the north via the Potrero Hills fault.
Pt. Reyes	0.8	Unsegmented (1.0)	N/A	47	12 ± 3	40 (0.2) 50 (0.6) 60 (0.2)	NE	R	7.0	0.05 (0.2) 0.3 (0.6) 0.5 (0.2)	Cao <i>et al.</i> (2003)

Table 1. Bay Area Time-Independent Seismic Source Parameters

Fault Name	Probability of Activity ¹	Rupture Scenario ²	Segment Name	Rupture Length ³	Width ⁴	Dip ⁵	Direction of Dip ⁶	Sense of Slip ⁷	Magnitude ⁸	Slip Rate ⁹	Notes
Quien Sabe	1.0	Unsegmented (1.0)	N/A	23	10	90	N/A	SS	6.4	0.1 (0.2) 1.0 (0.6) 2.0 (0.2)	Cao <i>et al.</i> (2003)
San Andreas (Southern)	1.0	Unsegmented (1.0)	N/A	312	12 ± 2	90	N/A	SS	7.8	28 (0.2) 33 (0.6) 38 (0.2)	Characterization from URS.
Sargent	0.8	Unsegmented (1.0)	Sargent	52	15 ± 3	80 ± 10	SW	RO	6.9	1.5 (0.3) 3.0 (0.4) 4.5 (0.3)	Characterization based on WGNCEP (1996). Geodetic measurements indicative of right slip across the southern Sargent fault (Prescott and Burford, 1976), evidence for creep of about 3-4 mm/yr, as well as associated historical microseismicity suggest that the Sargent fault is an independent seismic source. The Sargent fault experienced triggered slip during the 1989 M _w 6.9 Loma Prieta earthquake (Aydin, 1982). A Probability of Activity of less than 1.0 (0.9) considers that fault slip may occur coseismically as creep or during large magnitude events on the San Andreas fault.
Southeast Extension of Hayward (zone)	1.0	Unsegmented (1.0)	N/A	26	10	90	N/A	SS/RO	6.4	1.0 (0.2) 3.0 (0.6) 5.0 (0.2)	Characterization based on WGNCEP (1996), Graymer <i>et al.</i> (2006), and Fenton and Hitchcock (2001).
Southern Midland	0.8	Unsegmented (1.0)	N/A	26	15 ± 5	70	W	RO	6.6	0.1 (0.3) 0.5 (0.4) 1.0 (0.3)	Activity and rate is inferred from displacement of late Tertiary (and possibly early Pleistocene) strata in seismic reflection profiles (Weber-Band, 1998) and apparent displacement of basal peat (Holocene) inferred from analysis of Atwater (1982) data (this study). Tip of fault is inferred by CDOG (1982) to extend above the base of the Tertiary Markley Formation to depths of about 1.5 km, and possibly shallower. Minimum fault depth not constrained by data in CDOG (1982).
Thornton Arch (zone)	0.2	Floating Earthquake (1.0)	N/A	N/A	15 ± 5	70	S (E-W strike)	RO	6.0 (0.3) 6.25 (0.4) 6.5 (0.3)	0.05 (0.3) 0.10 (0.4) 0.15 (0.3)	Possible localization of Quaternary uplift suggesting the presence of active blind fault(s) is inferred based on the deflection of the Mokelumne River north around an arch mapped in the subsurface from oil and gas exploration data (California Division of Oil and Gas, 1982). EW strike - based on the orientation of the mapped arch.
Vernalis	0.8	Floating Earthquake (1.0)	N/A	46	15 ± 3	70 ± 10	W	RO	6.25 (0.2) 6.5 (0.4) 6.75 (0.4)	0.07 (0.3) 0.25 (0.4) 0.5 (0.3)	Quaternary activity of the Vernalis fault is inferred from the distribution of older Quaternary deposits (CDMG 1:25,000 San Jose quadrangle) that indicate differential uplift across the fault. Sterling (1992) describes stratigraphic and structural relationships imaged by seismic reflection data indicating "movement as recently as late Pliocene." The slip rate is estimated to be comparable to the estimated rate for the West Tracy fault.

Table 1. Bay Area Time-Independent Seismic Source Parameters

Fault Name	Probability of Activity ¹	Rupture Scenario ²	Segment Name	Rupture Length ³	Width ⁴	Dip ⁵	Direction of Dip ⁶	Sense of Slip ⁷	Magnitude ⁸	Slip Rate ⁹	Notes
Verona/Williams Thrust System	1.0	Unsegmented (0.6)	N/A	22	21 ± 2	30 (0.1) 45 (0.6) 60 (0.3)	NE	R	6.7	0.1 (0.2) 0.7 (0.5) 1.4 (0.3)	In this model, the Verona/Williams fault is the near surface expression of a deeper east-to northeast-dipping blind thrust fault that underlies the Livermore Valley (Unruh and Sawyer, 1997; Sawyer, 1998). This model explains fault and fold deformation in the Livermore Valley (including the Los Positas fault, Livermore thrust and Springtown anticline) as secondary structures that either root into the deeper structure or are secondary structures in the hanging wall of the Verona/Williams thrust. These secondary structures are non-seismogenic and are not treated as independent seismic sources. The slip rate distribution is from Savy and Foxall (2002). Fault tip is estimated to be at a depth of 3 km (0.5) or 5 km (0.5).
		Segmented (0.4)	Verona	10	10	30 (0.2) 45 (0.4) 60 (0.4)	NE	R	6.2	0.1 (0.2) 0.7 (0.5) 1.4 (0.3)	Characterization of the fault is based on information summarized in Herd and Brabb (1980), Hart (1980, 1981a,b), Jahns and Harding (1982), and source parameters developed by the Thrust Fault Subgroup of Working Group 1999 (WGCEP (2003) subgroup). The total length of the fault is approximately 7-9 km. Field observations and trenching described by Herd and Brabb (1980) provide evidence for late Quaternary surface-rupturing events on the fault. A 5.65-km-long-segment of the fault is included in an Alquist-Priolo zone (Hart, 1980, 1981a,b). The slip rate distribution is from Savy and Foxall (2002). Fault tip is estimated to be at a depth of 3 km (0.5) or 5 km (0.5).
			Williams	13	13	30 (0.1) 45 (0.6) 60 (0.3)	NE	R	6.3	0.1 (0.2) 0.3 (0.6) 1.0 (0.2)	Characterization of the fault is based on the following. The total length of the fault is based on mapping by Dibblee (1980,1981). Carpenter <i>et al.</i> (1984) show the fault as a southwest-vergent thrust fault. The CDWR (1979) suggested the fault was active based on displacements observed in Plio-Pleistocene Livermore gravels in the Hetch-Hetchy tunnel and the occurrence of moderate seismicity adjacent to its trace. In the absence of any reported slip rate estimates, a rate of slip comparable to Verona fault is used. Fault tip is estimated to be at a depth of 3 km (0.5) or 5 km (0.5).
			Las Positas P(a) = 0.7	17.5	15 ± 3	90	N/A	SS	6.5	0.1 (0.2) 0.3 (0.6) 1.0 (0.2)	Characterization is based on information summarized by Carpenter <i>et al.</i> (1980,1984) as follows. The total length of ~17.5 km is based on geologic mapping and air photo interpretation. Movement on both southern and northern fault traces extends up into Holocene deposits: faulting may have occurred as recently as 500 to 1,000 years ago. The average slip rate for the north branch of the Las Positas fault zone is 0.4 mm/yr; the range of rates obtained from observed vertical offset and inferred horizontal-to-vertical ratios and age estimates is 0.02 to 0.9 mm/yr.
West Napa	1.0	Unsegmented (0.15)	St. Helena/Dry Creek + West Napa	52	15 ± 3	90	N/A	SS	6.9	1.0 (0.3) 2.0 (0.3) 3.0 (0.3) 4.0 (0.1)	Characterization is based on recent compilation and mapping of the West Napa fault by Hanson and Wesling (2006 and 2007) and Clahan <i>et al.</i> (2005) conducted in support of the USGS Quaternary fault database for Northern California (Graymer <i>et al.</i> , 2006). The slip rate for the West Napa is not well constrained, but was previously considered to be on the order of 1 mm/yr (1 ± 1 mm/yr, Cao <i>et al.</i> , 2003). Several recent studies and observations suggest

Table 1. Bay Area Time-Independent Seismic Source Parameters

Fault Name	Probability of Activity ¹	Rupture Scenario ²	Segment Name	Rupture Length ³	Width ⁴	Dip ⁵	Direction of Dip ⁶	Sense of Slip ⁷	Magnitude ⁸	Slip Rate ⁹	Notes
		Floating Earthquake (0.35)	N/A	N/A	15 ± 3	90	N/A	SS	6.5	0.5 (0.1) 1.0 (0.3) 2.0 (0.3) 3.0 (0.2) 4/0 (0.1)	the slip rate is higher. These include: 1) more detailed mapping of the fault zone (Hanson and Wesling, 2006, 2007) that shows that the fault is better expressed geomorphically than had been recognized previously with evidence for recent (< 600 to 700 years B. P.) displacement; 2) comparison of slip budgets between the regions north and south of Carquinez Strait suggests that a significant amount of slip is being transferred from the North Calaveras fault to the West Napa fault via the Cull Canyon/Laffette/Reliz Valley fault zone; and 3) a recent analysis of GPS data with the preferred model indicating a rate of 4 ± 3 mm/yr (d'Alessio <i>et al.</i> , 2005).
		Segmented (0.15)	St. Helena/Dry Creek	24	15 ± 3	90	N/A	SS	6.6	1.0 (0.5) 2.0 (0.2) 3.0 (0.1)	
			West Napa	38	15 ± 3	90	N/A	SS	6.8	1.0 (0.5) 2.0 (0.2) 3.0 (0.1)	
		Segmented + Floating Earthquake (0.35)	Floating Earthquake on West Napa	N/A	15 ± 3	90	N/A	SS	6.4	1.0 (0.5) 2.0 (0.2) 3.0 (0.1)	
			St. Helena/Dry Creek	N/A	15 ± 3	90	N/A	SS	6.4	1.0 (0.5) 2.0 (0.2) 3.0 (0.1)	
West Tracy	0.9	Floating Earthquake (1.0)	N/A	30	15 ± 3	70 ± 10	W	RO	6.25 (0.2) 6.5 (0.4) 6.75 (0.4)	0.07 (0.3) 0.25 (0.4) 0.5 (0.3)	Quaternary activity of the West Tracy fault is inferred from the distribution of older Quaternary deposits (CDMG 1:25,000 San Jose quadrangle) that indicate differential uplift across the fault. Very limited data is available to estimate the rate of slip and recent fault behavior. The rate of reverse-oblique slip is inferred to be approximately half the rate estimated for the Midway/Black Butte fault zone. A lower bound of 0.07 mm/yr on the slip rate is estimated based on total vertical separation of about 800 ft (244 m) of a basal Miocene unconformity across the fault as reported by Sterling (1992), and an assumed duration of deformation (active during the past ~3.5 Ma).
Wragg Canyon	0.7	Unsegmented (1.0)	N/A	17	15 ± 3	90	N/A	SS	6.5	0.1 (0.2) 0.3 (0.6) 0.5 (0.2)	Fault mapped by Sims <i>et al.</i> (1973) along Wragg Canyon; O'Connell <i>et al.</i> (2001) inferred that small earthquakes with strike-slip focal mechanisms are associated with the fault. We adopted a P(a) = 1 based on data in O'Connell <i>et al.</i> (2001) showing a spatial association of seismicity with the Wragg Canyon fault. The slip rate was derived from a kinematic model whereby at least some slip on the Pittsburg-Kirby Hills fault is transferred to the Wragg Canyon fault through a restraining stepover across the Potrero Hills. In this model, the slip rate on Wragg Canyon fault (0.3 ± 0.2 mm/yr) is assumed to be somewhat less than the Pittsburg-Kirby Hills fault (0.5 ± 0.2 mm/yr).
Zayante-Vergeles	1.0	Unsegmented (1.0)	N/A	58	12	70 ± 10	SW	R	6.9	0.1 ± 0.1	Cao <i>et al.</i> (2003); Dip information from USGS Quaternary Database

¹ Probability of Activity: Independent seismic source ($M \geq 6.0$) and repeated displacements in late-Quaternary or historical activity (1.0); Late Pleistocene or inferred association with historical seismicity (0.7); activity inferred from fault geometry considered likely to move under current tectonic regime (0.5).

² Weight assigned according to likelihood of occurrence of rupture scenario.

³ Rupture length in kilometers.

⁴ Down-dip width of fault rupture. Unless otherwise stated, weights are 0.4 for the best estimate and 0.3 for the upper and lower bound estimates.

⁵ Inclination of fault plane, measured from the horizontal. Dips are not varied unless otherwise stated. Weights are 0.4 for the best estimate and 0.3 for the upper and lower bound estimates.

⁶ Direction of inclination of the fault plane. N/A infers a vertical fault plane.

Table 1. Bay Area Time-Independent Seismic Source Parameters

⁷ SS – strike-slip; R – reverse; OR – oblique-reverse.

⁸ Unless otherwise stated, uncertainties in the best estimate magnitude are ± 0.3 magnitude unit. Weights are 0.2, 0.6, and 0.2 unless otherwise stated. A single magnitude value is weighted 1.0.

⁹ Slip rate based on paleoseismic data. Unless otherwise stated, weights are 0.2, 0.6, and 0.2.

Table 2. Bay Area Time-Dependent Seismic Source Parameters

Fault Name	Probability of Activity ¹	Rupture Source ²	Segment Name	Rupture Length ³	Width ⁴	Dip ⁵	Direction of Dip ⁶	Sense of Slip ⁷	Magnitude ⁸	Year	Rate of Characteristic Event ⁹			Activity Rate		
											5%	5%	Mean	95%	Mean	95%
		SAS	Santa Cruz Mountains	62	15	90	N/A	SS	6.87 7.03 7.19	2005:	0.00E+00	4.31E-04	1.79E-03	0.00E+00	1.77E-03	7.34E-03
										2050:	0.00E+00	2.19E-03	8.26E-03	0.00E+00	9.01E-03	3.39E-02
										2100:	0.00E+00	4.77E-03	1.92E-02	0.00E+00	1.96E-02	7.90E-02
										2200:	0.00E+00	7.37E-03	3.02E-02	0.00E+00	3.03E-02	1.24E-01
		SAP	Peninsula	85	13	90	N/A	SS	6.97 7.15 7.31	2005:	0.00E+00	1.31E-03	5.60E-03	0.00E+00	4.32E-03	1.85E-02
										2050:	0.00E+00	2.61E-03	9.56E-03	0.00E+00	8.63E-03	3.16E-02
										2100:	0.00E+00	3.71E-03	1.41E-02	0.00E+00	1.23E-02	4.66E-02
										2200:	0.00E+00	4.44E-03	1.64E-02	0.00E+00	1.47E-02	5.43E-02
		SAN	North Coast	191	11	90	N/A	SS	7.30 7.45 7.59	2005:	0.00E+00	2.12E-04	9.31E-04	0.00E+00	1.15E-03	5.04E-03
										2050:	0.00E+00	4.14E-04	1.67E-03	0.00E+00	2.24E-03	9.06E-03
2100:	0.00E+00									6.07E-04	2.25E-03	0.00E+00	3.29E-03	1.22E-02		
2200:	0.00E+00									8.10E-04	2.99E-03	0.00E+00	4.38E-03	1.62E-02		
SAO	Offshore	135	11	90	N/A	SS	7.13 7.29 7.44	2005:	0.00E+00	1.80E-04	8.87E-04	0.00E+00	7.50E-04	3.70E-03		
								2050:	0.00E+00	4.04E-04	1.70E-03	0.00E+00	1.69E-03	7.10E-03		
								2100:	0.00E+00	7.08E-04	2.67E-03	0.00E+00	2.96E-03	1.11E-02		
								2200:	0.00E+00	1.16E-03	4.33E-03	0.00E+00	4.83E-03	1.81E-02		
SAS+SAP	Peninsula + Santa Cruz Mountains	147		90	N/A	SS	7.28 7.42 7.55	2005:	3.87E-05	1.01E-03	3.22E-03	2.03E-04	5.33E-03	1.69E-02		
								2050:	1.46E-04	2.06E-03	5.83E-03	7.68E-04	1.08E-02	3.06E-02		
								2100:	2.08E-04	3.14E-03	9.59E-03	1.09E-03	1.65E-02	5.03E-02		
								2200:	2.46E-04	4.09E-03	1.28E-02	1.29E-03	2.15E-02	6.69E-02		
SAN+SAO	Offshore + North Coast	326	11	90	N/A	SS	7.55 7.70 7.83	2005:	2.05E-05	9.43E-04	2.95E-03	1.73E-04	7.96E-03	2.49E-02		
								2050:	2.82E-04	1.65E-03	4.50E-03	2.38E-03	1.40E-02	3.80E-02		
								2100:	4.05E-04	2.35E-03	5.94E-03	3.42E-03	1.98E-02	5.01E-02		
								2200:	4.87E-04	3.17E-03	7.99E-03	4.11E-03	2.67E-02	6.74E-02		
SAS+SAP+SAN	North Coast + Peninsula + Santa Cruz Mountains	338	13 ± 3	90	N/A	SS	7.62 7.76 7.89	2005:	0.00E+00	1.66E-05	8.98E-05	0.00E+00	1.57E-04	8.47E-04		
								2050:	0.00E+00	2.71E-05	1.10E-04	0.00E+00	2.56E-04	1.04E-03		
								2100:	0.00E+00	3.68E-05	1.34E-04	0.00E+00	3.47E-04	1.27E-03		
								2200:	0.00E+00	4.64E-05	1.58E-04	0.00E+00	4.38E-04	1.49E-03		
SAP+SAN+SAO	Offshore + North Coast + Peninsula	411	11 ± 2	90	N/A	SS	7.67 7.82 7.97	2005:	0.00E+00	4.43E-05	2.82E-04	0.00E+00	4.84E-04	3.08E-03		
								2050:	0.00E+00	7.34E-05	4.21E-04	0.00E+00	8.02E-04	4.60E-03		
								2100:	0.00E+00	1.01E-04	4.99E-04	0.00E+00	1.10E-03	5.46E-03		
								2200:	0.00E+00	1.31E-04	5.96E-04	0.00E+00	1.43E-03	6.52E-03		
SAS+SAP+SAN+S AO	Offshore + North Coast + Peninsula + Santa Cruz Mountains (1906)	473	13 ± 2	90	N/A	SS	7.75 7.90 8.06	2005:	7.82E-05	1.46E-03	4.25E-03	9.74E-04	1.81E-02	5.30E-02		
								2050:	5.97E-04	2.30E-03	6.16E-03	7.44E-03	2.86E-02	7.66E-02		
								2100:	1.03E-03	3.08E-03	7.74E-03	1.29E-02	3.83E-02	9.63E-02		
								2200:	1.31E-03	3.94E-03	9.02E-03	1.64E-02	4.90E-02	1.12E-01		
Floating Earthquake	N/A	N/A	13 ± 3	90	N/A	SS	6.9	2005:	1.62E-04	1.81E-03	6.49E-03	3.87E-04	4.33E-03	1.55E-02		
								2050:	1.99E-04	3.72E-03	1.32E-02	4.76E-04	8.89E-03	3.16E-02		
								2100:	2.09E-04	5.80E-03	2.14E-02	5.00E-04	1.39E-02	5.12E-02		
								2200:	2.12E-04	8.03E-03	3.12E-02	5.07E-04	1.92E-02	7.45E-02		

Table 2. Bay Area Time-Dependent Seismic Source Parameters

Fault Name	Probability of Activity ¹	Rupture Source ²	Segment Name	Rupture Length ³	Width ⁴	Dip ⁵	Direction of Dip ⁶	Sense of Slip ⁷	Magnitude ⁸	Year	Rate of Characteristic Event ⁹			Activity Rate		
											5%	5%	Mean	95%	Mean	95%
Hayward – Rodgers Creek	1.0	HS	Southern Hayward	53	12 ± 2	90	N/A	SS	6.42 6.67 6.90	2005: 2050: 2100: 2200:	8.66E-04	4.24E-03	1.08E-02	1.56E-03	7.63E-03	1.95E-02
											1.15E-03	5.13E-03	1.28E-02	2.06E-03	9.23E-03	2.31E-02
											1.28E-03	5.75E-03	1.48E-02	2.31E-03	1.04E-02	2.66E-02
											1.38E-03	6.41E-03	1.65E-02	2.49E-03	1.15E-02	2.96E-02
		HN	North Hayward	35	12 ± 2	90	N/A	SS	6.20 6.49 6.73	2005: 2050: 2100: 2200:	9.57E-04	5.17E-03	1.46E-02	1.44E-03	7.77E-03	2.19E-02
											1.05E-03	5.48E-03	1.54E-02	1.58E-03	8.25E-03	2.32E-02
											1.14E-03	5.75E-03	1.57E-02	1.72E-03	8.66E-03	2.37E-02
1.20E-03	6.06E-03										1.64E-02	1.81E-03	9.13E-03	2.47E-02		
HS+HN	Hayward	88	12 ± 2	90	N/A	SS	6.71 6.90 7.09	2005: 2050: 2100: 2200:	7.36E-04	3.38E-03	8.65E-03	1.72E-03	7.91E-03	2.03E-02		
									8.37E-04	3.88E-03	1.03E-02	1.96E-03	9.10E-03	2.42E-02		
									9.21E-04	4.26E-03	1.14E-02	2.16E-03	9.97E-03	2.66E-02		
									1.02E-03	4.67E-03	1.28E-02	2.38E-03	1.10E-02	3.01E-02		
RC	Rodgers Creek	63	12 ± 2	90	N/A	SS	6.83 6.98 7.14	2005: 2050: 2100: 2200:	1.56E-03	5.93E-03	1.44E-02	4.16E-03	1.58E-02	3.85E-02		
									1.72E-03	6.49E-03	1.71E-02	4.58E-03	1.73E-02	4.56E-02		
									1.89E-03	6.97E-03	1.88E-02	5.05E-03	1.86E-02	5.02E-02		
									2.23E-03	7.59E-03	2.07E-02	5.93E-03	2.02E-02	5.50E-02		
HN+RC	North Hayward + Rodgers Creek	98	12 ± 2	90	N/A	SS	6.96 7.11 7.27	2005: 2050: 2100: 2200:	4.10E-05	7.60E-04	2.34E-03	1.29E-04	2.38E-03	7.35E-03		
									4.49E-05	8.25E-04	2.53E-03	1.41E-04	2.59E-03	7.95E-03		
									4.91E-05	8.81E-04	2.78E-03	1.54E-04	2.76E-03	8.73E-03		
									4.91E-05	9.50E-04	2.97E-03	1.54E-04	2.98E-03	9.32E-03		
HS+HN+RC	Hayward + Rodgers Creek	151	12 ± 2	90	N/A	SS	7.11 7.26 7.40	2005: 2050: 2100: 2200:	6.14E-05	4.11E-04	1.11E-03	2.39E-04	1.60E-03	4.35E-03		
									6.76E-05	4.59E-04	1.32E-03	2.64E-04	1.79E-03	5.14E-03		
									7.33E-05	4.98E-04	1.43E-03	2.86E-04	1.94E-03	5.60E-03		
									7.95E-05	5.44E-04	1.63E-03	3.10E-04	2.12E-03	6.37E-03		
Floating Earthquake	N/A	N/A	12 ± 2	90	N/A	SS	6.90	2005: 2050: 2100: 2200:	1.02E-04	2.52E-04	4.80E-04	2.44E-04	6.02E-04	1.15E-03		
									1.09E-04	2.59E-04	4.85E-04	2.61E-04	6.20E-04	1.16E-03		
									1.19E-04	2.70E-04	4.94E-04	2.84E-04	6.45E-04	1.18E-03		
									1.35E-04	2.90E-04	5.46E-04	3.23E-04	6.94E-04	1.30E-03		
Calaveras	1.0	CS	Southern Calaveras	19	11 ± 2	90	N/A	SS	0.0 5.79 6.12	2005: 2050: 2100: 2200:	0.00E+00	1.17E-02	3.77E-02	0.00E+00	1.60E-02	5.15E-02
											0.00E+00	1.21E-02	4.03E-02	0.00E+00	1.66E-02	5.52E-02
											0.00E+00	1.25E-02	4.15E-02	0.00E+00	1.70E-02	5.68E-02
											0.00E+00	1.30E-02	4.24E-02	0.00E+00	1.78E-02	5.80E-02
		CC	Central Calaveras	59	11 ± 2	90	N/A	SS	5.79 6.23 6.61	2005: 2050: 2100: 2200:	8.25E-04	6.40E-03	1.80E-02	1.00E-03	7.78E-03	2.19E-02
											1.97E-03	8.52E-03	2.49E-02	2.40E-03	1.04E-02	3.03E-02
2.10E-03	9.12E-03										2.63E-02	2.55E-03	1.11E-02	3.20E-02		
2.38E-03	9.57E-03										2.70E-02	2.90E-03	1.16E-02	3.29E-02		
CS+CC	South + Central Calaveras	78	11 ± 2	90	N/A	SS	5.93 6.36 6.68	2005: 2050: 2100: 2200:	0.00E+00	2.16E-03	7.92E-03	0.00E+00	2.85E-03	1.04E-02		
									0.00E+00	2.74E-03	1.01E-02	0.00E+00	3.61E-03	1.33E-02		
									0.00E+00	2.94E-03	1.09E-02	0.00E+00	3.88E-03	1.44E-02		
									0.00E+00	3.09E-03	1.14E-02	0.00E+00	4.08E-03	1.50E-02		
CN	Northern Calaveras	45	13 ± 2	90	N/A	SS	6.62 6.78 6.93	2005: 2050: 2100: 2200:	1.10E-03	5.14E-03	1.45E-02	2.28E-03	1.06E-02	3.00E-02		
									1.23E-03	5.50E-03	1.57E-02	2.54E-03	1.14E-02	3.26E-02		
									1.35E-03	5.82E-03	1.68E-02	2.79E-03	1.20E-02	3.48E-02		
									1.56E-03	6.26E-03	1.81E-02	3.23E-03	1.30E-02	3.74E-02		
CC+CN	Central + Northern Calaveras	104	13 ± 2	90	N/A	SS	6.72 6.91 7.08	2005: 2050: 2100: 2200:	0.00E+00	1.37E-04	1.00E-03	0.00E+00	3.24E-04	2.37E-03		
									0.00E+00	1.65E-04	1.14E-03	0.00E+00	3.91E-04	2.70E-03		
									0.00E+00	1.81E-04	1.28E-03	0.00E+00	4.28E-04	3.02E-03		
									0.00E+00	1.97E-04	1.36E-03	0.00E+00	4.67E-04	3.21E-03		

Table 2. Bay Area Time-Dependent Seismic Source Parameters

Fault Name	Probability of Activity ¹	Rupture Source ²	Segment Name	Rupture Length ³	Width ⁴	Dip ⁵	Direction of Dip ⁶	Sense of Slip ⁷	Magnitude ⁸	Year	Rate of Characteristic Event ⁹			Activity Rate		
											5%	5%	Mean	95%	Mean	95%
		CS+CC+CN	Northern + Central + Southern Calaveras	123	11 ± 2	90	N/A	SS	6.76 6.94 7.11	2005:	0.00E+00	8.05E-04	2.81E-03	0.00E+00	1.99E-03	6.96E-03
										2050:	0.00E+00	9.38E-04	3.40E-03	0.00E+00	2.32E-03	8.42E-03
										2100:	0.00E+00	1.00E-03	3.58E-03	0.00E+00	2.48E-03	8.85E-03
		2200:	0.00E+00	1.07E-03	3.71E-03	0.00E+00	2.65E-03	9.17E-03								
		Floating Earthquake	N/A	N/A	11 ± 2	90	N/A	SS	6.2	2005:	6.17E-04	2.63E-03	6.66E-03	7.83E-04	3.34E-03	8.45E-03
										2050:	6.92E-04	2.73E-03	6.67E-03	8.78E-04	3.46E-03	8.47E-03
										2100:	7.43E-04	2.85E-03	6.88E-03	9.43E-04	3.62E-03	8.73E-03
										2200:	8.39E-04	3.11E-03	7.86E-03	1.06E-03	3.95E-03	9.98E-03
		Floating Earthquake on CS+CC	N/A	N/A	11 ± 2	90	N/A	SS	6.2	2005:	2.10E-03	1.04E-02	2.50E-02	2.66E-03	1.32E-02	3.17E-02
2050:	2.22E-03									1.07E-02	2.51E-02	2.81E-03	1.36E-02	3.18E-02		
2100:	2.37E-03									1.13E-02	2.64E-02	3.00E-03	1.43E-02	3.35E-02		
2200:	2.55E-03									1.23E-02	2.88E-02	3.24E-03	1.56E-02	3.66E-02		
Concord – Green Valley	1.0	CON	Concord	20	16 ± 2	90	N/A	SS	5.79 6.25 6.65	2005:	1.56E-04	1.88E-03	5.70E-03	1.91E-04	2.30E-03	6.97E-03
										2050:	2.02E-04	2.06E-03	6.03E-03	2.47E-04	2.51E-03	7.36E-03
										2100:	2.21E-04	2.21E-03	6.63E-03	2.70E-04	2.70E-03	8.10E-03
		2200:	2.66E-04	2.41E-03	7.06E-03	3.25E-04	2.94E-03	8.63E-03								
		GVS	Southern Green Valley	22	14 ± 2	90	N/A	SS	5.81 6.24 6.60	2005:	6.22E-05	8.78E-04	2.85E-03	7.57E-05	1.07E-03	3.47E-03
										2050:	8.50E-05	9.57E-04	3.08E-03	1.03E-04	1.16E-03	3.75E-03
										2100:	9.77E-05	1.02E-03	3.20E-03	1.19E-04	1.25E-03	3.90E-03
										2200:	1.16E-04	1.11E-03	3.49E-03	1.41E-04	1.35E-03	4.25E-03
		CON+GVS	Concord + Southern Green Valley	42	14 ± 2	90	N/A	SS	6.20 6.58 6.87	2005:	2.78E-05	5.99E-04	2.00E-03	4.42E-05	9.54E-04	3.19E-03
										2050:	3.28E-05	6.52E-04	2.13E-03	5.23E-05	1.04E-03	3.40E-03
										2100:	4.30E-05	6.99E-04	2.29E-03	6.85E-05	1.11E-03	3.64E-03
										2200:	5.32E-05	7.60E-04	2.52E-03	8.47E-05	1.21E-03	4.01E-03
		GVN	Northern Green Valley	14	14 ± 2	90	N/A	SS	5.56 6.02 6.43	2005:	1.98E-04	2.36E-03	7.05E-03	2.17E-04	2.59E-03	7.74E-03
										2050:	2.33E-04	2.55E-03	7.56E-03	2.55E-04	2.80E-03	8.31E-03
										2100:	2.73E-04	2.71E-03	7.66E-03	3.00E-04	2.98E-03	8.41E-03
										2200:	3.14E-04	2.92E-03	8.23E-03	3.45E-04	3.21E-03	9.04E-03
		GVS+GVN	Green Valley	36	14 ± 2	90	N/A	SS	6.11 6.48 6.77	2005:	8.35E-05	1.20E-03	3.78E-03	1.22E-04	1.76E-03	5.53E-03
										2050:	1.03E-04	1.31E-03	4.23E-03	1.51E-04	1.92E-03	6.19E-03
										2100:	1.18E-04	1.40E-03	4.41E-03	1.72E-04	2.05E-03	6.44E-03
										2200:	1.39E-04	1.52E-03	4.81E-03	2.04E-04	2.22E-03	7.03E-03
		CON+GVS+GVN	Concord+Green Valley	56	14 ± 2	90	N/A	SS	6.42 6.71 6.95	2005:	2.53E-04	2.32E-03	7.37E-03	4.67E-04	4.27E-03	1.36E-02
2050:	3.06E-04									2.57E-03	7.91E-03	5.64E-04	4.73E-03	1.46E-02		
2100:	3.70E-04									2.77E-03	8.24E-03	6.82E-04	5.11E-03	1.52E-02		
2200:	4.63E-04									3.05E-03	8.76E-03	8.54E-04	5.62E-03	1.62E-02		
Floating Earthquake	N/A	N/A	14 ± 2	90	N/A	SS	6.2	2005:	1.06E-04	2.40E-03	1.07E-02	1.36E-04	3.07E-03	1.37E-02		
								2050:	1.18E-04	2.47E-03	1.08E-02	1.51E-04	3.16E-03	1.39E-02		
								2100:	1.23E-04	2.56E-03	1.10E-02	1.57E-04	3.28E-03	1.41E-02		
								2200:	1.32E-04	2.74E-03	1.13E-02	1.69E-04	3.51E-03	1.44E-02		
San Gregorio	1.0	SGS	Southern San Gregorio	66	12 ± 2	90	N/A	SS	6.76 6.96 7.12	2005:	0.00E+00	8.17E-04	3.09E-03	0.00E+00	2.04E-03	7.71E-03
										2050:	0.00E+00	8.96E-04	3.33E-03	0.00E+00	2.24E-03	8.32E-03
										2100:	0.00E+00	9.75E-04	3.58E-03	0.00E+00	2.43E-03	8.94E-03
		2200:	0.00E+00	1.11E-03	3.83E-03	0.00E+00	2.77E-03	9.55E-03								
		SGN	Northern San Gregorio	110	13 ± 2	90	N/A	SS	7.07 7.23 7.40	2005:	0.00E+00	1.41E-03	5.03E-03	0.00E+00	5.42E-03	1.93E-02
										2050:	0.00E+00	1.58E-03	5.45E-03	0.00E+00	6.06E-03	2.09E-02
										2100:	0.00E+00	1.73E-03	5.81E-03	0.00E+00	6.66E-03	2.23E-02
2200:	0.00E+00									1.97E-03	6.23E-03	0.00E+00	7.58E-03	2.39E-02		

Table 2. Bay Area Time-Dependent Seismic Source Parameters

Fault Name	Probability of Activity ¹	Rupture Source ²	Segment Name	Rupture Length ³	Width ⁴	Dip ⁵	Direction of Dip ⁶	Sense of Slip ⁷	Magnitude ⁸	Year	Rate of Characteristic Event ⁹			Activity Rate			
											5%	5%	Mean	95%	Mean	95%	
		SGS+SGN	Northern + Southern San Gregorio						7.30	2005:	0.00E+00	9.22E-04	2.93E-03	0.00E+00	4.94E-03	1.57E-02	
									7.44	2050:	0.00E+00	1.03E-03	3.33E-03	0.00E+00	5.51E-03	1.78E-02	
									7.58	2100:	0.00E+00	1.15E-03	3.52E-03	0.00E+00	6.16E-03	1.89E-02	
										2200:	0.00E+00	1.33E-03	4.01E-03	0.00E+00	7.13E-03	2.15E-02	
		Floating Earthquake	N/A	N/A	13 ± 2	90	N/A	SS		6.9	2005:	3.05E-04	7.23E-04	1.23E-03	7.35E-04	1.74E-03	2.96E-03
											2050:	3.21E-04	7.45E-04	1.24E-03	7.73E-04	1.79E-03	2.99E-03
											2100:	3.34E-04	7.76E-04	1.25E-03	8.04E-04	1.87E-03	3.02E-03
											2200:	3.50E-04	8.37E-04	1.45E-03	8.44E-04	2.02E-03	3.49E-03
Greenville	1.0	GS	Southern Greenville	24	15 ± 3	90	N/A	SS	6.40	2005:	3.26E-05	1.08E-03	2.80E-03	5.46E-05	1.81E-03	4.69E-03	
									6.60	2050:	9.32E-05	1.19E-03	2.90E-03	1.56E-04	1.99E-03	4.85E-03	
									6.78	2100:	1.91E-04	1.31E-03	3.08E-03	3.20E-04	2.19E-03	5.16E-03	
										2200:	3.30E-04	1.51E-03	3.44E-03	5.52E-04	2.53E-03	5.76E-03	
		GN	Northern Greenville	27	15 ± 3	90	N/A	SS		6.45	2005:	1.16E-05	1.03E-03	2.82E-03	2.06E-05	1.82E-03	4.99E-03
										6.66	2050:	6.08E-05	1.12E-03	2.80E-03	1.08E-04	1.98E-03	4.96E-03
										6.84	2100:	1.39E-04	1.23E-03	3.14E-03	2.46E-04	2.18E-03	5.57E-03
											2200:	2.32E-04	1.43E-03	3.67E-03	4.11E-04	2.53E-03	6.50E-03
		GS+GN	Southern+Northern Greenville	51	15 ± 3	90	N/A	SS		6.78	2005:	9.29E-05	5.32E-04	1.29E-03	2.34E-04	1.34E-03	3.26E-03
										6.94	2050:	1.16E-04	5.79E-04	1.36E-03	2.93E-04	1.46E-03	3.43E-03
										7.11	2100:	1.38E-04	6.38E-04	1.48E-03	3.49E-04	1.61E-03	3.73E-03
											2200:	1.75E-04	7.40E-04	1.71E-03	4.42E-04	1.87E-03	4.31E-03
		Floating Earthquake	N/A	N/A	15 ± 3	90	N/A	SS		6.2	2005:	5.82E-05	1.49E-04	2.73E-04	7.44E-05	1.91E-04	3.49E-04
											2050:	6.17E-05	1.54E-04	2.74E-04	7.89E-05	1.96E-04	3.50E-04
											2100:	6.37E-05	1.60E-04	2.85E-04	8.15E-05	2.04E-04	3.64E-04
											2200:	6.55E-05	1.72E-04	3.20E-04	8.38E-05	2.20E-04	4.10E-04
Mt Diablo	1.0	MTD	Mt. Diablo	31	17 ± 2	30 (0.2)	NE	R	6.48	2005:	3.97E-04	2.71E-03	6.72E-03	7.07E-04	4.84E-03	1.20E-02	
						45 (0.6)			2050:	5.52E-04	2.97E-03	7.45E-03	9.84E-04	5.29E-03	1.33E-02		
						50 (0.2)			2100:	6.16E-04	3.23E-03	7.89E-03	1.10E-03	5.75E-03	1.41E-02		
									2200:	6.64E-04	3.66E-03	8.99E-03	1.18E-03	6.53E-03	1.60E-02		

¹ Probability of Activity: Holocene or historical activity (1.0); Late Pleistocene or inferred association with historical seismicity (0.7); activity inferred from fault geometry considered likely to move under current tectonic regime (0.5).

² Weight assigned according to likelihood of occurrence of rupture scenario.

³ Rupture length in kilometers.

⁴ Down-dip width of fault rupture. Unless otherwise stated, weights are 0.4 for the best estimate and 0.3 for the upper and lower bound estimates.

⁵ Inclination of fault plane, measured from the horizontal. Dips are not varied unless otherwise stated. Weights are 0.4 for the best estimate and 0.3 for the upper and lower bound estimates.

⁶ Direction of inclination of the fault plane. N/A infers a vertical fault plane.

⁷ SS – strike-slip; R – reverse; OR – oblique-reverse.

⁸ Unless otherwise stated, uncertainties in the best estimate magnitude are ± 0.3 magnitude unit. Weights are 0.2, 0.6, and 0.2 unless otherwise stated.

⁹ Slip rate based on paleoseismic data. Unless otherwise stated, weights are 0.2, 0.6, and 0.2.

Topical Area: Seismology

Table 3
Mean Expert Weights for Probability Models Applied to the SFBR Fault Systems
(Table 5.5, WGCEP, 2003)

Fault System	Poisson	Empirical	BPT	BPT-step	Time-Predictable
San Andreas	0.100	0.181	0.154	0.231	0.335
Hayward/Rodger's Creek	0.123	0.285	0.131	0.462	—
Calaveras	0.227	0.315	0.142	0.315	—
Concord/Green Valley	0.246	0.277	0.123	0.354	—
San Gregorio	0.196	0.292	0.115	0.396	—
Greenville	0.231	0.288	0.131	0.350	—
Mt. Diablo Thrust	0.308	0.396	0.092	0.204	—

**Table 4
Empirical Model Factors**

Model	Extrapolated Annual Number of Events for Year:			
	2005	2055	2105	2205
A	0.014	0.014	0.014	0.014
B	0.016	0.016	0.016	0.016
C	0.011	0.011	0.011	0.011
D	0.020	0.020	0.020	0.020
E	0.016	0.018	0.020	0.025
F	0.018	0.026	0.034	0.050
Empirical Factors Based on Long Term Rate of 0.031				
Minimum	0.355	0.355	0.355	0.355
Average	0.512	0.567	0.622	0.733
Maximum	0.645	0.850	1.107	1.623

Table 5
Ground Motions for Return Periods of 100 to 2,500 Years in 2005

Site	PGA (g's)			
	100 years	200 years	500 years	2,500 years
Clifton Court	0.22	0.29	0.40	0.66
Delta Cross Channel	0.15	0.19	0.25	0.37
Montezuma Slough	0.27	0.35	0.47	0.74
Sacramento	0.12	0.15	0.20	0.30
Sherman Island	0.24	0.31	0.41	0.64
Stockton	0.13	0.17	0.22	0.32

Topical Area: Seismology

Table 6a
Controlling Seismic Sources at a Return Period of 100 Years in 2005

Location	PGA	1.0 Sec SA
Clifton Court	Southern Midland Mt. Diablo	Mt. Diablo Hayward-Rodgers Creek
Delta Cross Channel	Southern Midland Northern Midland Zone	Mt. Diablo
Montezuma Slough	Concord-Green Valley	Concord-Green Valley
Sacramento	Northern Midland Zone	Mt. Diablo San Andreas
Sherman Island	Southern Midland	Southern Midland Hayward-Rodgers Creek San Andreas
Stockton	Southern Midland Hayward-Rodgers Creek Calaveras	Hayward-Rodgers Creek San Andreas
<p>Note: Seismic sources are ordered by contribution.</p>		

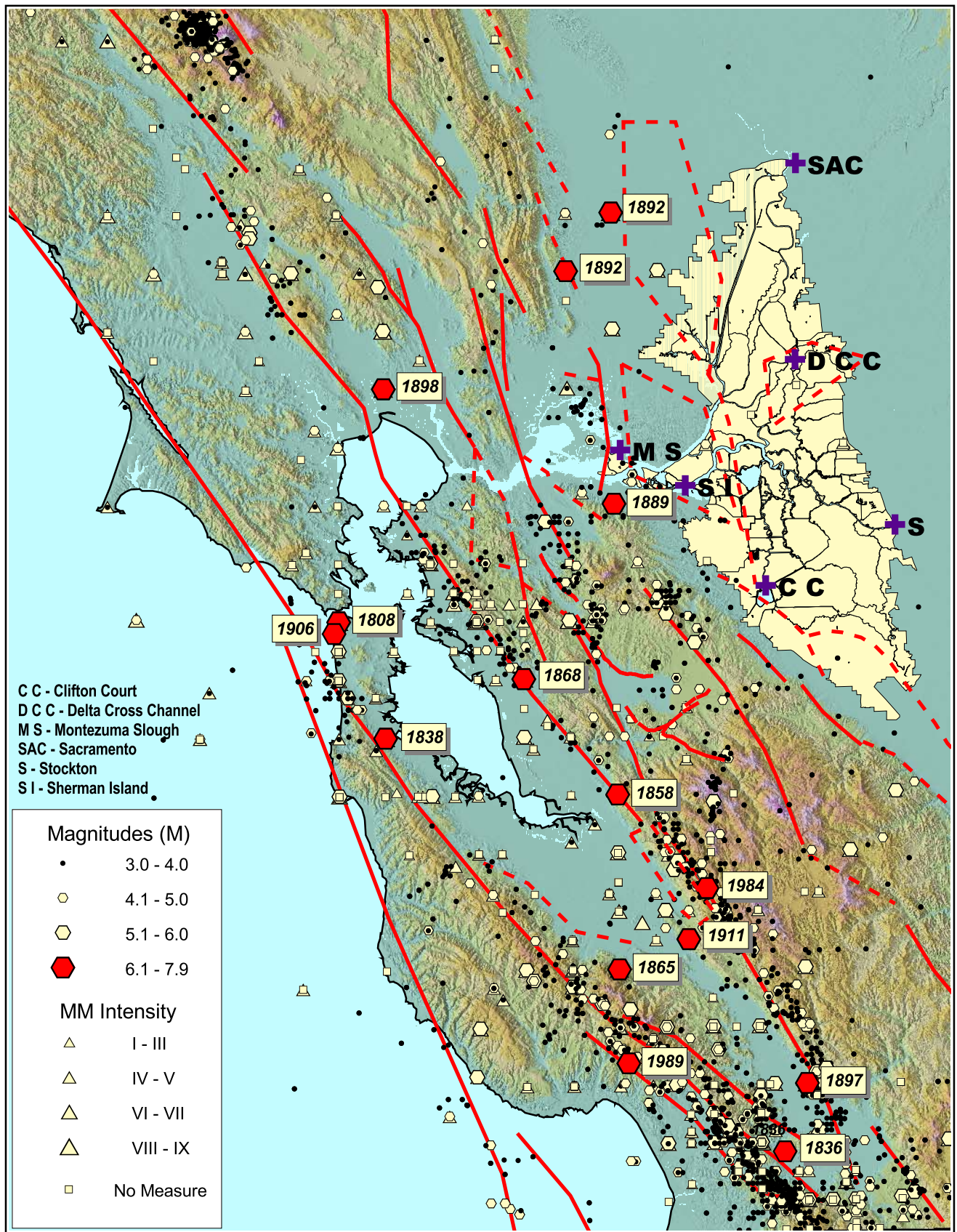
Topical Area: Seismology

Table 6b
Controlling Seismic Sources at a Return Period of 2,500 Years in 2005

Location	PGA	1.0 Sec SA
Clifton Court	Southern Midland	Southern Midland
Delta Cross Channel	Southern Midland Northern Midland Zone	Cascadia Subduction Zone Southern Midland
Montezuma Slough	Pittsburg-Kirby Hills	Pittsburg-Kirby Hills
Sacramento	Northern Midland Zone	Cascadia Subduction Zone
Sherman Island	Southern Midland Montezuma Hills Zone	Southern Midland
Stockton	Southern Midland	Cascadia Subduction Zone

Note:
Seismic sources are ordered by contribution.

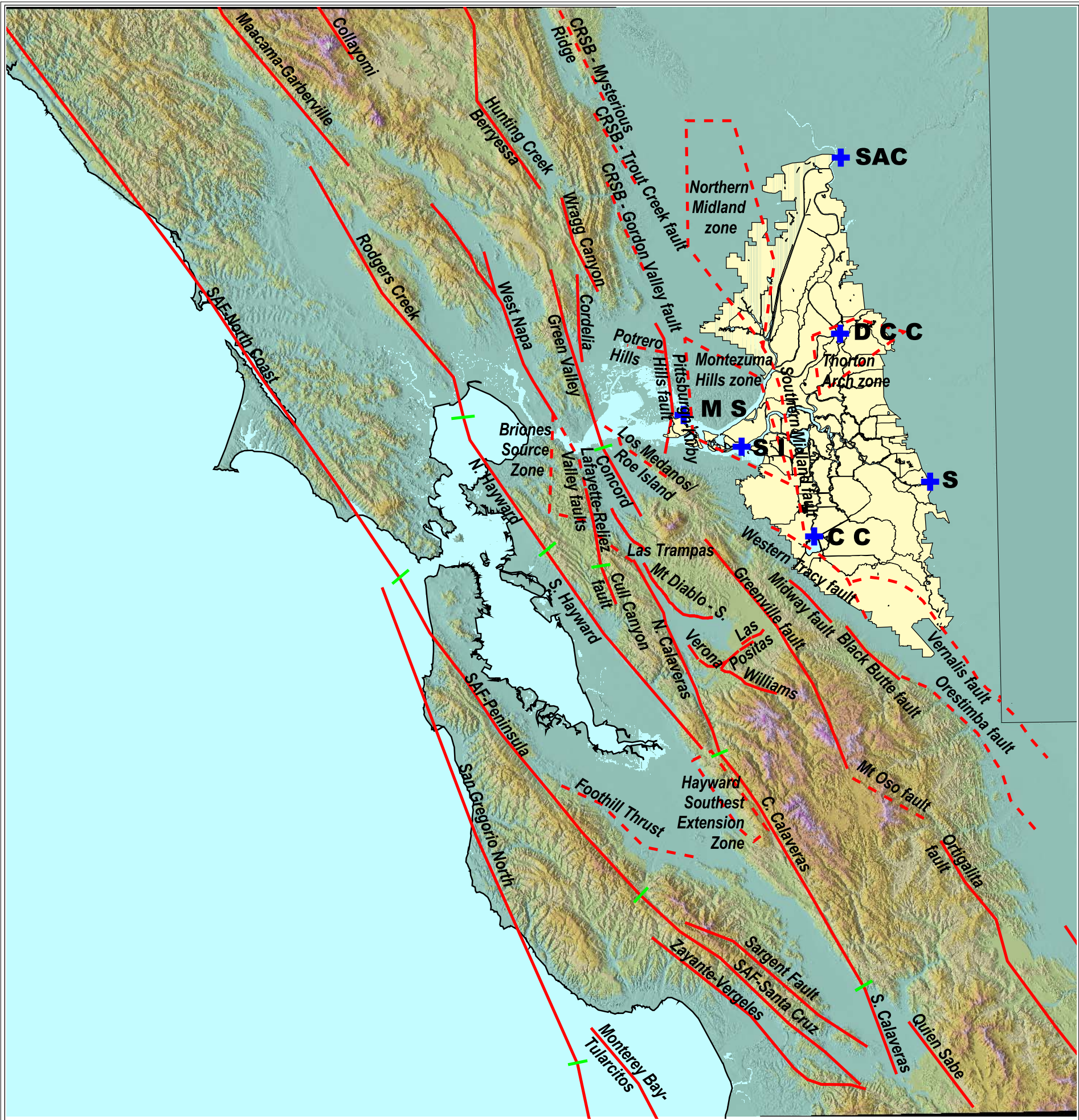
Figures



Delta Risk Analysis
 California
 Project No. 26815621

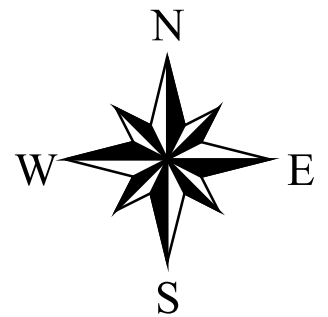
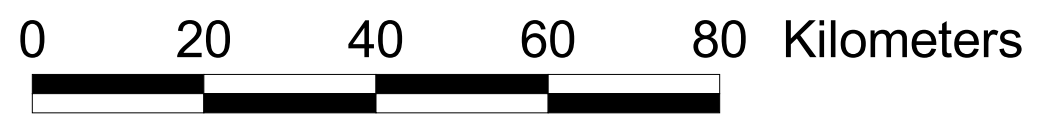
**ACTIVE FAULTS AND HISTORICAL SEISMICITY
 OF THE SAN FRANCISCO BAY REGION
 (M >= 3.0), 1800 - 2006**

Figure
 1



- Legal Delta Boundary V. 2002-4
- Surficial faults used in the hazard analysis
- Blind faults used in the hazard analysis
- Bounds of delta islands

CRSB - Coast Range Sierran Block
 SAF - San Andreas Fault



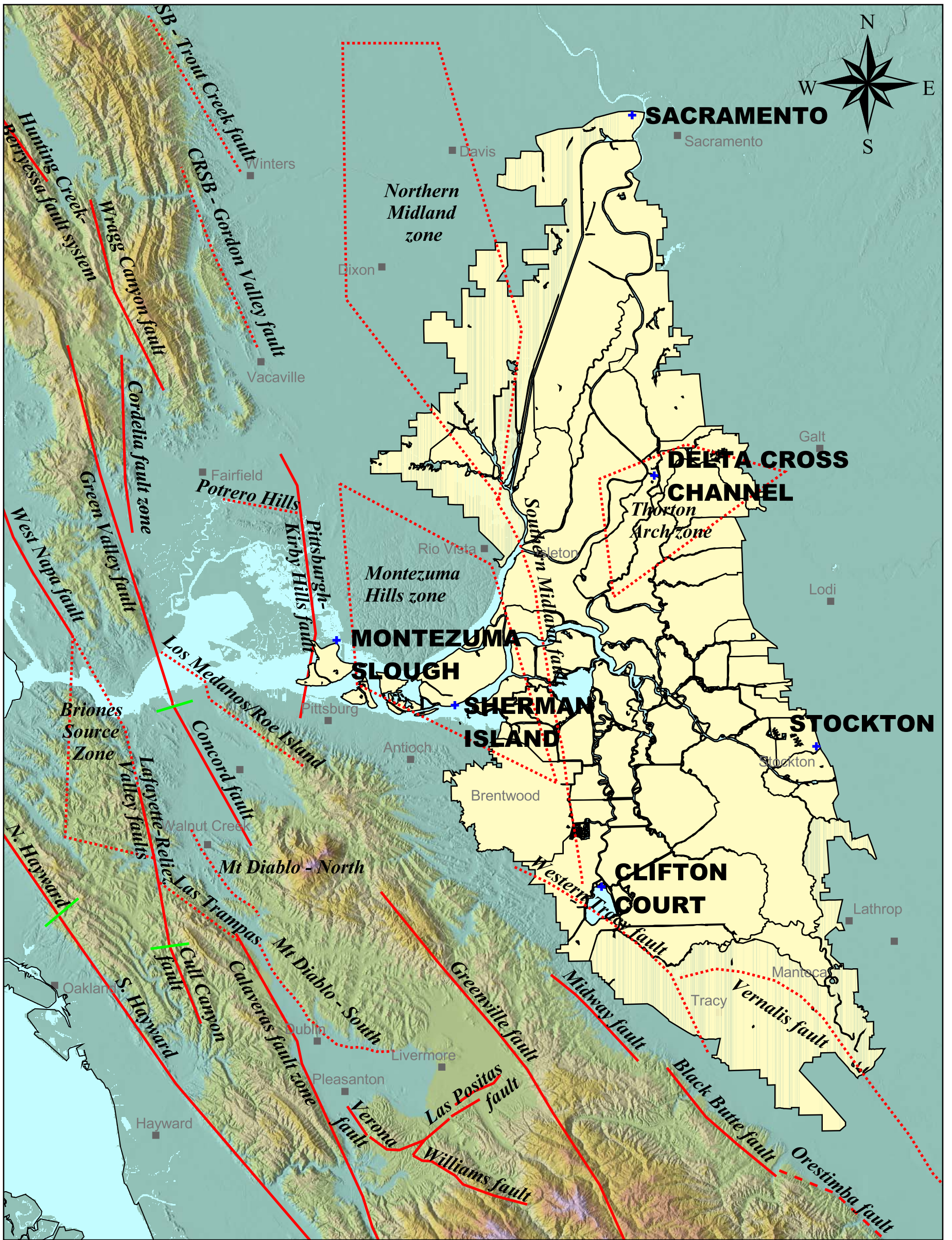
- C C - Clifton Court
- D C C - Delta Cross Channel
- M S - Montezuma Slough
- SAC - Sacramento
- S I - Sherman Island
- S - Stockton



Project No. #####
 Delta Risk Analysis
 California

**ACTIVE FAULTS OF THE
 SAN FRANCISCO BAY REGION**

**Figure
 2**



0 10 20 30 Miles

0 10 20 30 40 50 Kilometers

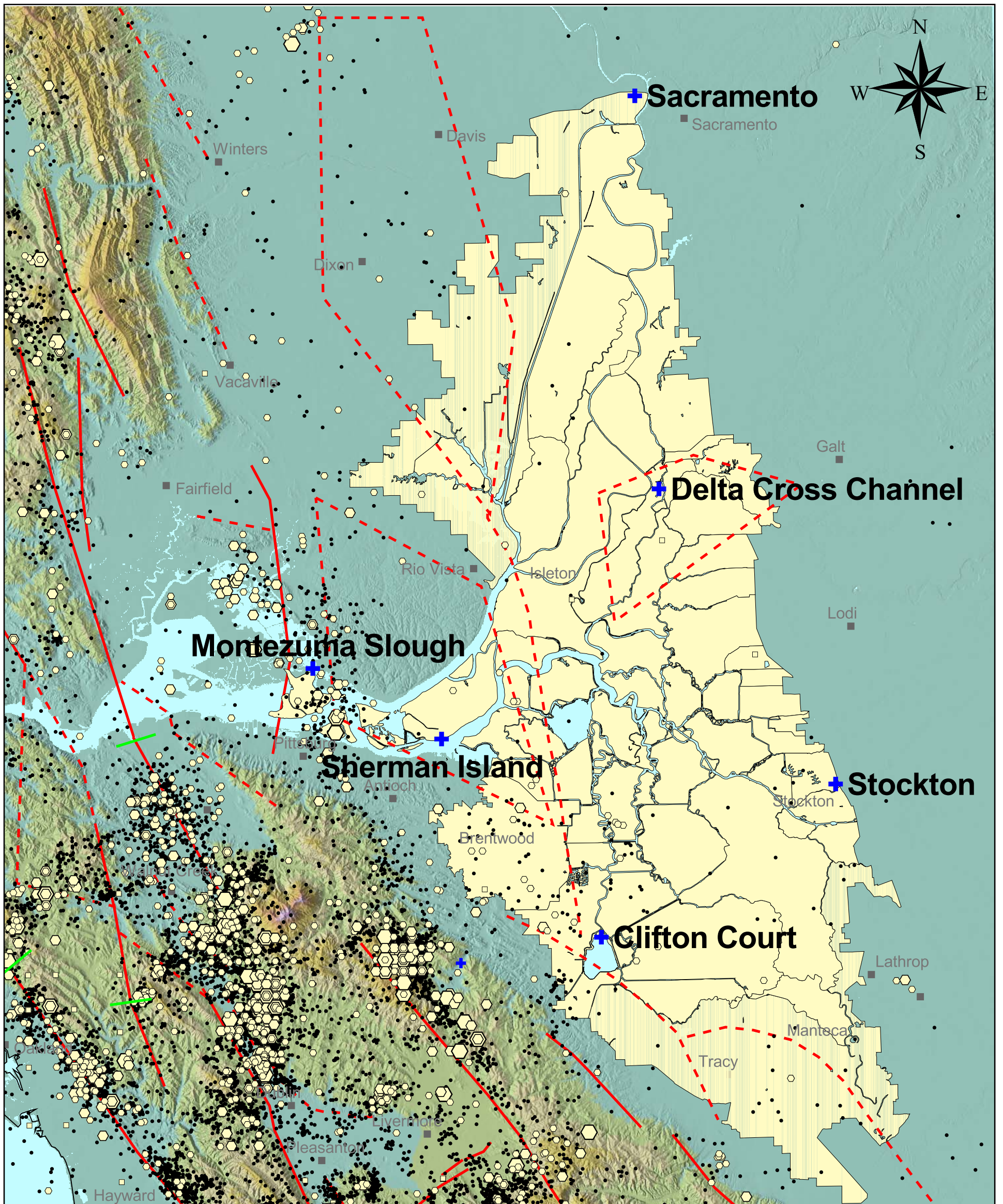
- Legal Delta Boundary V. 2002-4
- Surficial faults used in the hazard analysis
- Blind faults used in the hazard analysis
- Bounds of delta islands
- CRSB - Coast Range Sierran Block



Delta Risk Management Strategy, California
Project No. 26815431

ACTIVE FAULTS IN THE SITE REGION

Figure 3a



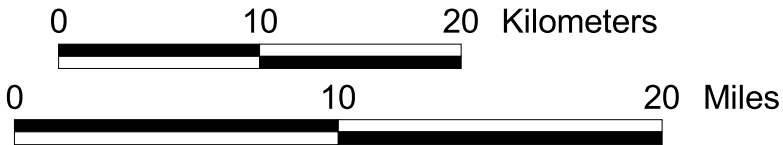
Magnitudes (M)	MM Intensity
• 0.0 - 1.9	△ I - III
○ 2.0 - 2.9	△ IV - V
◐ 3.0 - 3.9	△ VI - VII
◑ ≥ 4.0	△ VIII - IX
	□ No Measure

 Legal Delta Boundary V. 2002-4

 Surficial faults used in the hazard analysis

 Blind faults used in the hazard analysis

 Bounds of delta islands

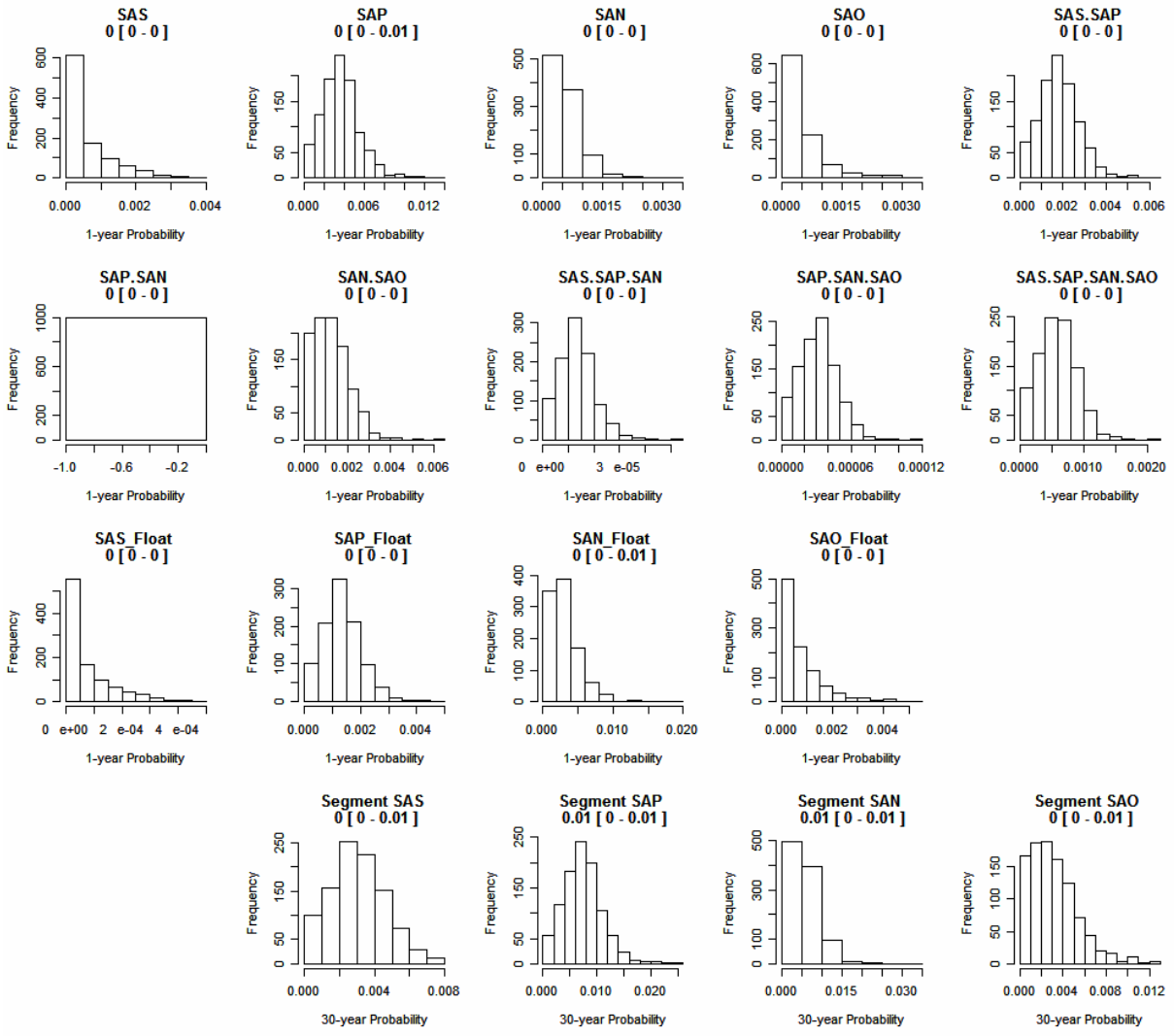


Delta Risk Management Strategy, California

Project No. 26815431

CONTEMPORARY SEISMICITY (1966 TO 2006) IN THE SITE REGION

Figure 3b



Delta Risk\Figures\TimePred2005.grf 1/31/07 3:45 PM

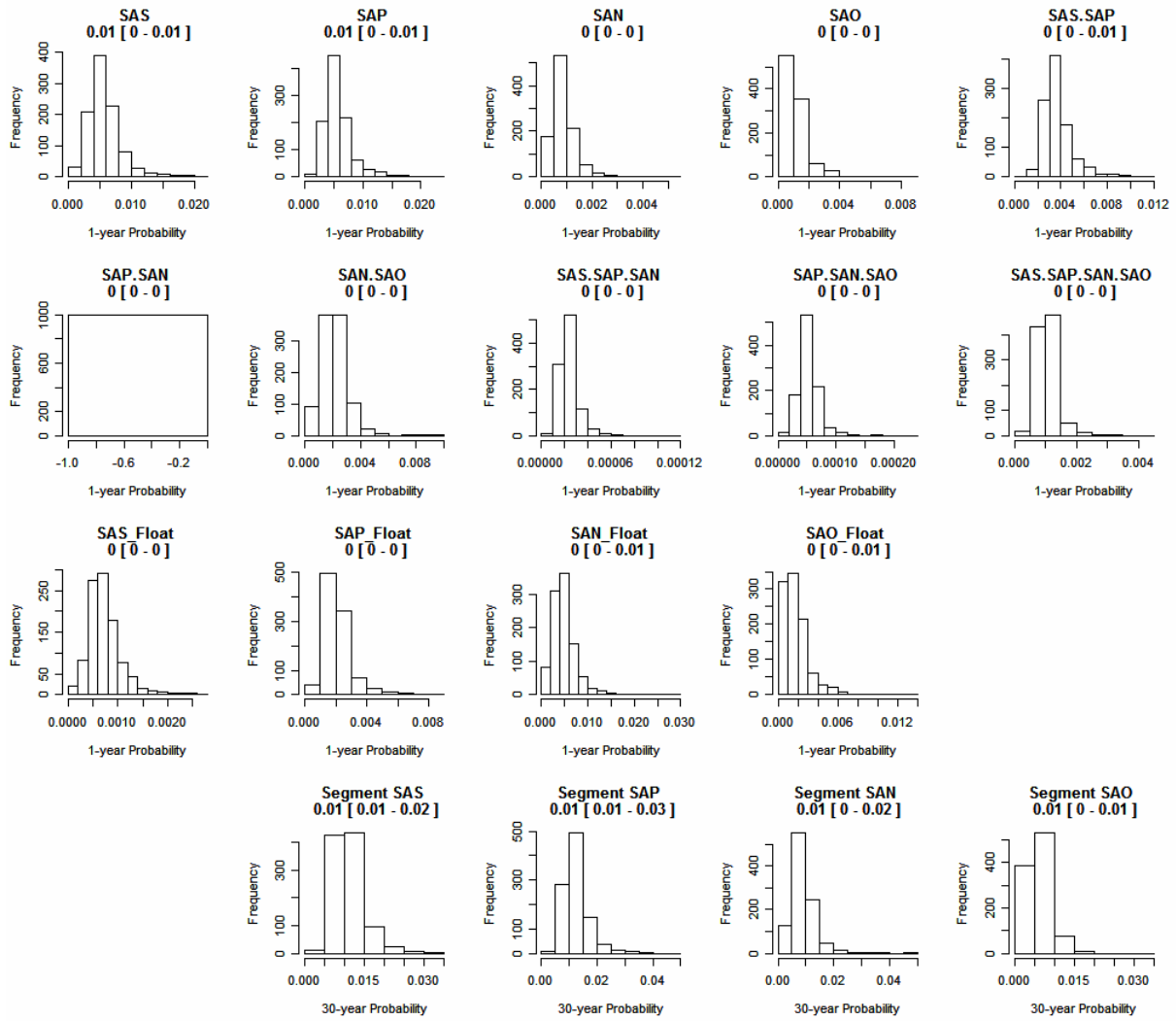


DELTA RISK
MANAGEMENT STRATEGY
California

Project No. 26815621

Time-Dependent Probabilities
for the San Andreas Rupture Scenarios for 2005

Figure
4

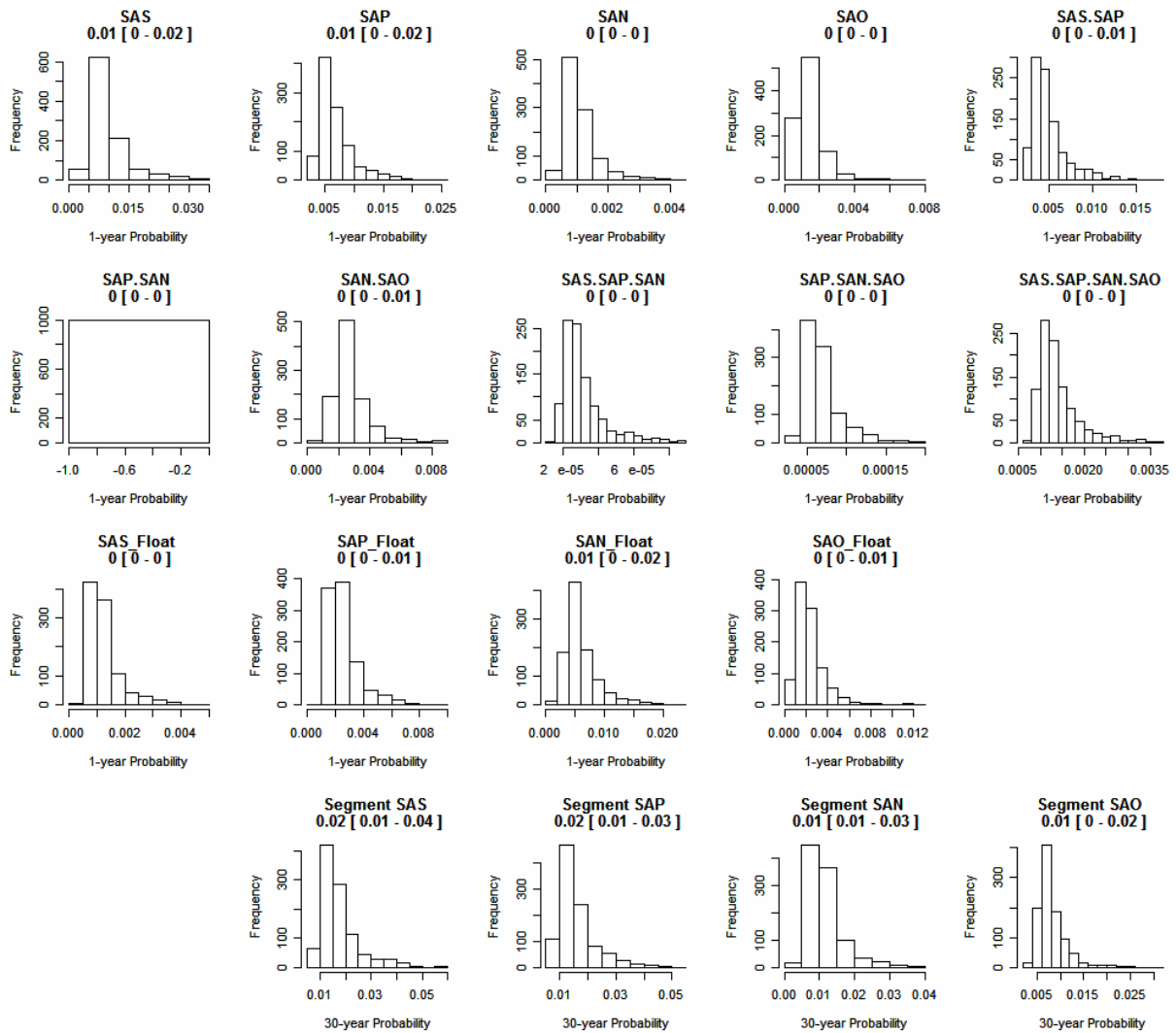


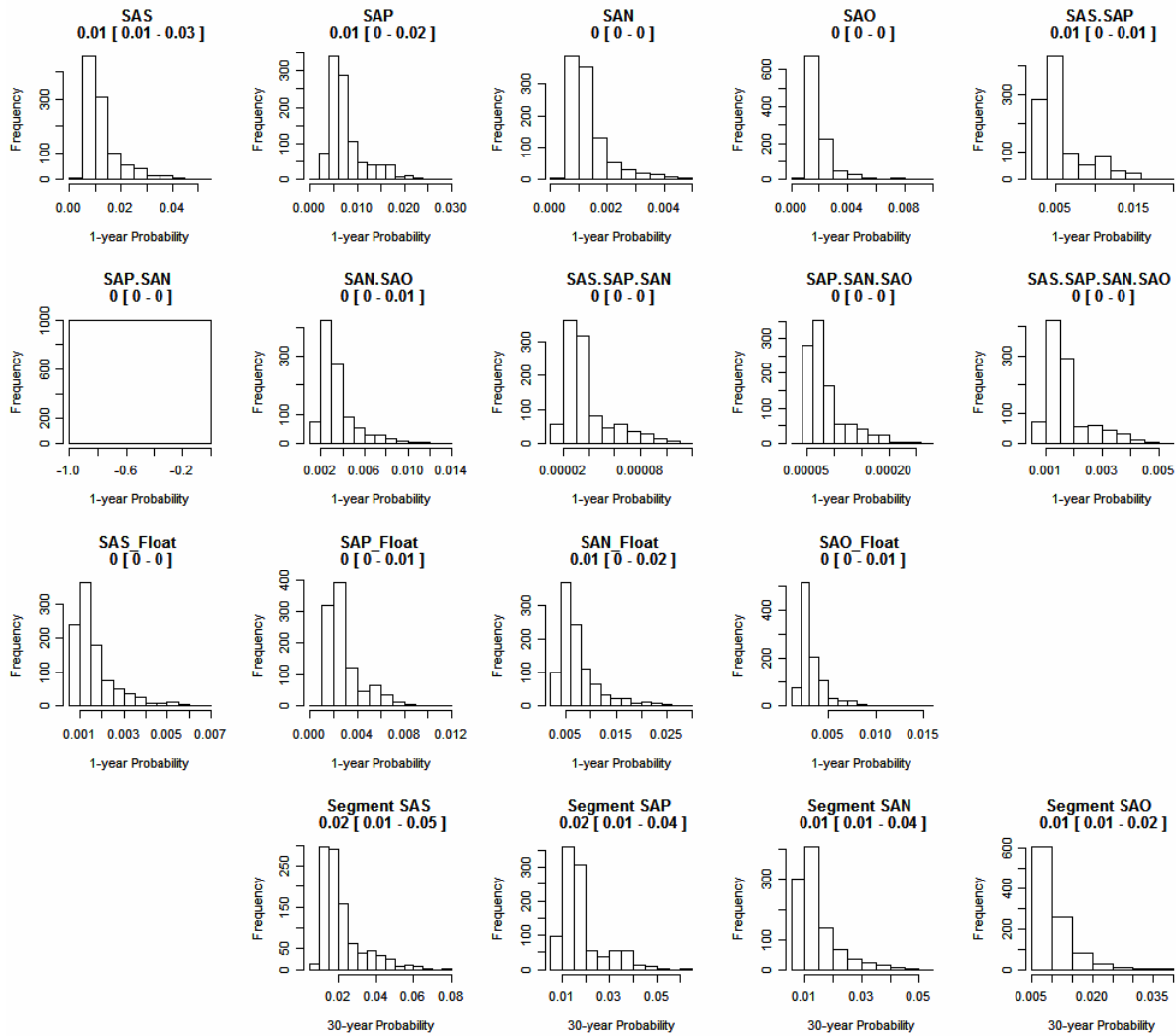
DELTA RISK
MANAGEMENT STRATEGY
California

Project No. 26815621

Time-Dependent Probabilites
for the San Andreas Rupture Scenarios for 2050

Figure
5



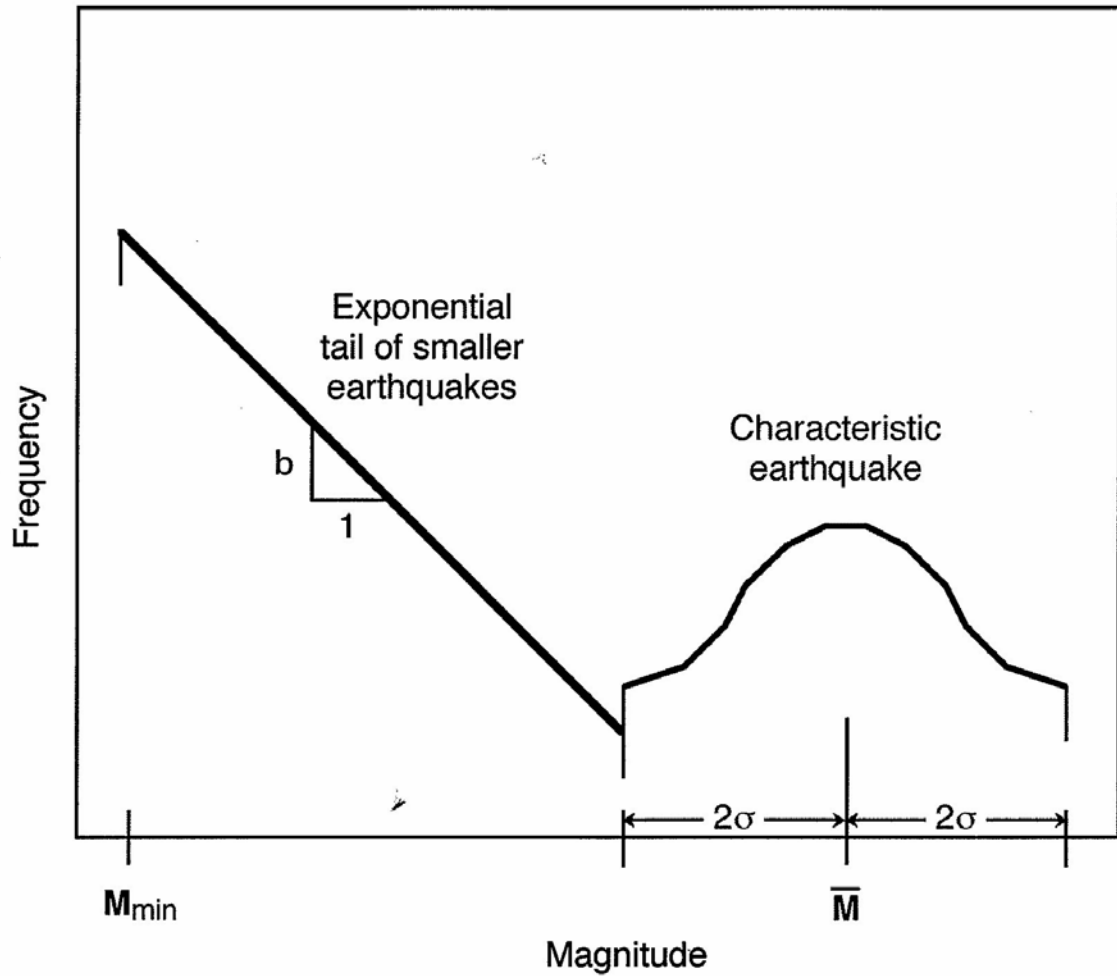


DELTA RISK
MANAGEMENT STRATEGY
California

Project No. 26815621

Time-Dependent Probabilities
for the San Andreas Rupture Scenarios for 2200

Figure
7



Source: WGCEP (2003) Figure 4.1

Delta Risk\Figures\Magpdf.grf 1/31/07:3:42 PM

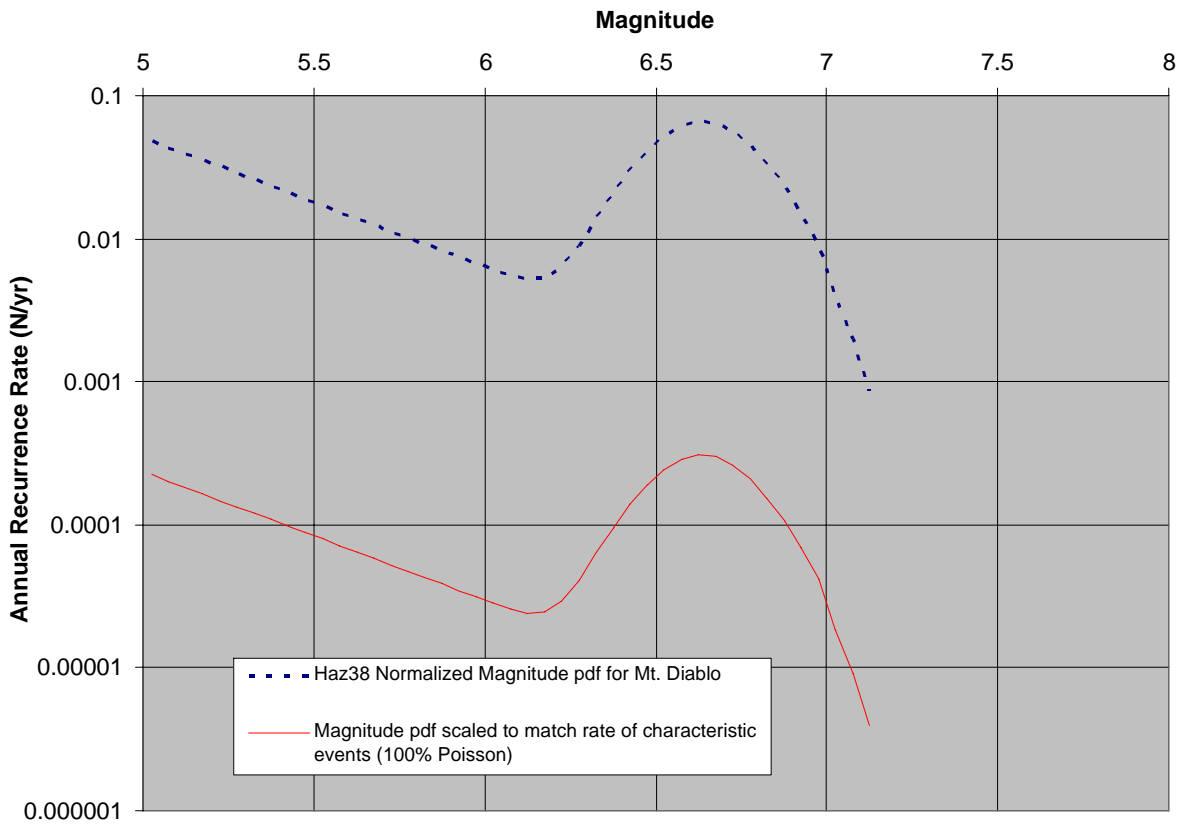


DELTA RISK
MANAGEMENT STRATEGY
California

Project No. 26815621

ILLUSTRATION OF MAGNITUDE PROBABILITY
DENSITY FUNCTION FOR TIME-DEPENDENT
SOURCES

Figure
8



Delta Risk\Figures\MtDiabloMagpdf.grf 1/31/073:43 PM

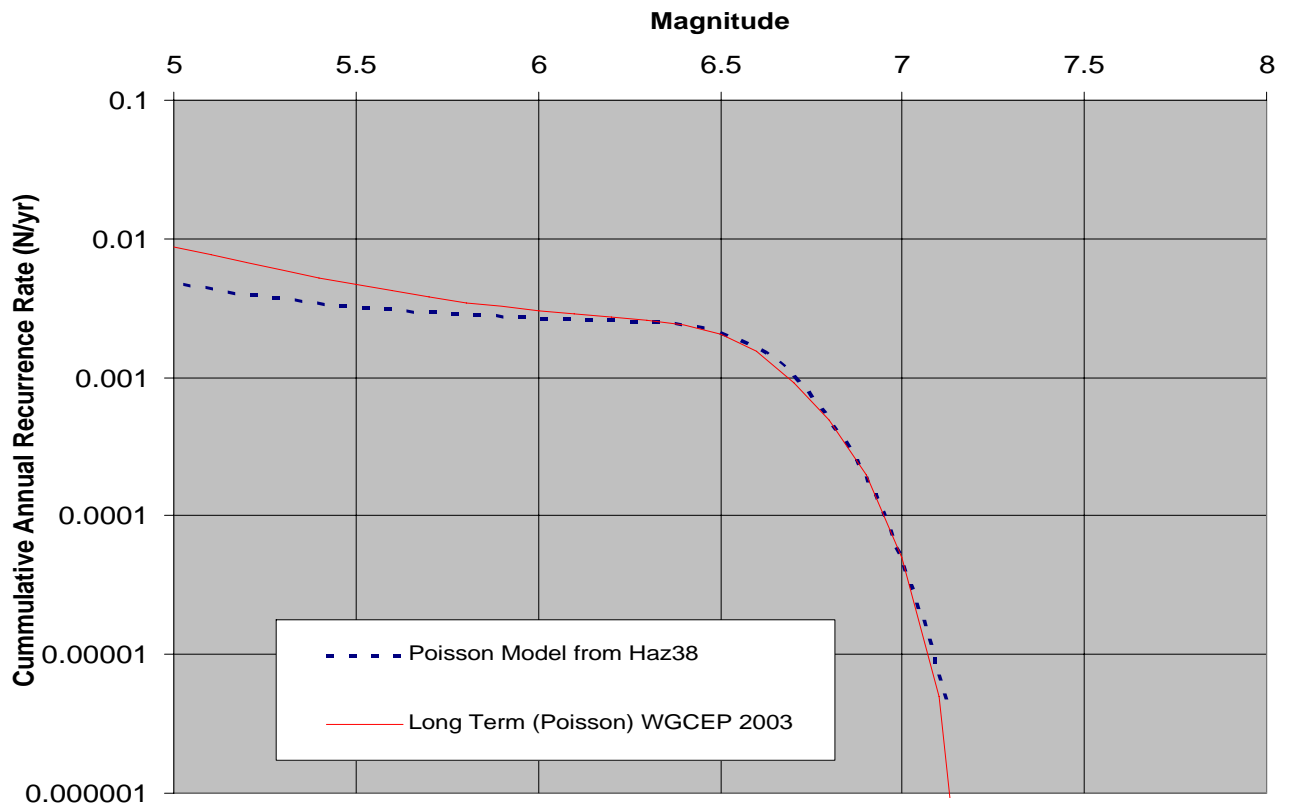


DELTA RISK
MANAGEMENT STRATEGY
California

Project No. 26815621

MAGNITUDE PROBABILITY DENSITY FUNCTION
FOR THE MT. DIABLO FAULT

Figure
9



Delta Risk\Figures\MtDiabloRecur.grf 1/31/07 3:43 PM

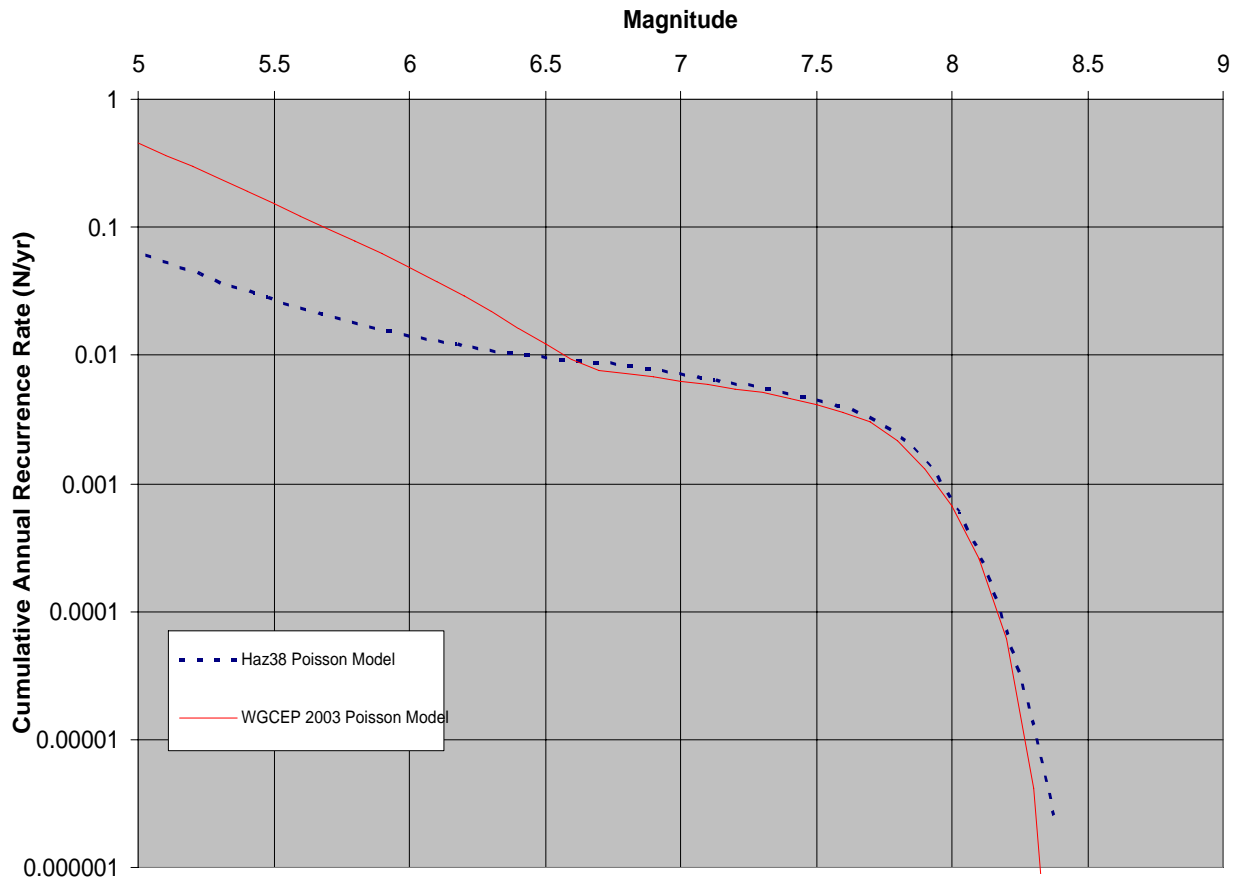


DELTA RISK
MANAGEMENT STRATEGY
California

Project No. 26815621

CUMULATIVE ANNUAL RECURRENCE CURVE
FOR THE MT. DIABLO FAULT

Figure
10



Delta Risk\Figures\SARrecur.grf 1/31/073:44 PM

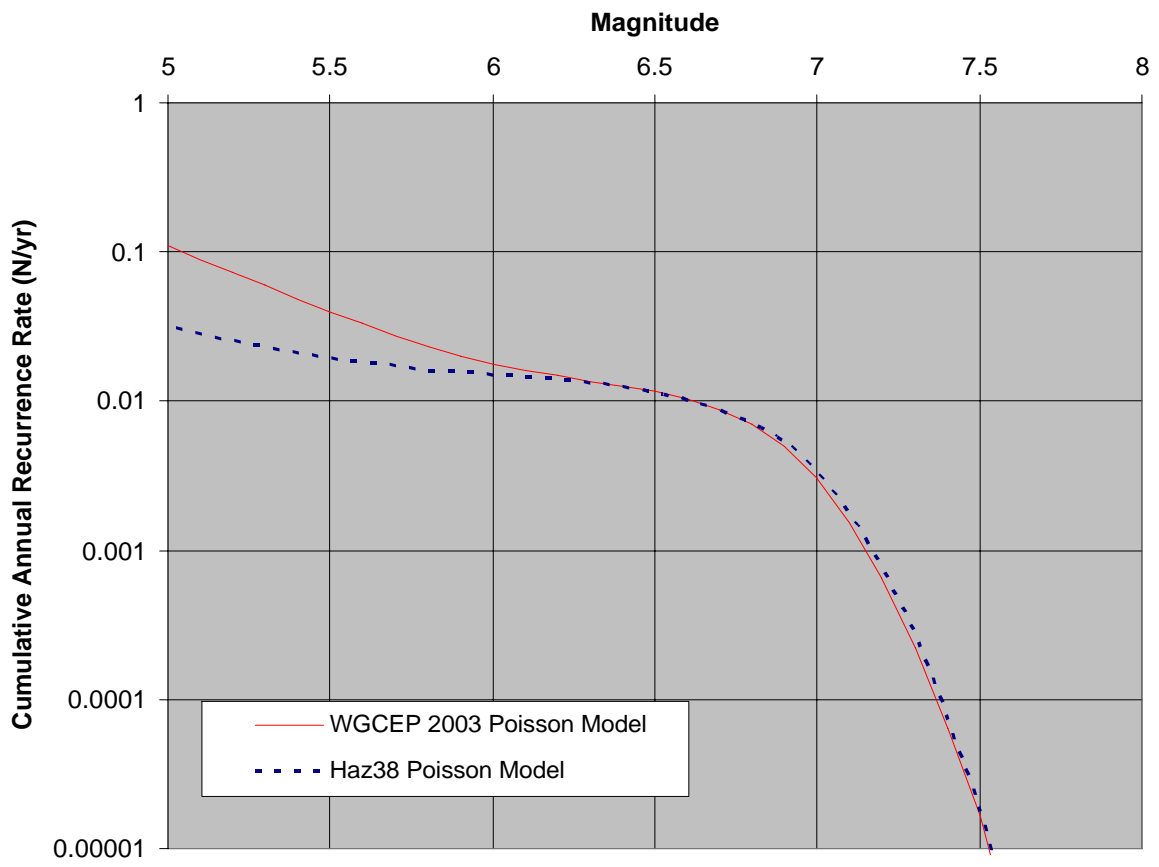


DELTA RISK
MANAGEMENT STRATEGY
California

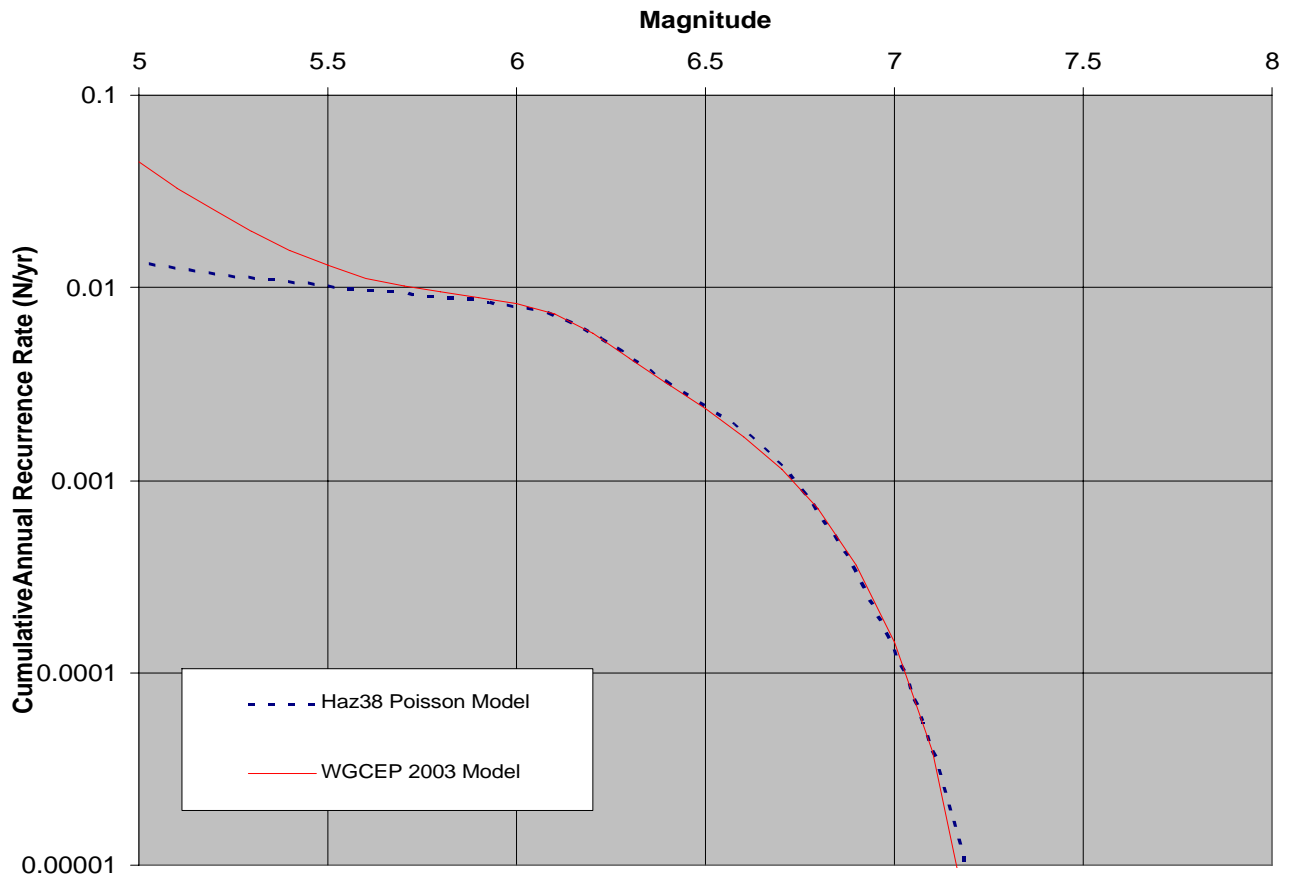
Project No. 26815621

CUMULATIVE ANNUAL RECURRENCE CURVE
FOR THE SAN ANDREAS FAULT

Figure
11



Delta Risk\Figures\HayRCRecur.grf 1/31/07 3:42 PM



Delta Risk\Figures\ConGV\Recur.grf 1/31/07 3:41 PM

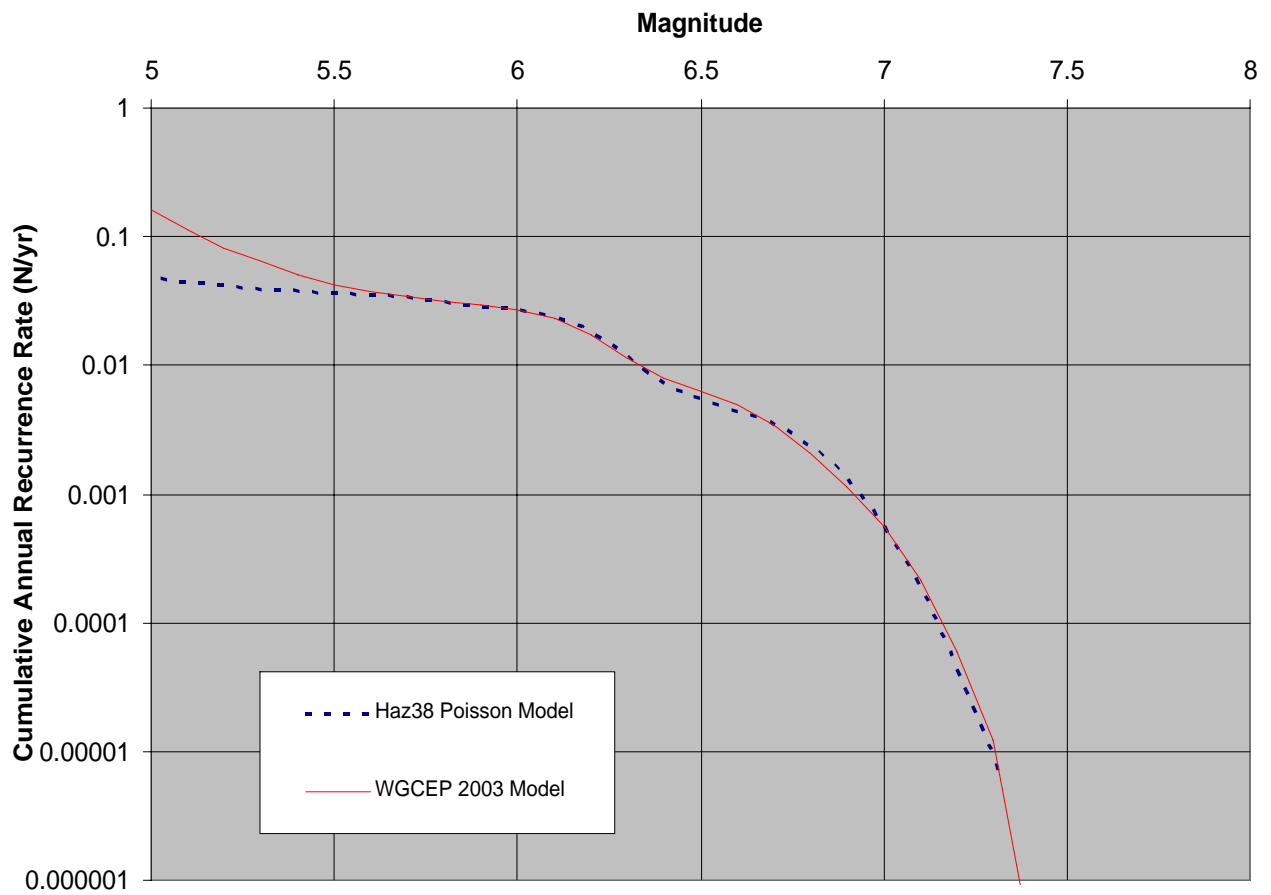


DELTA RISK
MANAGEMENT STRATEGY
California

Project No. 26815621

CUMULATIVE ANNUAL RECURRENCE CURVE
FOR THE CONCORD-GREEN VALLEY FAULT

Figure
13



Delta Risk\Figures\CaliRecur.grf 1/31/07 3:40 PM

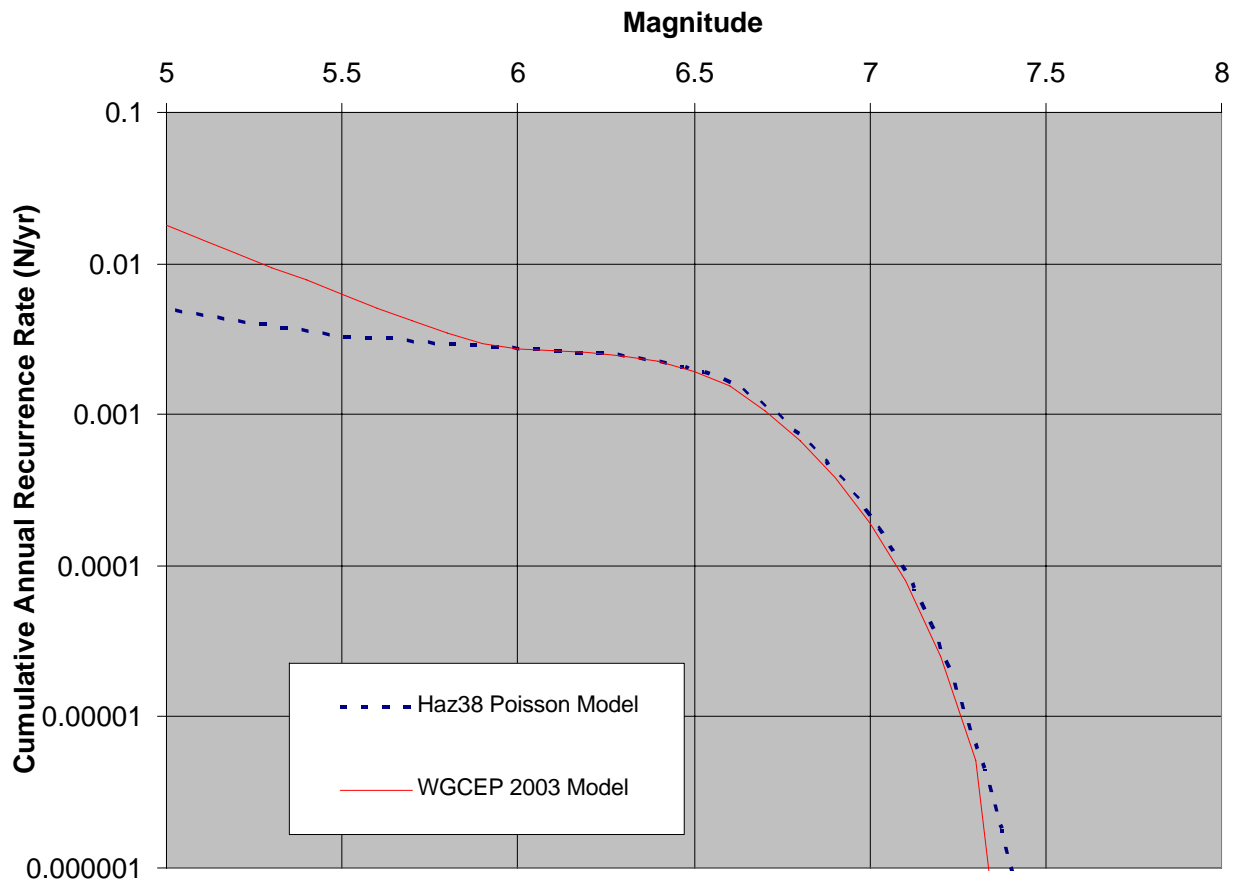


DELTA RISK
MANAGEMENT STRATEGY
California

Project No. 26815621

CUMULATIVE ANNUAL RECURRENCE CURVE
FOR THE CALAVERAS FAULT

Figure
14



Delta Risk\Figures\GreenRecur.grf 1/31/07 3:41 PM

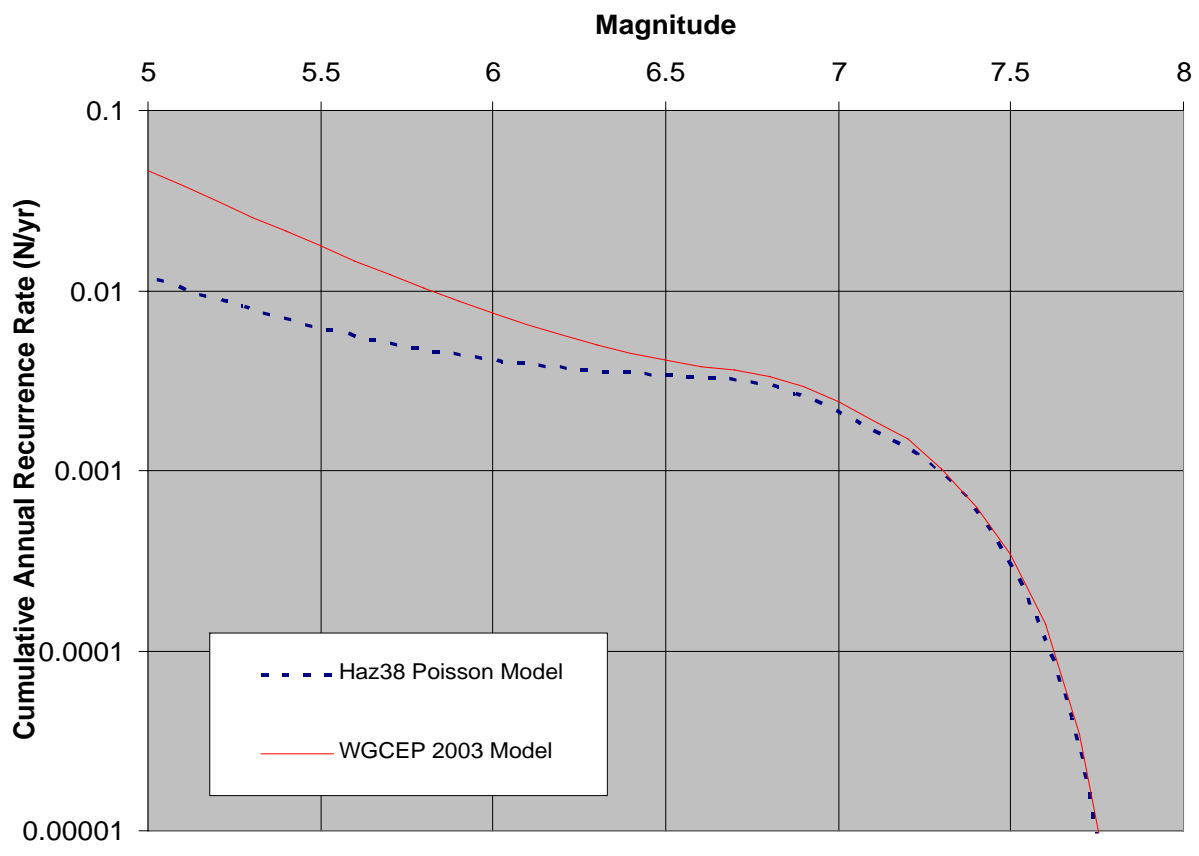


DELTA RISK
MANAGEMENT STRATEGY
California

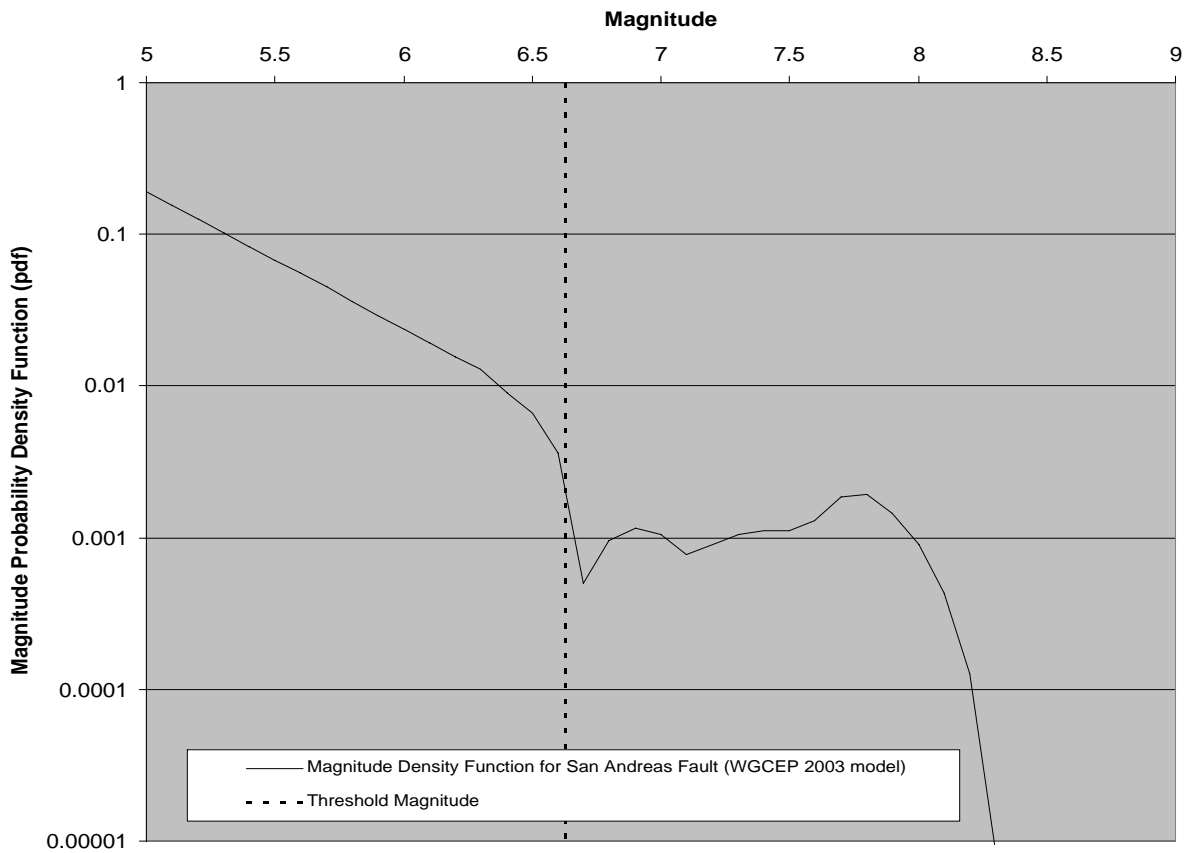
Project No. 26815621

CUMULATIVE ANNUAL RECURRENCE CURVE
FOR THE GREENVILLE FAULT

Figure
15



Delta Risk\Figures\SGRecur.grf 1/31/07 3:45 PM



Delta Risk\Figures\SAMagPdfRecur.grf 1/31/07 3:43 PM

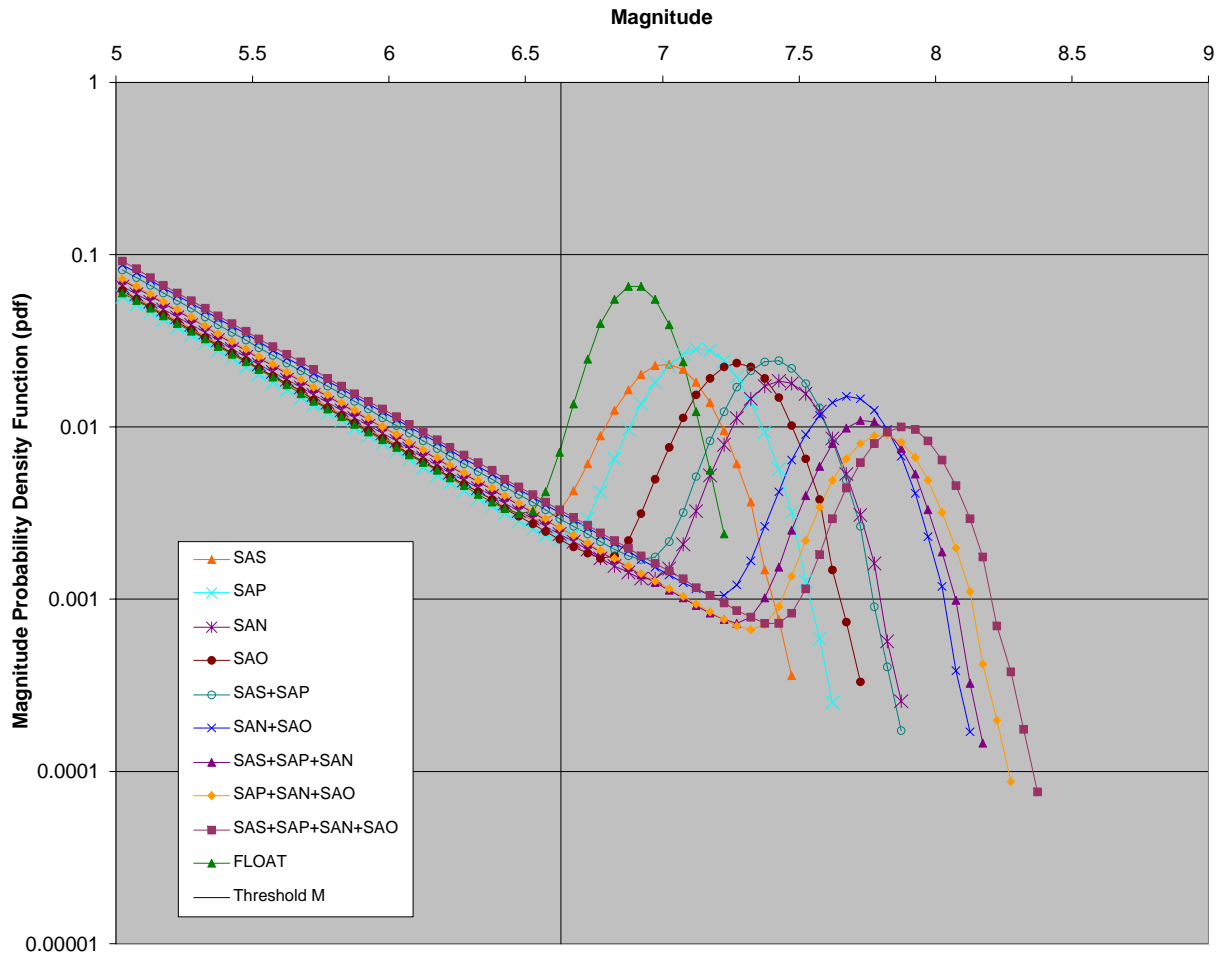


DELTA RISK
MANAGEMENT STRATEGY
California

Project No. 26815621

MAGNITUDE PROBABILITY DENSITY FUNCTION
FOR THE SAN ANDREAS FAULT
FROM WGCEP (2003)

Figure
17



Delta Risk\Figures\SARupsMagPdfs.grf 1/31/07 3:44 PM

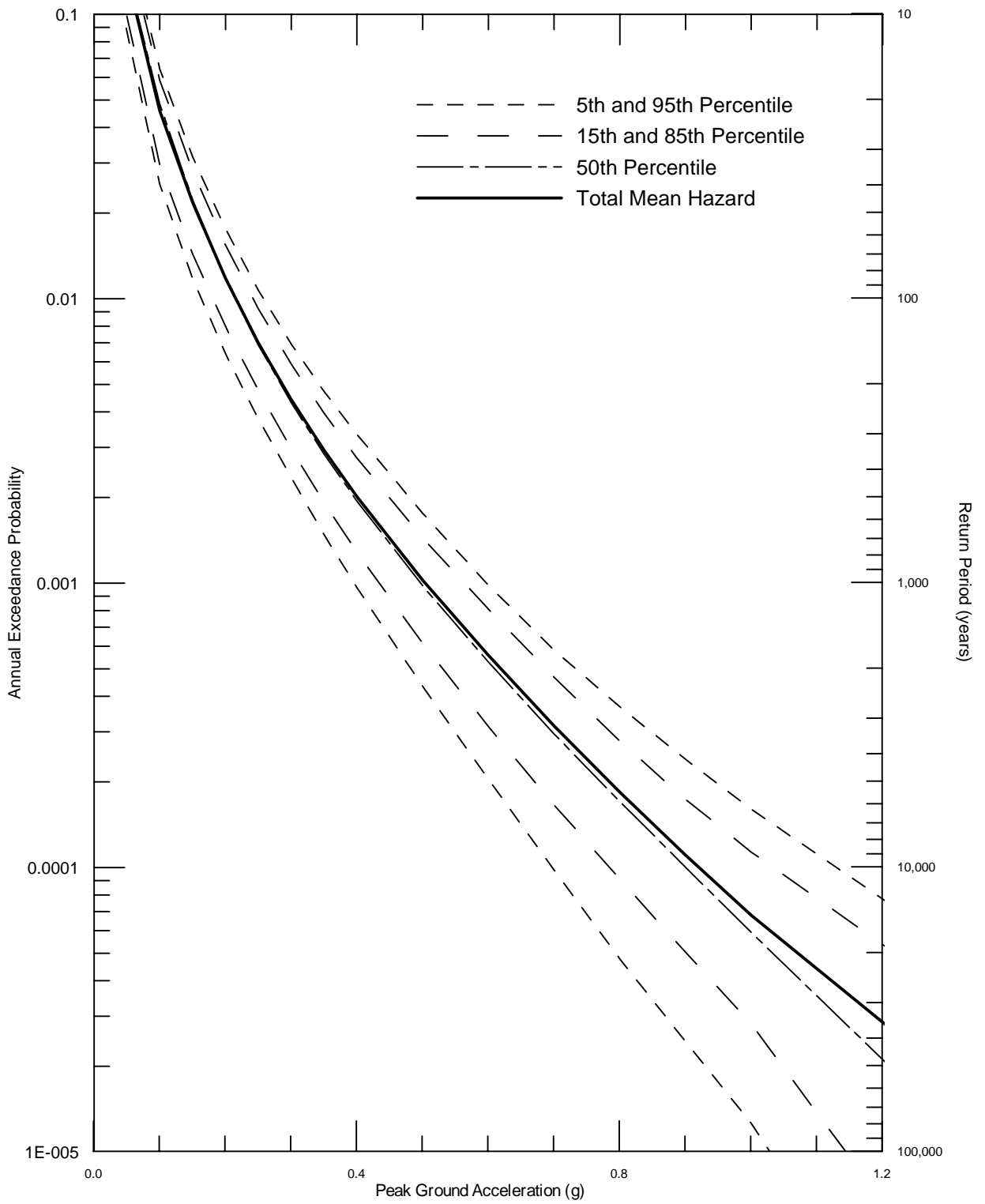


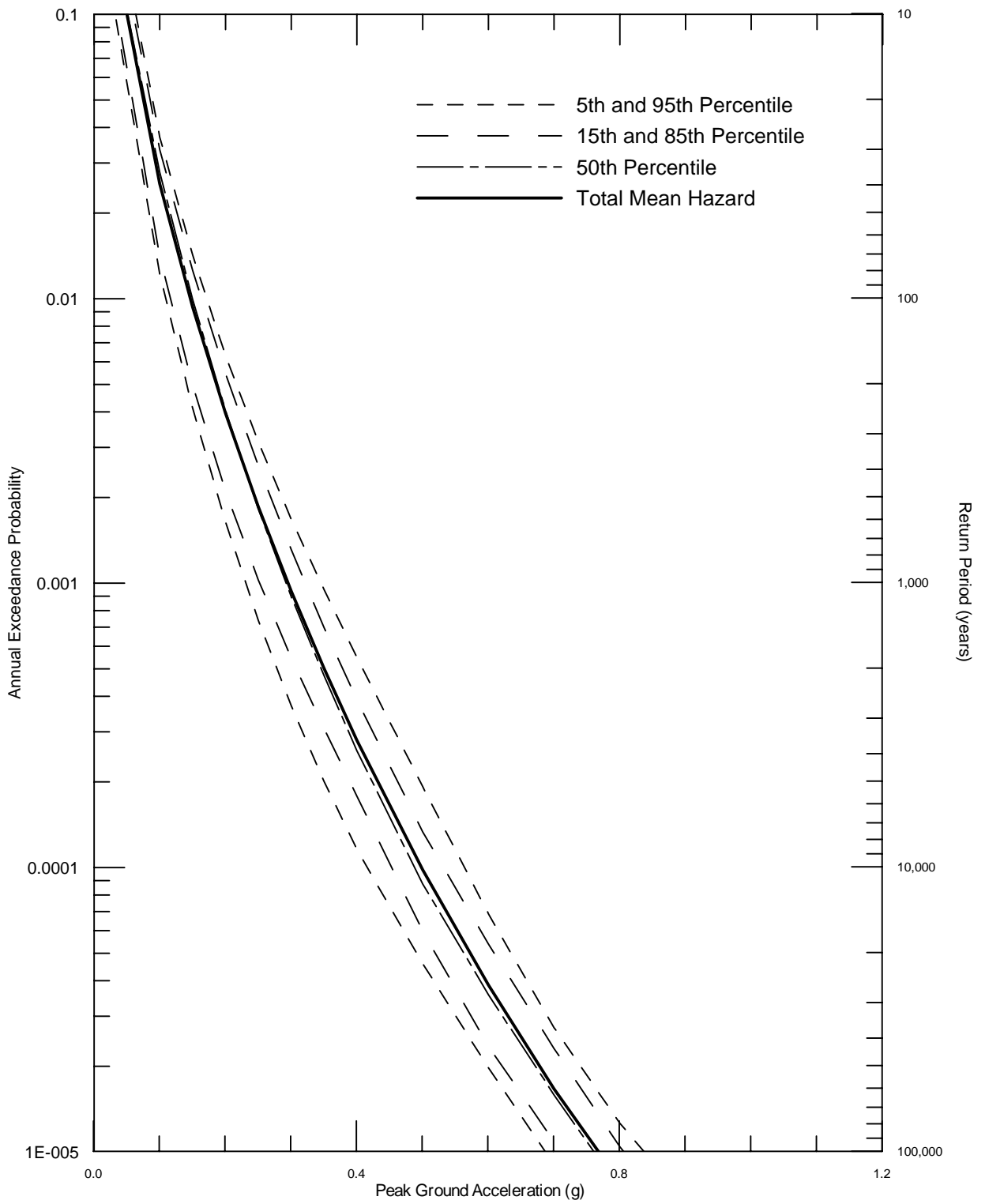
DELTA RISK
MANAGEMENT STRATEGY
California

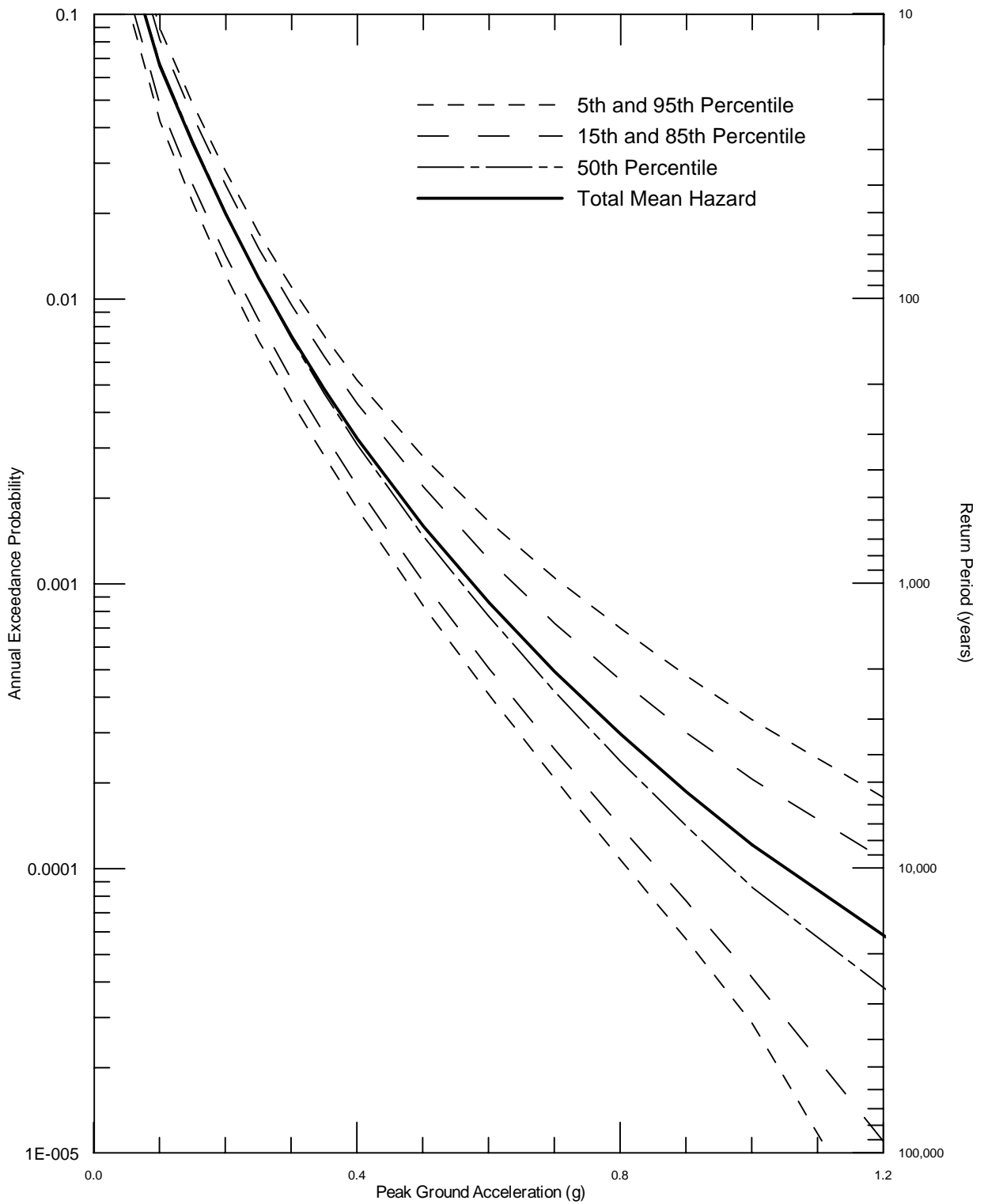
Project No. 26815621

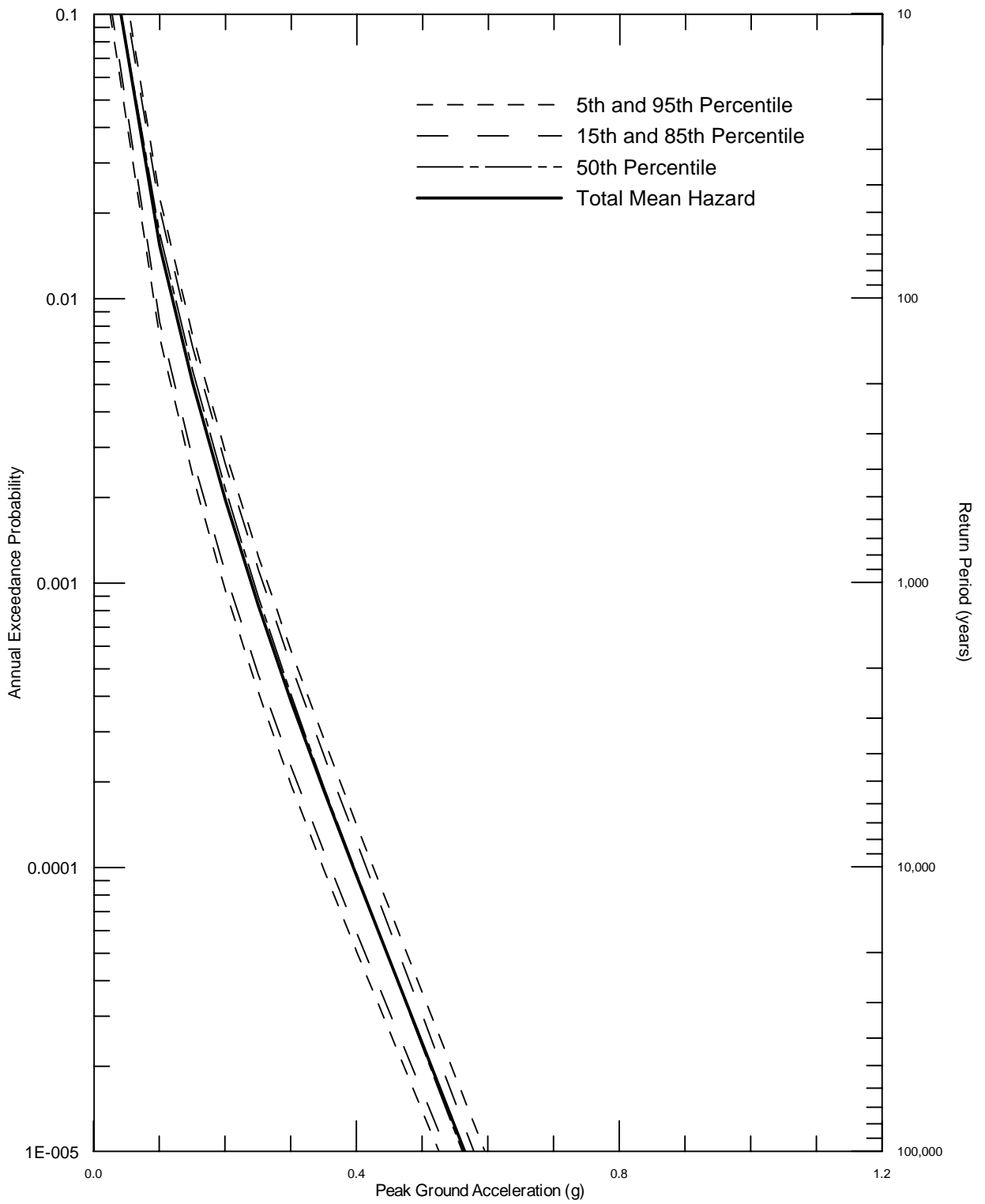
MAGNITUDE PROBABILITY DENSITY
FUNCTIONS FOR THE SAN ANDREAS
RUPTURE SOURCES

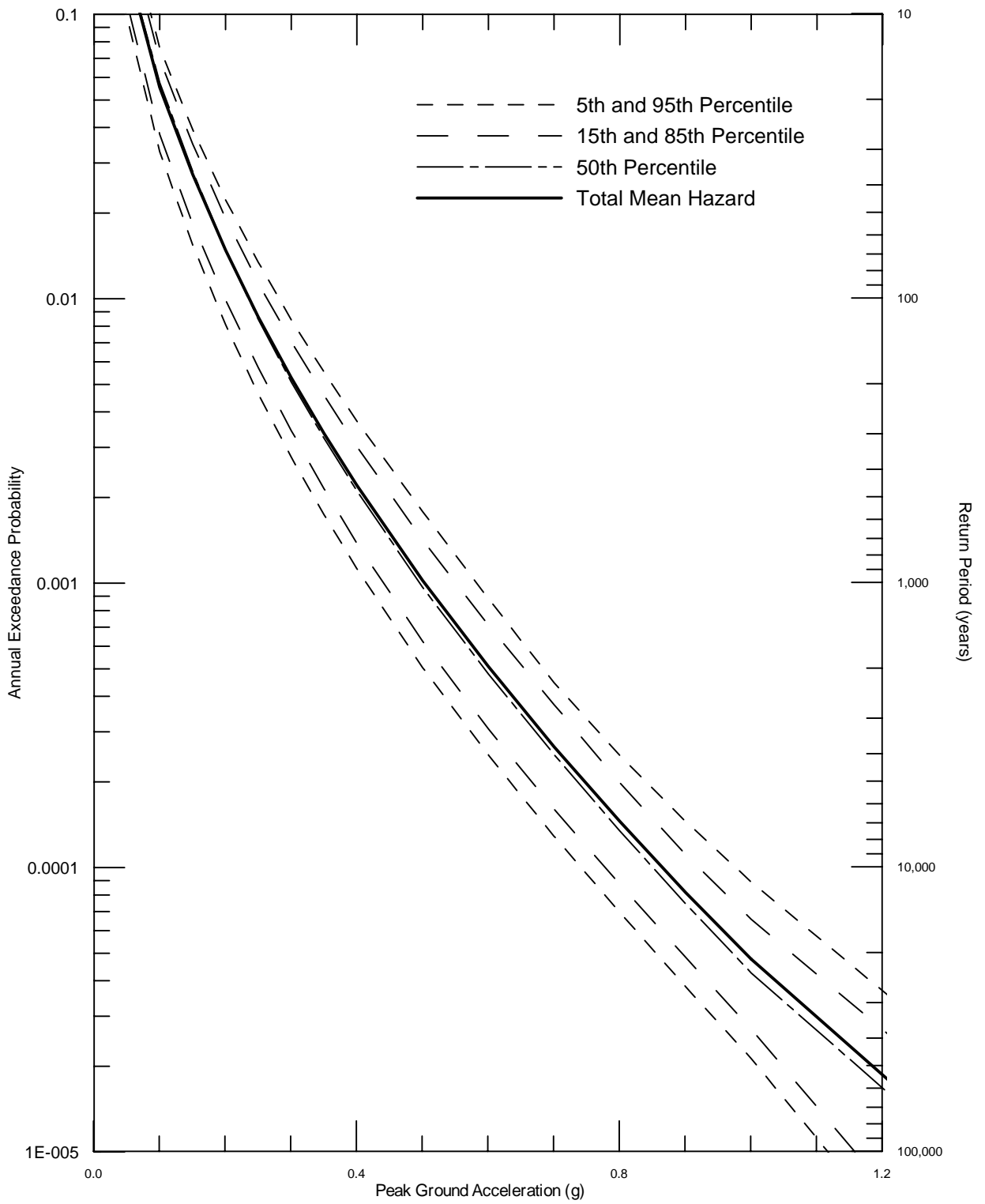
Figure
18

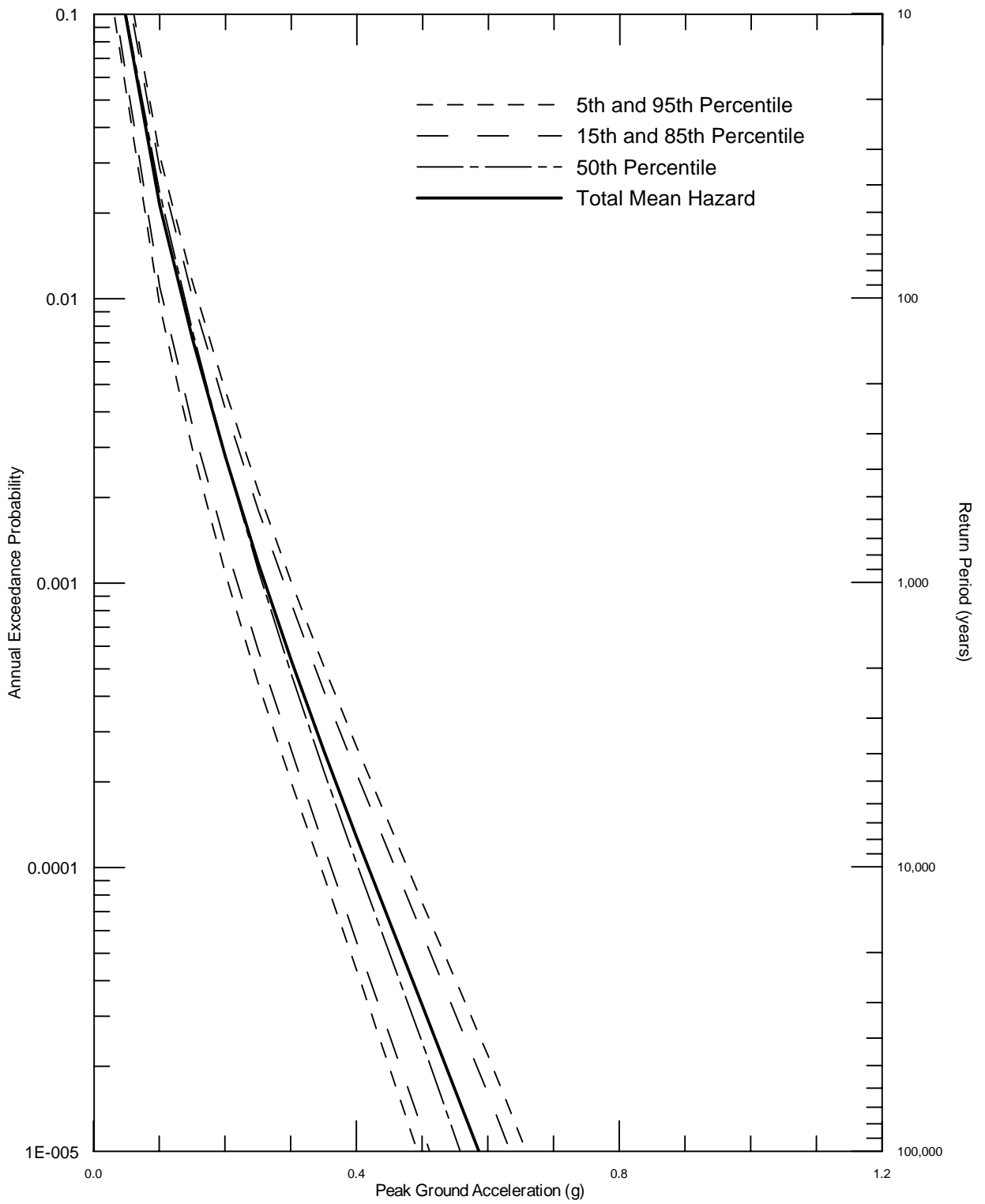










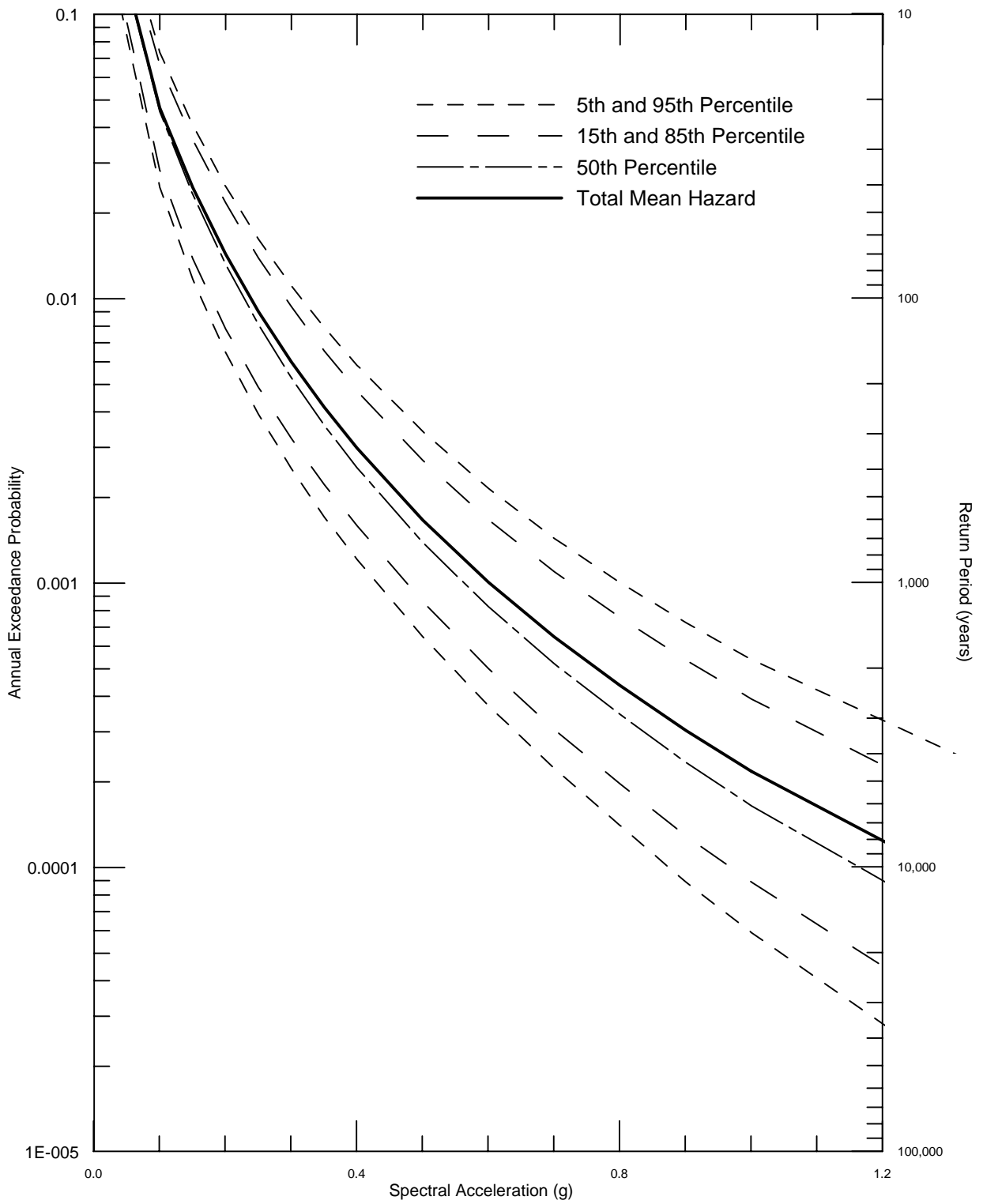


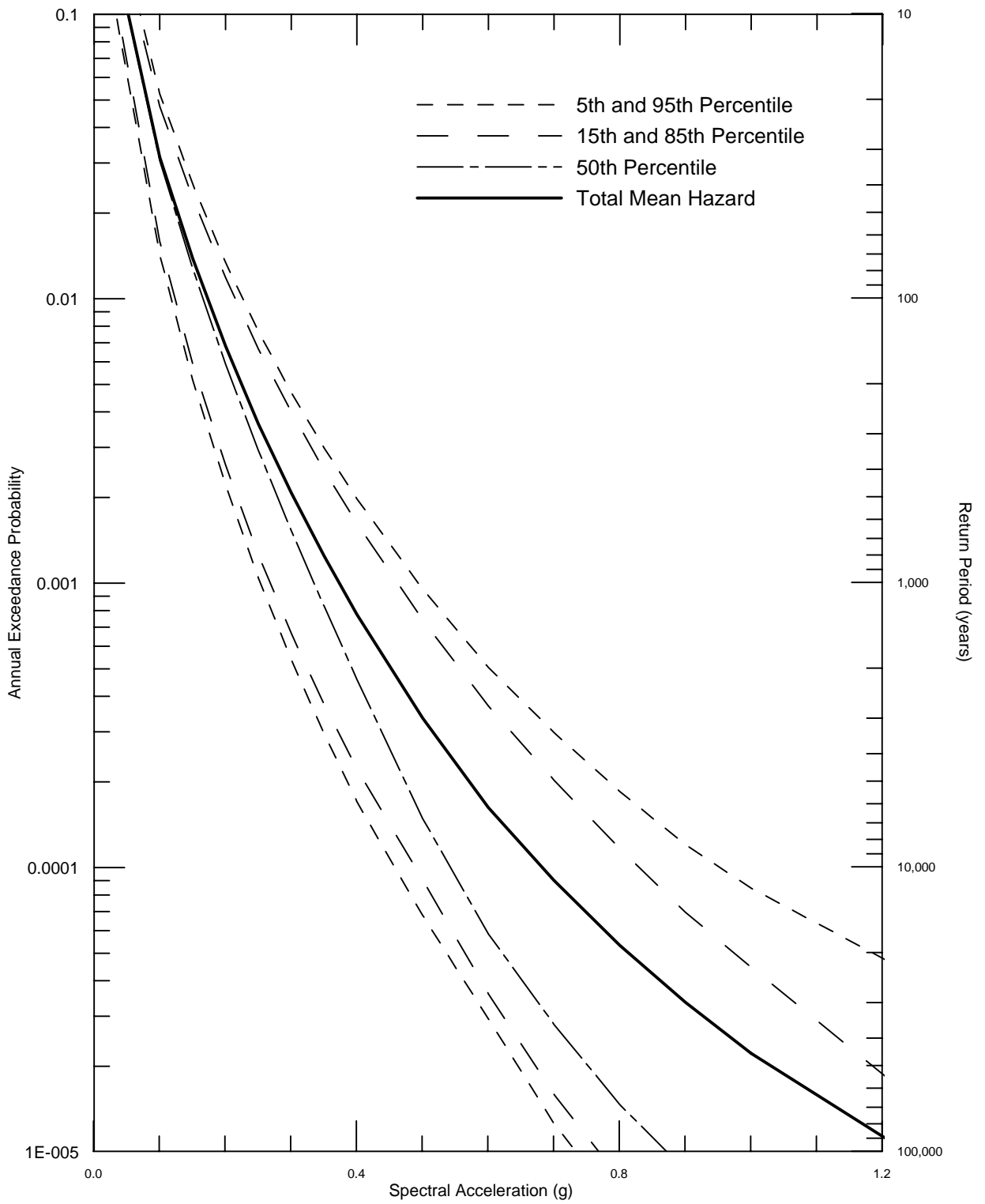
DELTA RISK
MANAGEMENT STRATEGY
CALIFORNIA

Project No. 26815900

TIME DEPENDENT SEISMIC HAZARD CURVES
FOR MEAN PEAK HORIZONTAL ACCELERATION
FOR STOCKTON FOR 2005

Figure
24



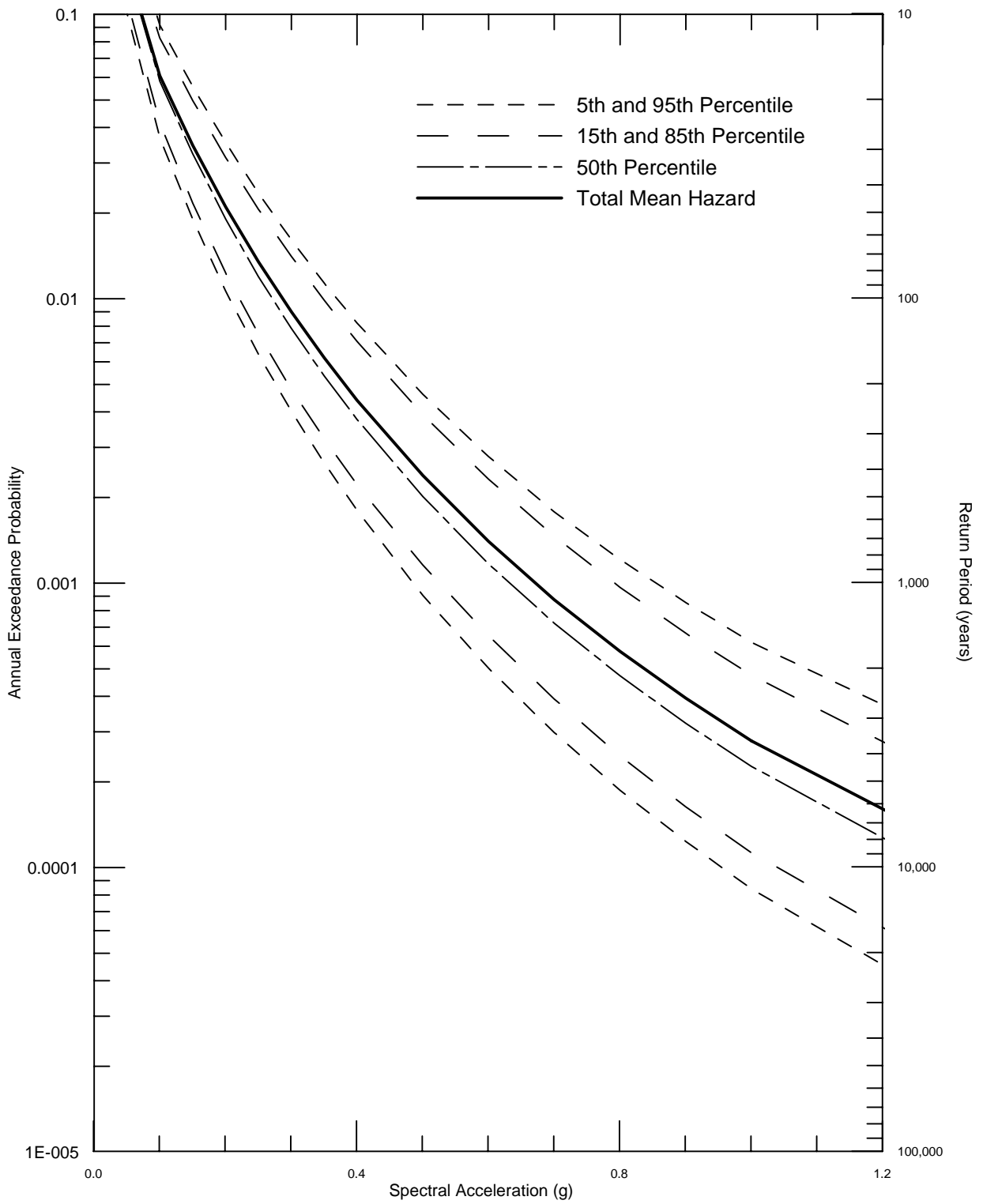


DELTA RISK
MANAGEMENT STRATEGY
CALIFORNIA

Project No. 26815900

TIME DEPENDENT SEISMIC HAZARD CURVES
FOR 1.0 SEC HORIZONTAL SPECTRAL
ACCELERATION FOR DELTA CROSS CHANNEL
FOR 2005

Figure
26

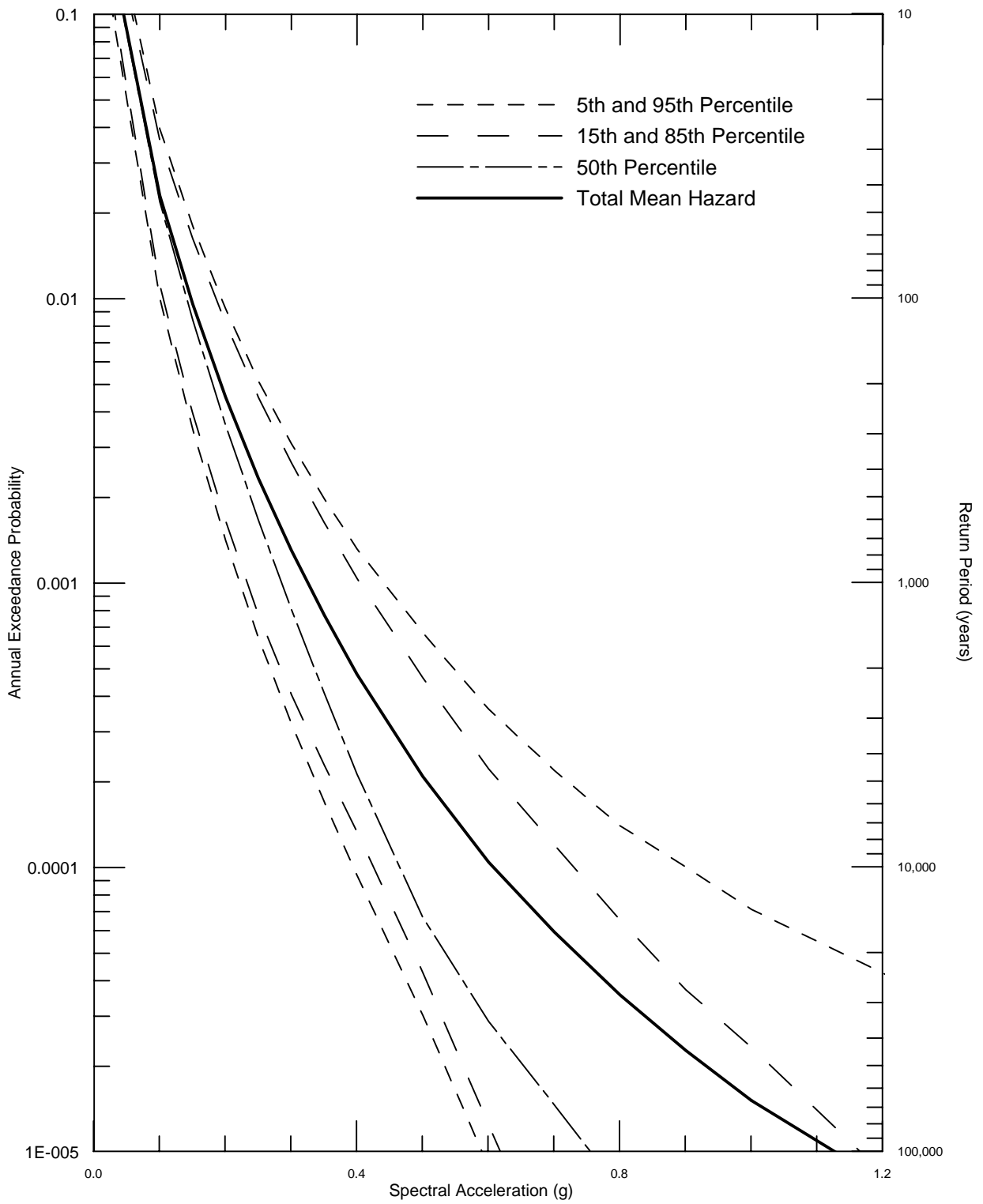


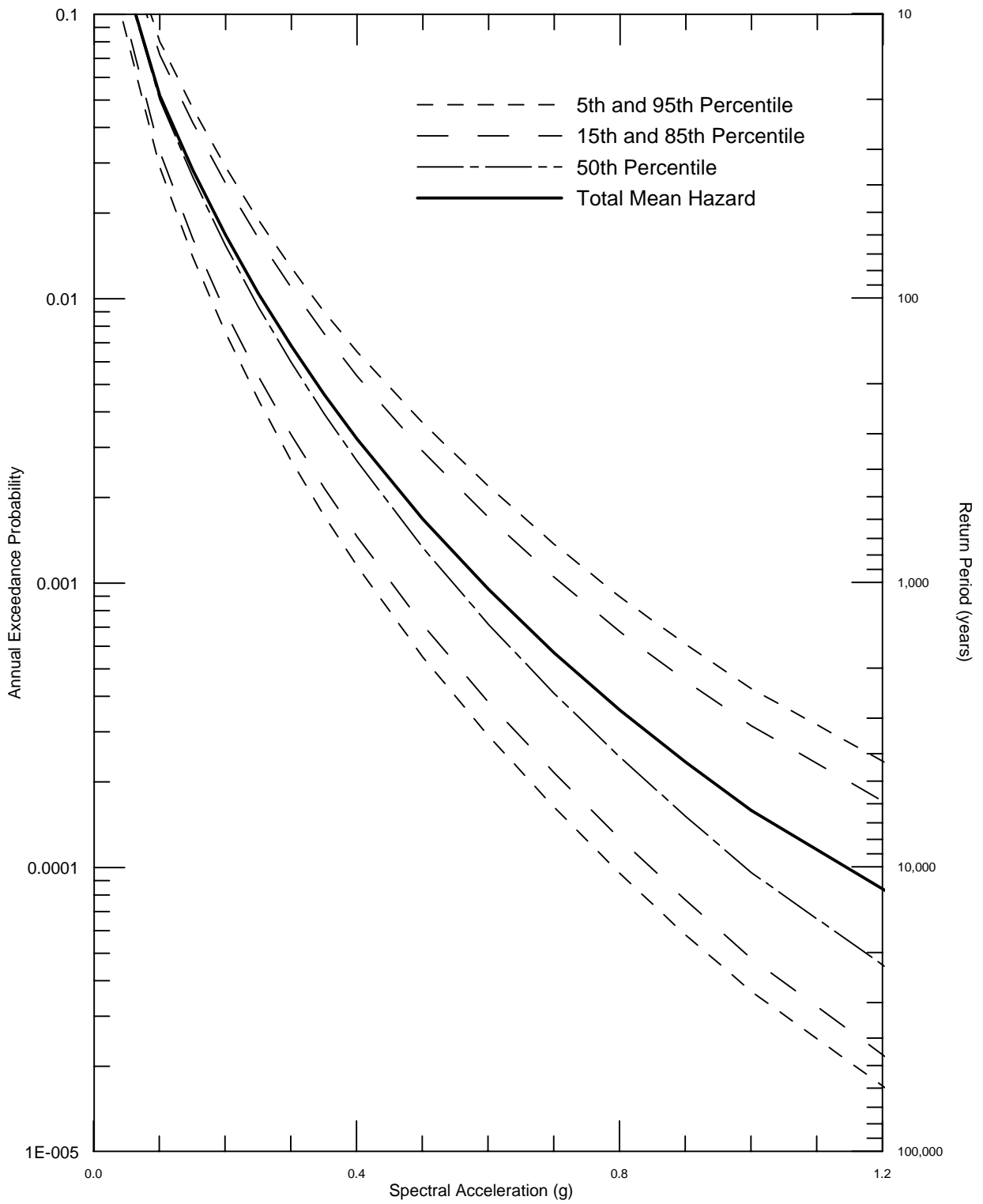
DELTA RISK
MANAGEMENT STRATEGY
CALIFORNIA

Project No. 26815900

TIME DEPENDENT SEISMIC HAZARD CURVES
FOR 1.0 SEC HORIZONTAL SPECTRAL
ACCELERATION FOR MONTEZUMA SLOUGH
FOR 2005

Figure
27



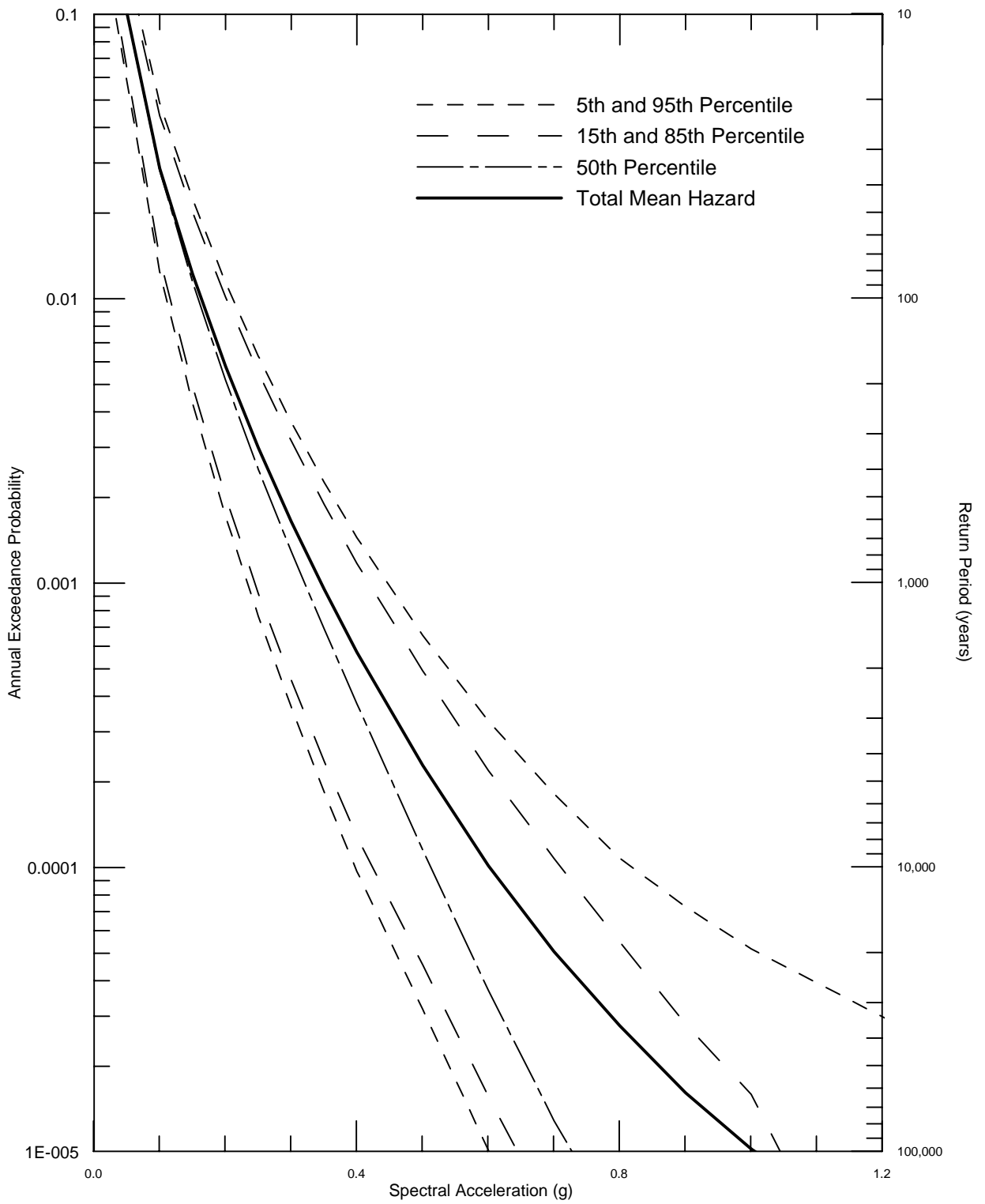


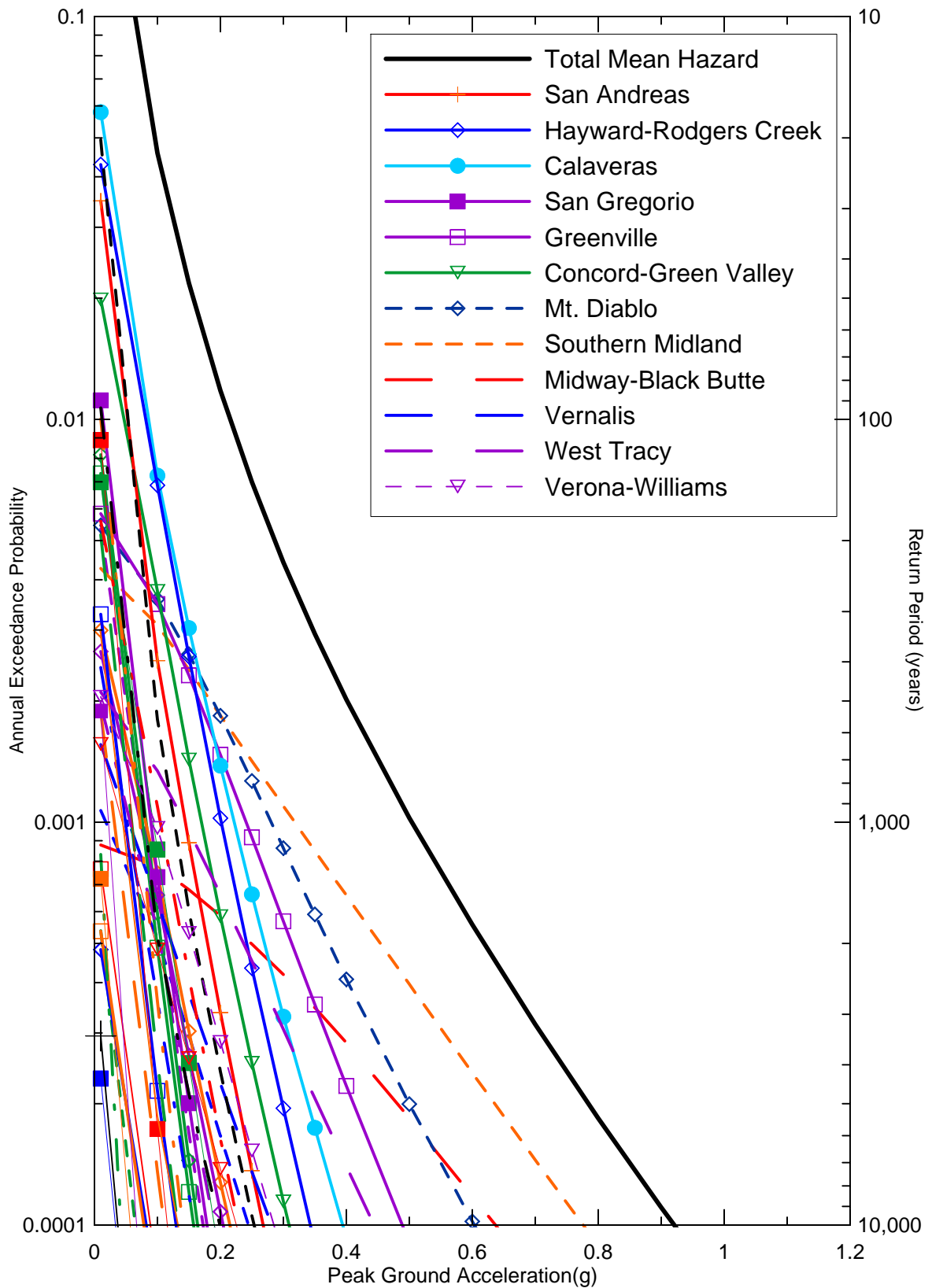
DELTA RISK
MANAGEMENT STRATEGY
CALIFORNIA

Project No. 26815900

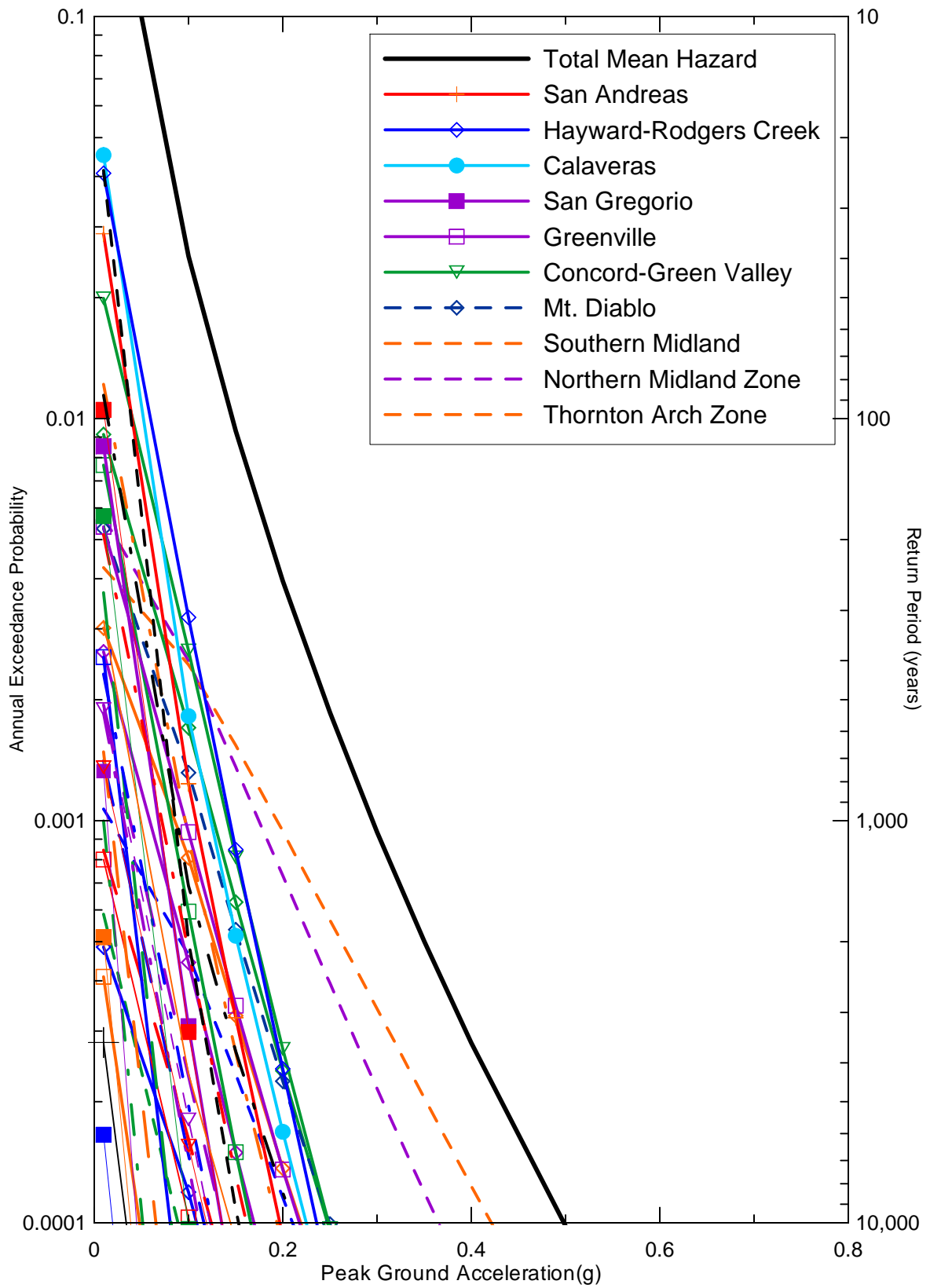
TIME DEPENDENT SEISMIC HAZARD CURVES
FOR 1.0 SEC HORIZONTAL SPECTRAL
ACCELERATION FOR SHERMAN ISLAND FOR 2005

Figure
29

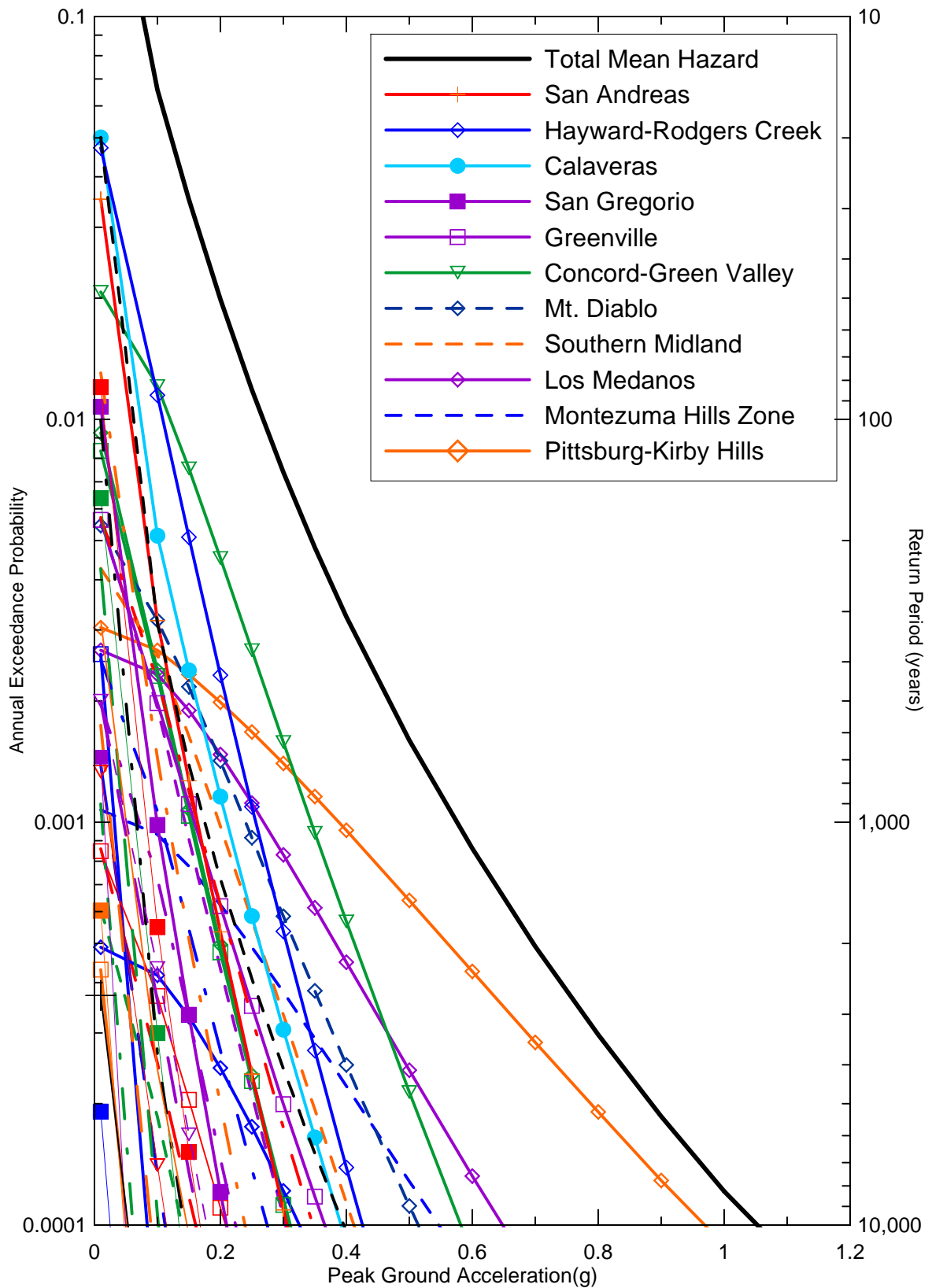




Delta Risk\figures\DR2-ppga-2005.grf



Delta Risk\figures\DR-4-pga-2005.grf



Delta Risk\figures\DR3-pga-2005.grf

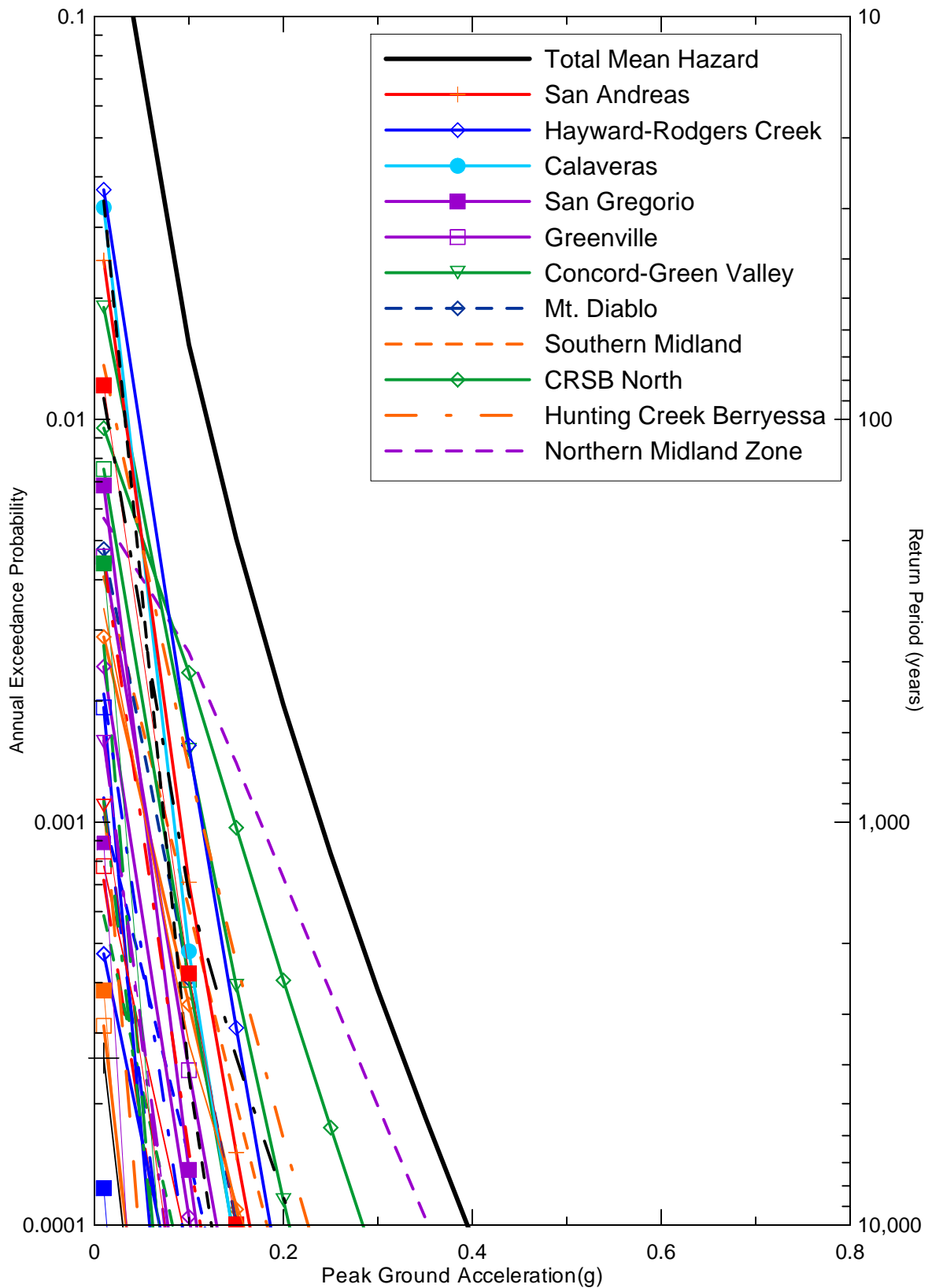


DELTA RISK
MANAGEMENT STRATEGY
CALIFORNIA

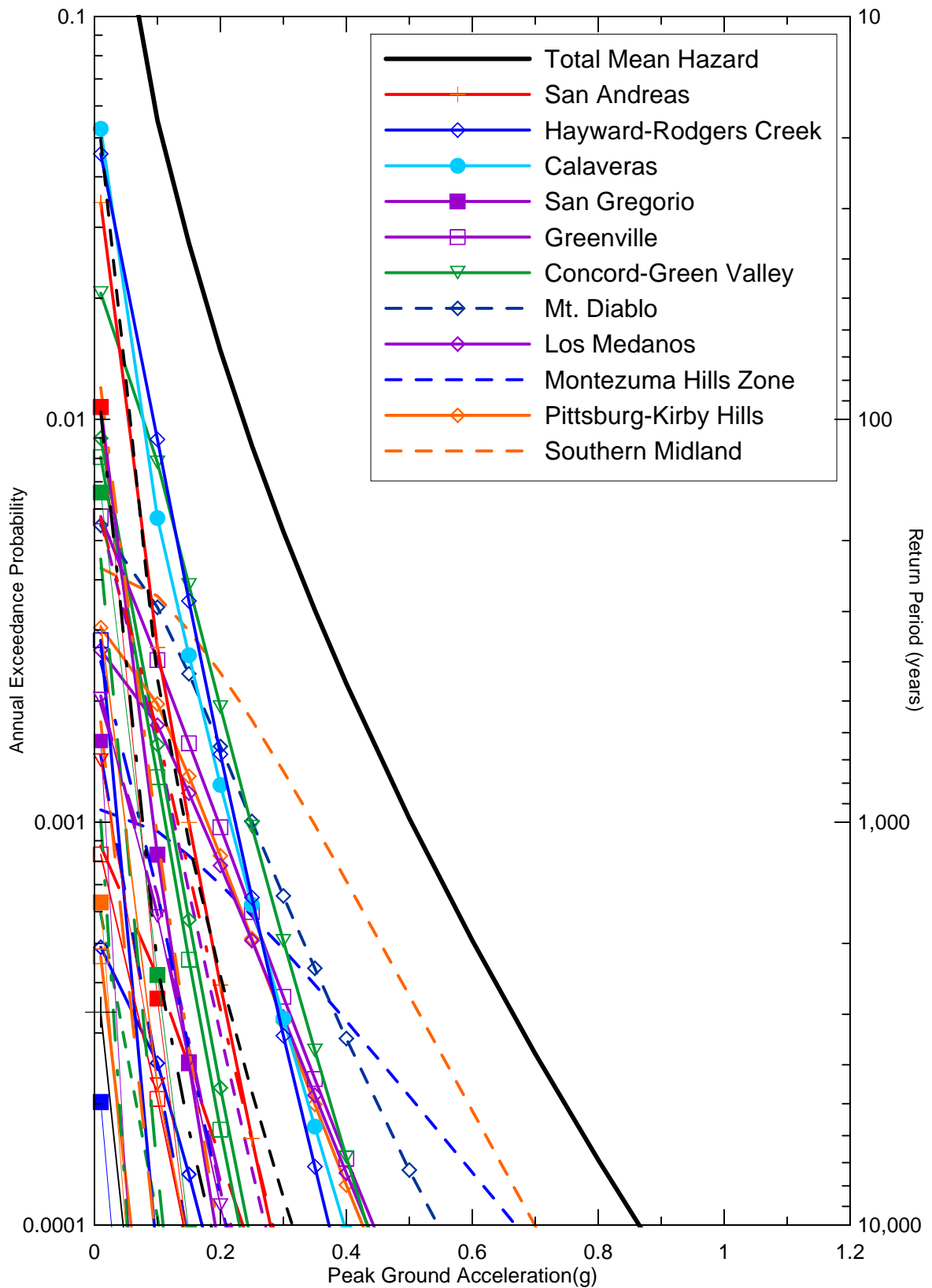
Project No. 26815900

SEISMIC SOURCE CONTRIBUTIONS TO MEAN
PEAK HORIZONTAL ACCELERATION TIME-
DEPENDENT HAZARD FOR MONTEZUMA SLOUGH
FOR 2005

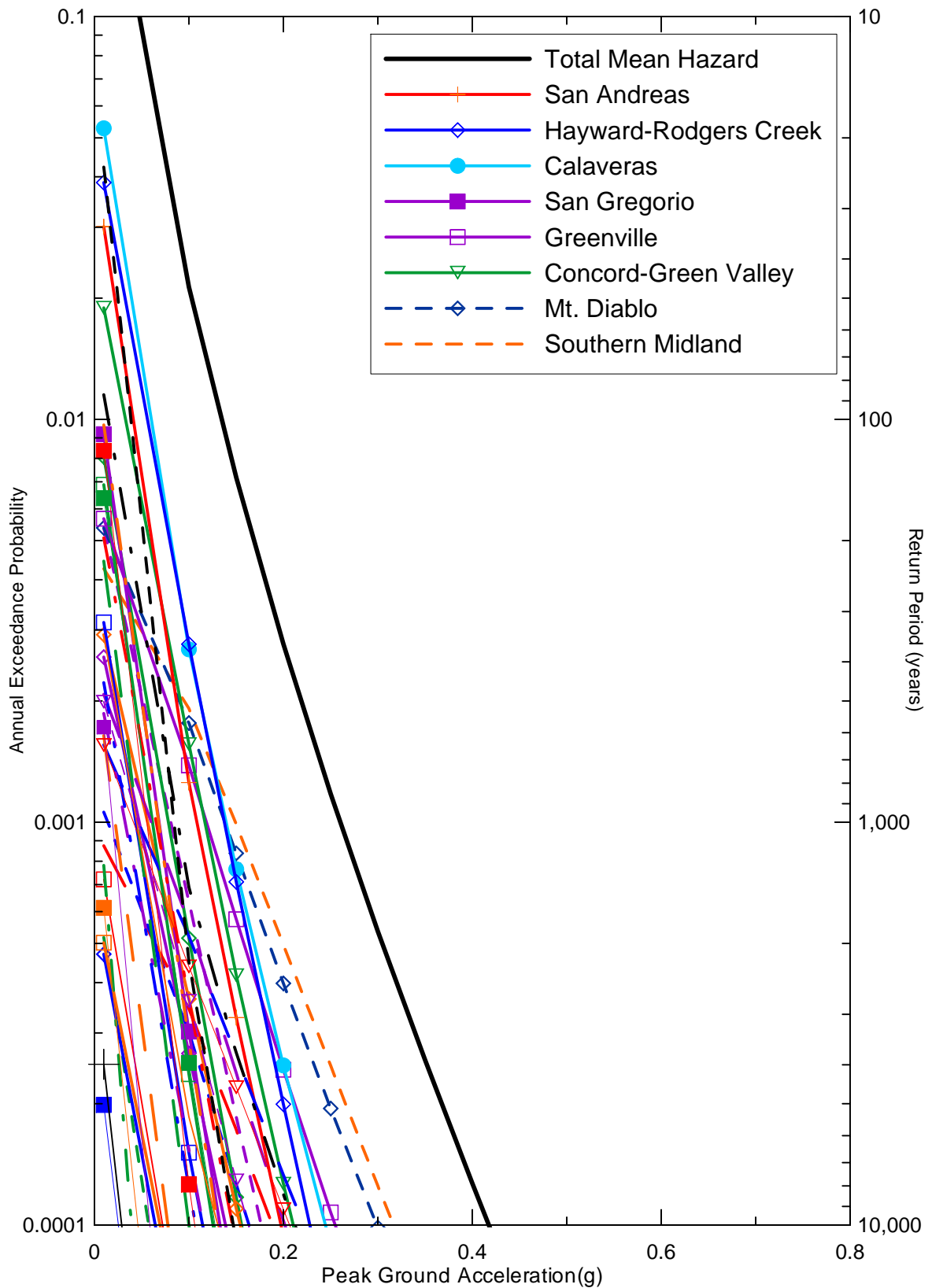
Figure
33



Delta Risk\figures\DR6-pga-2005.grf



Delta Risk\figures\DR1-pga-2005.grf



Delta Risk\figures\DR5-pga-2005.grf

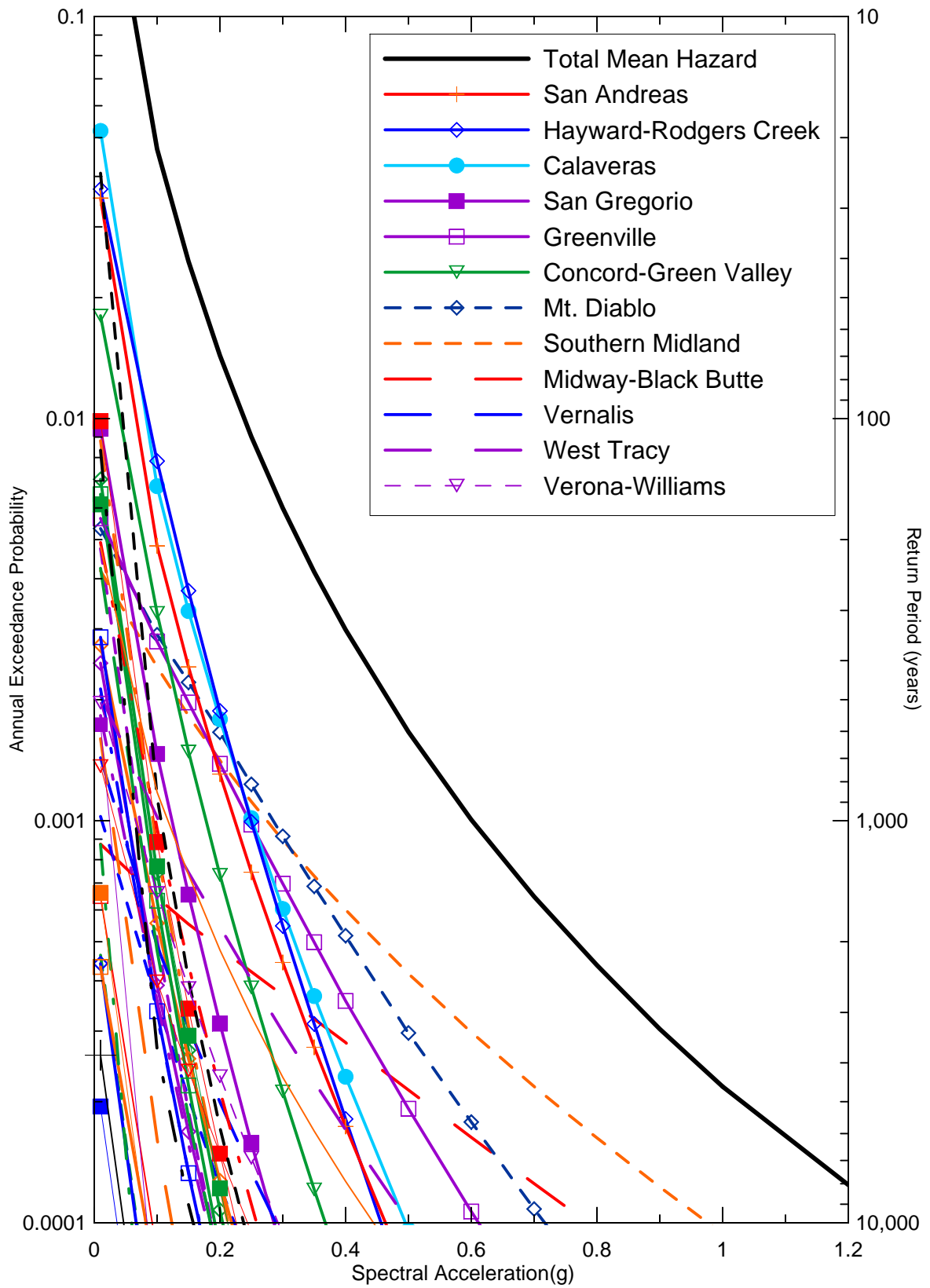


DELTA RISK
MANAGEMENT STRATEGY
CALIFORNIA

Project No. 26815900

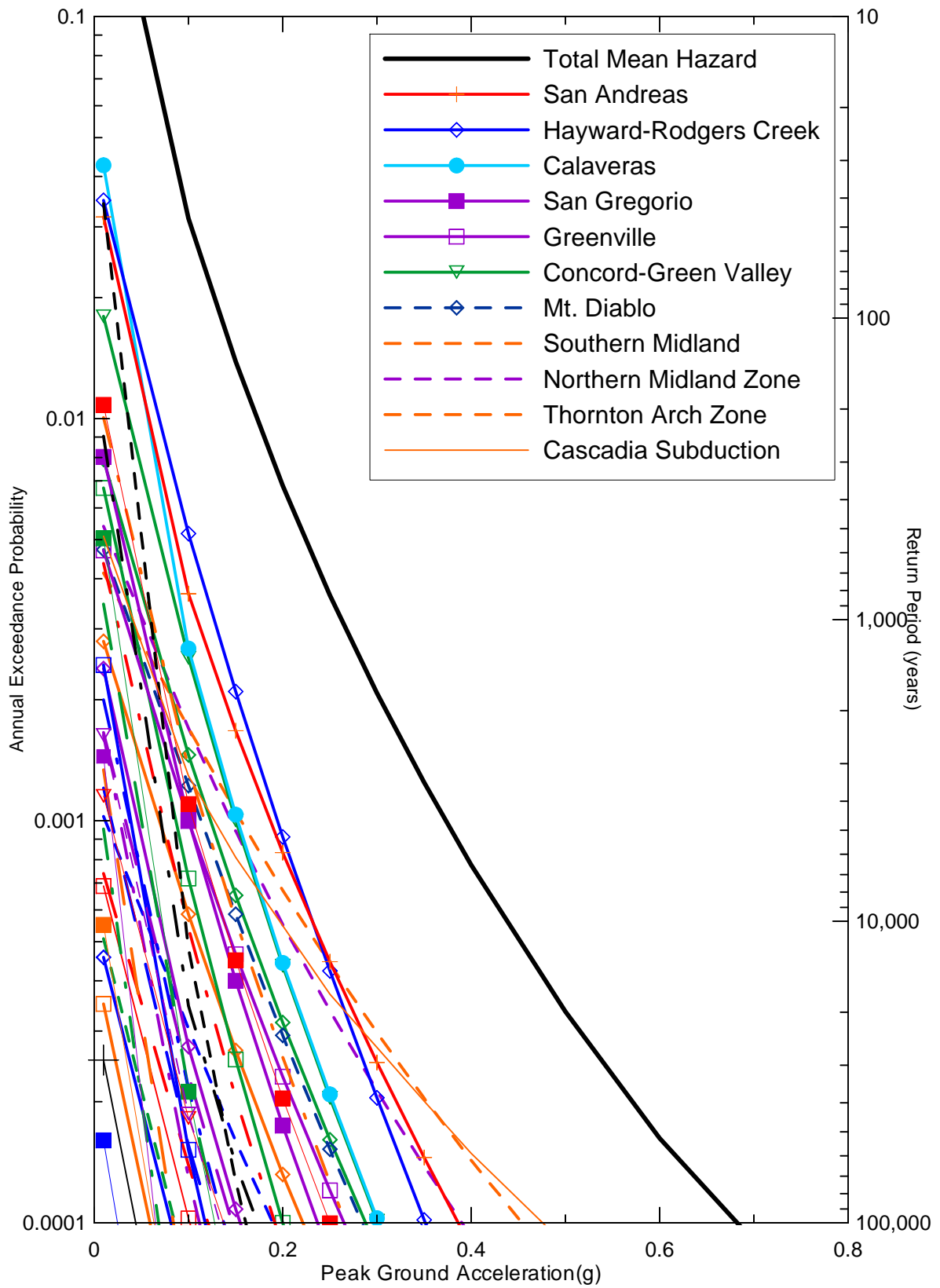
SEISMIC SOURCE CONTRIBUTIONS TO MEAN
PEAK HORIZONTAL ACCELERATION TIME-
DEPENDENT HAZARD FOR STOCKTON
FOR 2005

Figure
36



Delta Risk\figures\DR2-11-2005.grf

	<p>DELTA RISK MANAGEMENT STRATEGY CALIFORNIA</p>	<p>SEISMIC SOURCE CONTRIBUTIONS TO 1.0 SEC HORIZONTAL SPECTRAL ACCELERATION TIME- DEPENDENT HAZARD FOR CLIFTON COURT FOR 2005</p>	<p>Figure 37</p>
<p>Project No. 26815900</p>			



Delta Risk\figures\DR4-11-2005.grf

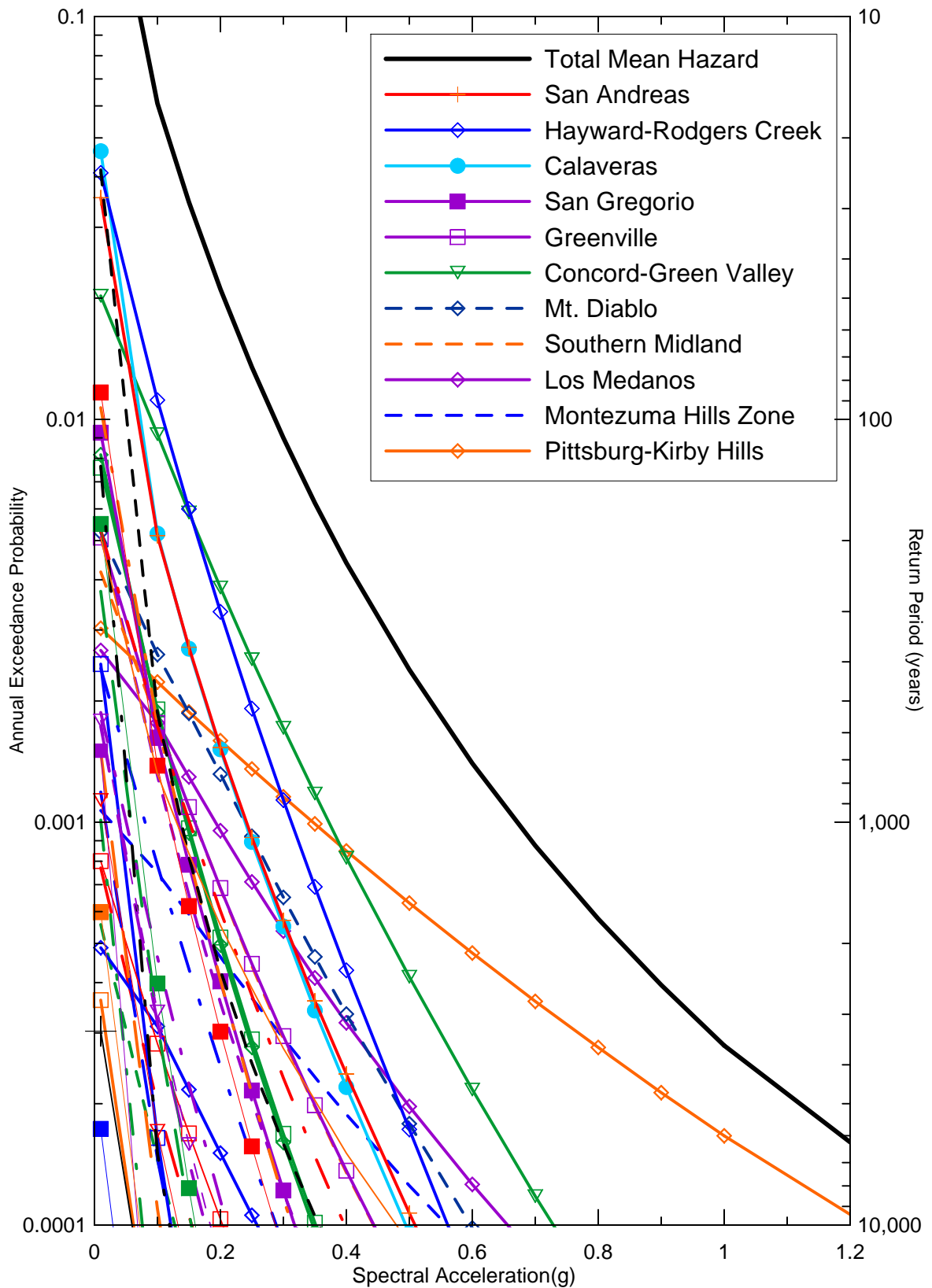


DELTA RISK
MANAGEMENT STRATEGY
CALIFORNIA

Project No. 26815900

SEISMIC SOURCE CONTRIBUTIONS TO 1.0 SEC
HORIZONTAL SPECTRAL ACCELERATION TIME-
DEPENDENT HAZARD FOR DELTA CROSS CHANNEL
FOR 2005

Figure
38



Delta Risk\figures\DR3-11-2005.grf

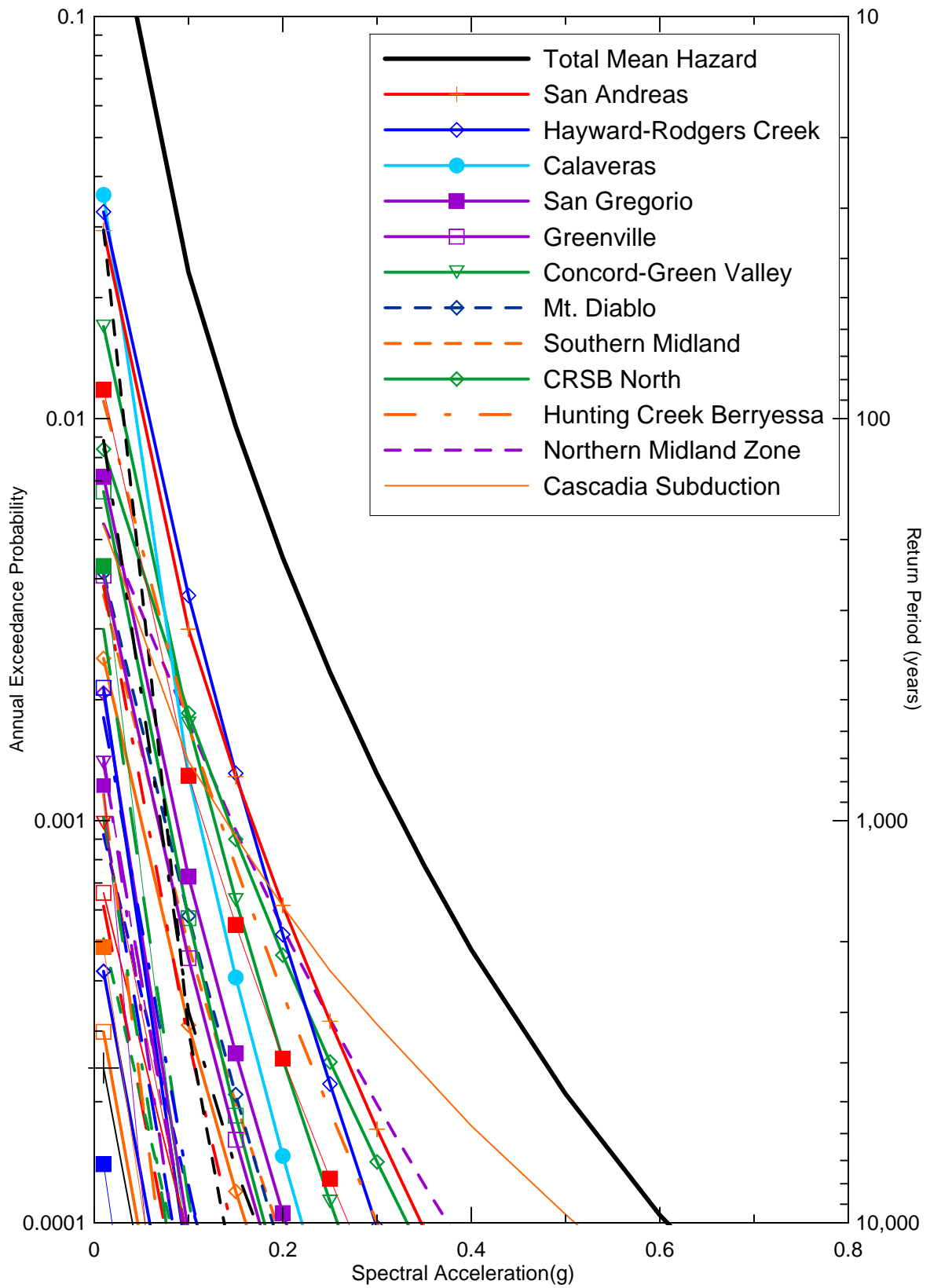


DELTA RISK
MANAGEMENT STRATEGY
CALIFORNIA

Project No. 26815900

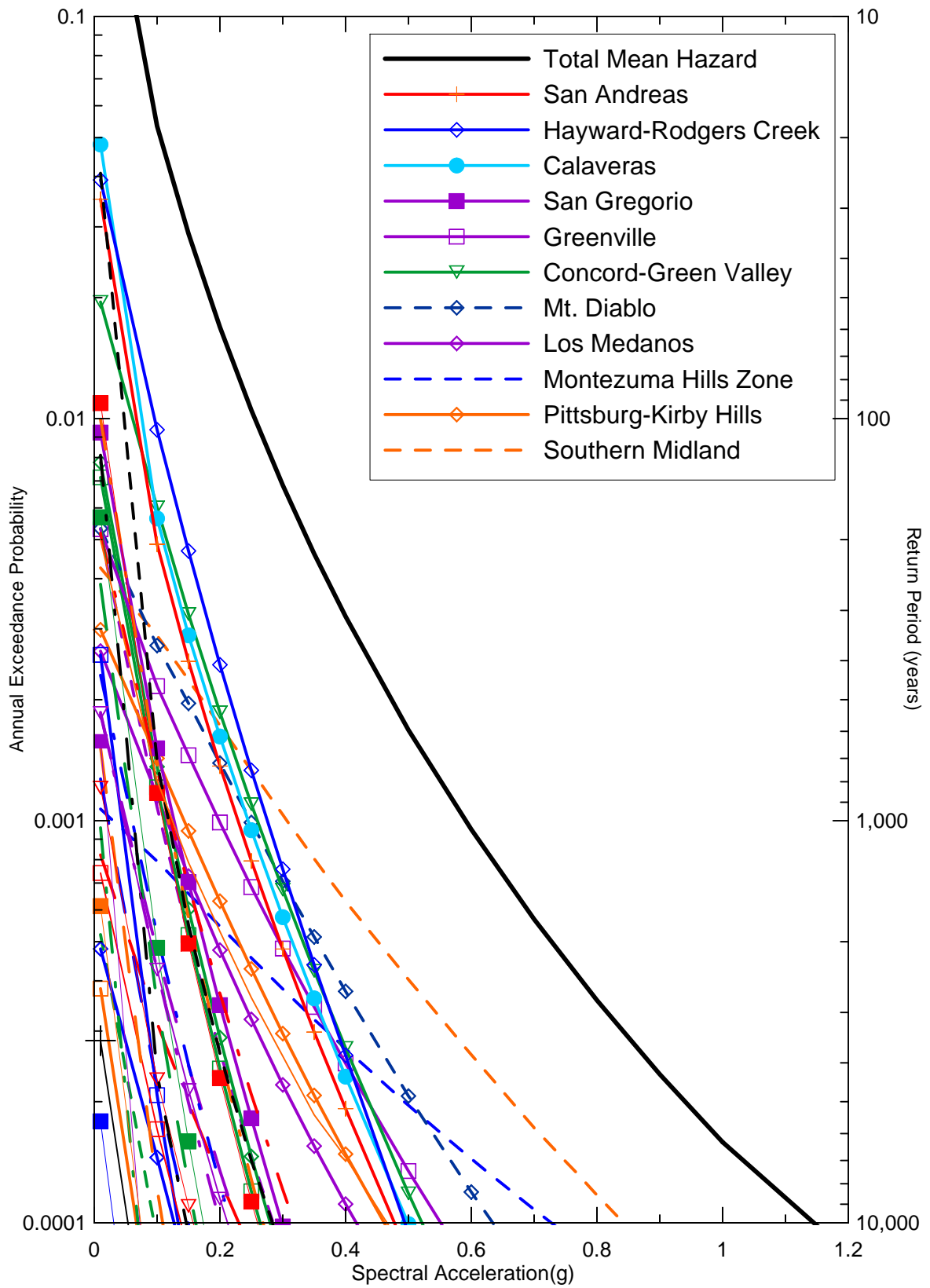
SEISMIC SOURCE CONTRIBUTIONS TO 1.0 SEC
HORIZONTAL SPECTRAL ACCELERATION TIME-
DEPENDENT HAZARD FOR MONTEZUMA SLOUGH
FOR 2005

Figure
39



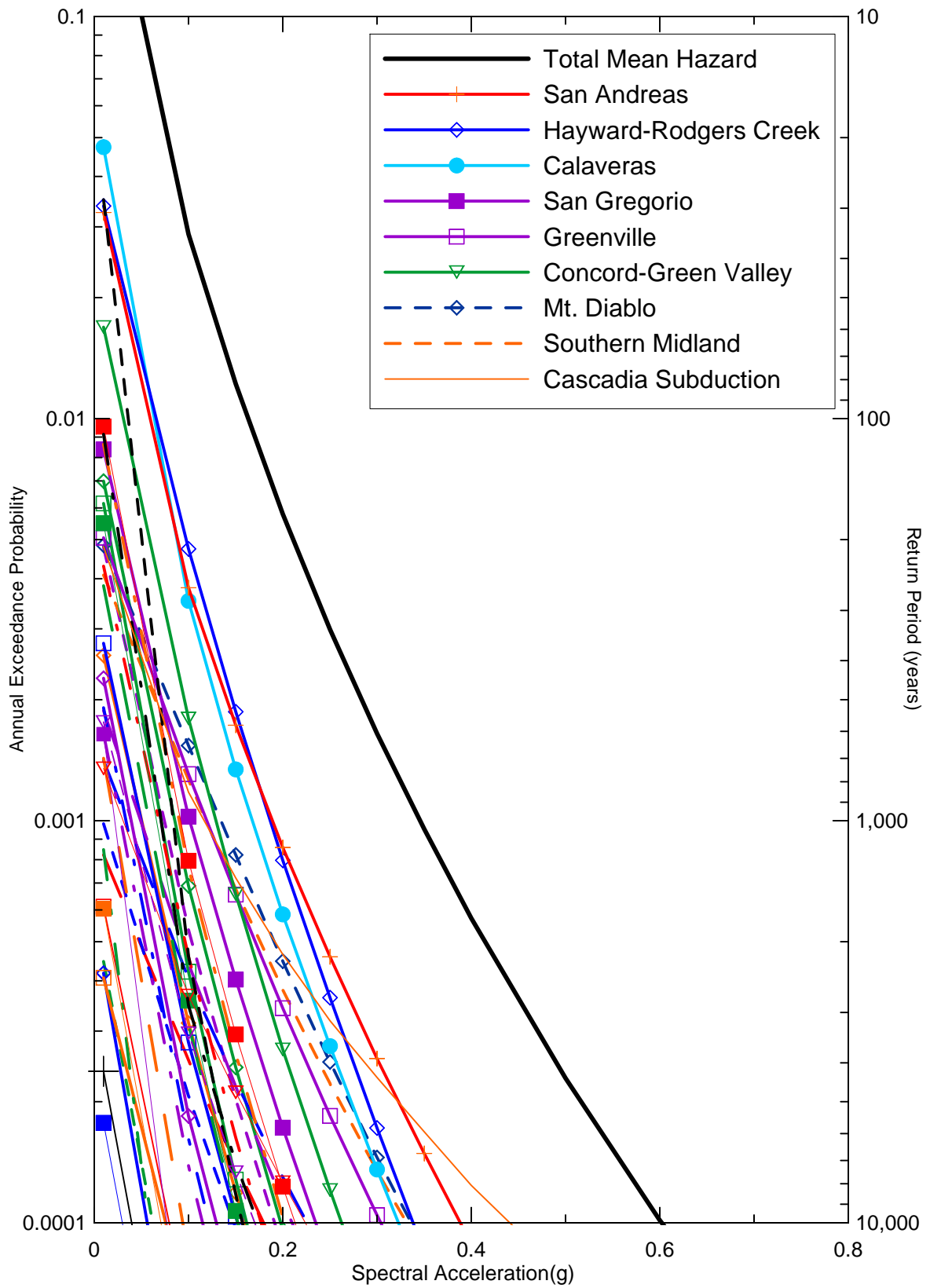
Delta Risk\figures\DR6-11-2005.grf

	<p>DELTA RISK MANAGEMENT STRATEGY CALIFORNIA</p>	<p>SEISMIC SOURCE CONTRIBUTIONS TO 1.0 SEC HORIZONTAL SPECTRAL ACCELERATION TIME- DEPENDENT HAZARD FOR SACRAMENTO FOR 2005</p>	<p>Figure 40</p>
<p>Project No. 26815900</p>			

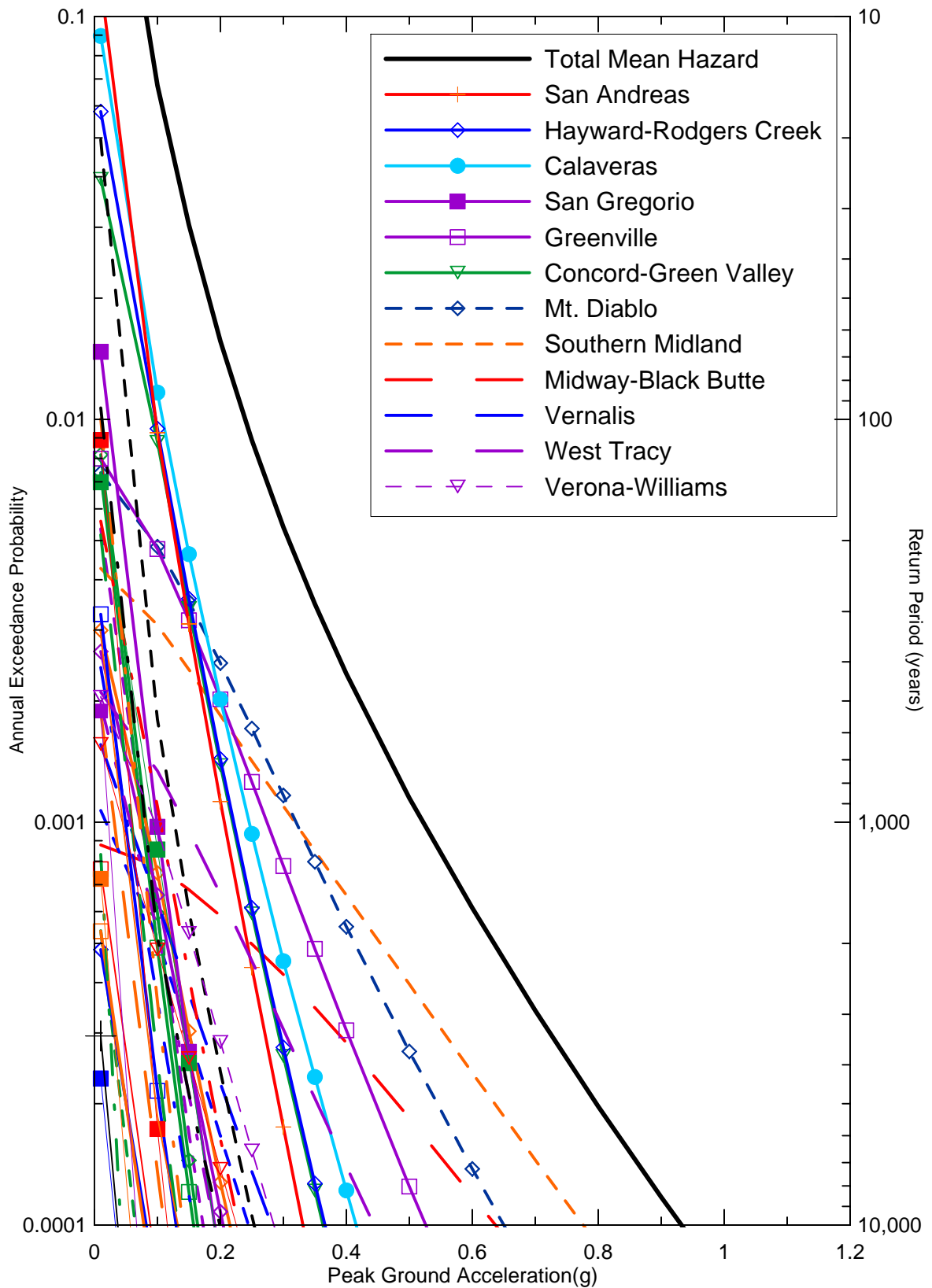


Delta Risk\figures\DR1-11-2005.grf

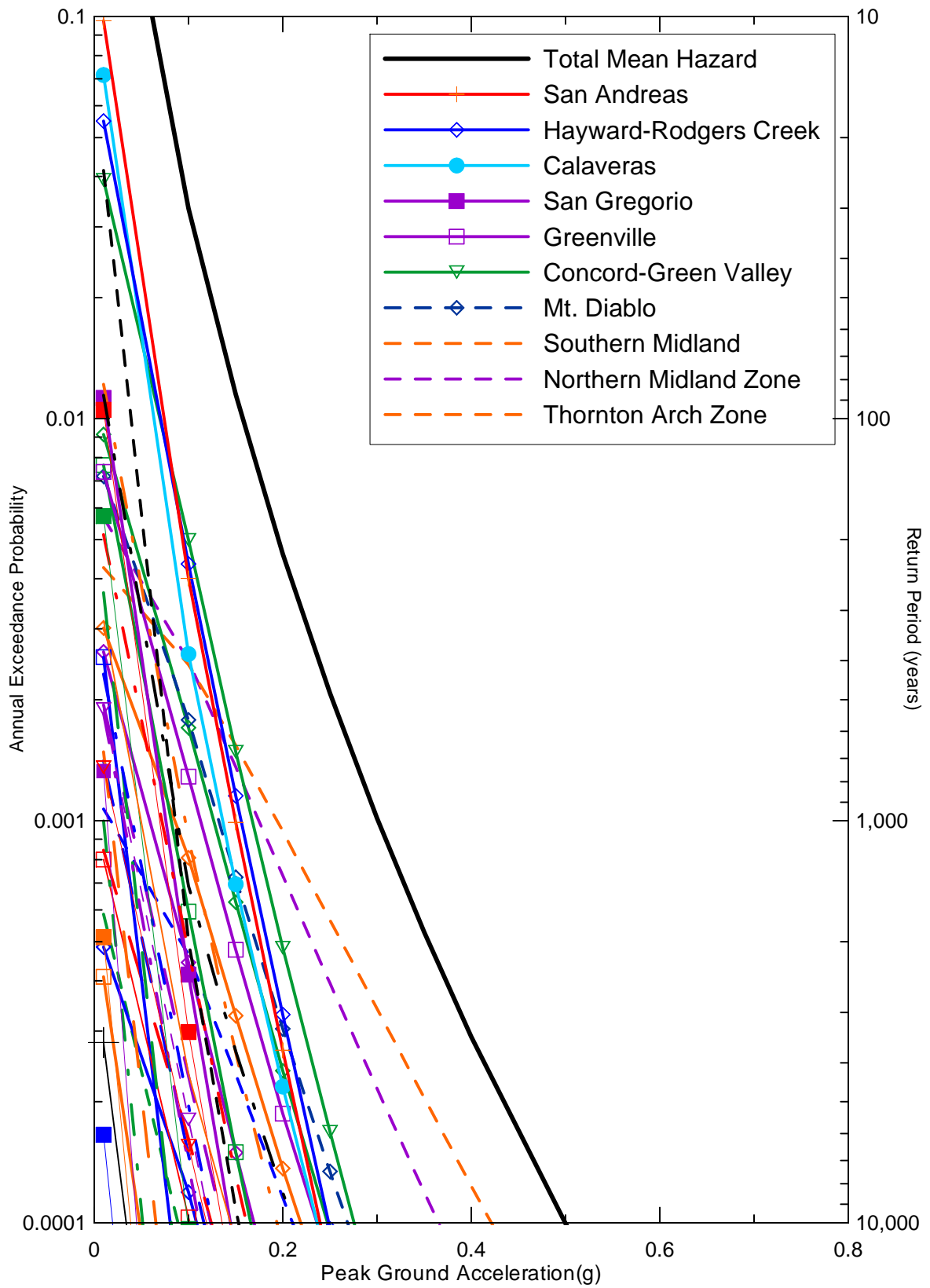
	<p>DELTA RISK MANAGEMENT STRATEGY CALIFORNIA</p>	<p>SEISMIC SOURCE CONTRIBUTIONS TO 1.0 SEC HORIZONTAL SPECTRAL ACCELERATION TIME- DEPENDENT HAZARD FOR SHERMAN ISLAND FOR 2005</p>	<p>Figure 41</p>
<p>Project No. 26815900</p>			



Delta Risk\figures\DR5-11-2005.grf



Delta Risk\figures\DR2-pga-2200.grf



Delta Risk\figures\DR4+pga-2200.grf

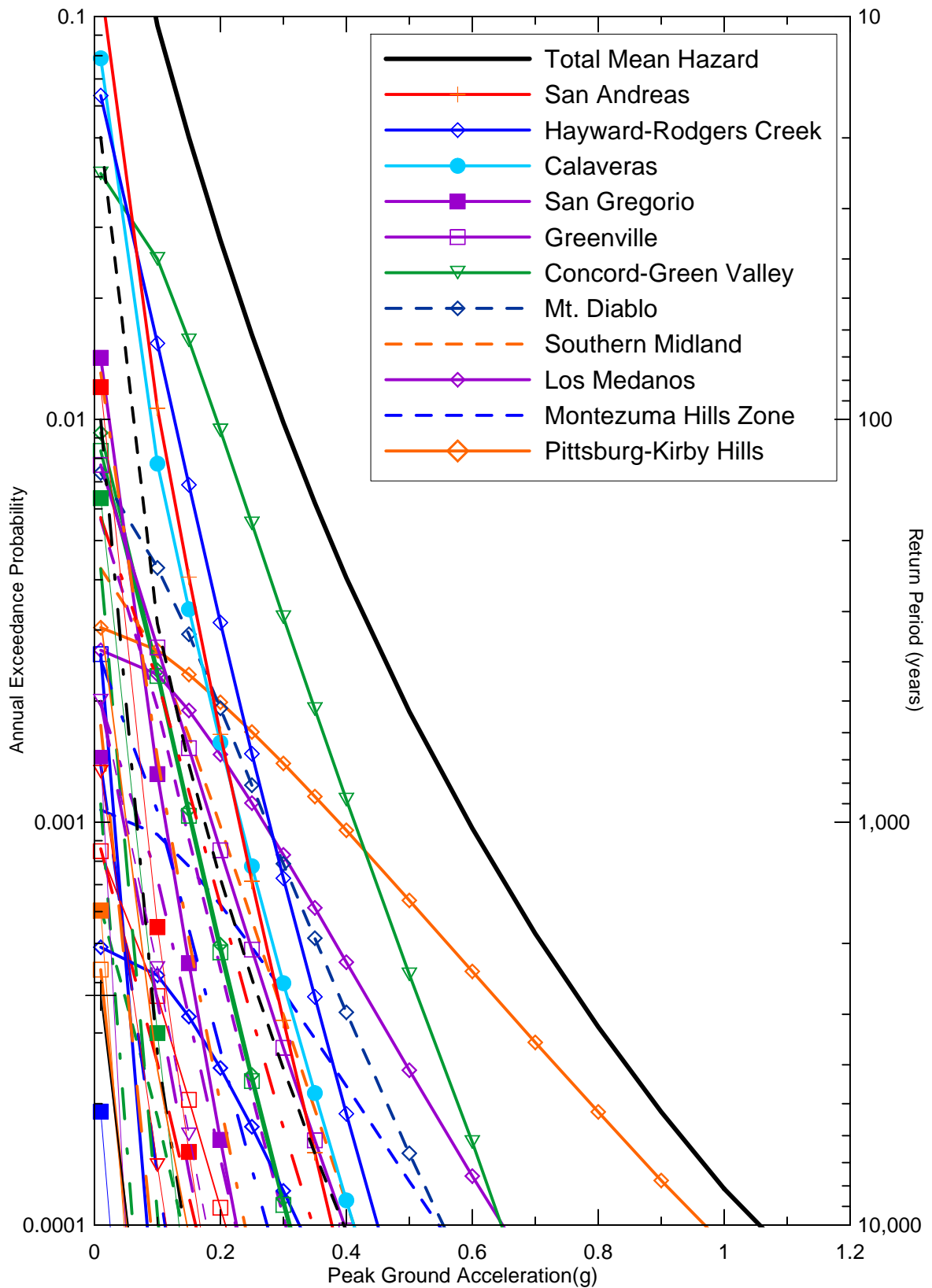


DELTA RISK
MANAGEMENT STRATEGY
CALIFORNIA

Project No. 26815900

SEISMIC SOURCE CONTRIBUTIONS TO MEAN
PEAK HORIZONTAL ACCELERATION TIME-
DEPENDENT HAZARD FOR DELTA CROSS CHANNEL
FOR 2200

Figure
44



Delta Risk\figures\DR3-pga-2200.grf

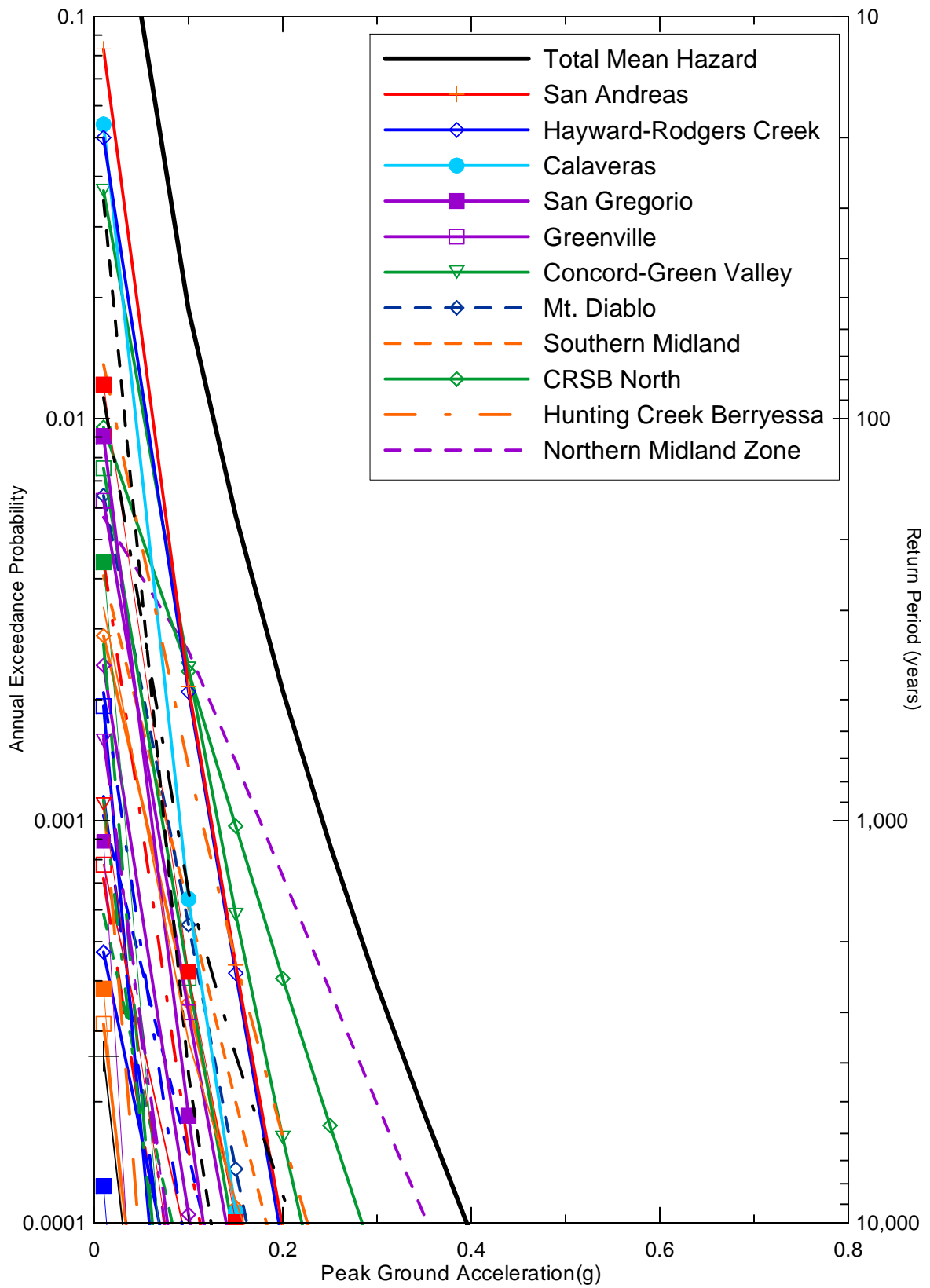


DELTA RISK
MANAGEMENT STRATEGY
CALIFORNIA

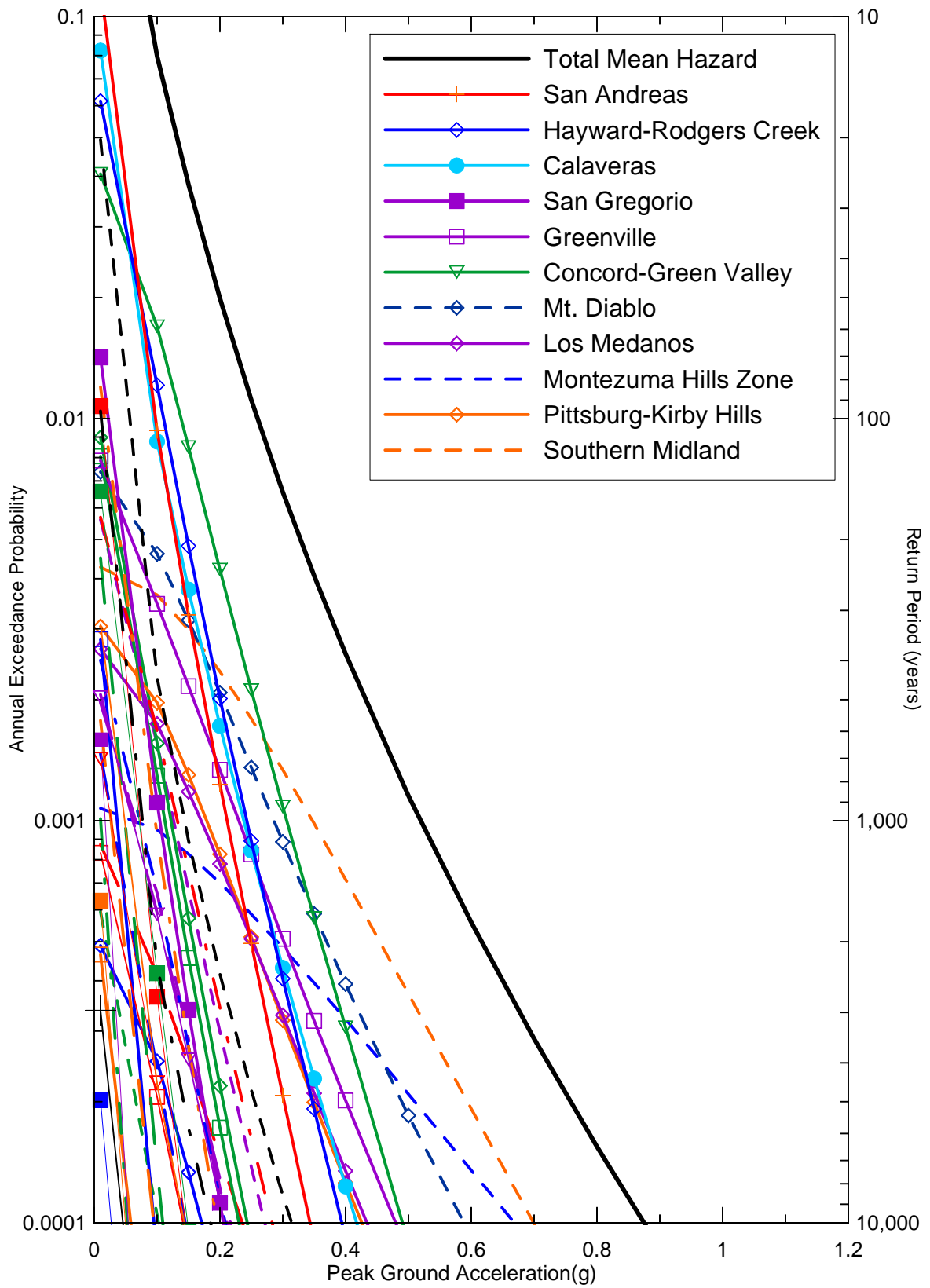
Project No. 26815900

SEISMIC SOURCE CONTRIBUTIONS TO MEAN
PEAK HORIZONTAL ACCELERATION TIME-
DEPENDENT HAZARD FOR MONTEZUMA SLOUGH
FOR 2200

Figure
45



Delta Risk\figures\DR6-pga-2200.grf



Delta Risk\figures\DR1-pga-2200.grf

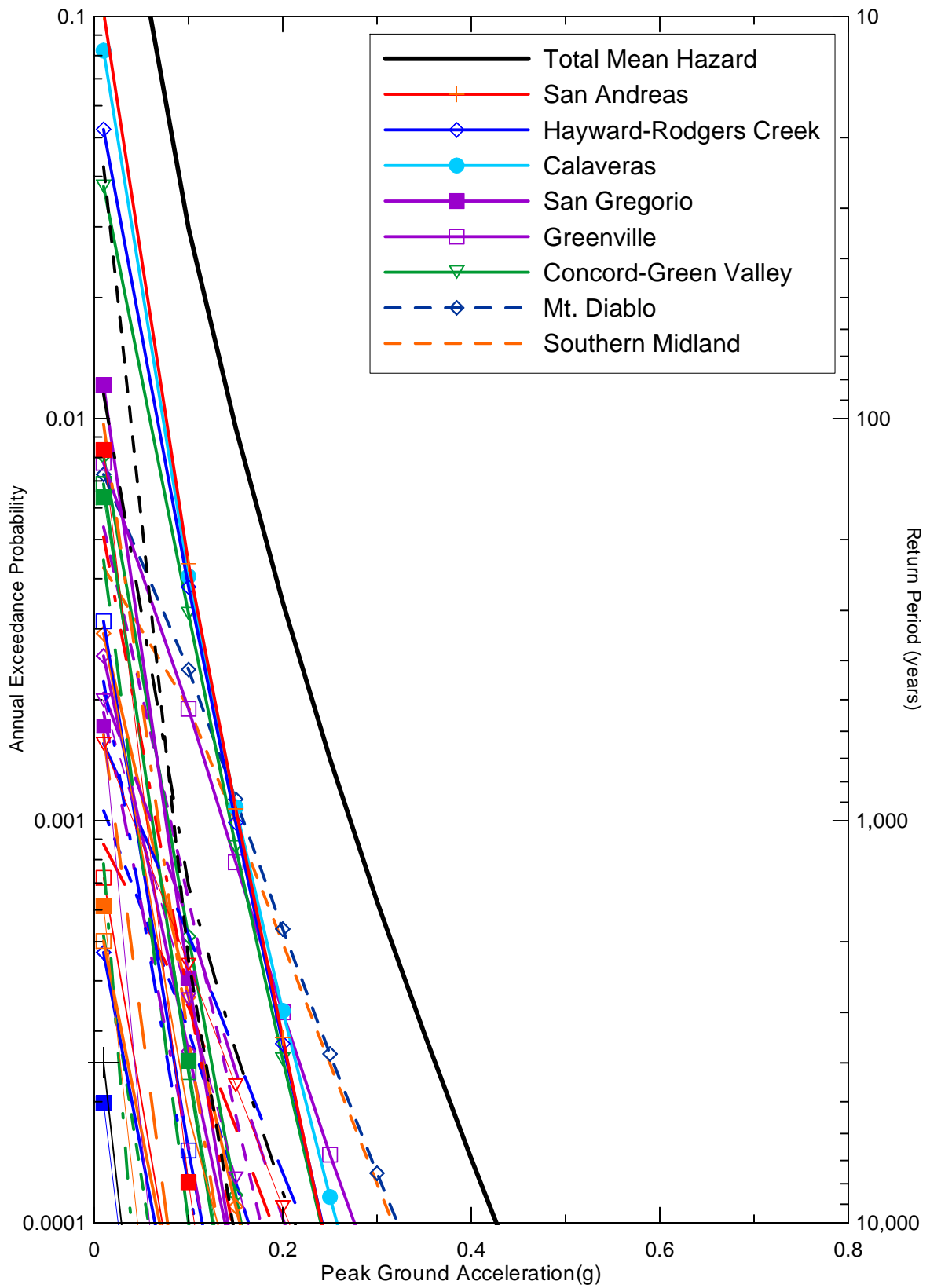


DELTA RISK
MANAGEMENT STRATEGY
CALIFORNIA

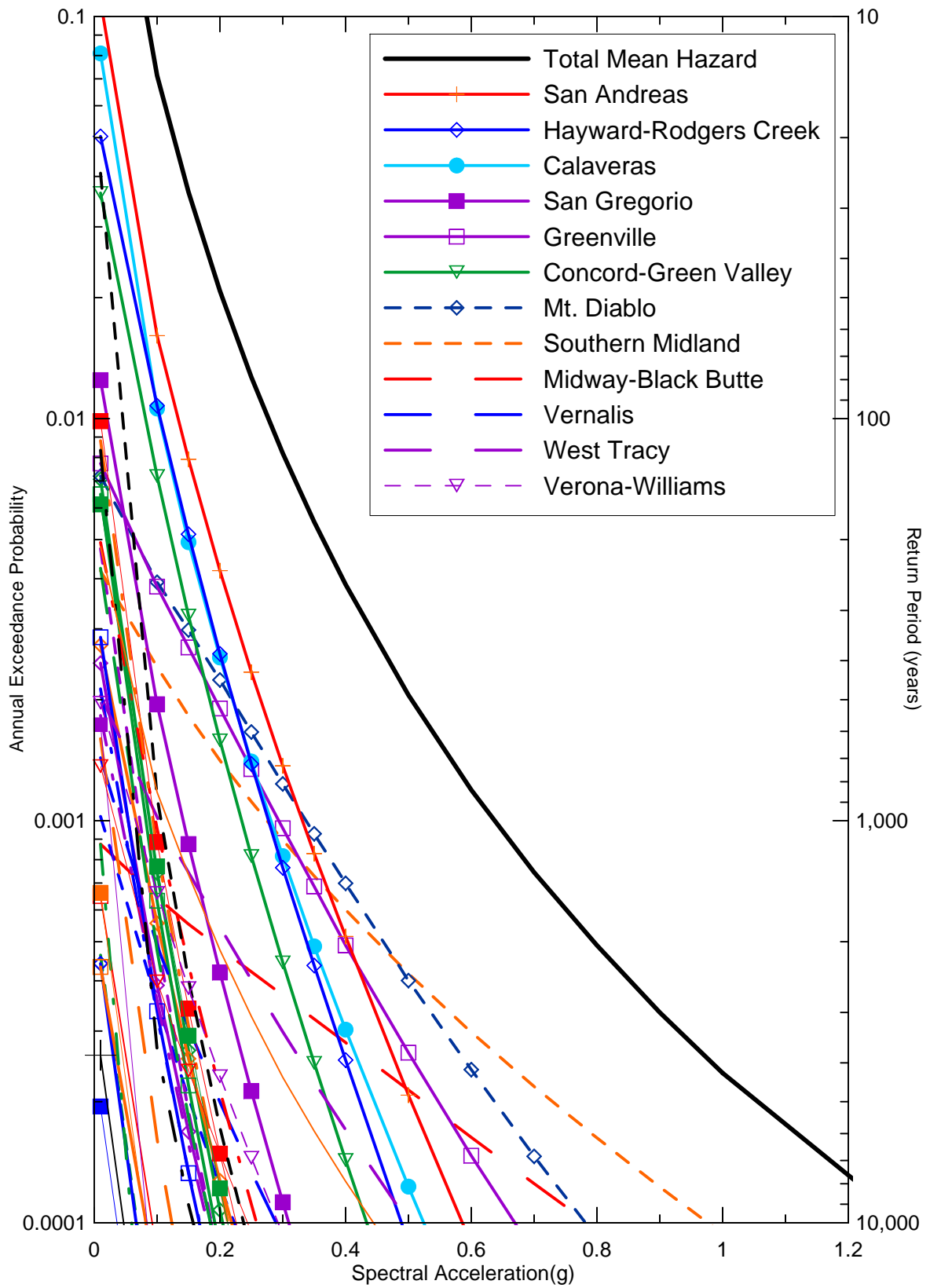
Project No. 26815900

SEISMIC SOURCE CONTRIBUTIONS TO MEAN
PEAK HORIZONTAL ACCELERATION TIME-
DEPENDENT HAZARD FOR SHERMAN ISLAND
FOR 2200

Figure
47



Delta Risk\figures\DR5-pga-2200.grf



Delta Risk\figures\DR2-11-2200.grf

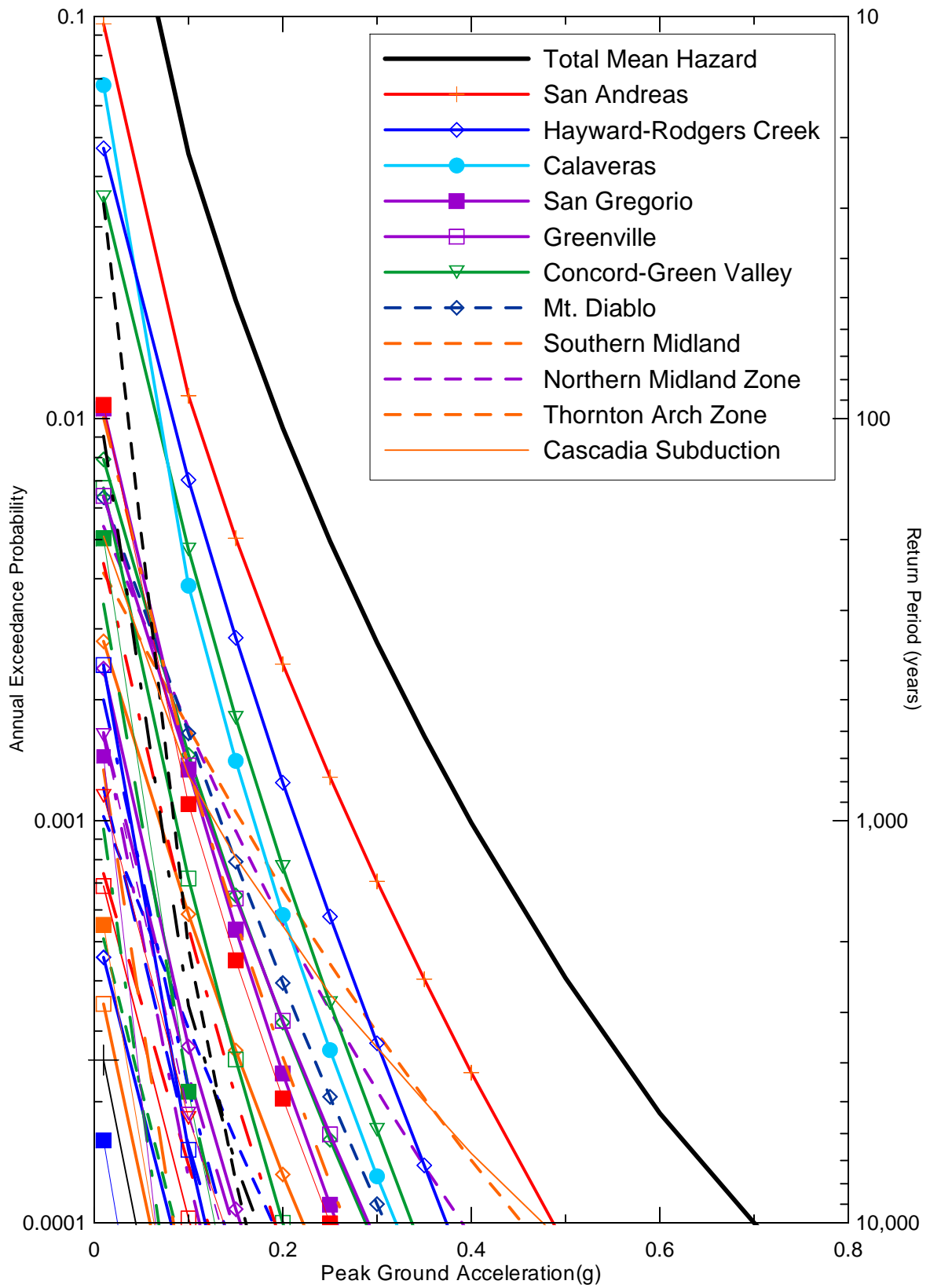


DELTA RISK
MANAGEMENT STRATEGY
CALIFORNIA

Project No. 26815900

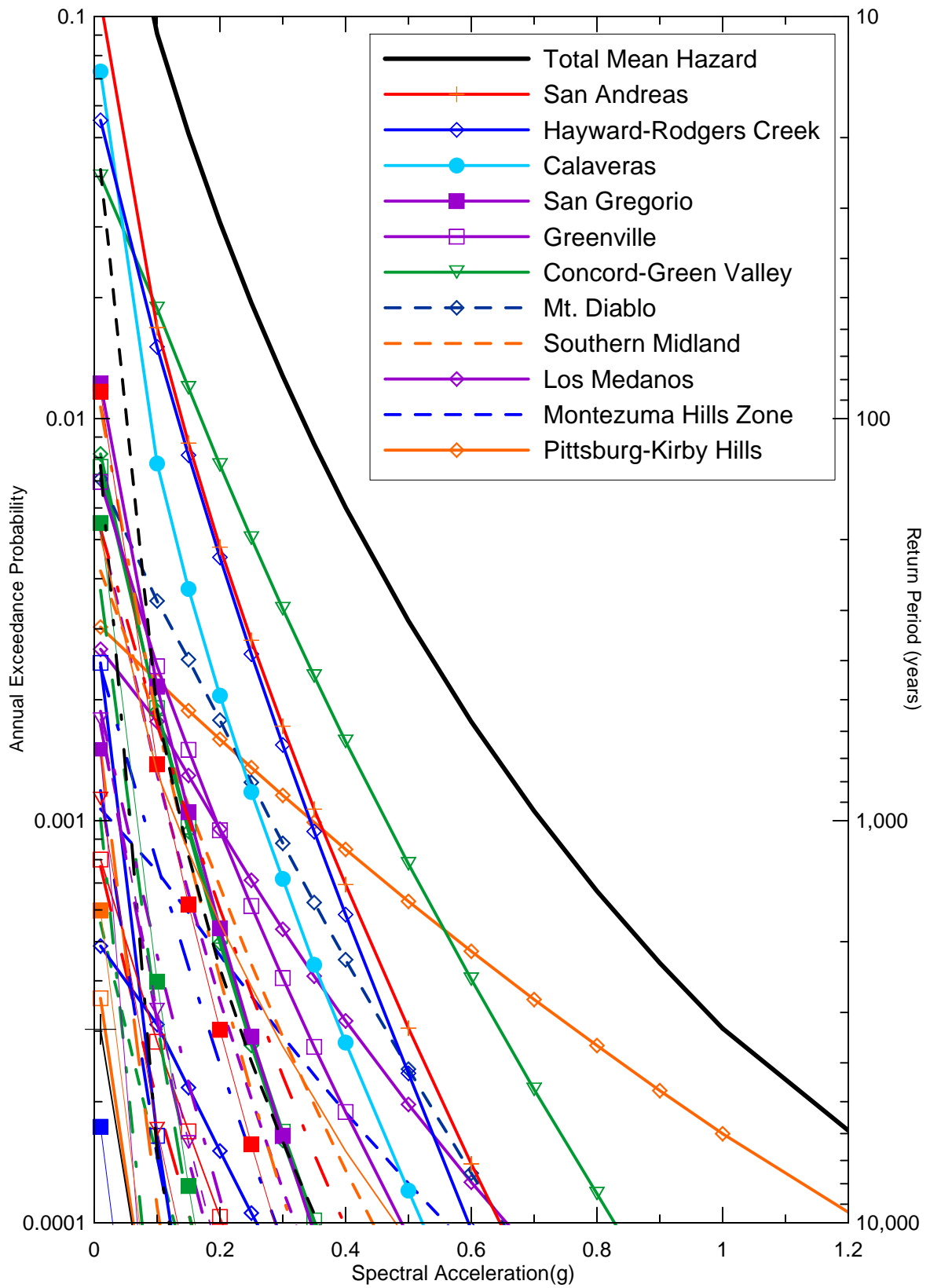
SEISMIC SOURCE CONTRIBUTIONS TO 1.0 SEC
HORIZONTAL SPECTRAL ACCELERATION TIME-
DEPENDENT HAZARD FOR CLIFTON COURT
FOR 2200

Figure
49



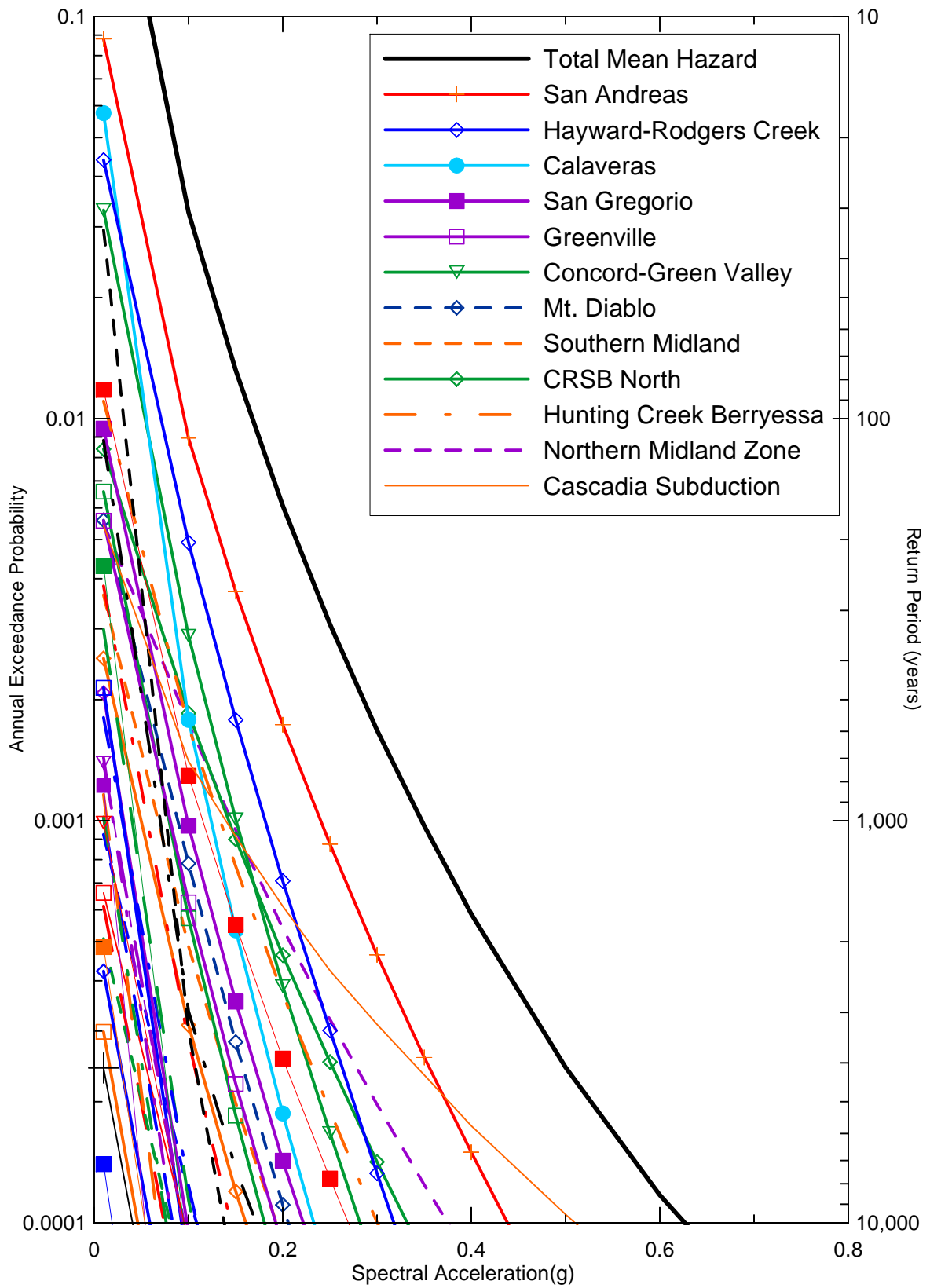
Delta Risk\figures\DR4-11-2200.grf

	<p>DELTA RISK MANAGEMENT STRATEGY CALIFORNIA</p>	<p>SEISMIC SOURCE CONTRIBUTIONS TO 1.0 SEC HORIZONTAL SPECTRAL ACCELERATION TIME- DEPENDENT HAZARD FOR DELTA CROSS CHANNEL FOR 2200</p>	<p>Figure 50</p>
<p>Project No. 26815900</p>			



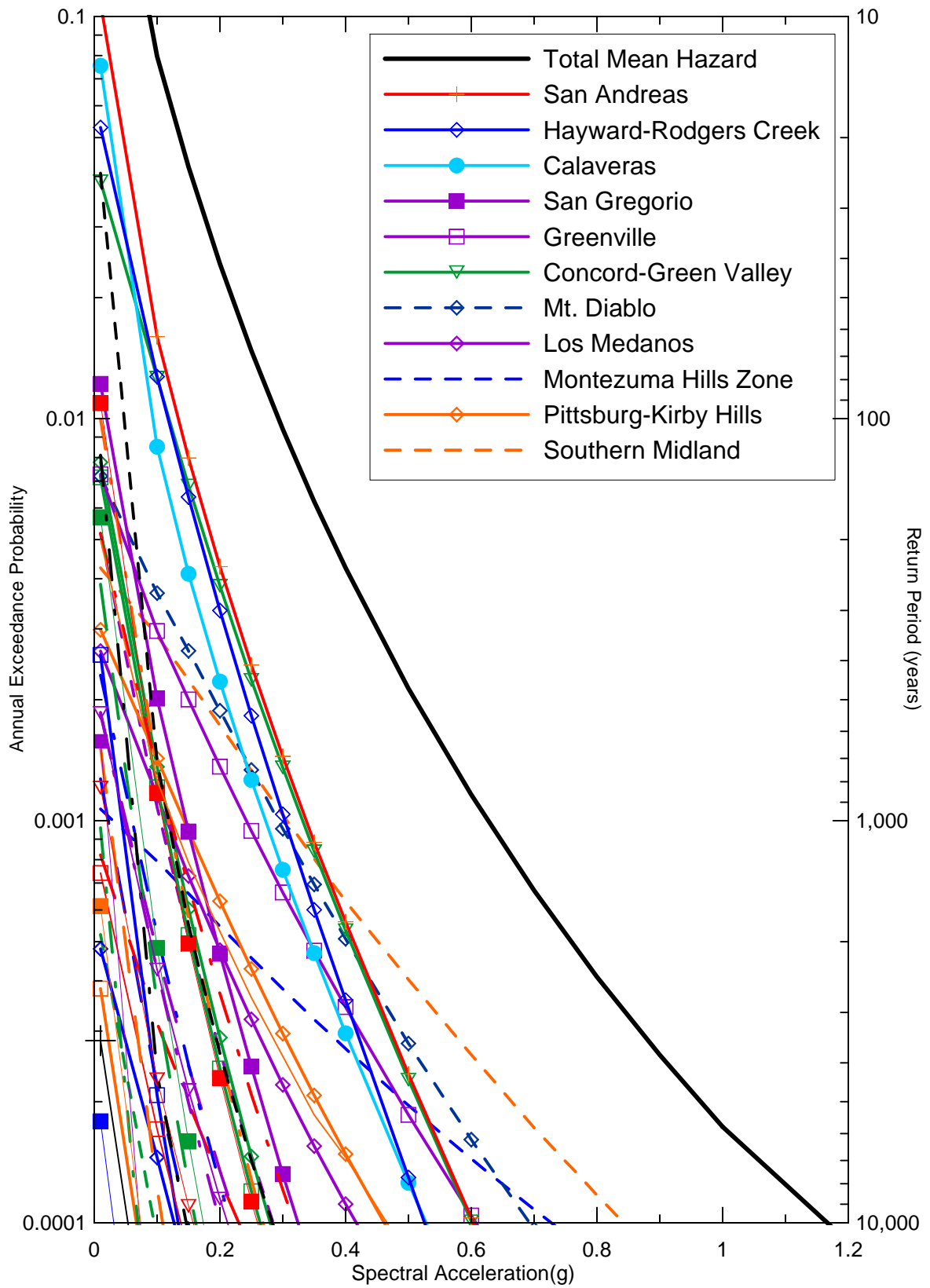
Delta Risk\figures\DR3-11-2200.grf

	<p>DELTA RISK MANAGEMENT STRATEGY CALIFORNIA</p>	<p>SEISMIC SOURCE CONTRIBUTIONS TO 1.0 SEC HORIZONTAL SPECTRAL ACCELERATION TIME- DEPENDENT HAZARD FOR MONTEZUMA SLOUGH FOR 2200</p>	<p>Figure 51</p>
<p>Project No. 26815900</p>			



Delta Risk\figures\DR6-11-2200.grf

	<p>DELTA RISK MANAGEMENT STRATEGY CALIFORNIA</p>	<p>SEISMIC SOURCE CONTRIBUTIONS TO 1.0 SEC HORIZONTAL SPECTRAL ACCELERATION TIME- DEPENDENT HAZARD FOR SACRAMENTO FOR 2200</p>	<p>Figure 52</p>
<p>Project No. 26815900</p>			



Delta Risk\figures\DR1-11-2200.grf

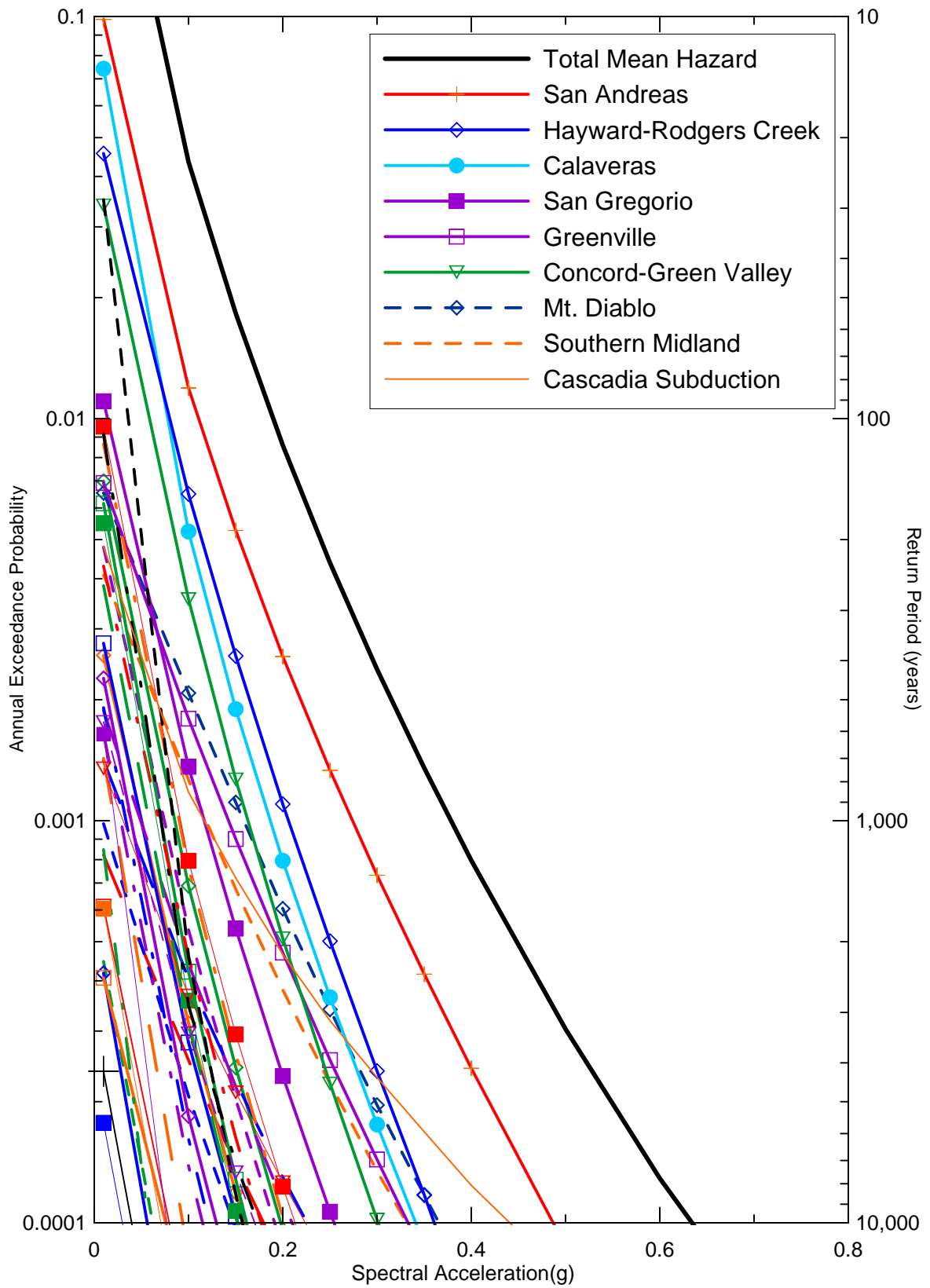


DELTA RISK
MANAGEMENT STRATEGY
CALIFORNIA

Project No. 26815900

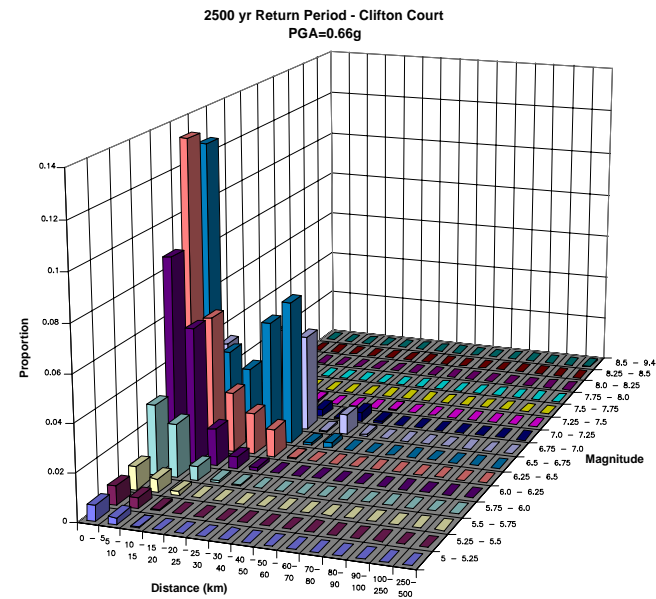
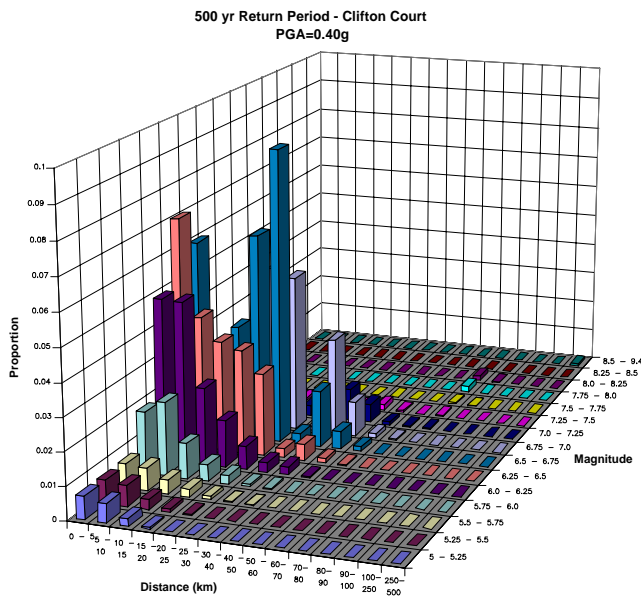
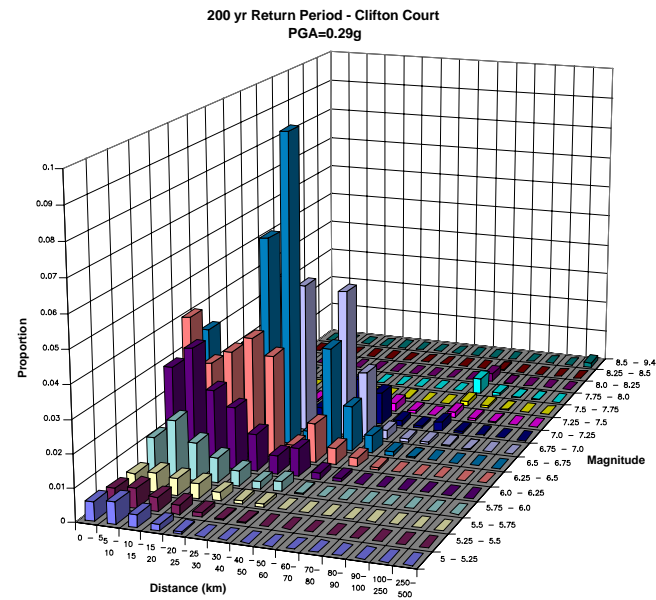
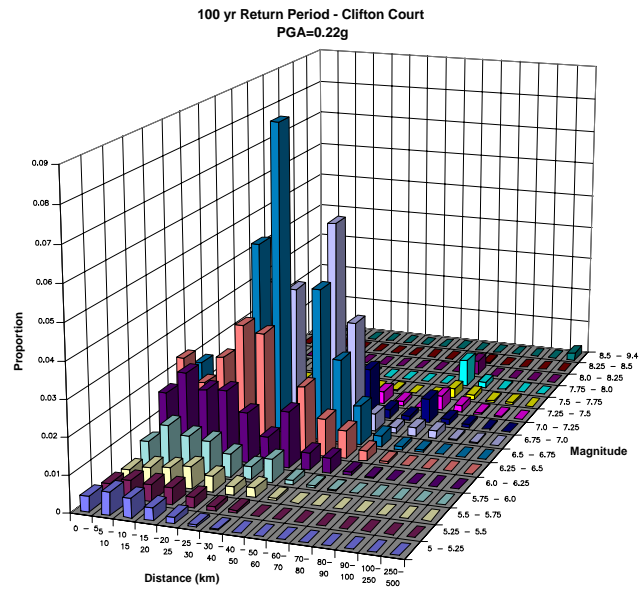
SEISMIC SOURCE CONTRIBUTIONS TO 1.0 SEC
HORIZONTAL SPECTRAL ACCELERATION TIME-
DEPENDENT HAZARD FOR SHERMAN ISLAND
FOR 2200

Figure
53



Delta Risk\figures\DR5-11-2200.grf

	<p>DELTA RISK MANAGEMENT STRATEGY CALIFORNIA</p>	<p>SEISMIC SOURCE CONTRIBUTIONS TO 1.0 SEC HORIZONTAL SPECTRAL ACCELERATION TIME- DEPENDENT HAZARD FOR STOCKTON FOR 2200</p>	<p>Figure 54</p>
<p>Project No. 26815900</p>			

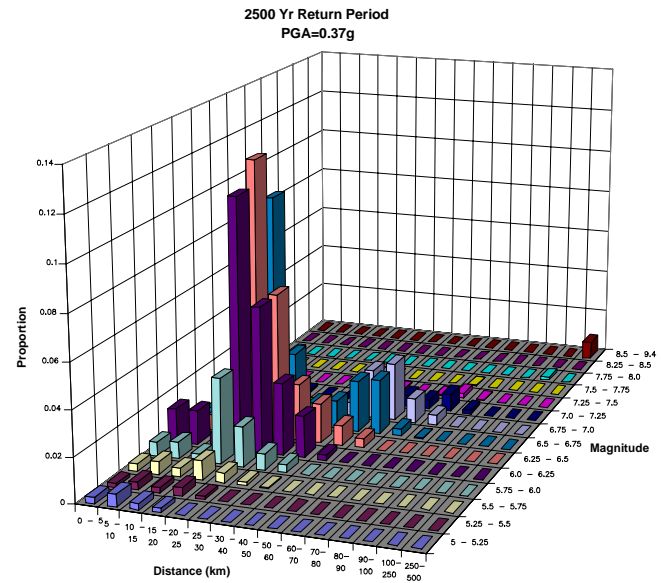
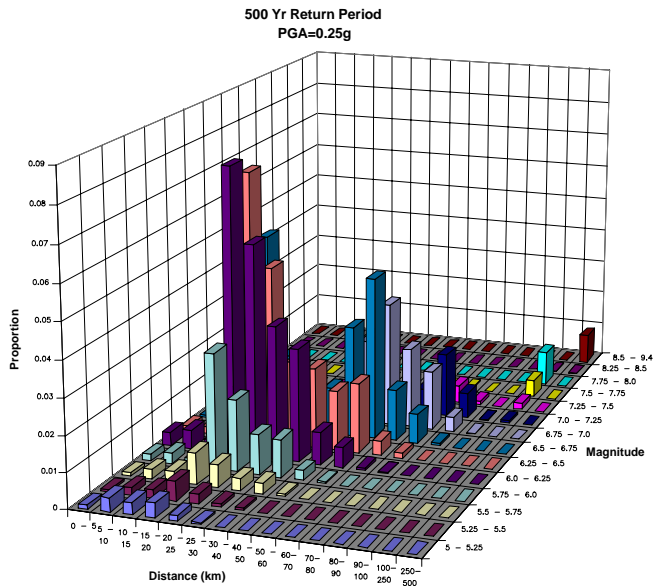
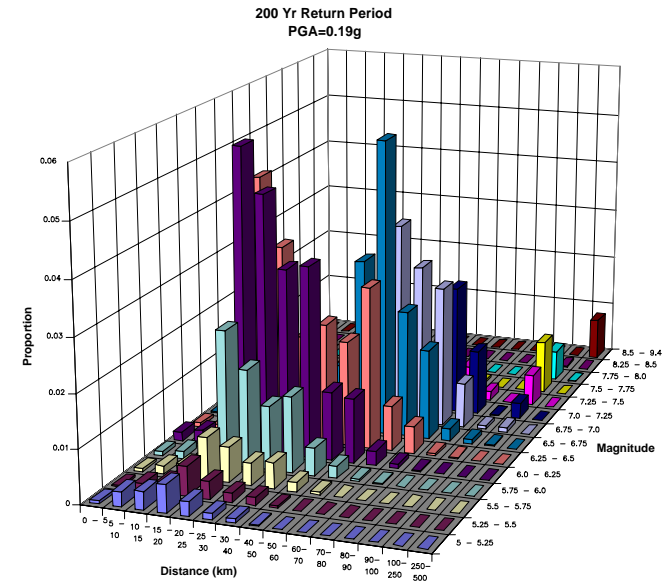
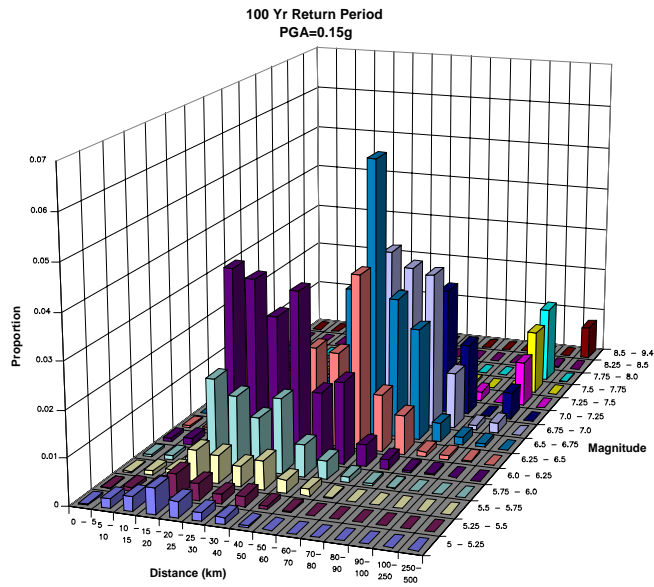


DELTA RISK MANAGEMENT STRATEGY
CALIFORNIA

PROJECT No. 26815621

MAGNITUDE AND DISTANCE CONTRIBUTIONS
TO THE MEAN PEAK HORIZONTAL
ACCELERATION HAZARD FOR
CLIFTON COURT FOR 2005

Figure
55

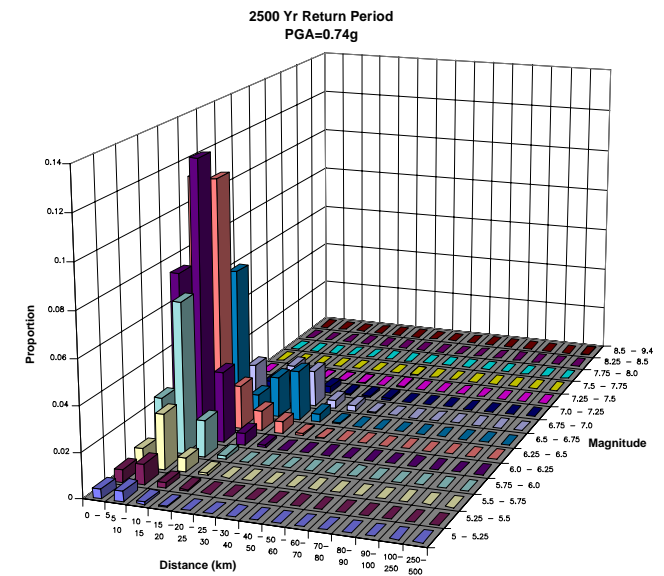
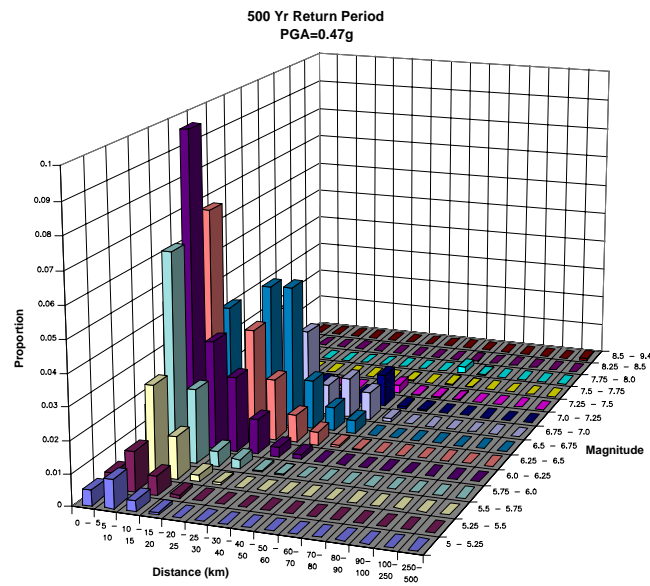
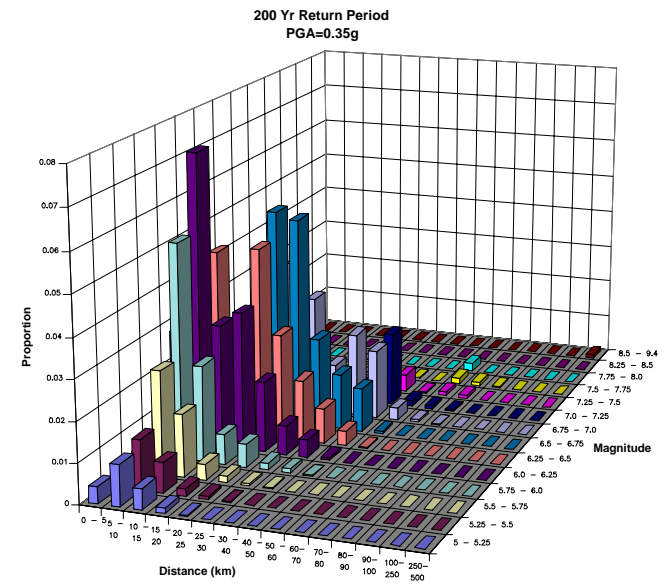
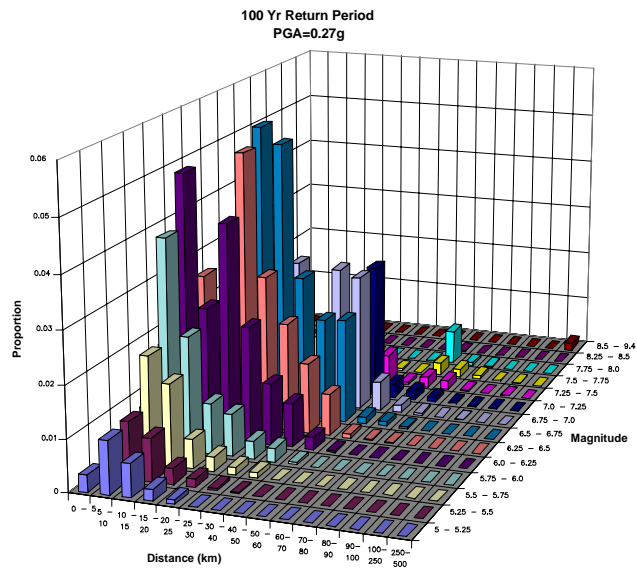


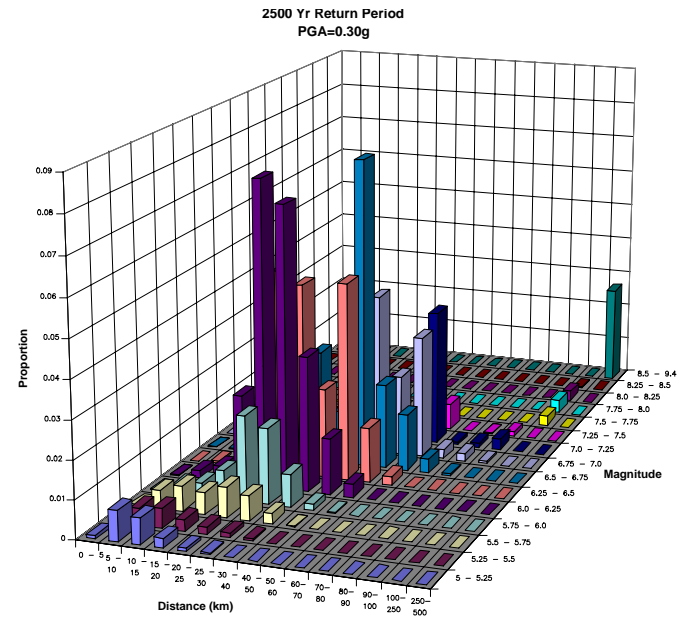
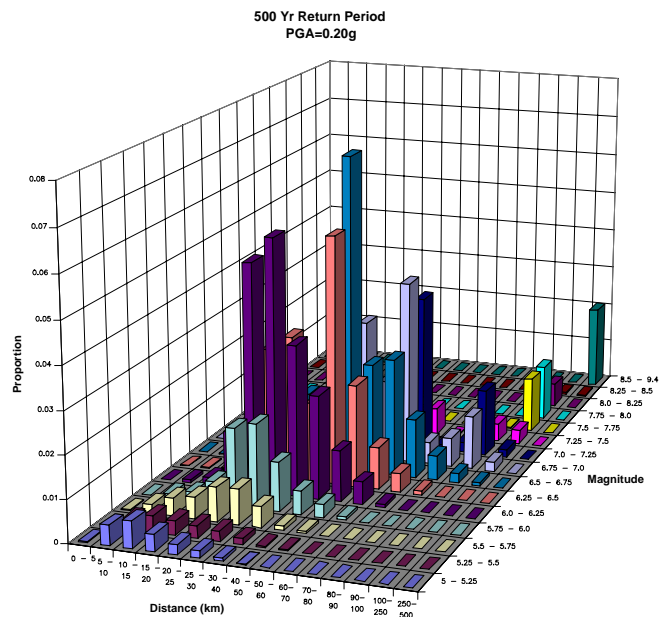
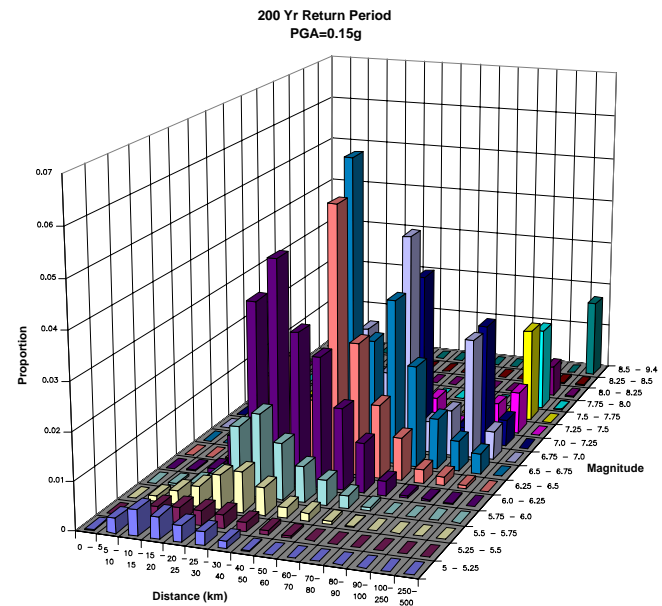
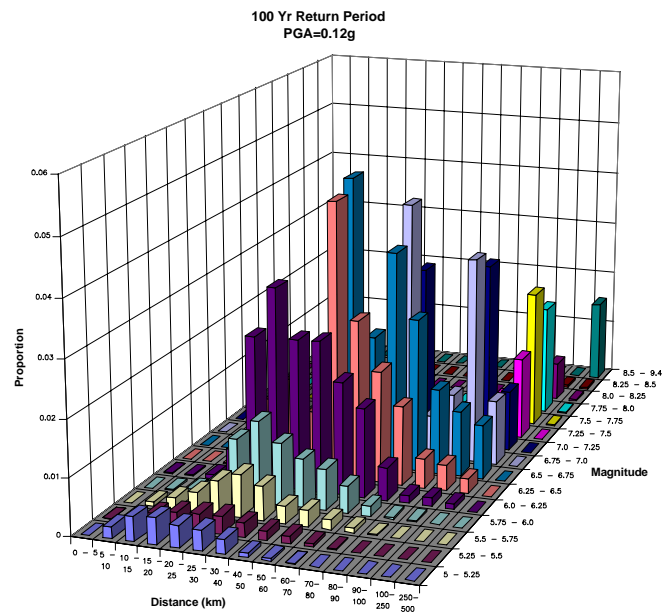
DELTA RISK MANAGEMENT STRATEGY
CALIFORNIA

PROJECT No. 26815621

MAGNITUDE AND DISTANCE CONTRIBUTIONS
TO THE MEAN PEAK HORIZONTAL
ACCELERATION HAZARD FOR
DELTA CROSS CHANNEL FOR 2005

Figure
56



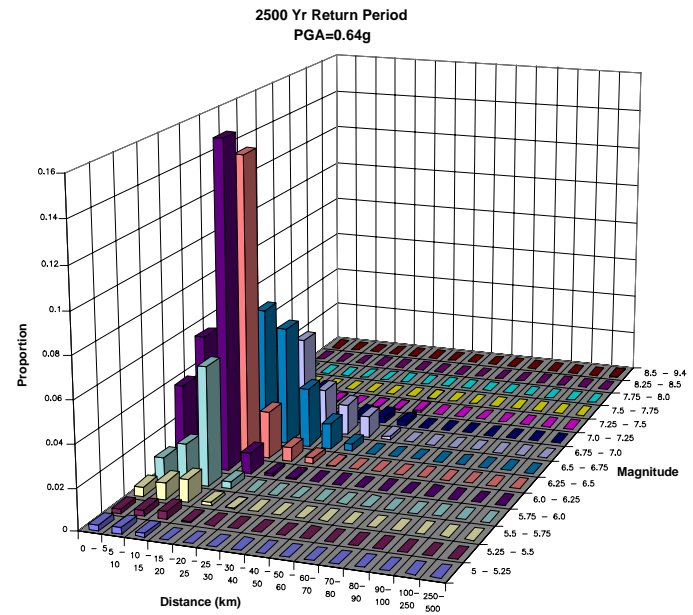
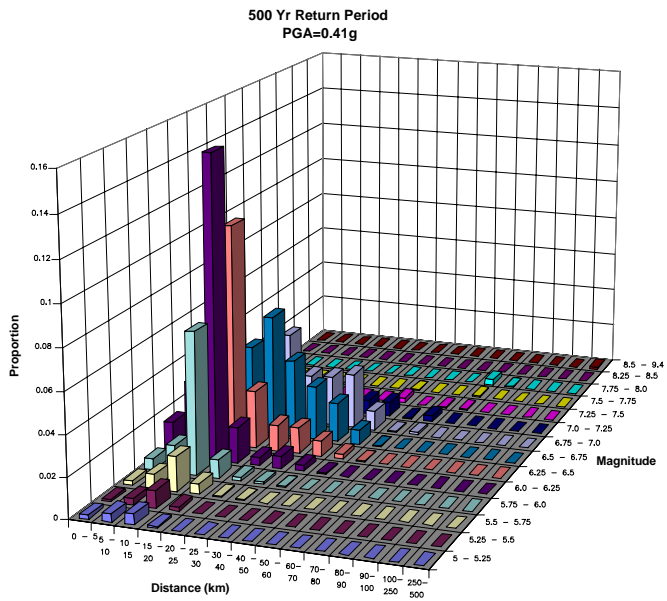
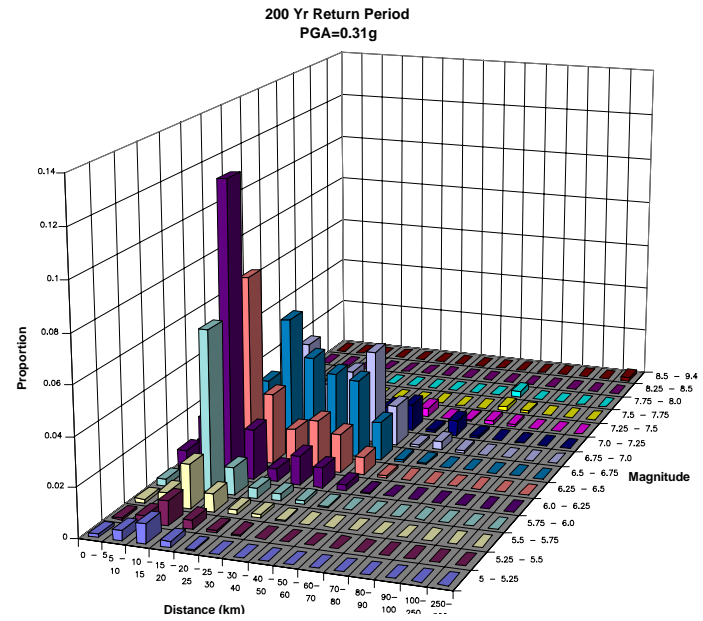
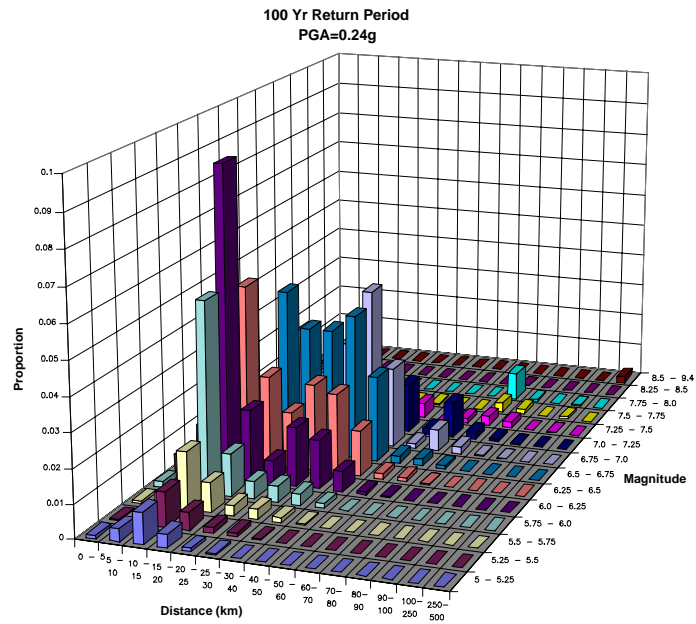


DELTA RISK MANAGEMENT STRATEGY
CALIFORNIA

PROJECT No. 26815621

MAGNITUDE AND DISTANCE CONTRIBUTIONS
TO THE MEAN PEAK HORIZONTAL
ACCELERATION HAZARD FOR
SACRAMENTO FOR 2005

Figure
58

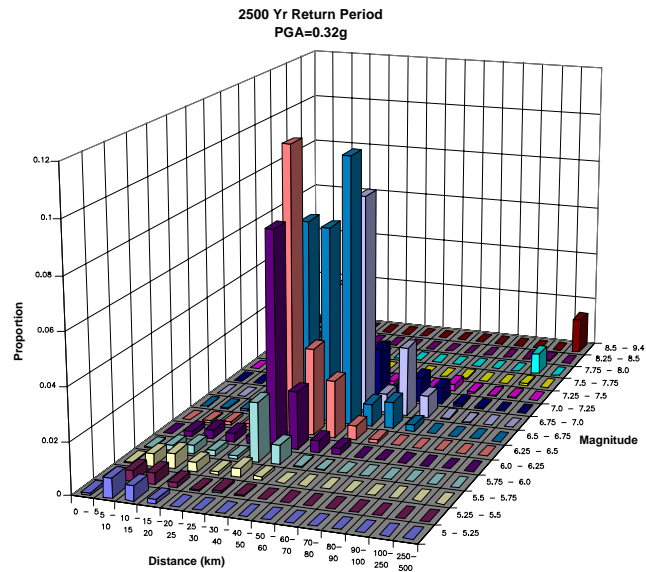
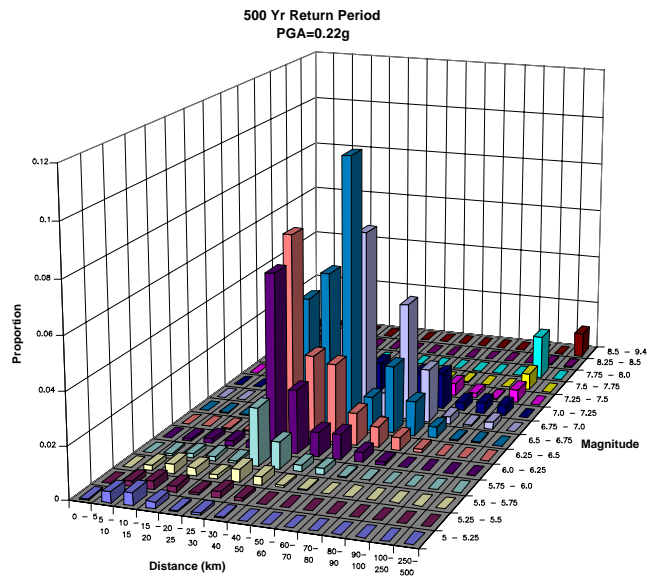
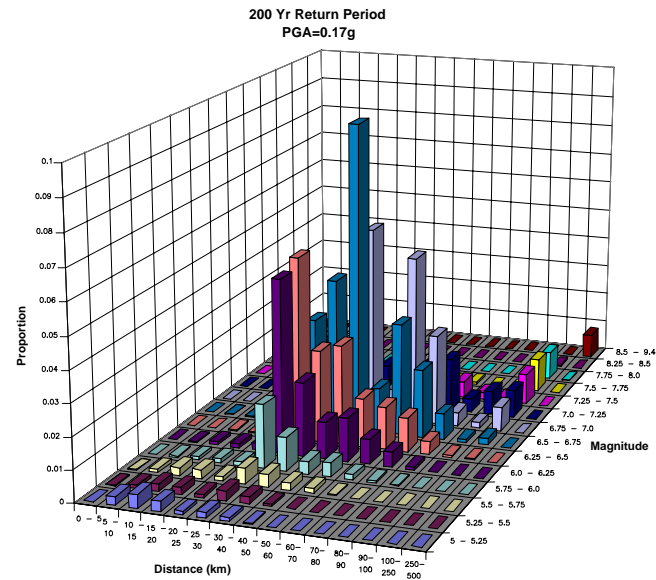
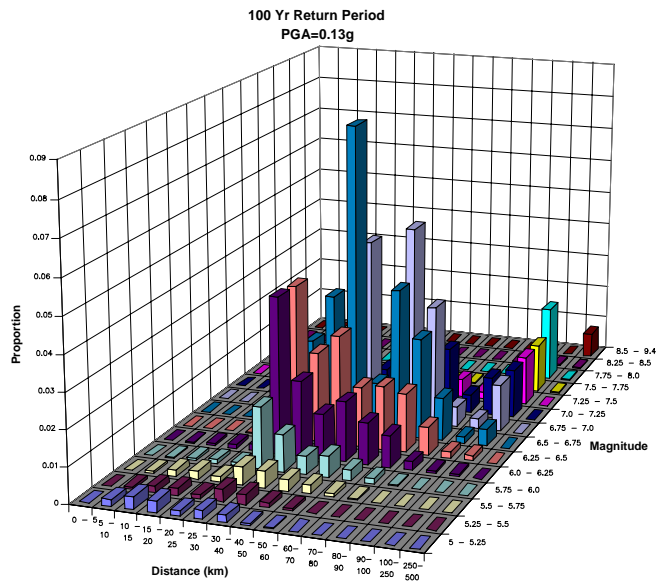


DELTA RISK MANAGEMENT STRATEGY
CALIFORNIA

PROJECT No. 26815621

MAGNITUDE AND DISTANCE CONTRIBUTIONS
TO THE MEAN PEAK HORIZONTAL
ACCELERATION HAZARD FOR
SHERMAN ISLAND FOR 2005

Figure
59



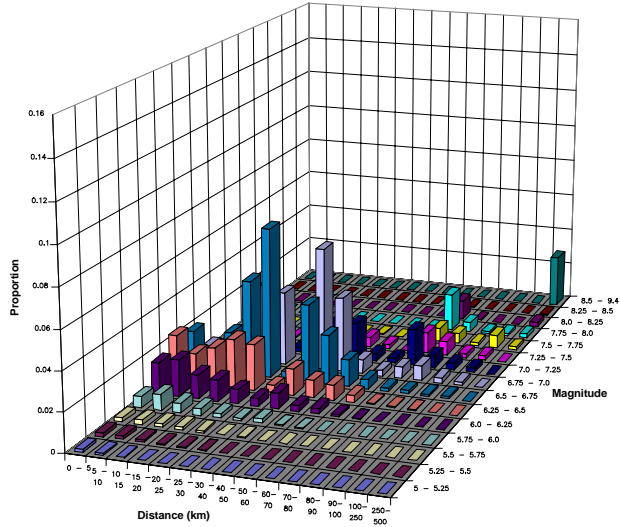
DELTA RISK MANAGEMENT STRATEGY
CALIFORNIA

PROJECT No. 26815621

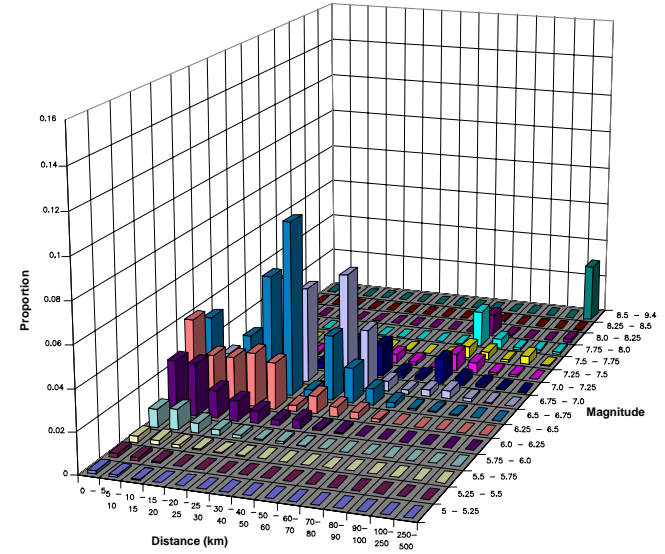
MAGNITUDE AND DISTANCE CONTRIBUTIONS
TO THE MEAN PEAK HORIZONTAL
ACCELERATION HAZARD FOR
STOCKTON FOR 2005

Figure
60

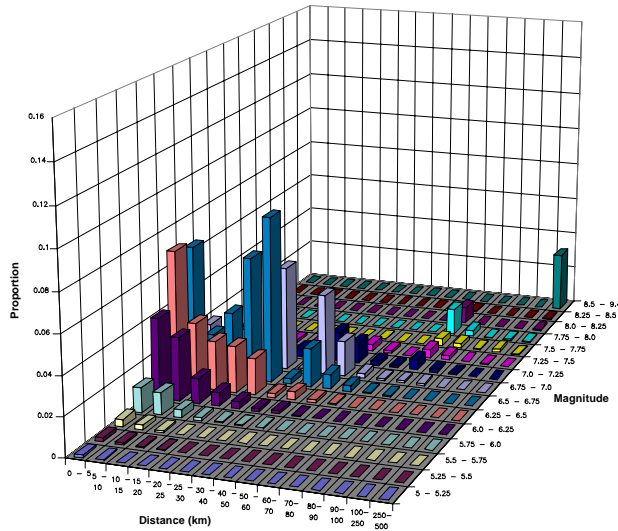
100 Yr Return Period
PGA=0.24g



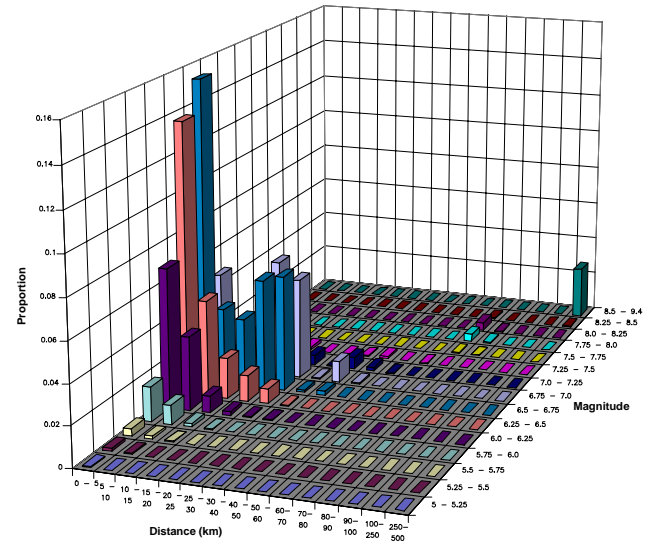
200 Yr Return Period
PGA=0.32g



500 Yr Return Period
PGA=0.47g



2500 Yr Return Period
PGA=0.82g



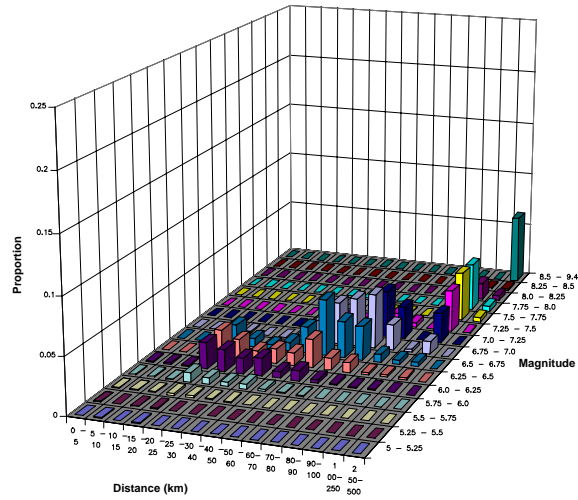
DELTA RISK MANAGEMENT STRATEGY
CALIFORNIA

PROJECT No. 26815621

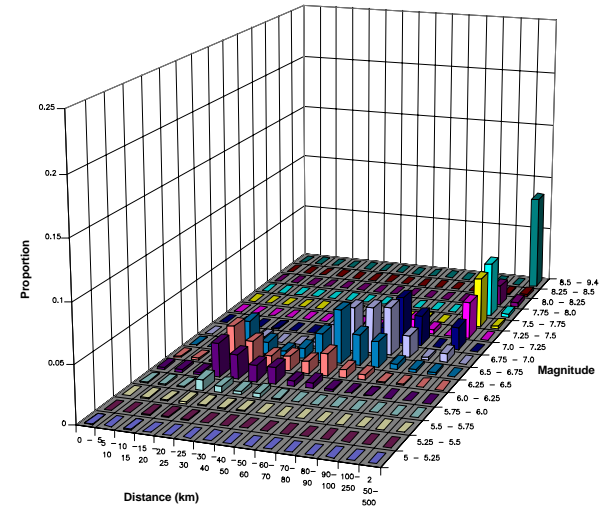
MAGNITUDE AND DISTANCE CONTRIBUTIONS
TO THE 1.0 SEC HORIZONTAL SPECTRAL
ACCELERATION HAZARD FOR
CLIFTON COURT FOR 2005

Figure
61

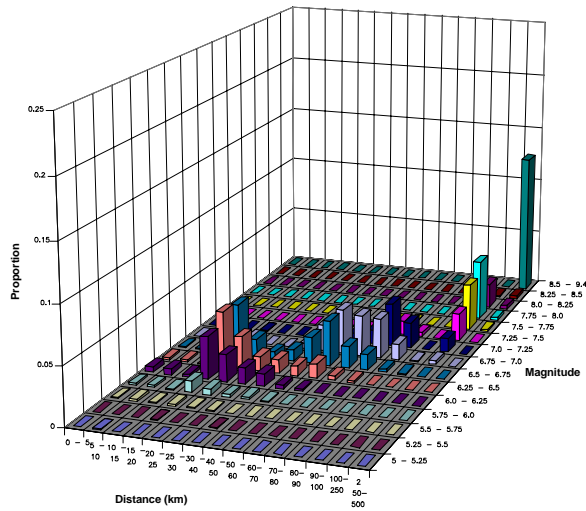
100 Yr Return Period
PGA=0.17g



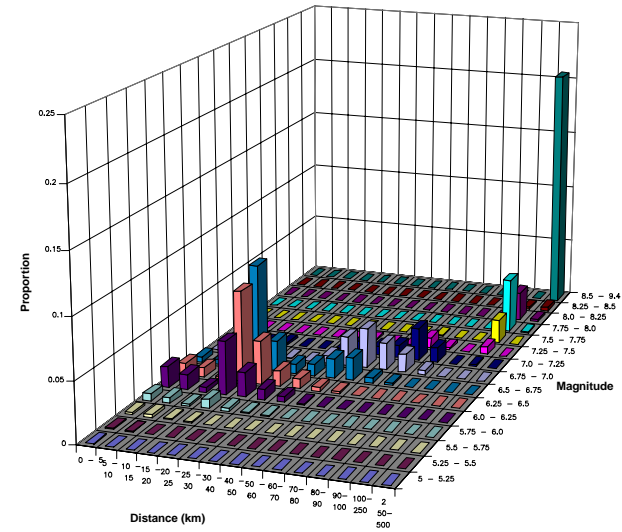
200 Yr Return Period
PGA=0.22g



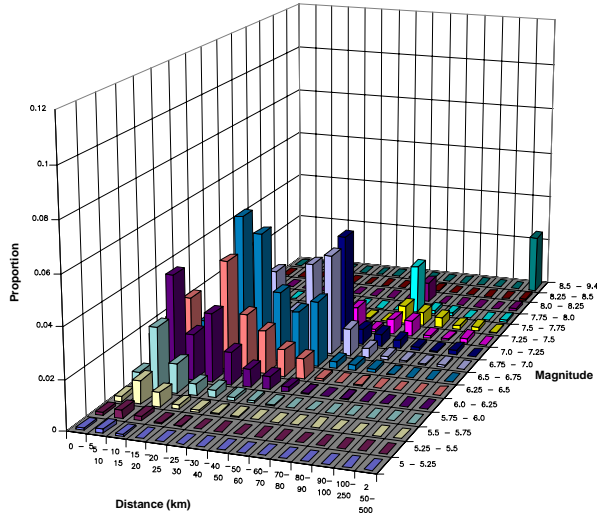
500 Yr Return Period
PGA=0.30g



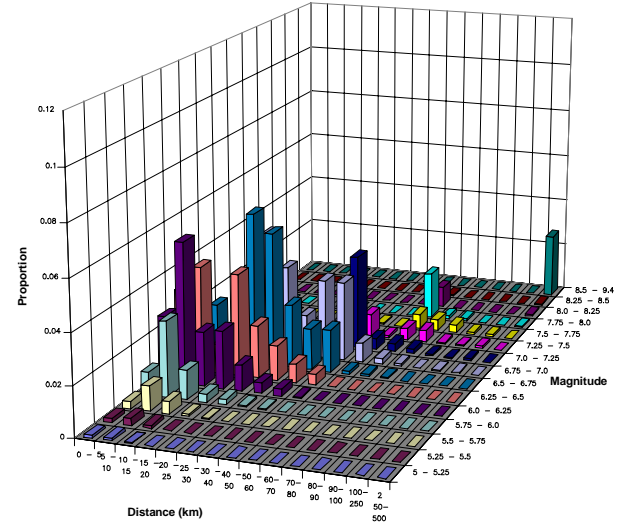
2500 Yr Return Period
PGA=0.48g



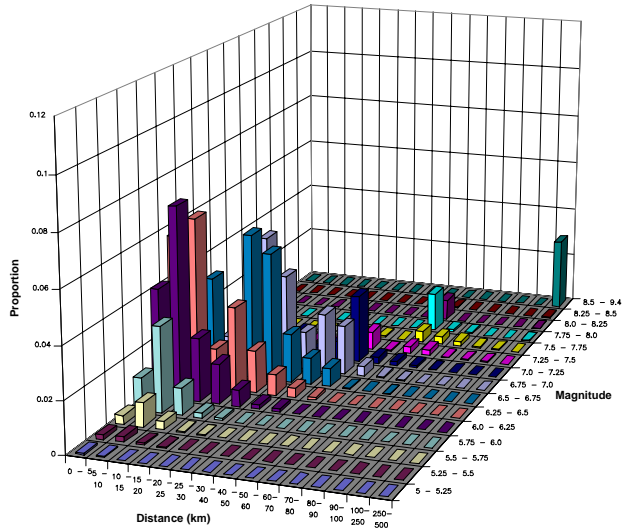
100 Yr Return Period
PGA=0.29g



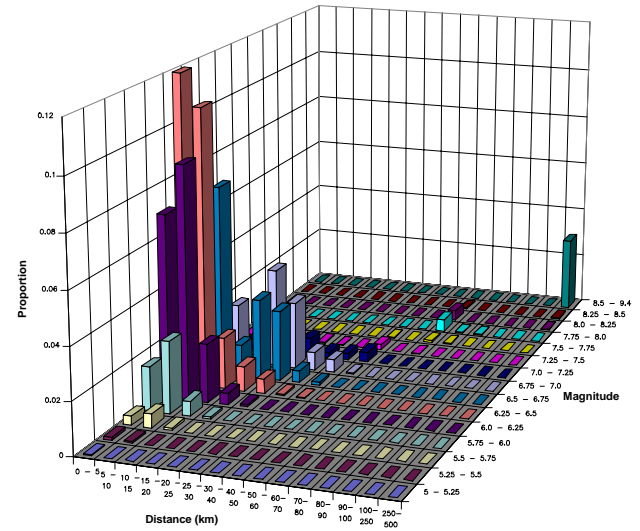
200 Yr Return Period
PGA=0.38g



500 Yr Return Period
PGA=0.53g



2500 Yr Return Period
PGA=0.90g



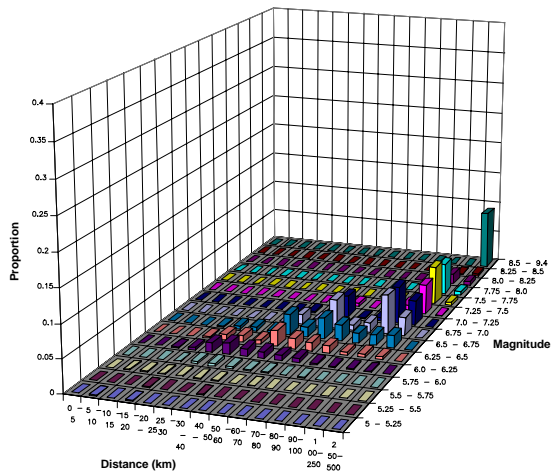
DELTA RISK MANAGEMENT STRATEGY
CALIFORNIA

PROJECT No. 26815621

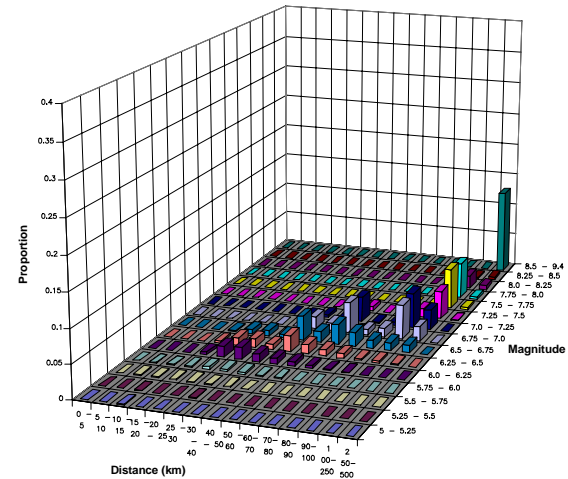
MAGNITUDE AND DISTANCE CONTRIBUTIONS
TO THE 1.0 SEC HORIZONTAL SPECTRAL
ACCELERATION HAZARD FOR
MONTEZUMA SLOUGH FOR 2005

Figure
63

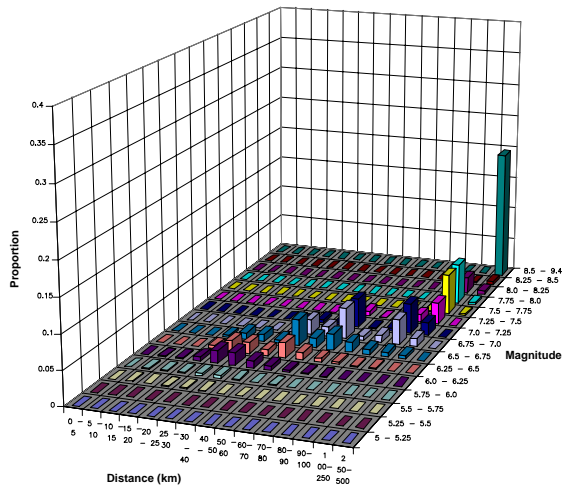
100 Yr Return Period
PGA=0.15g



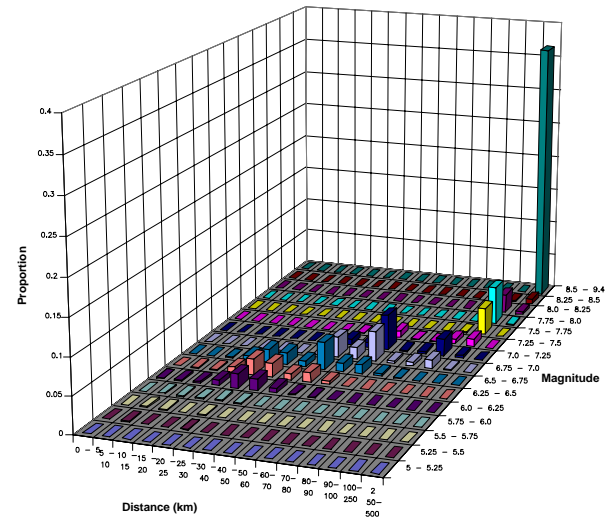
200 Yr Return Period
PGA=0.19g



500 Yr Return Period
PGA=0.26g



2500 Yr Return Period
PGA=0.42g

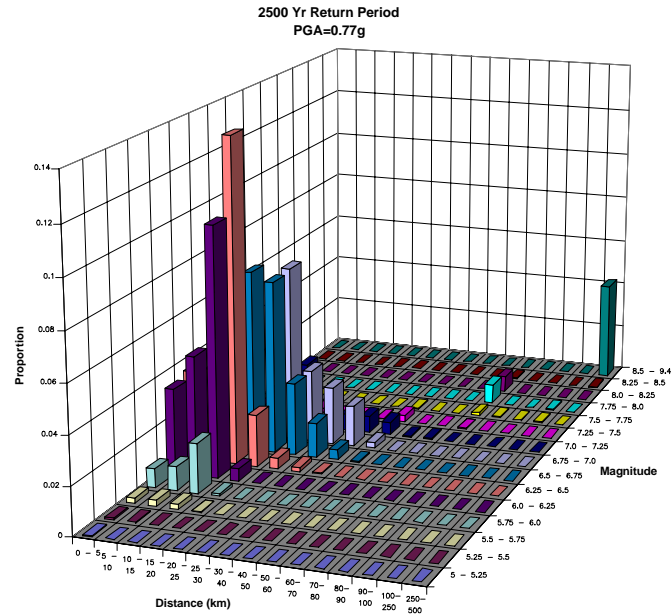
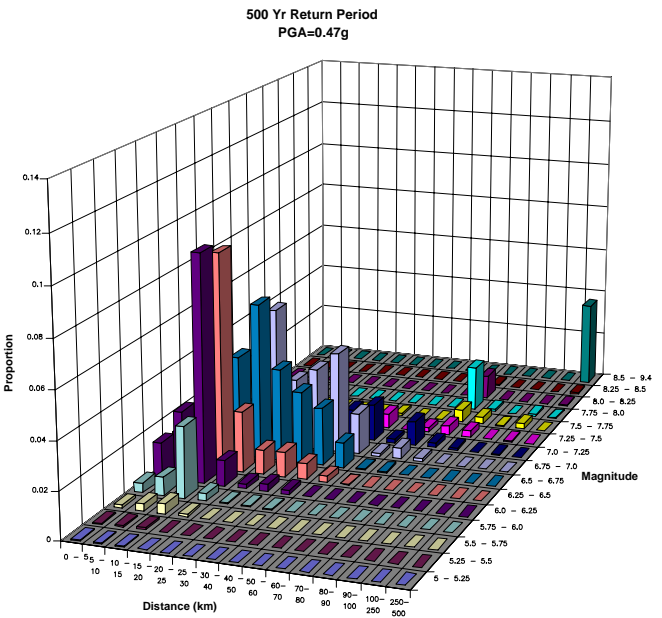
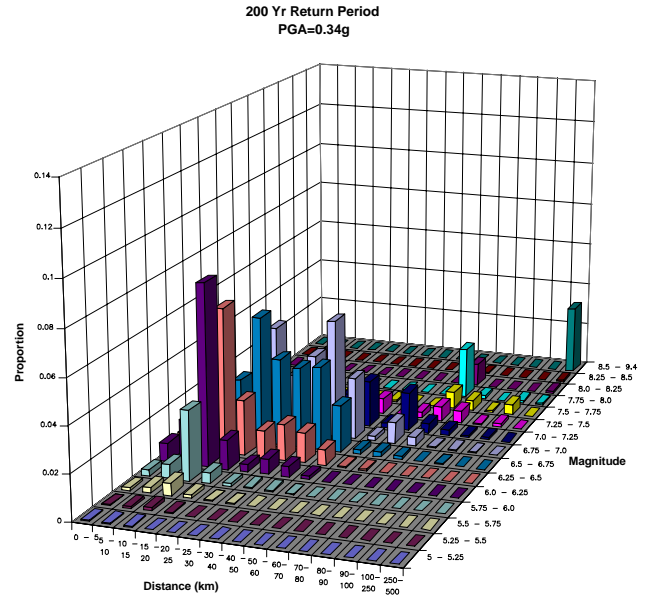
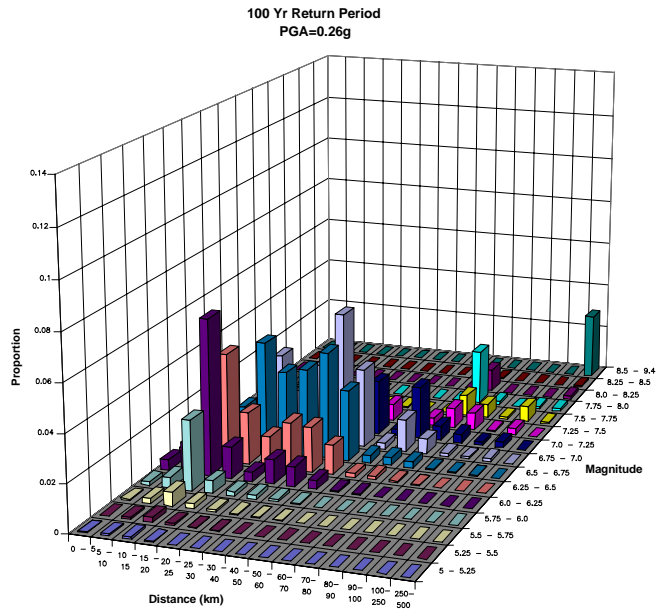


DELTA RISK MANAGEMENT STRATEGY
CALIFORNIA

PROJECT No. 26815621

MAGNITUDE AND DISTANCE CONTRIBUTIONS
TO THE 1.0 SEC HORIZONTAL SPECTRAL
ACCELERATION HAZARD FOR
SACRAMENTO FOR 2005

Figure
64



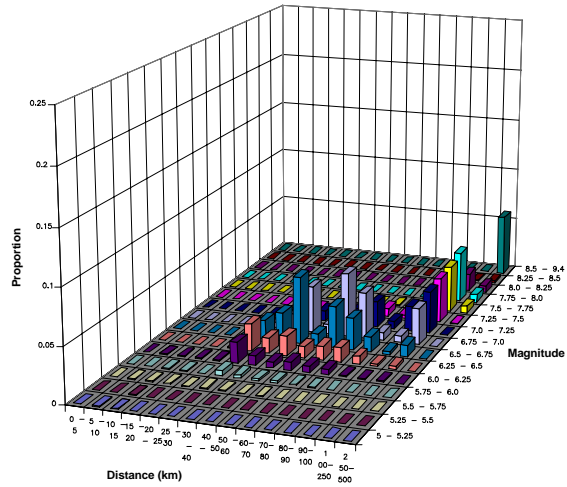
DELTA RISK MANAGEMENT STRATEGY
CALIFORNIA

PROJECT No. 26815621

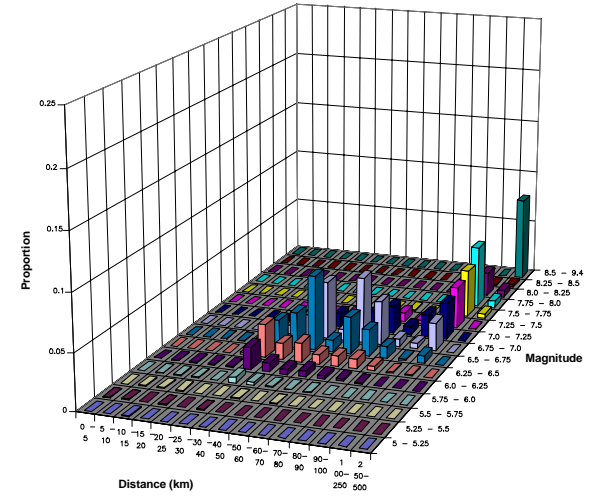
MAGNITUDE AND DISTANCE CONTRIBUTIONS
TO THE 1.0 SEC HORIZONTAL SPECTRAL
ACCELERATION HAZARD FOR
SHERMAN ISLAND FOR 2005

Figure
65

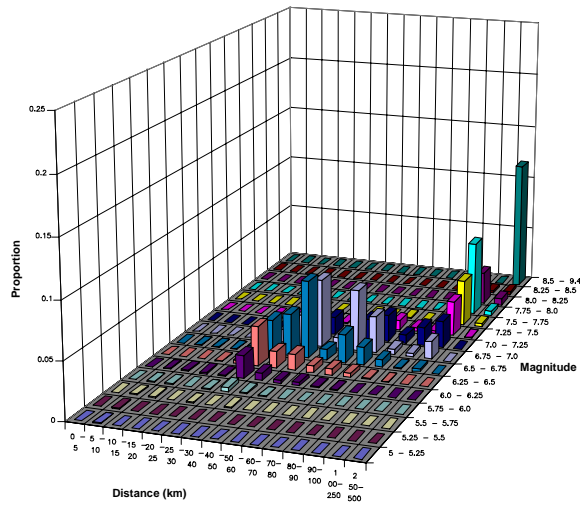
100 Yr Return Period
PGA=0.16g



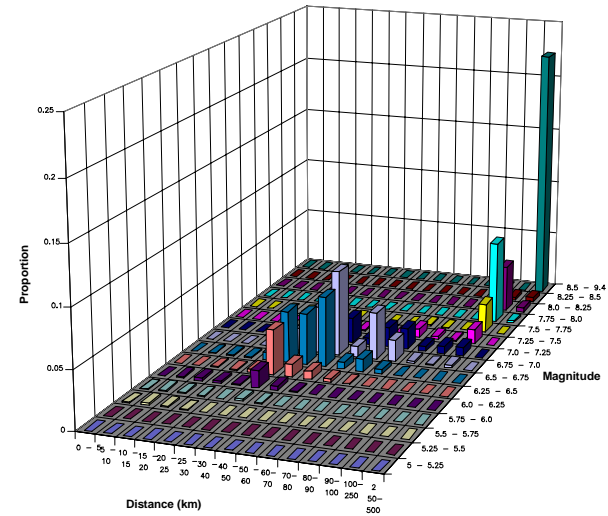
200 Yr Return Period
PGA=0.21g



500 Yr Return Period
PGA=0.28g



2500 Yr Return Period
PGA=0.44g

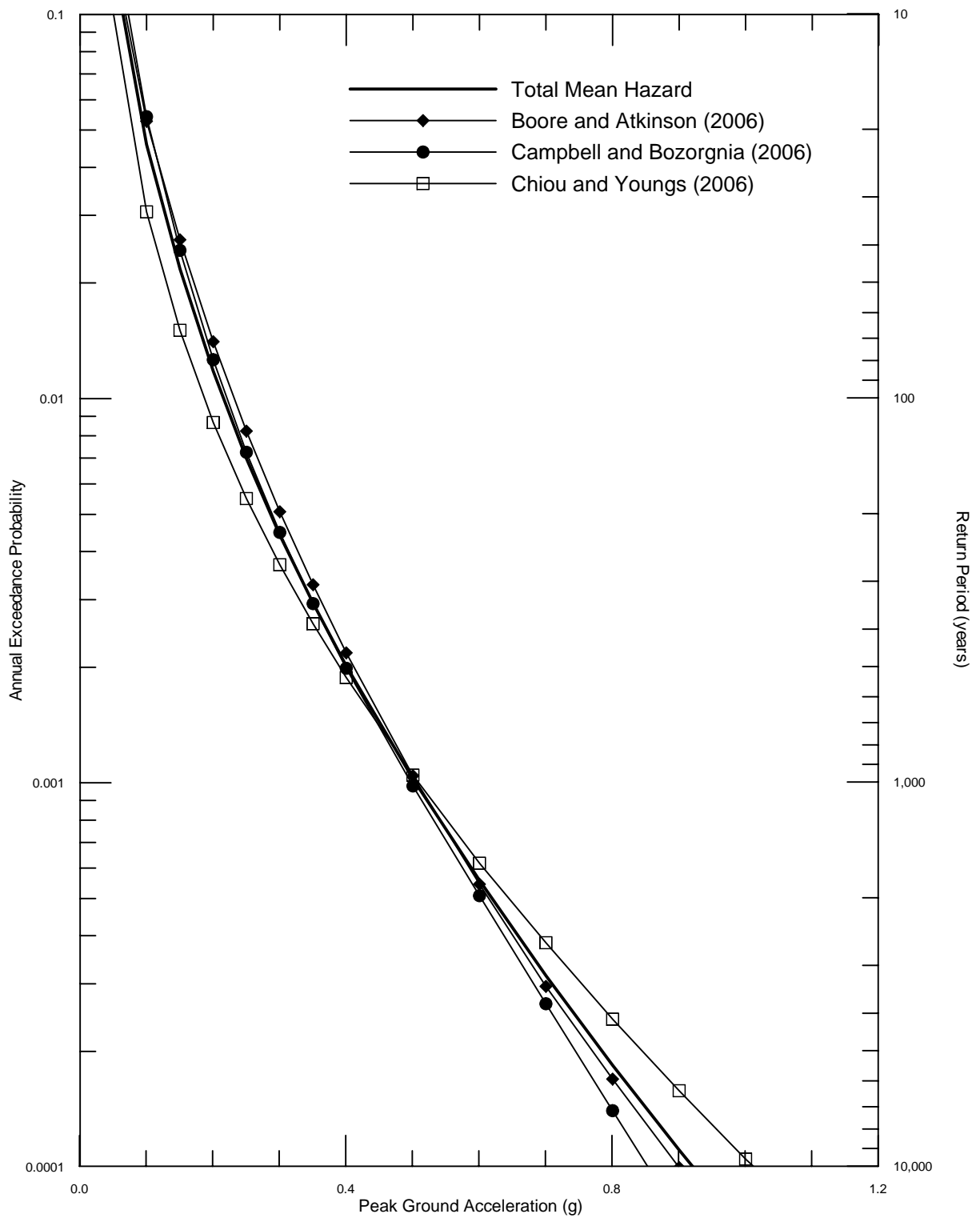


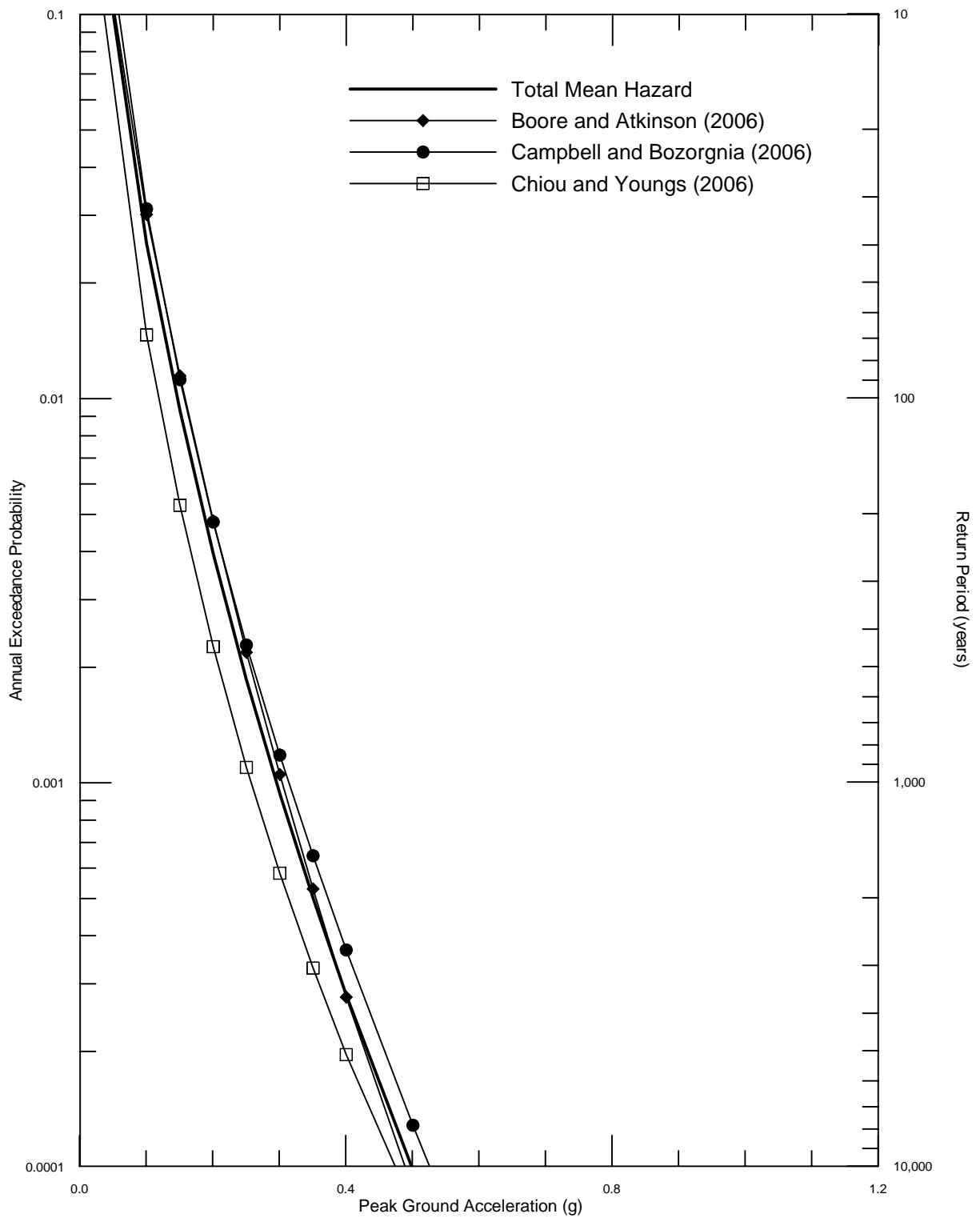
DELTA RISK MANAGEMENT STRATEGY
CALIFORNIA

PROJECT No. 26815621

MAGNITUDE AND DISTANCE CONTRIBUTIONS
TO THE 1.0 SEC HORIZONTAL SPECTRAL
ACCELERATION HAZARD FOR
STOCKTON FOR 2005

Figure
66



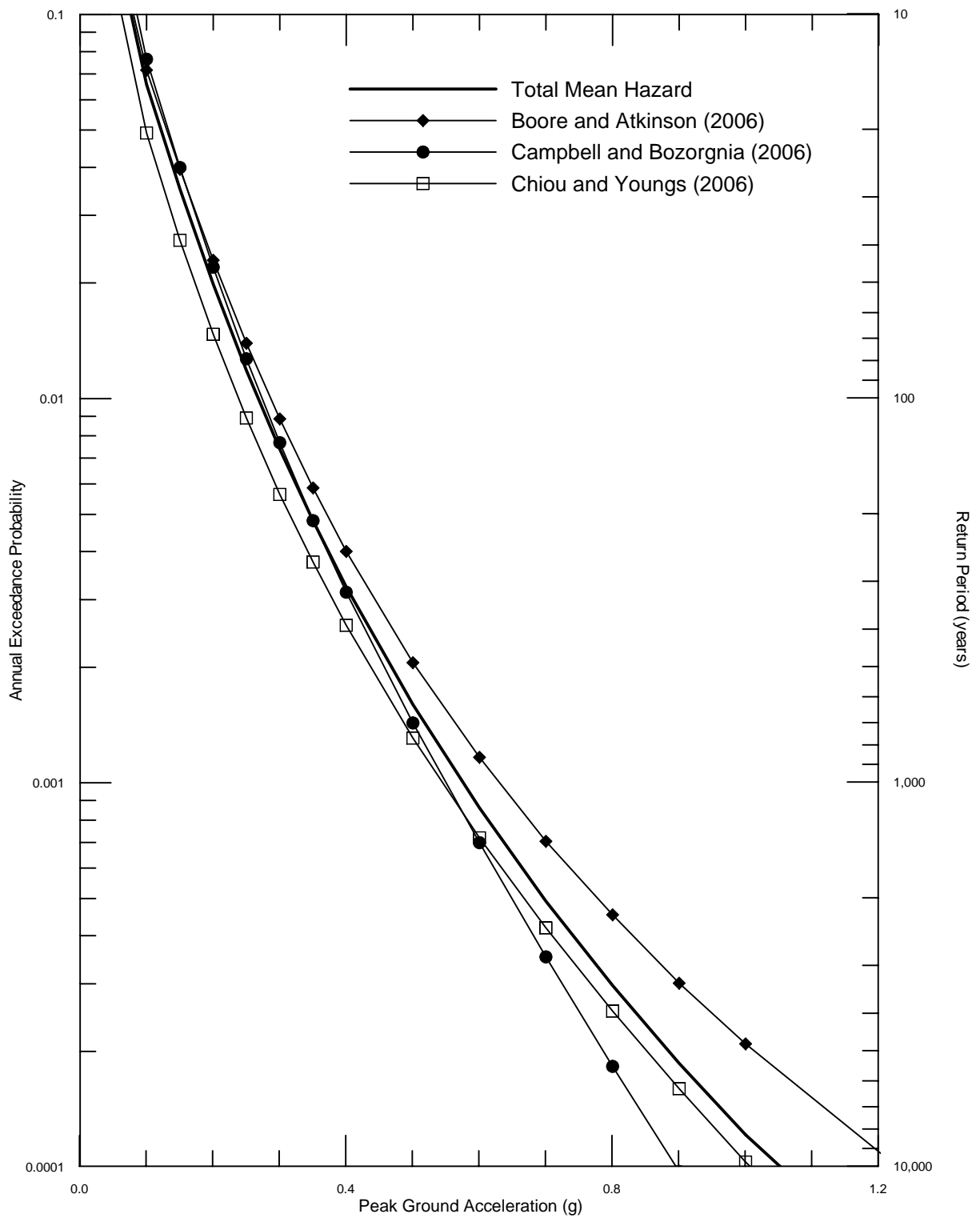


DELTA RISK
MANAGEMENT STRATEGY
CALIFORNIA

Project No. 26815900

SENSITIVITY OF MEAN PEAK
HORIZONTAL ACCELERATION TIME-DEPENDENT
HAZARD TO ATTENUATION RELATIONSHIPS
FOR DELTA CROSS CHANNEL FOR 2005

Figure
68

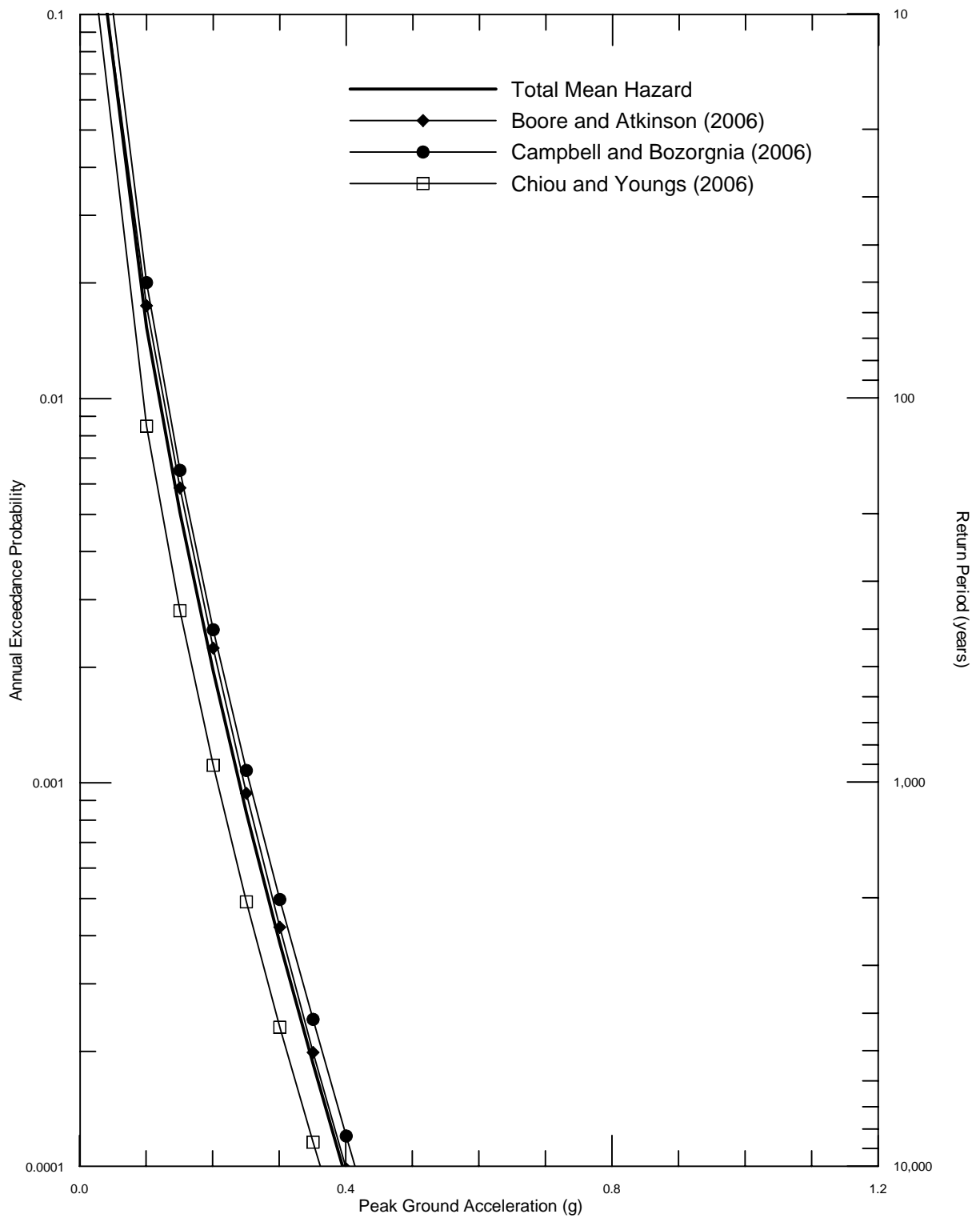


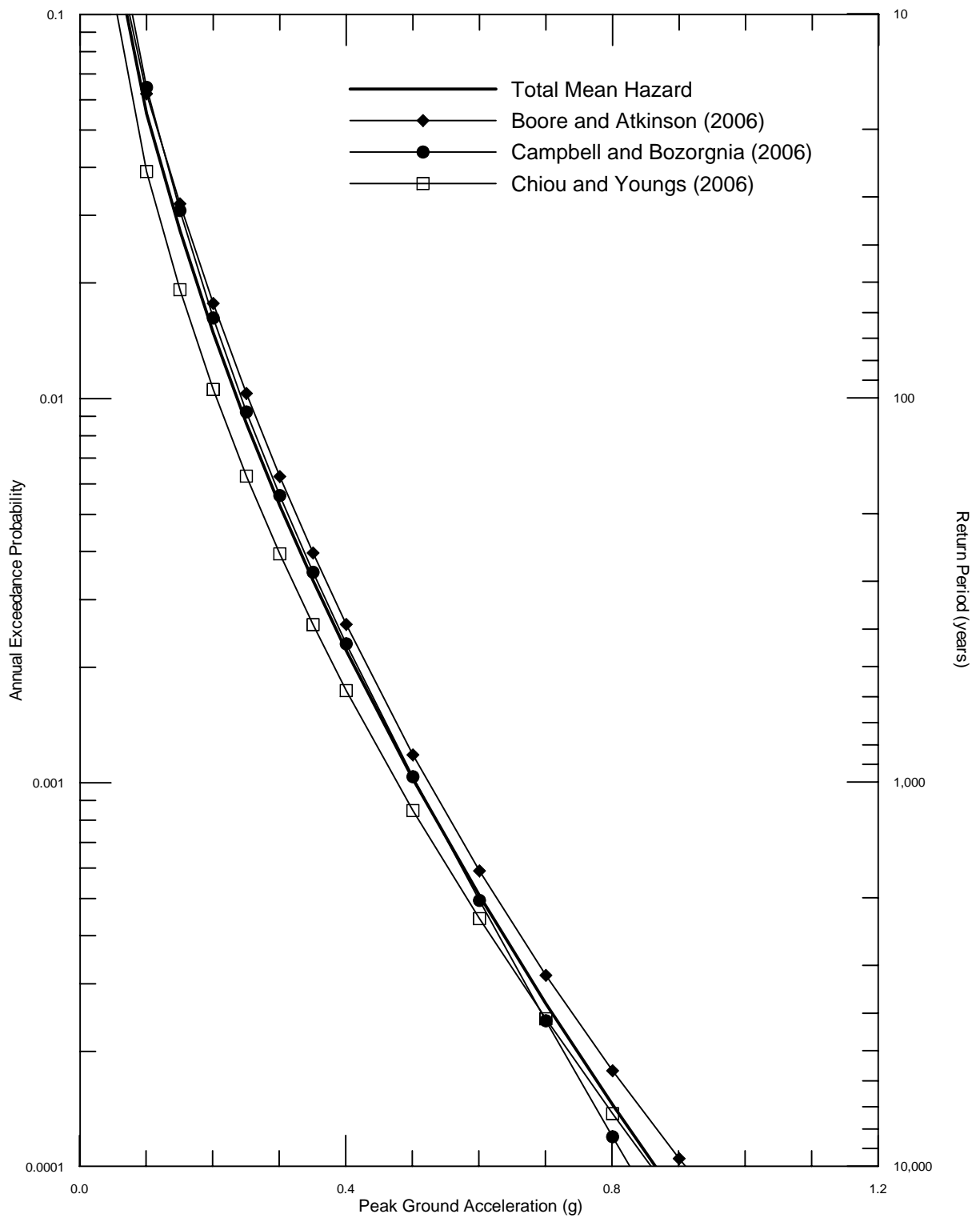
DELTA RISK
MANAGEMENT STRATEGY
CALIFORNIA

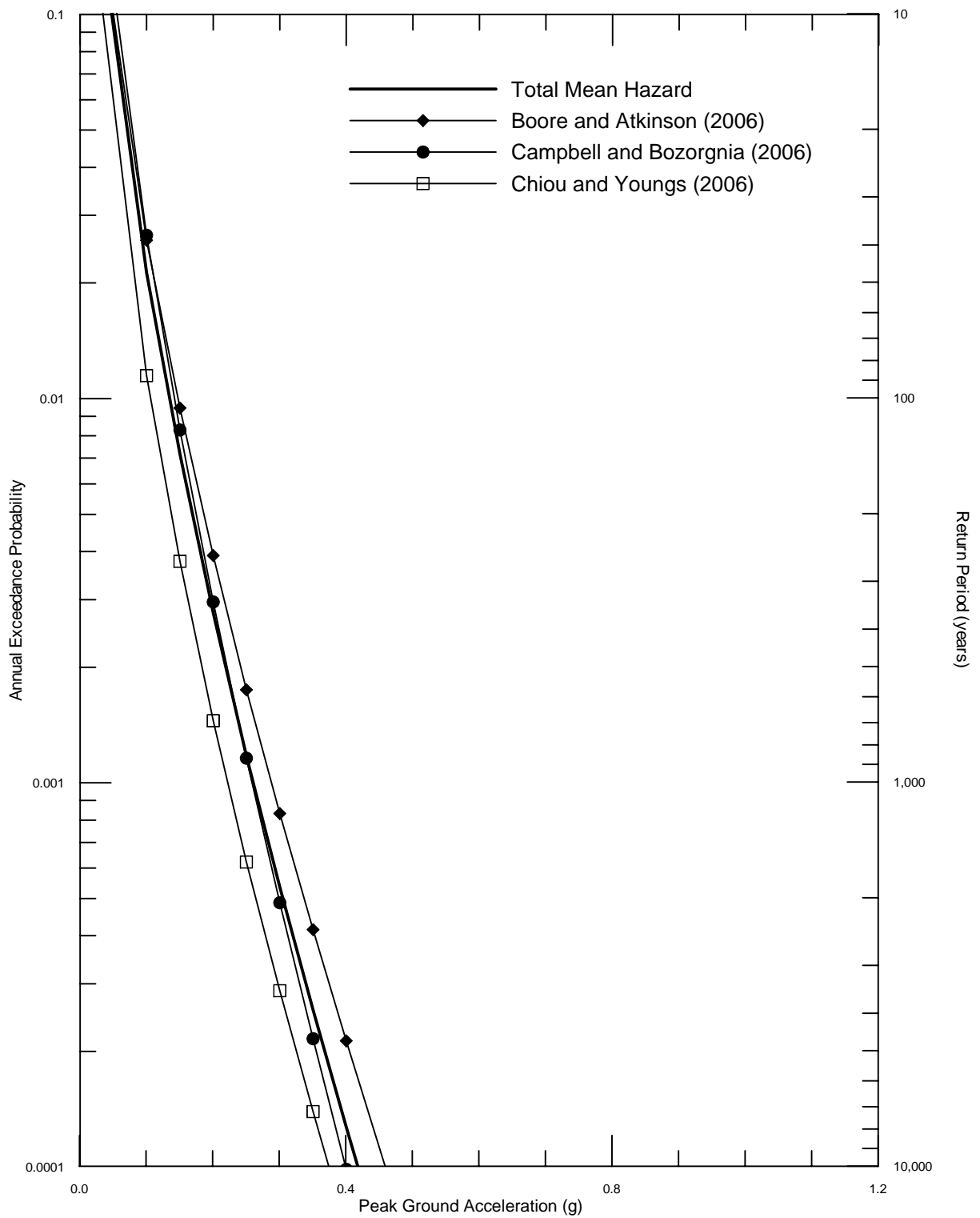
Project No. 26815900

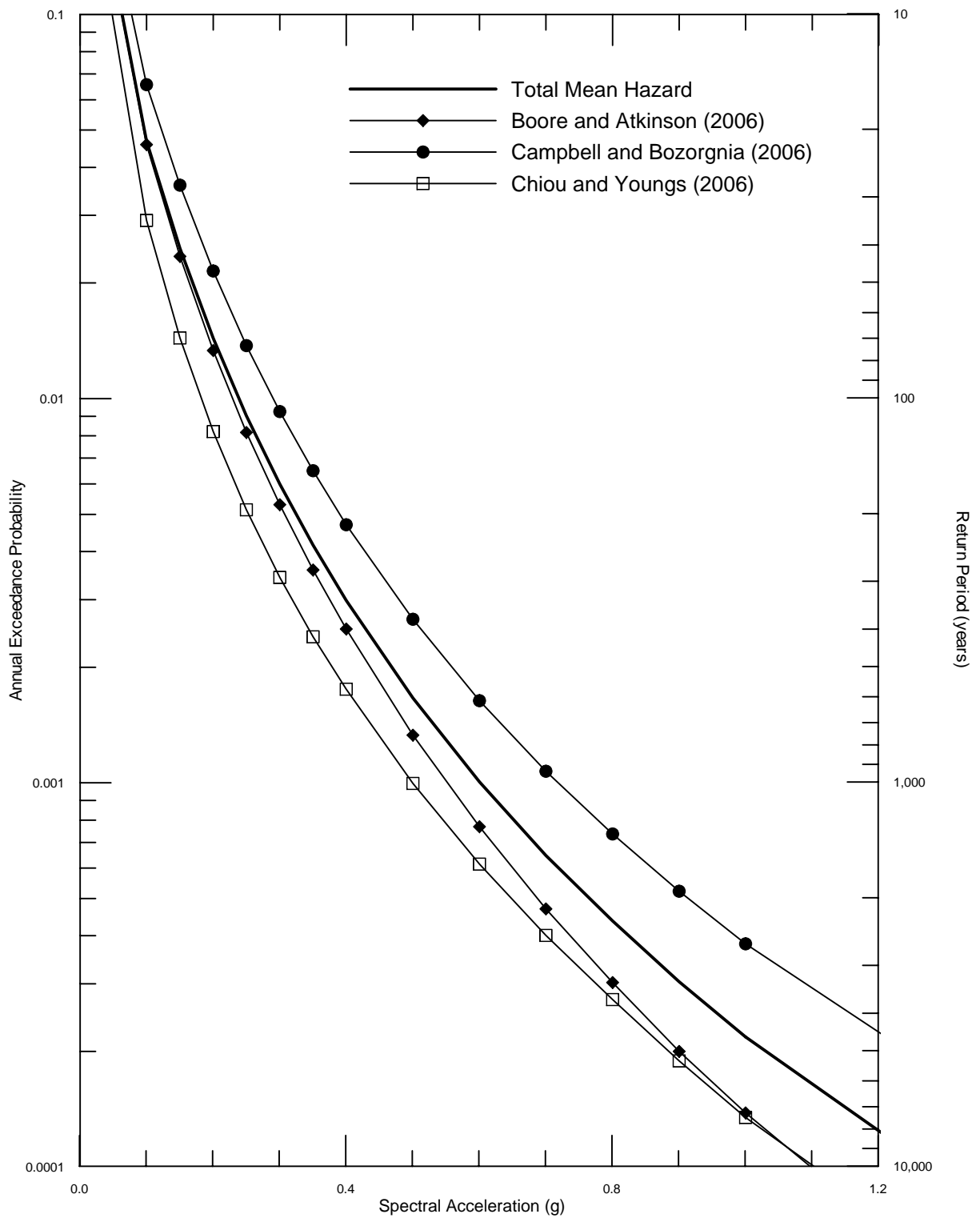
SENSITIVITY OF MEAN PEAK
HORIZONTAL ACCELERATION TIME-DEPENDENT
HAZARD TO ATTENUATION RELATIONSHIPS
FOR MONTEZUMA SLOUGH FOR 2005

Figure
69







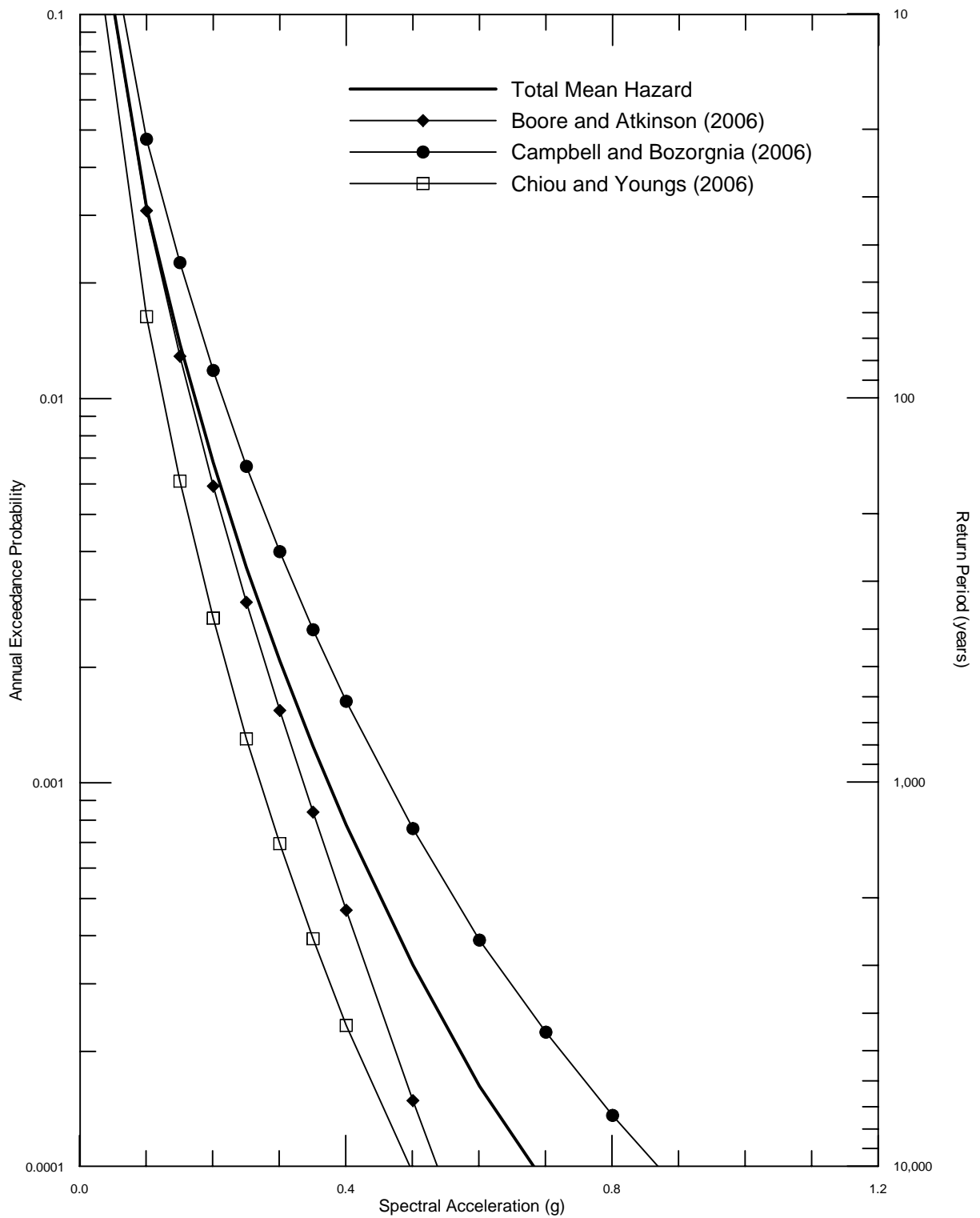


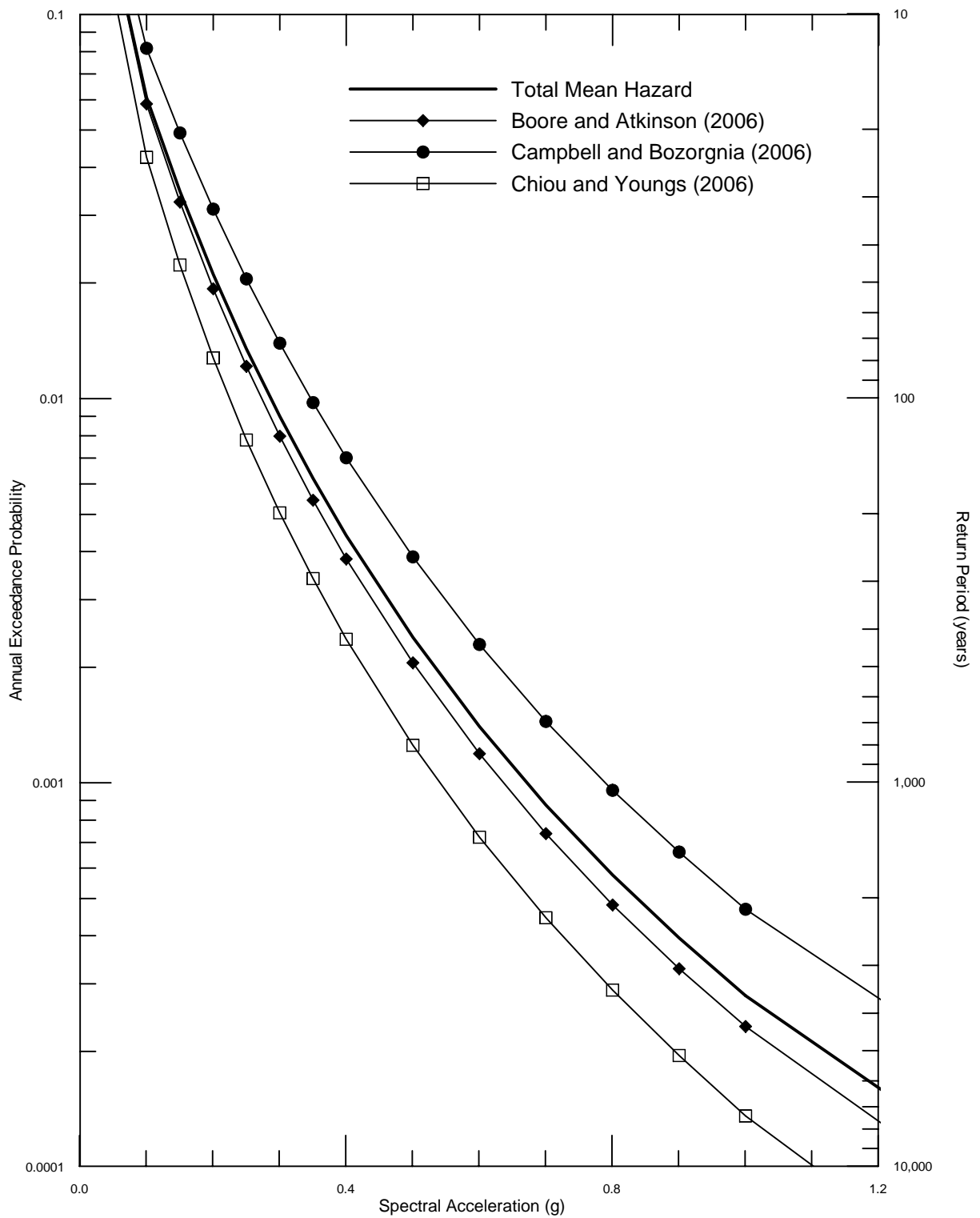
DELTA RISK
MANAGEMENT STRATEGY
CALIFORNIA

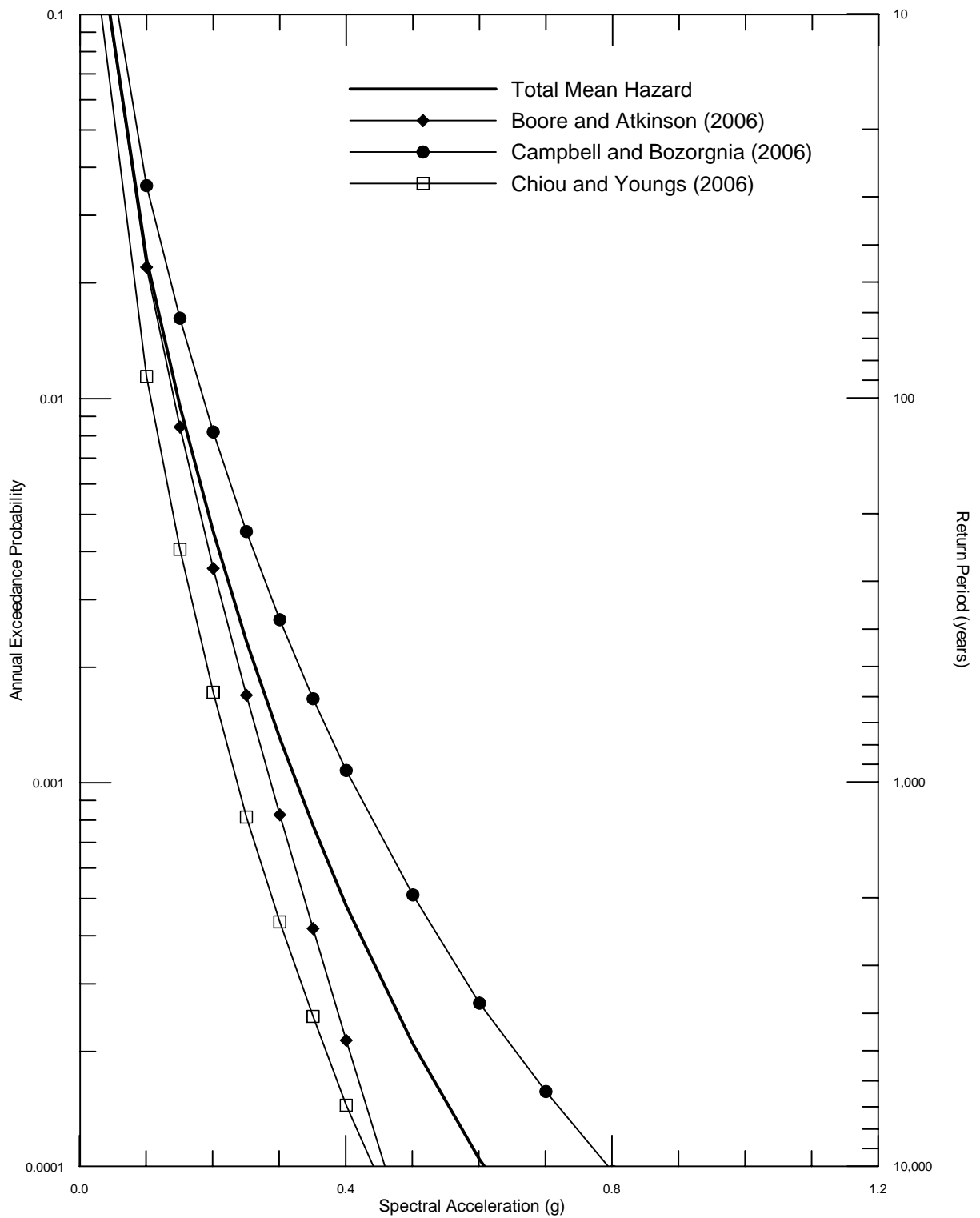
Project No. 26815900

SENSITIVITY OF 1.0 SEC SPECTRAL
HORIZONTAL ACCELERATION TIME-DEPENDENT
HAZARD TO ATTENUATION RELATIONSHIPS
FOR CLIFTON COURT FOR 2005

Figure
73





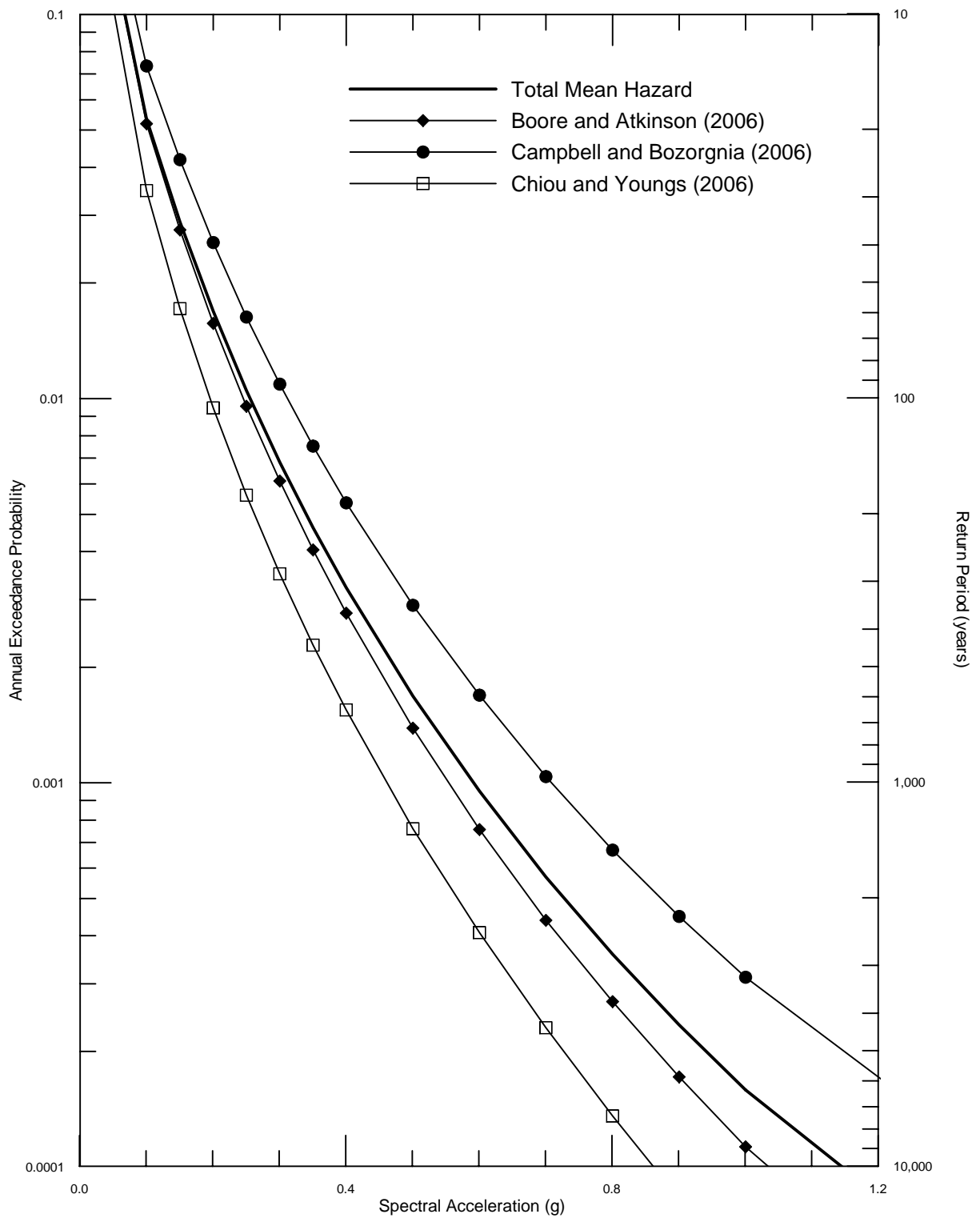


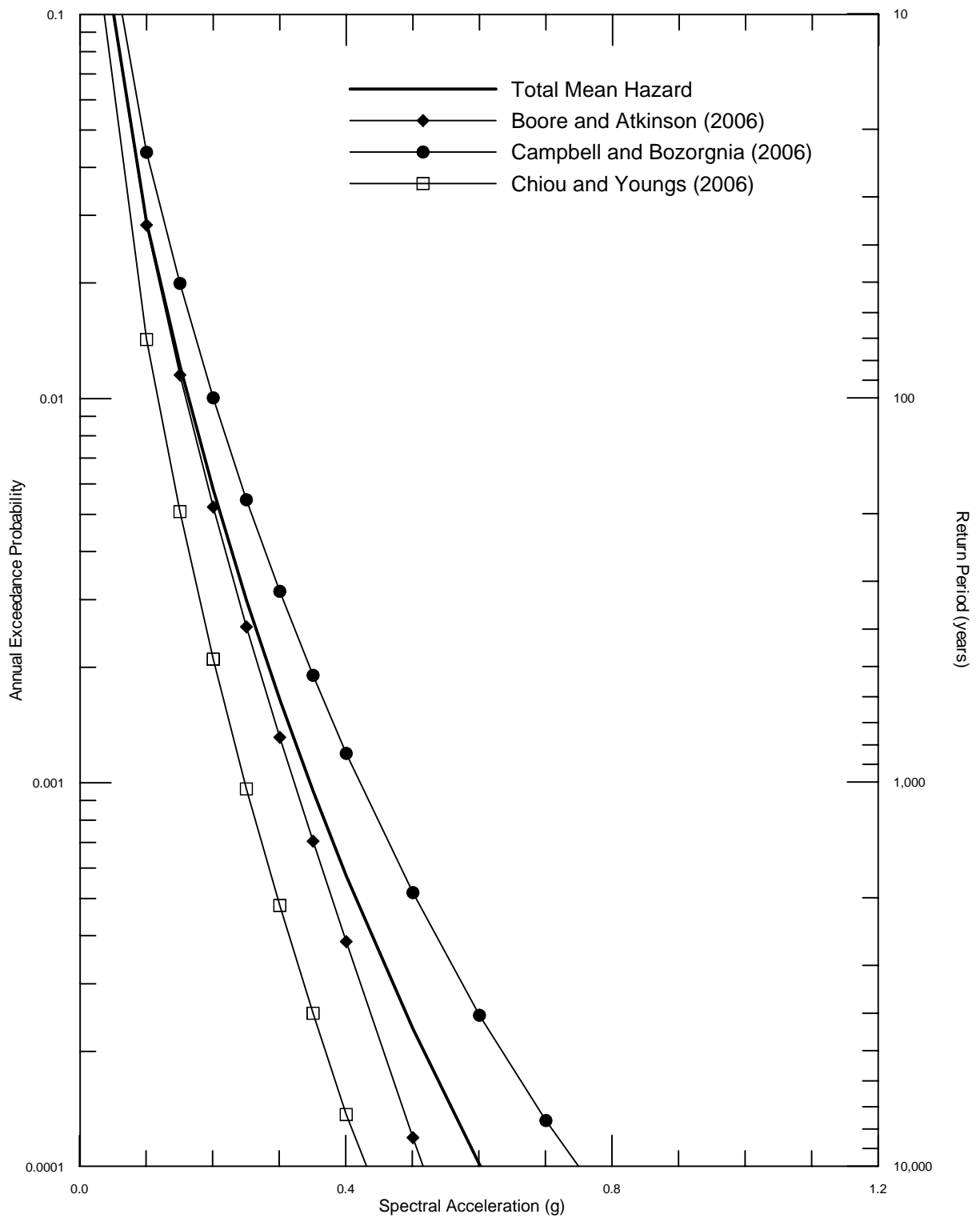
DELTA RISK
MANAGEMENT STRATEGY
CALIFORNIA

Project No. 26815900

SENSITIVITY OF 1.0 SEC SPECTRAL
HORIZONTAL ACCELERATION TIME-DEPENDENT
HAZARD TO ATTENUATION RELATIONSHIPS
FOR SACRAMENTO FOR 2005

Figure
76



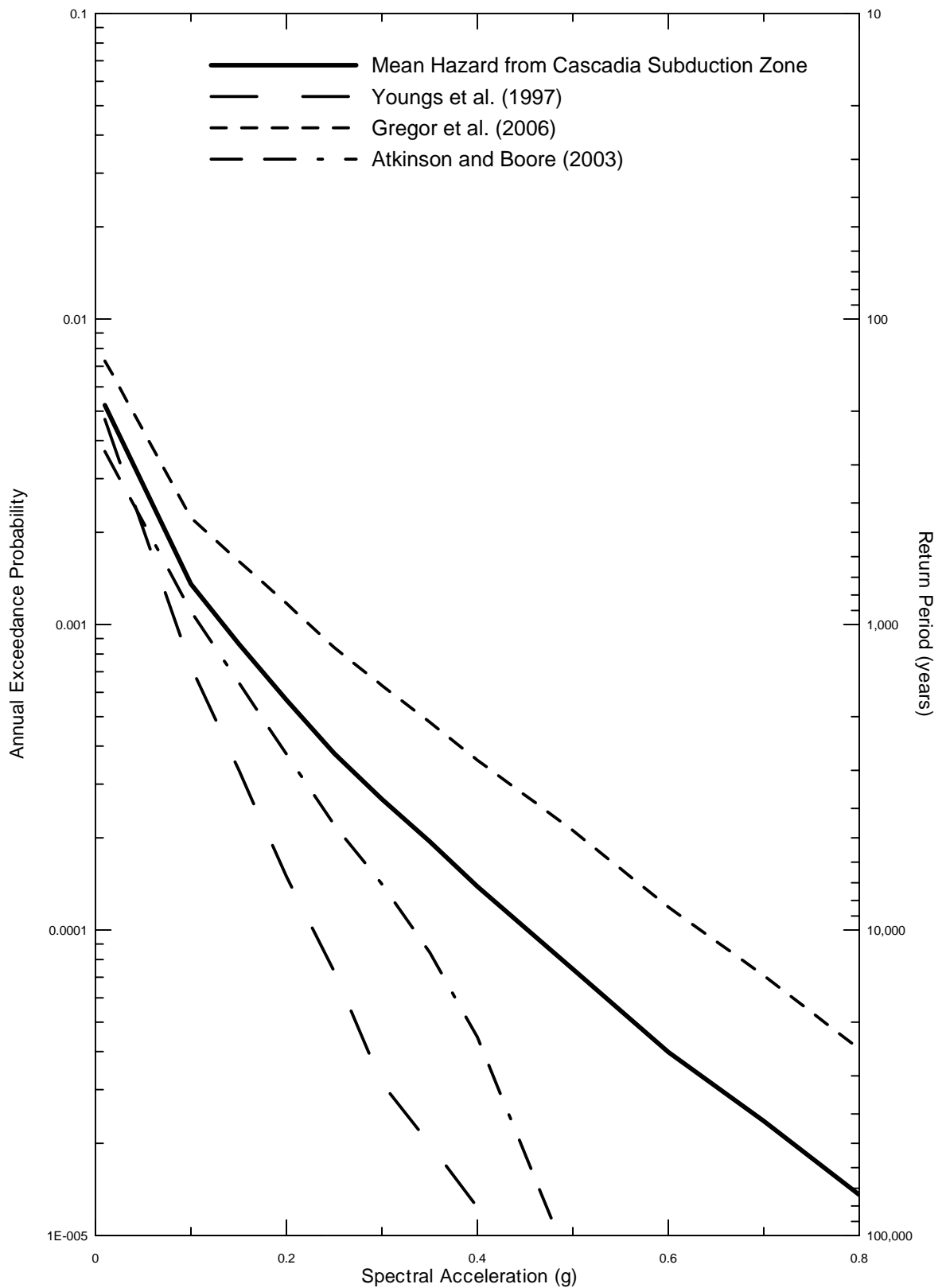


DELTA RISK
MANAGEMENT STRATEGY
CALIFORNIA

Project No. 26815900

SENSITIVITY OF 1.0 SEC SPECTRAL
HORIZONTAL ACCELERATION TIME-DEPENDENT
HAZARD TO ATTENUATION RELATIONSHIPS
FOR STOCKTON FOR 2005

Figure
78

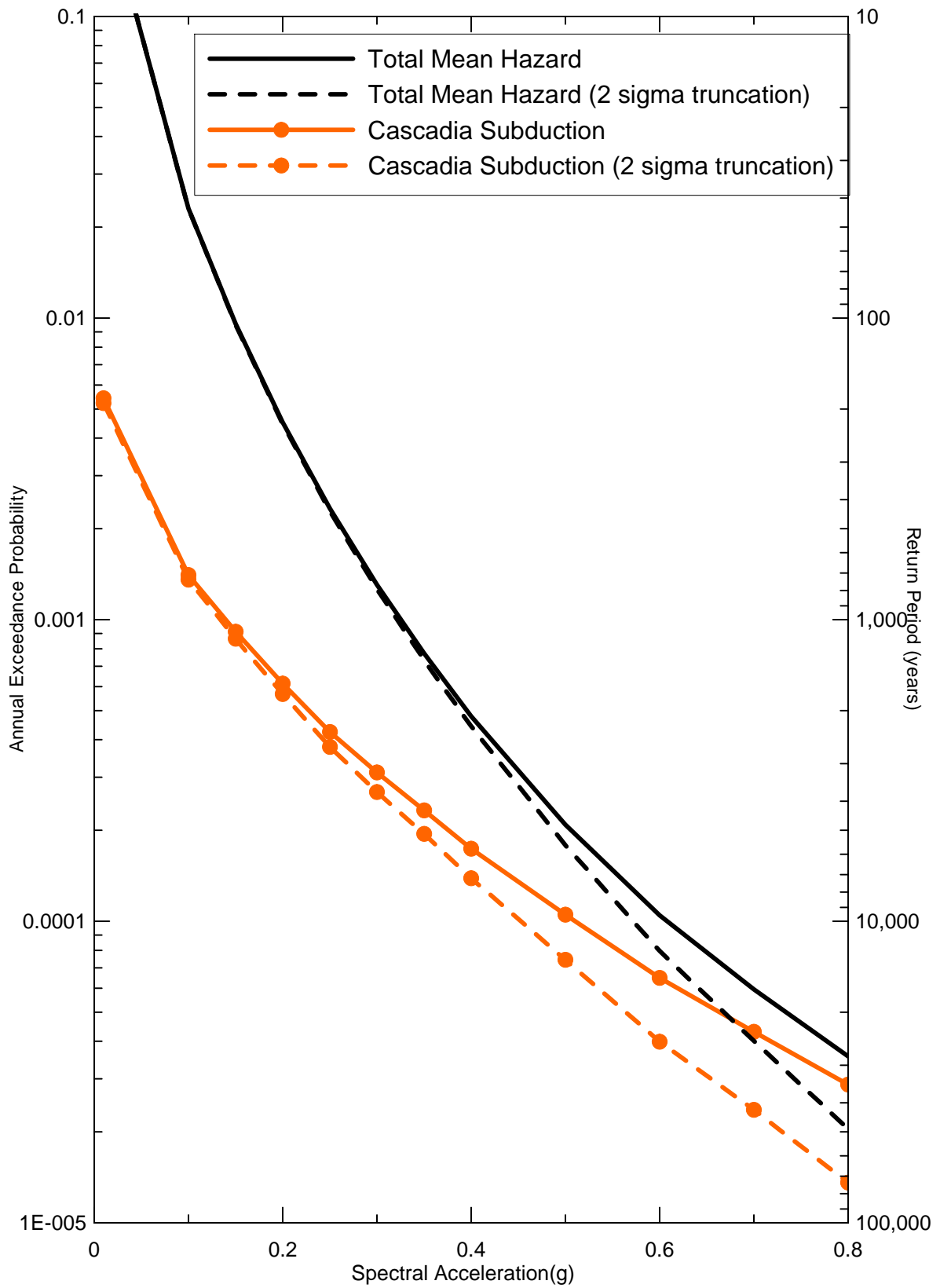


DELTA RISK
MANAGEMENT STRATEGY
California

Project No. 26815621

SENSITIVITY OF CASCADIA SUBDUCTION ZONE
1.0 SEC HORIZONTAL ACCELERATION HAZARD TO
SUBDUCTION ATTENUATION RELATIONSHIPS
FOR SACRAMENTO FOR 2005

Figure
79



Delta Risk\figures\DR6-11-2005cas.grf

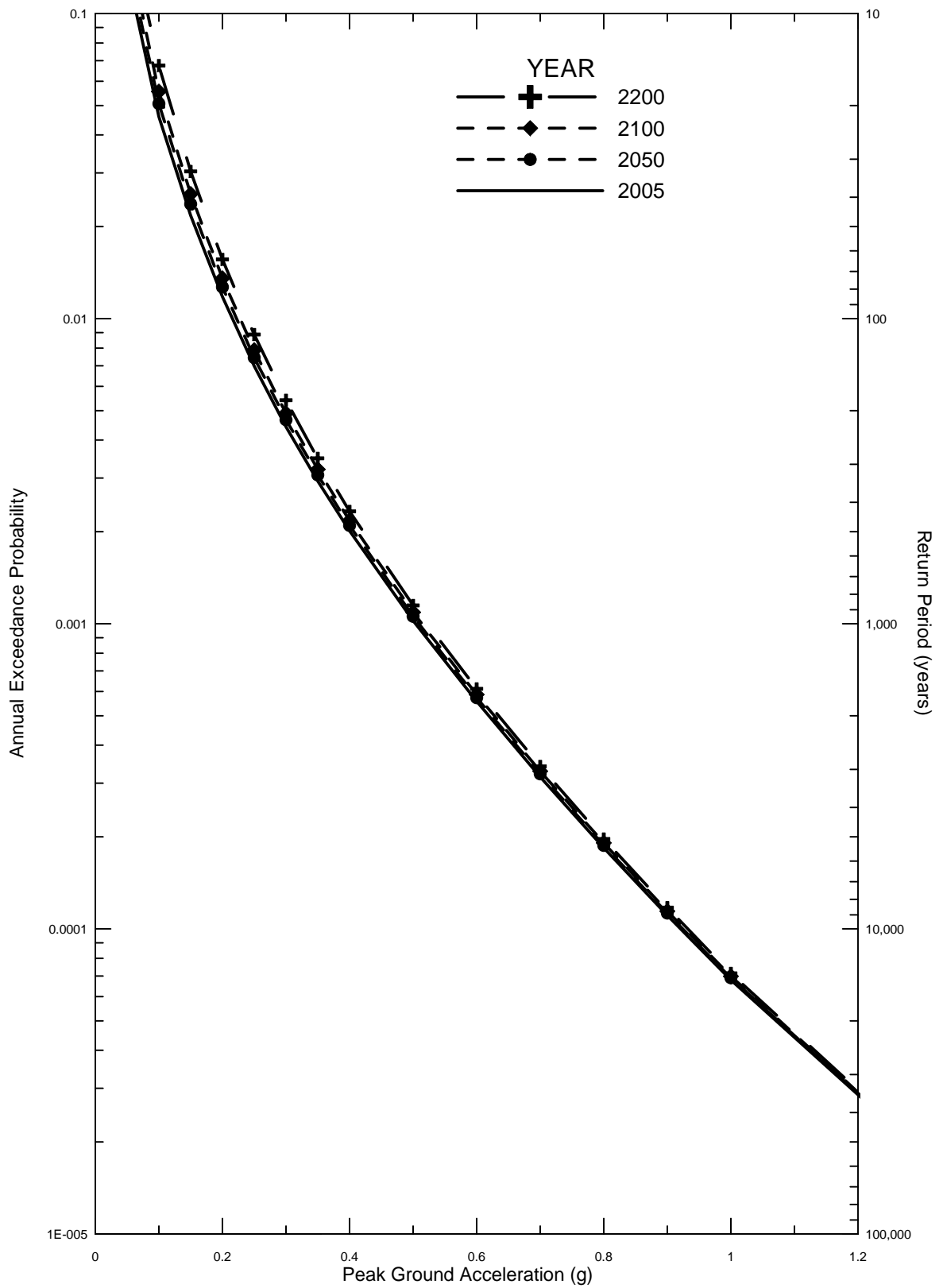


DELTA RISK
MANAGEMENT STRATEGY
CALIFORNIA

Project No. 26815621

1.0 SEC HORIZONTAL SPECTRAL ACCELERATION
HAZARD FOR SACRAMENTO FOR 2005:
EFFECT OF TRUNCATING SIGMA FOR
CASCADIA SUBDUCTION ZONE

Figure
80



delta Risk\Figures\DR2-pga-ALL.grf 6/3/07 4:26 PM

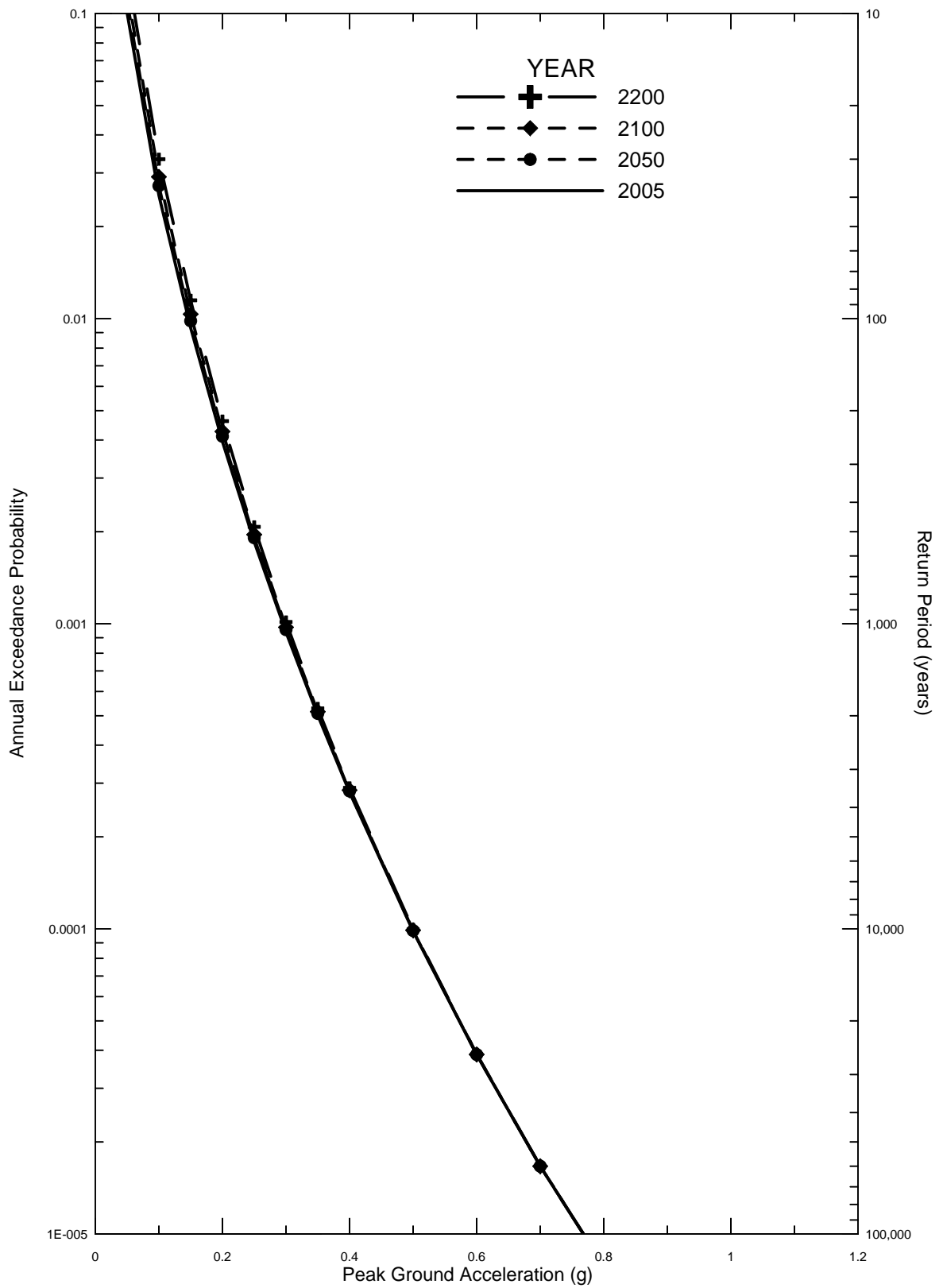


DELTA RISK
MANAGEMENT STRATEGY
California

Project No. 26815621

MEAN PEAK HORIZONTAL ACCELERATION
HAZARD FOR CLIFTON COURT
FOR 2005, 2050, 2100 AND 2200

Figure
81



delta Risk\Figures\DR4-pga-ALL.grf 6/3/07 4:25 PM

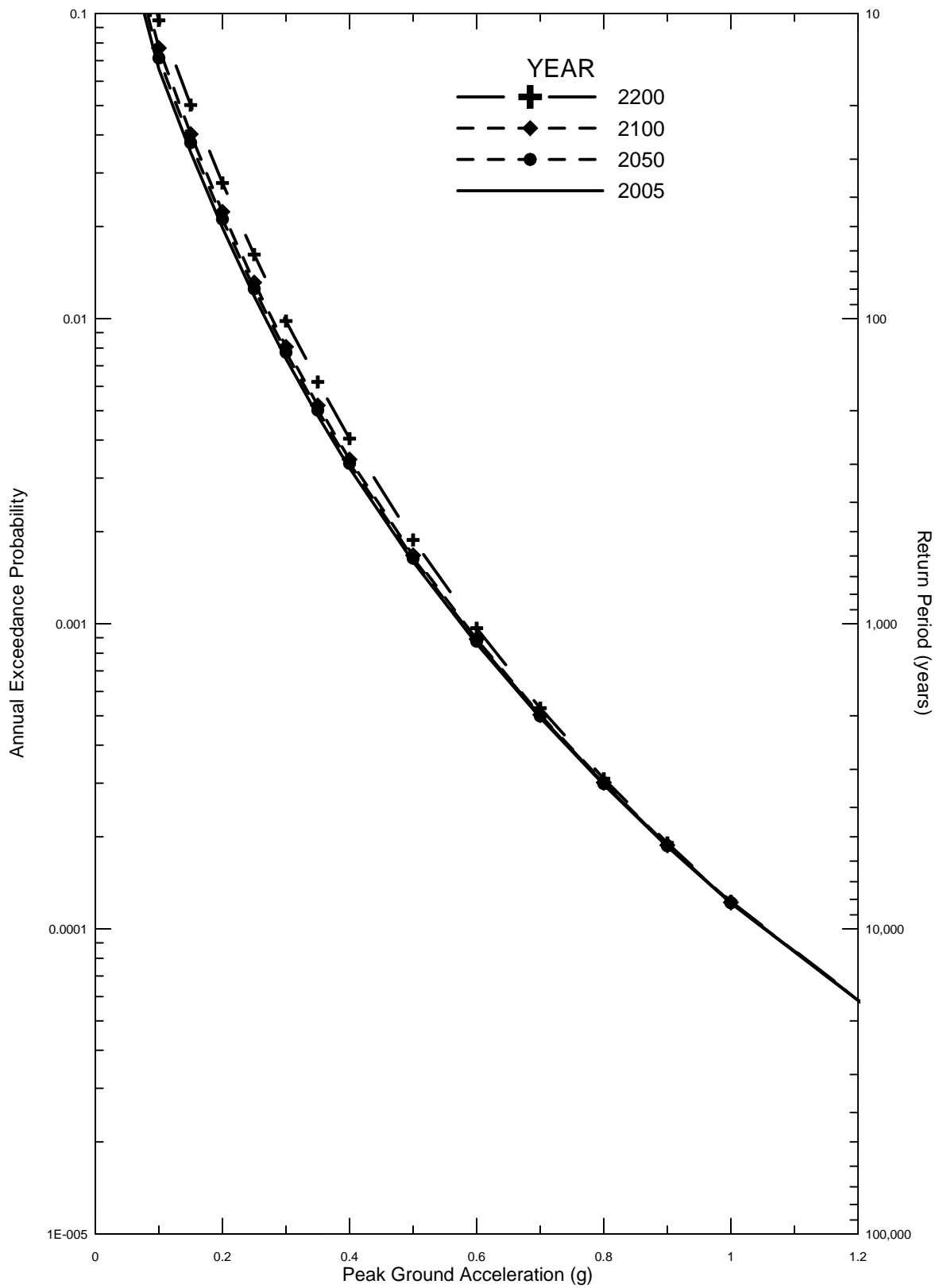


DELTA RISK
MANAGEMENT STRATEGY
California

Project No. 26815621

MEAN PEAK HORIZONTAL ACCELERATION
HAZARD FOR DELTA CROSS CHANNEL
FOR 2005, 2050, 2100 AND 2200

Figure
82



delta Risk\Figures\DR3-pga-ALL.grf 6/3/07 4:26 PM

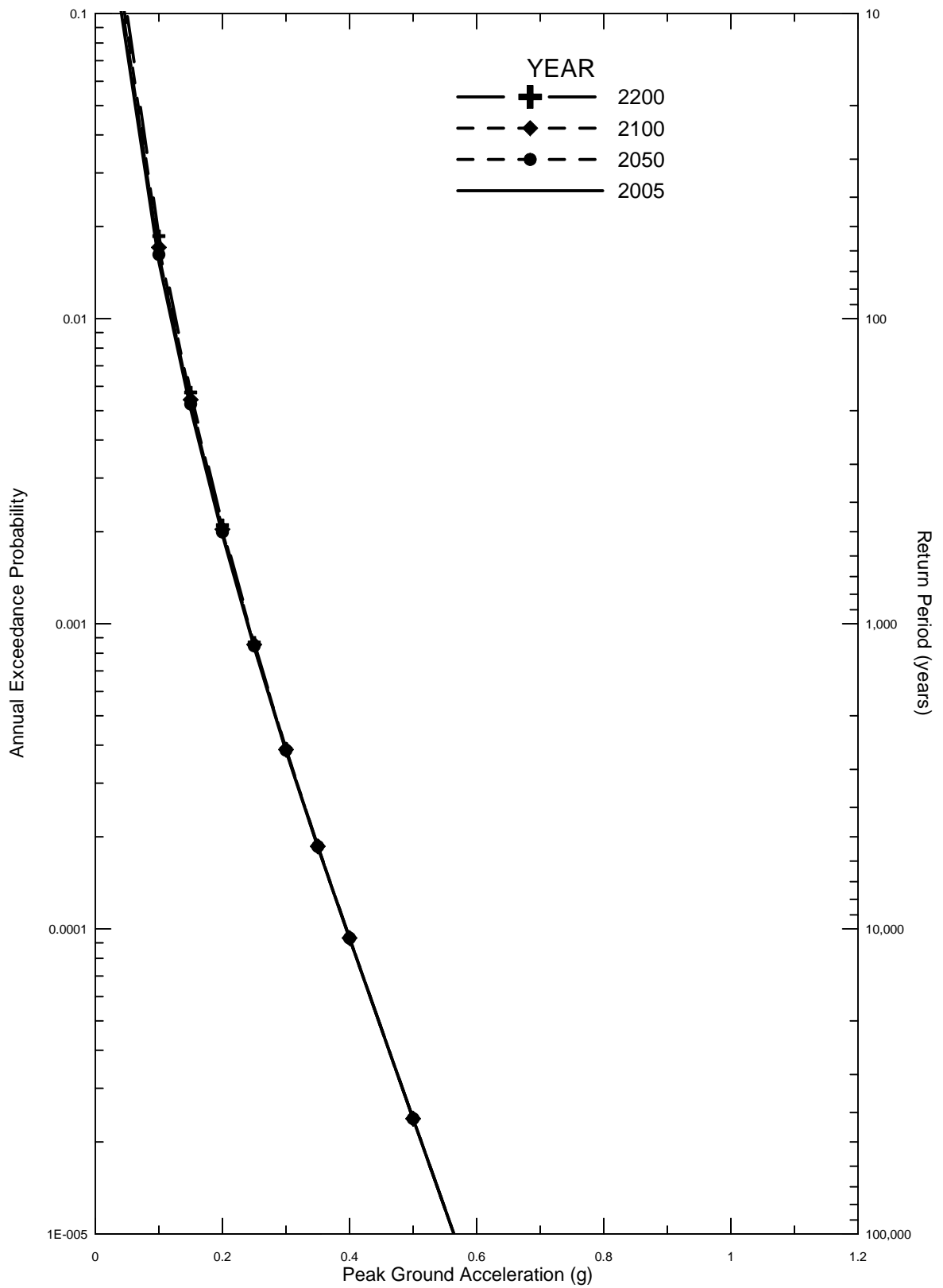


DELTA RISK
MANAGEMENT STRATEGY
California

Project No. 26815621

MEAN PEAK HORIZONTAL ACCELERATION
HAZARD FOR MONTEZUMA SLOUGH
FOR 2005, 2050, 2100 AND 2200

Figure
83



delta Risk\Figures\DR6-pga-ALL.grf 6/3/07 4:24 PM

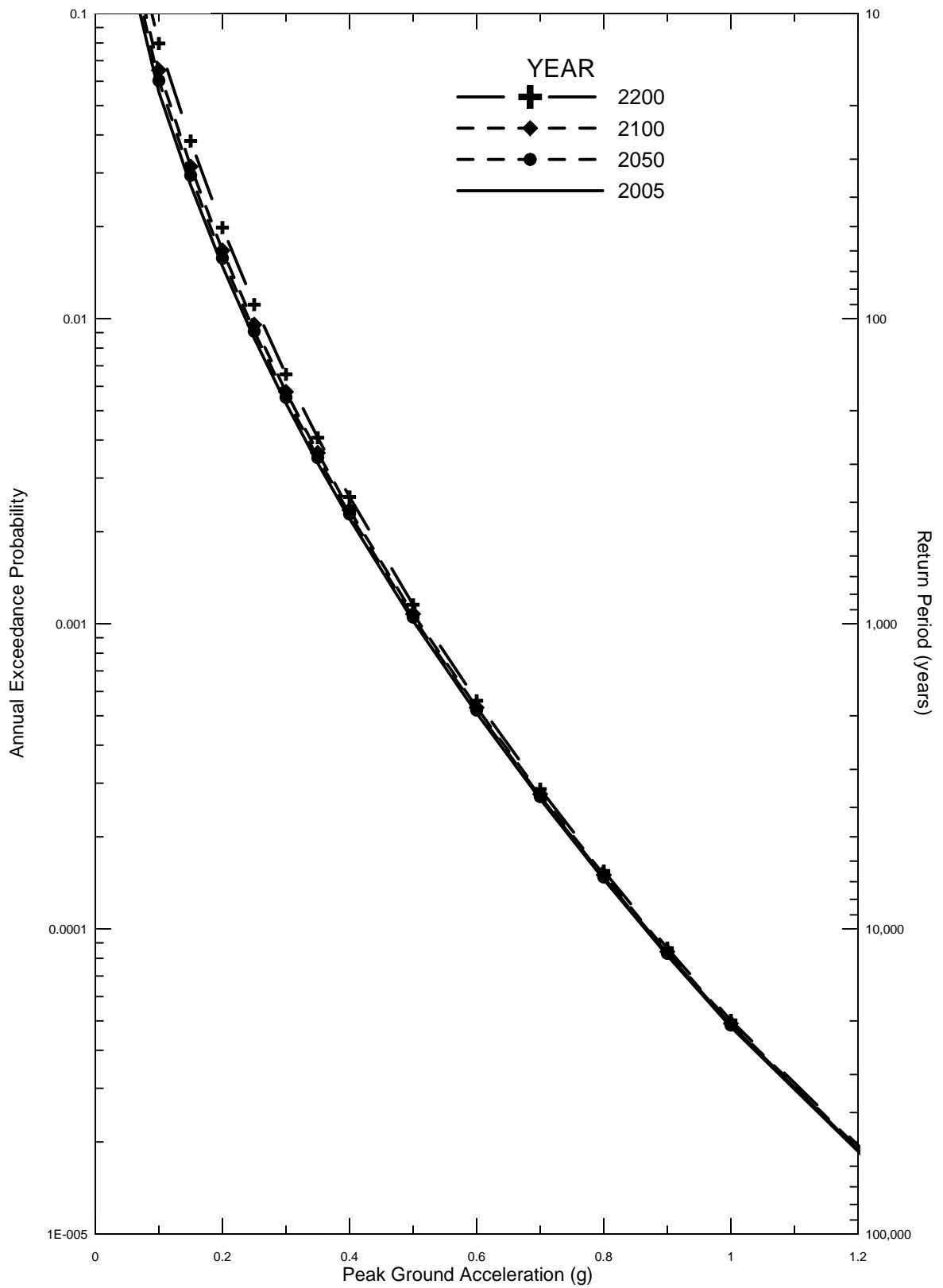


DELTA RISK
MANAGEMENT STRATEGY
California

Project No. 26815621

MEAN PEAK HORIZONTAL ACCELERATION
HAZARD FOR SACRAMENTO
FOR 2005, 2050, 2100 AND 2200

Figure
84



delta Risk\Figures\DR1-pga-ALL.grf 6/3/07 4:26 PM

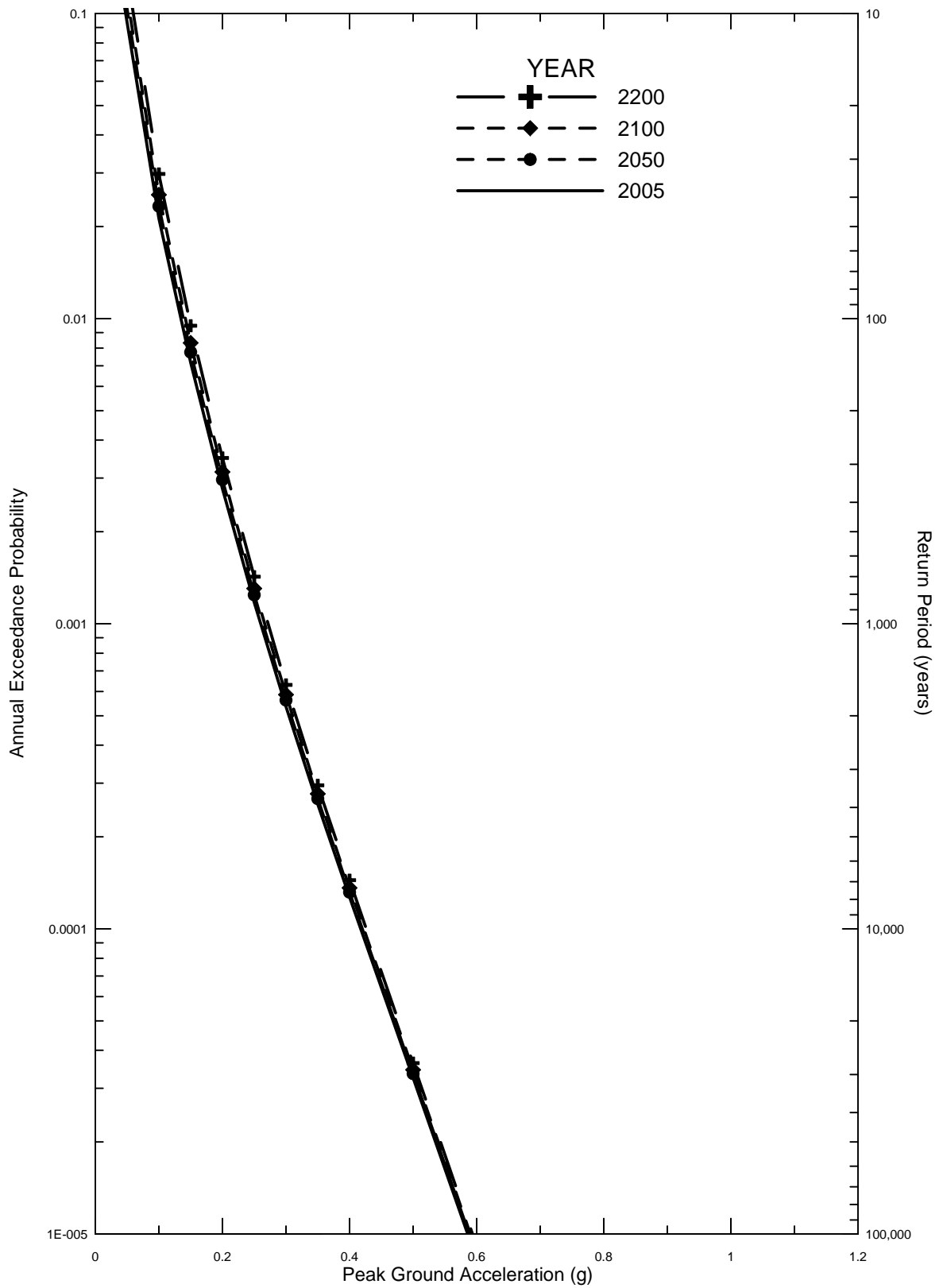


DELTA RISK
MANAGEMENT STRATEGY
California

Project No. 26815621

MEAN PEAK HORIZONTAL ACCELERATION
HAZARD FOR SHERMAN ISLAND
FOR 2005, 2050, 2100 AND 2200

Figure
85



Delta Risk\Figures\DR5-pga-ALL.grf 6/3/07 4:25 PM

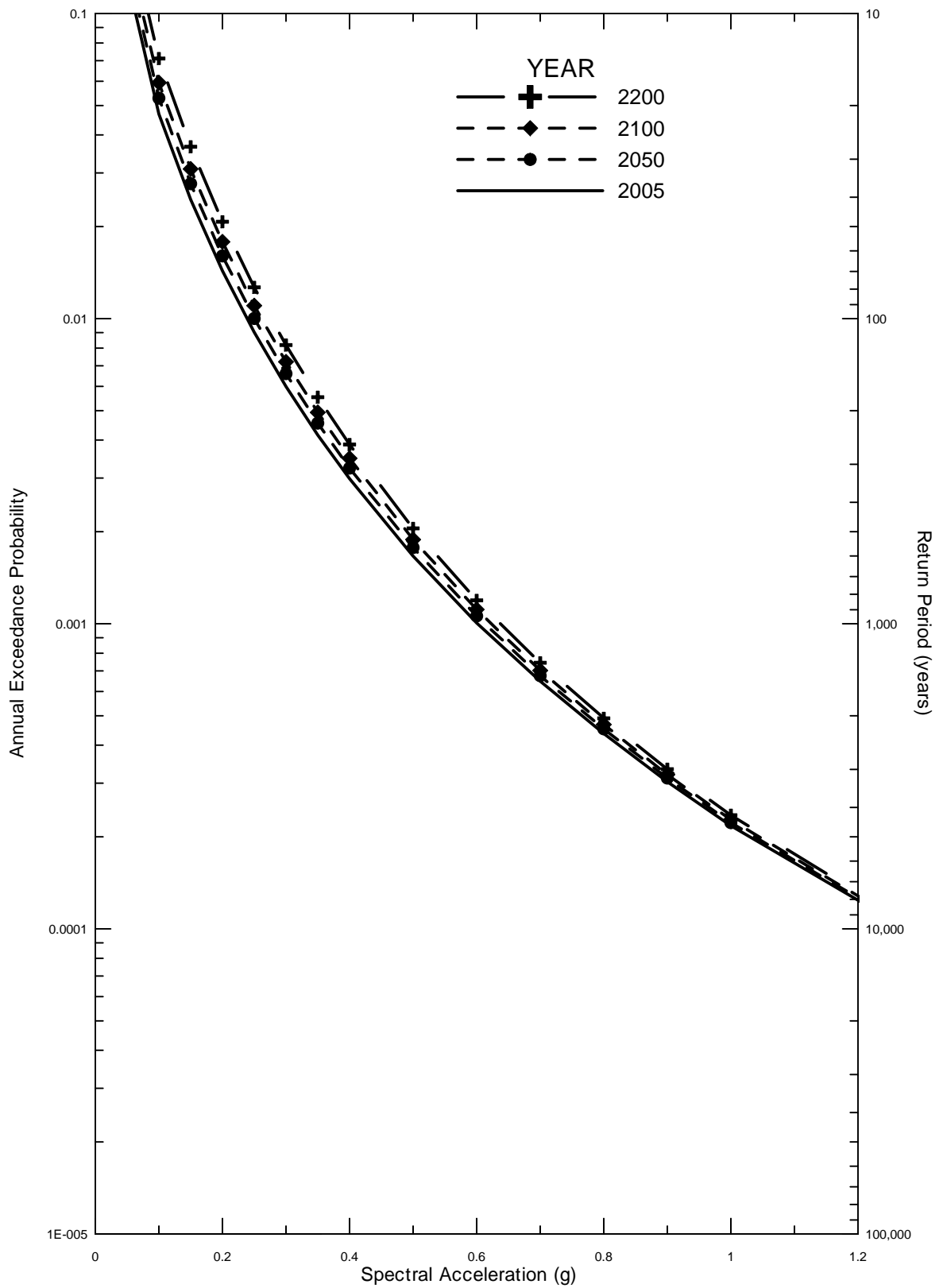


DELTA RISK
MANAGEMENT STRATEGY
California

Project No. 26815621

MEAN PEAK HORIZONTAL ACCELERATION
HAZARD FOR STOCKTON
FOR 2005, 2050, 2100 AND 2200

Figure
86



Delta Risk\Figures\DR2-11-ALL.grf 6/3/07 4:23 PM

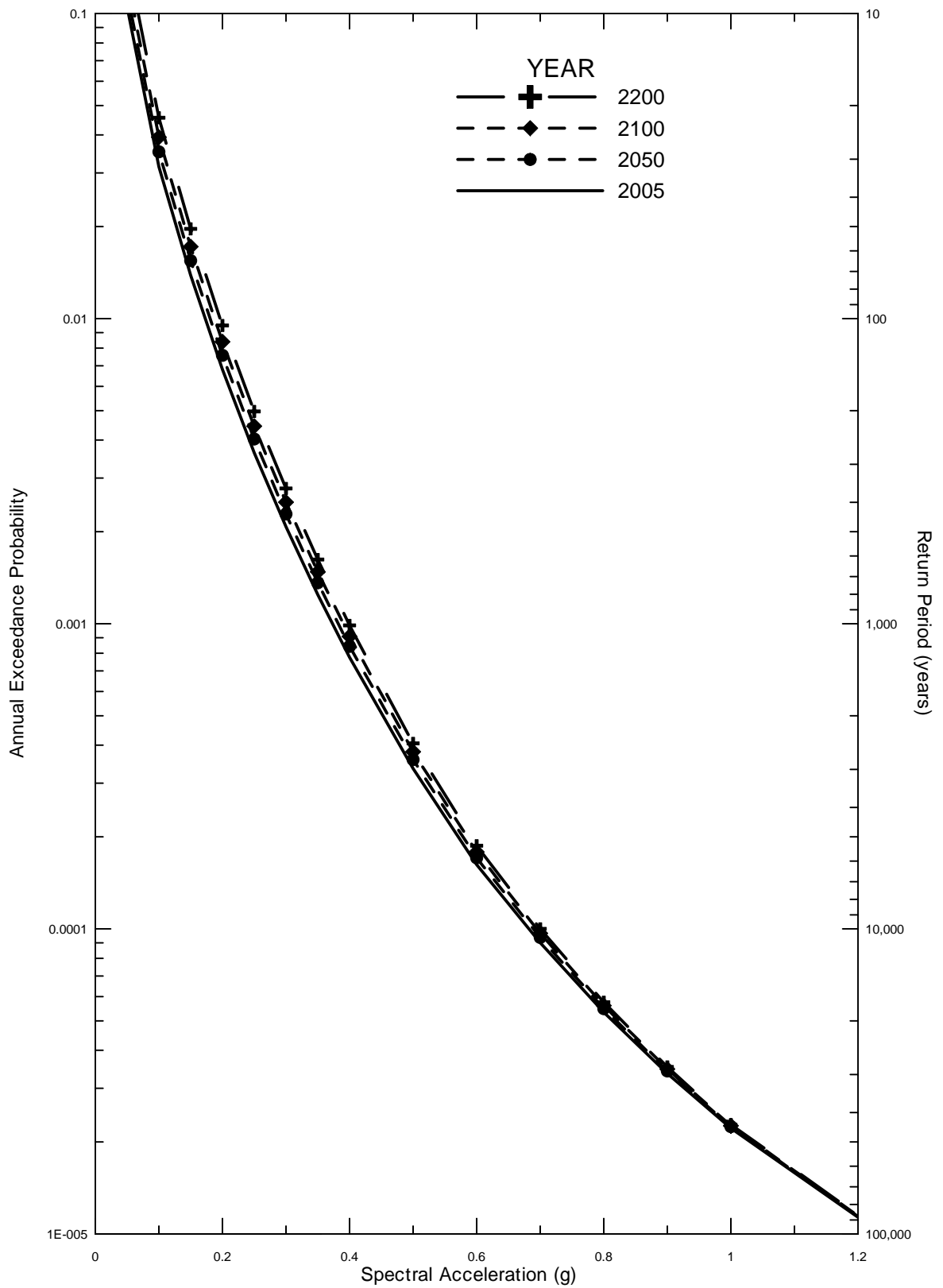


DELTA RISK
MANAGEMENT STRATEGY
California

Project No. 26815621

HORIZONTAL SPECTRAL ACCELERATION
HAZARD AT 1.0 SEC FOR CLIFTON COURT
FOR 2005, 2050, 2100 AND 2200

Figure
87



delta Risk\Figures\DR4-t1-ALL.grf 6/3/07 4:22 PM

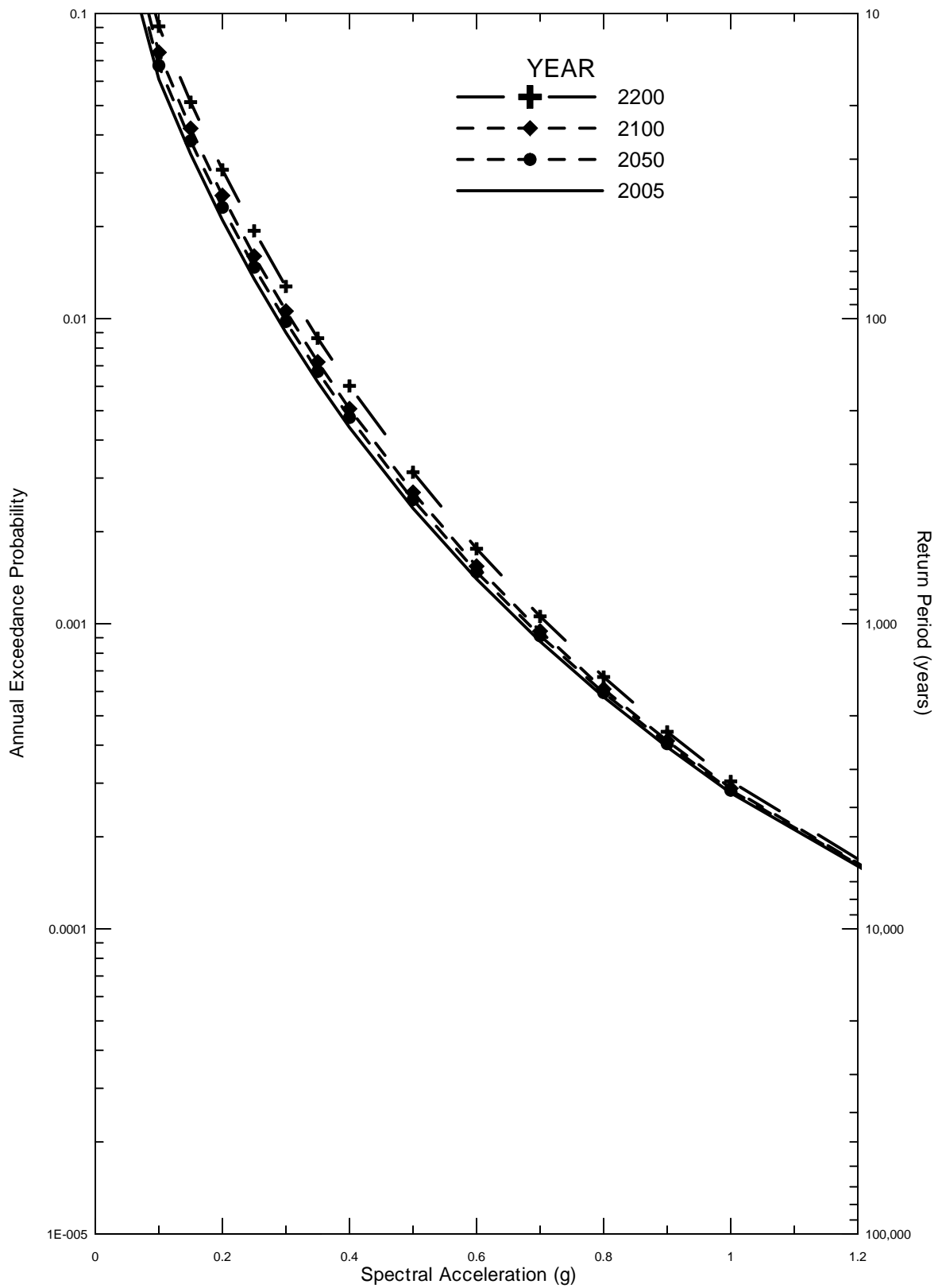


DELTA RISK
MANAGEMENT STRATEGY
California

Project No. 26815621

HORIZONTAL SPECTRAL ACCELERATION
HAZARD AT 1.0 SEC FOR DELTA CROSS CHANNEL
FOR 2005, 2050, 2100 AND 2200

Figure
88



delta Risk\Figures\DR3-11-ALL.grf 6/3/07 4:23 PM

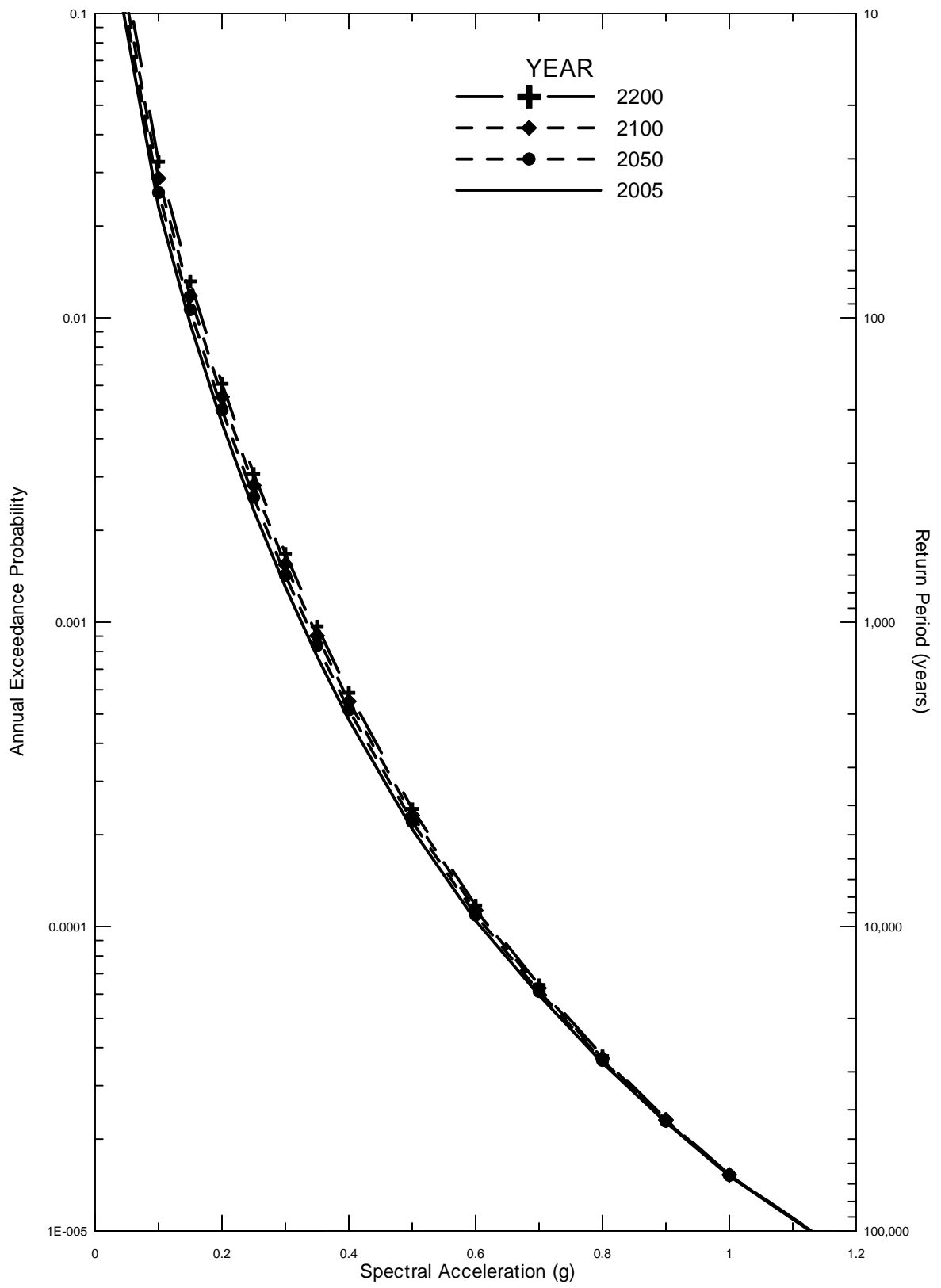


DELTA RISK
MANAGEMENT STRATEGY
California

Project No. 26815621

HORIZONTAL SPECTRAL ACCELERATION
HAZARD AT 1.0 SEC FOR MONTEZUMA SLOUGH
FOR 2005, 2050, 2100 AND 2200

Figure
89



Delta Risk\Figures\DR6-t1-ALL.grf 6/3/07 4:21 PM

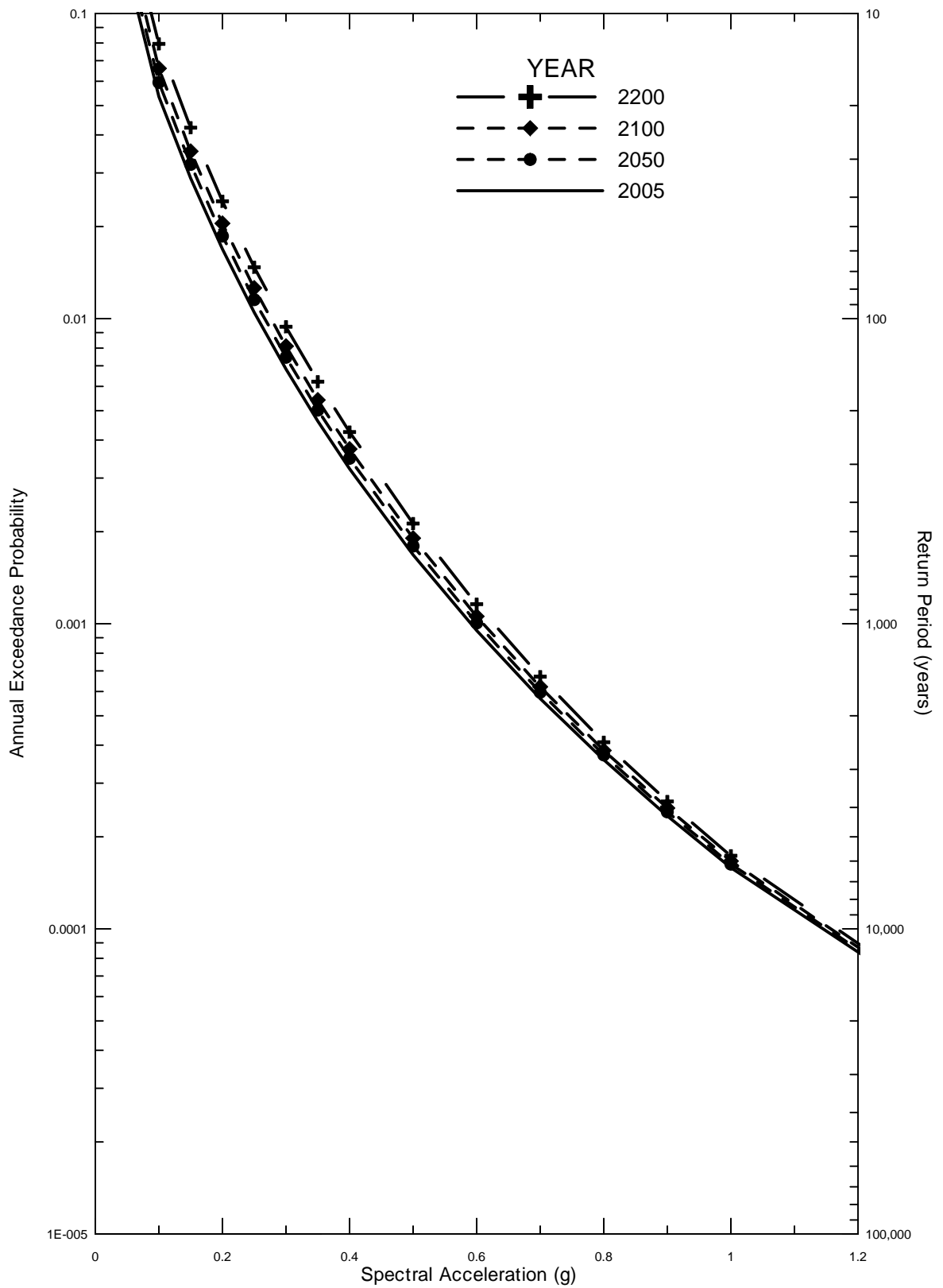


DELTA RISK
MANAGEMENT STRATEGY
California

Project No. 26815621

HORIZONTALSPECTRAL ACCELERATION
HAZARD AT 1.0 SEC FOR SACRAMENTO
FOR 2005, 2050, 2100 AND 2200

Figure
90



delta Risk\Figures\DR1-11-ALL.grf 6/3/07 4:24 PM

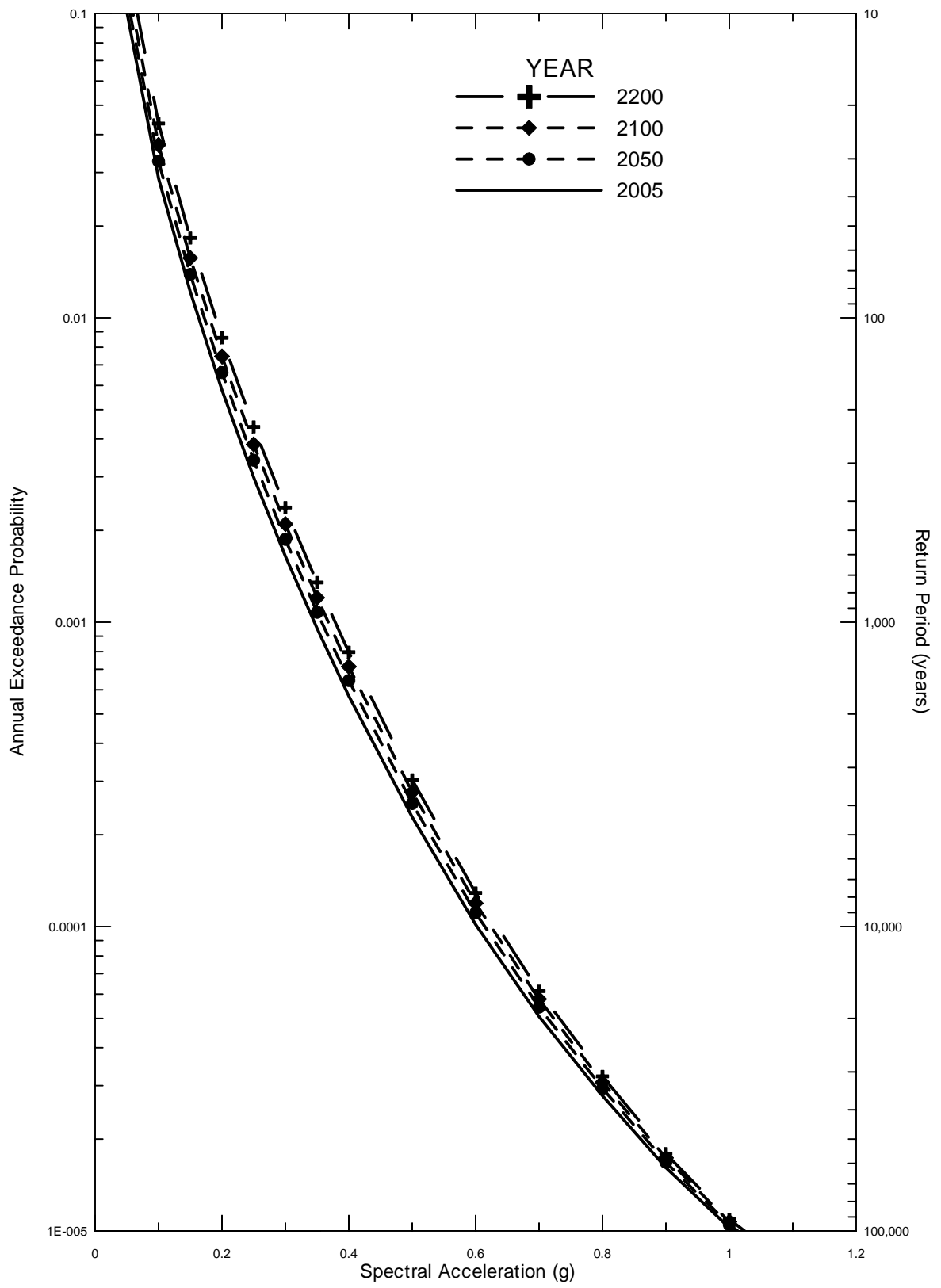


DELTA RISK
MANAGEMENT STRATEGY
California

Project No. 26815621

HORIZONTAL SPECTRAL ACCELERATION
HAZARD AT 1.0 SEC FOR SHERMAN ISLAND
FOR 2005, 2050, 2100 AND 2200

Figure
91



delta Risk\Figures\DR5-t1-ALL.grf 6/3/07 4:21 PM

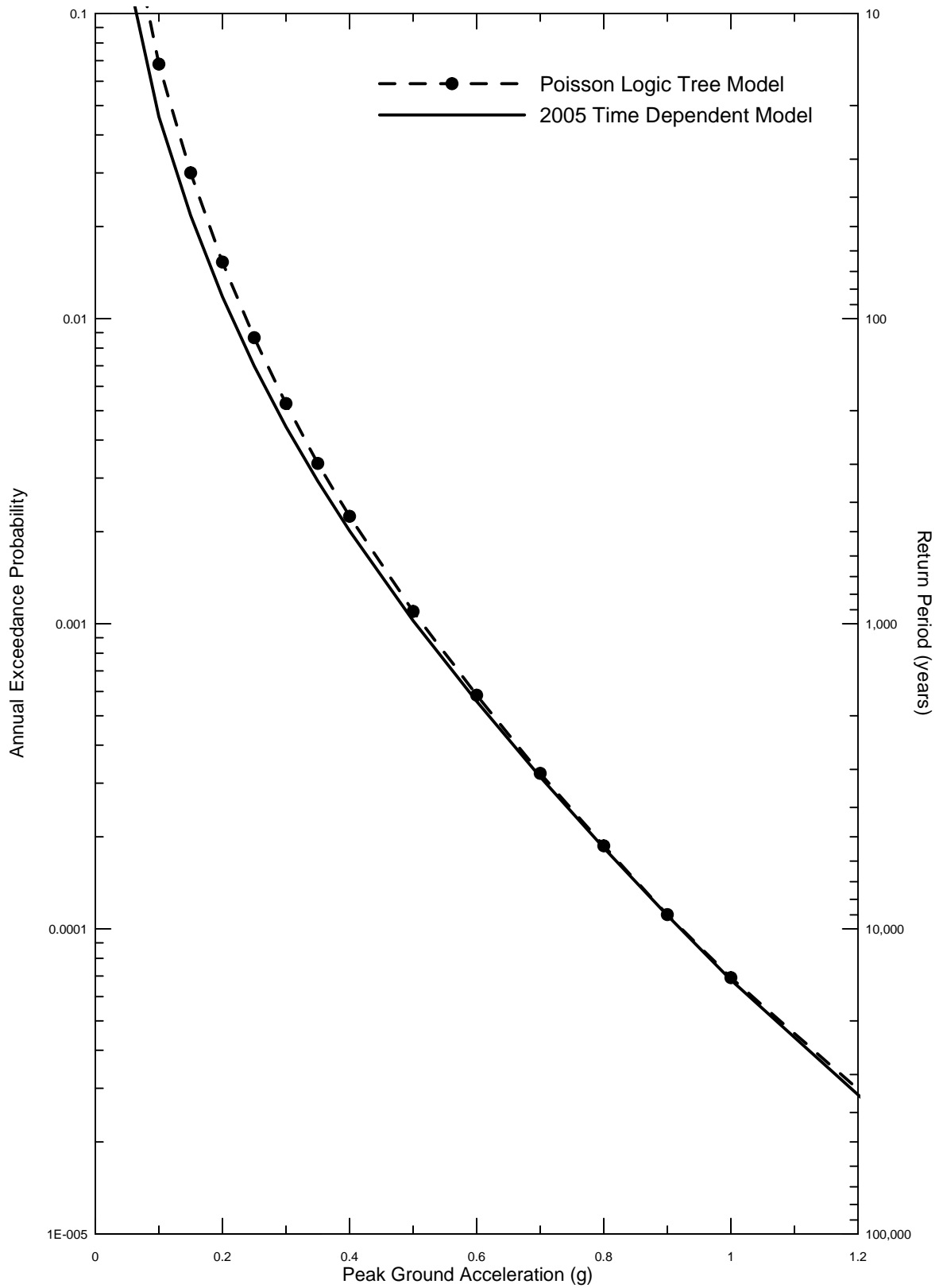


DELTA RISK
MANAGEMENT STRATEGY
California

Project No. 26815621

HORIZONTAL SPECTRAL ACCELERATION
HAZARD AT 1.0 SEC FOR STOCKTON
FOR 2005, 2050, 2100 AND 2200

Figure
92



delta Risk\Figures\DR2-pga-TDvP.gif 6/1/07 11:19 AM

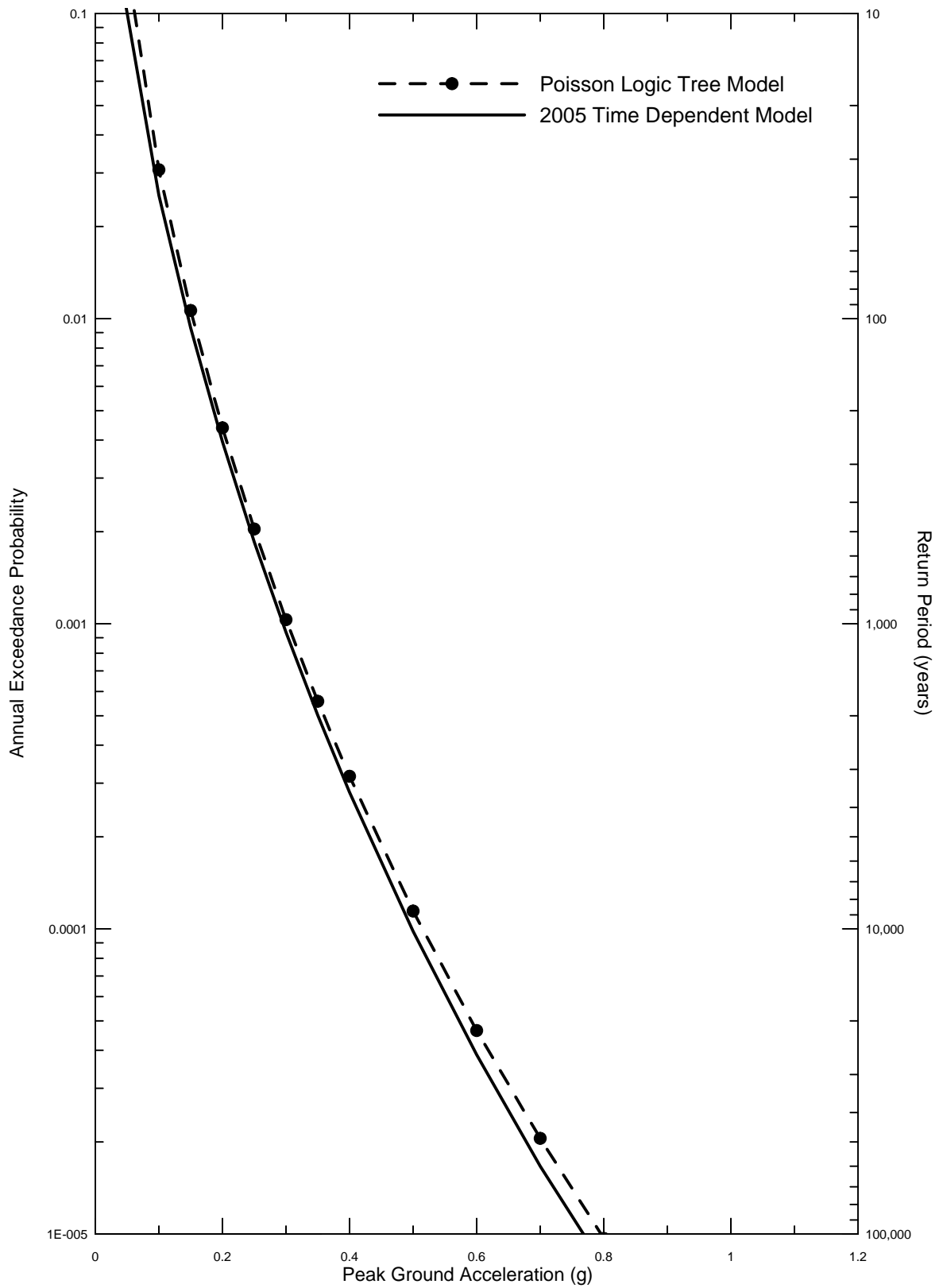


DELTA RISK
MANAGEMENT STRATEGY
California

Project No. 26815621

MEAN PEAK HORIZONTAL ACCELERATION
HAZARD TIME DEPENDENT AND POISSON MODELS
FOR CLIFTON COURT FOR 2005

Figure
93



delta Risk\Figures\DR4-pga-TDvP.gif 6/1/07 11:17 AM

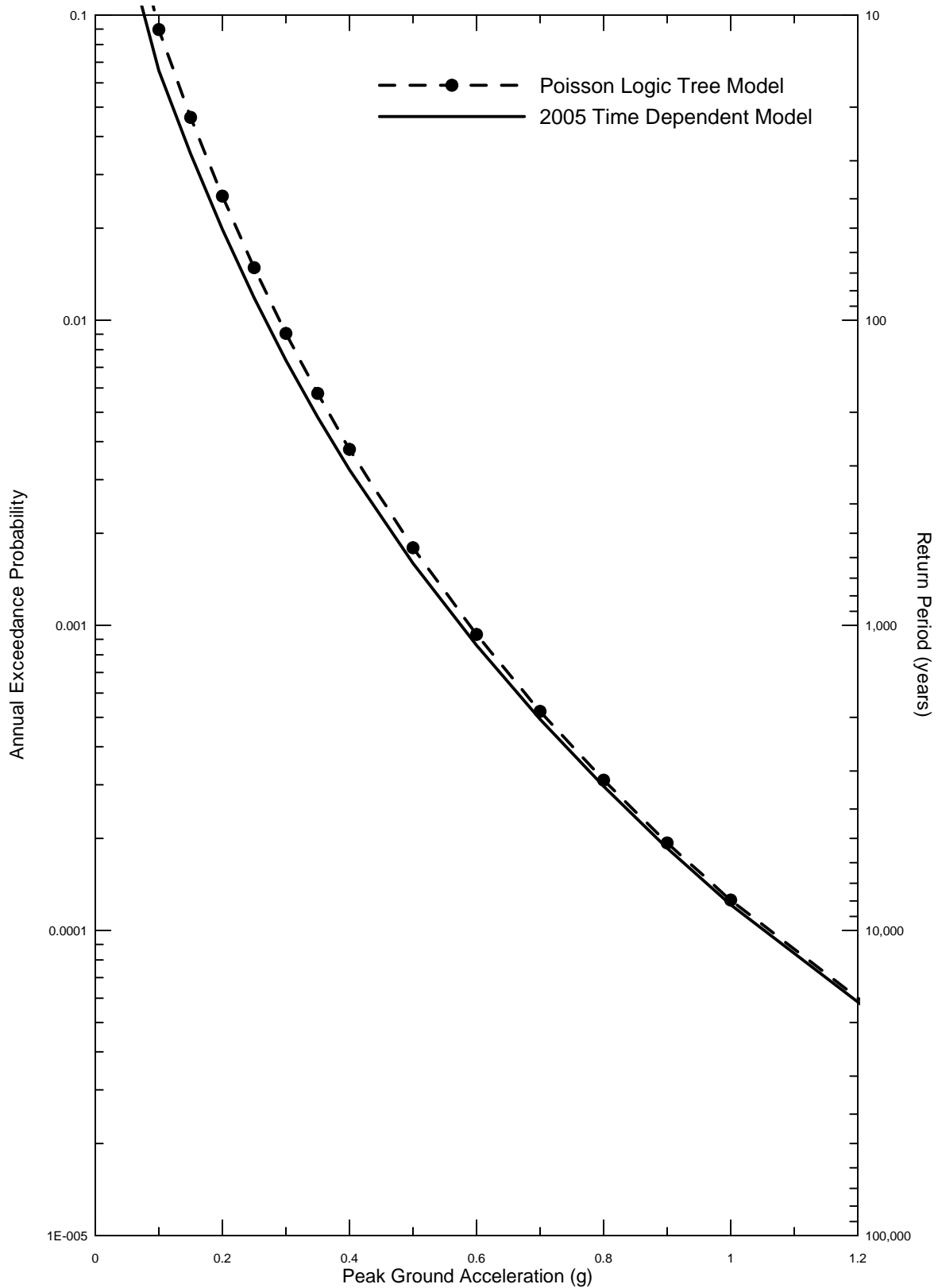


DELTA RISK
MANAGEMENT STRATEGY
California

Project No. 26815621

MEAN PEAK HORIZONTAL ACCELERATION
HAZARD TIME DEPENDENT AND POISSON MODELS
FOR DELTA CROSS CHANNEL FOR 2005

Figure
94



delta Risk\Figures\DR3-pga-TDvP.gif 6/1/07 11:18 AM

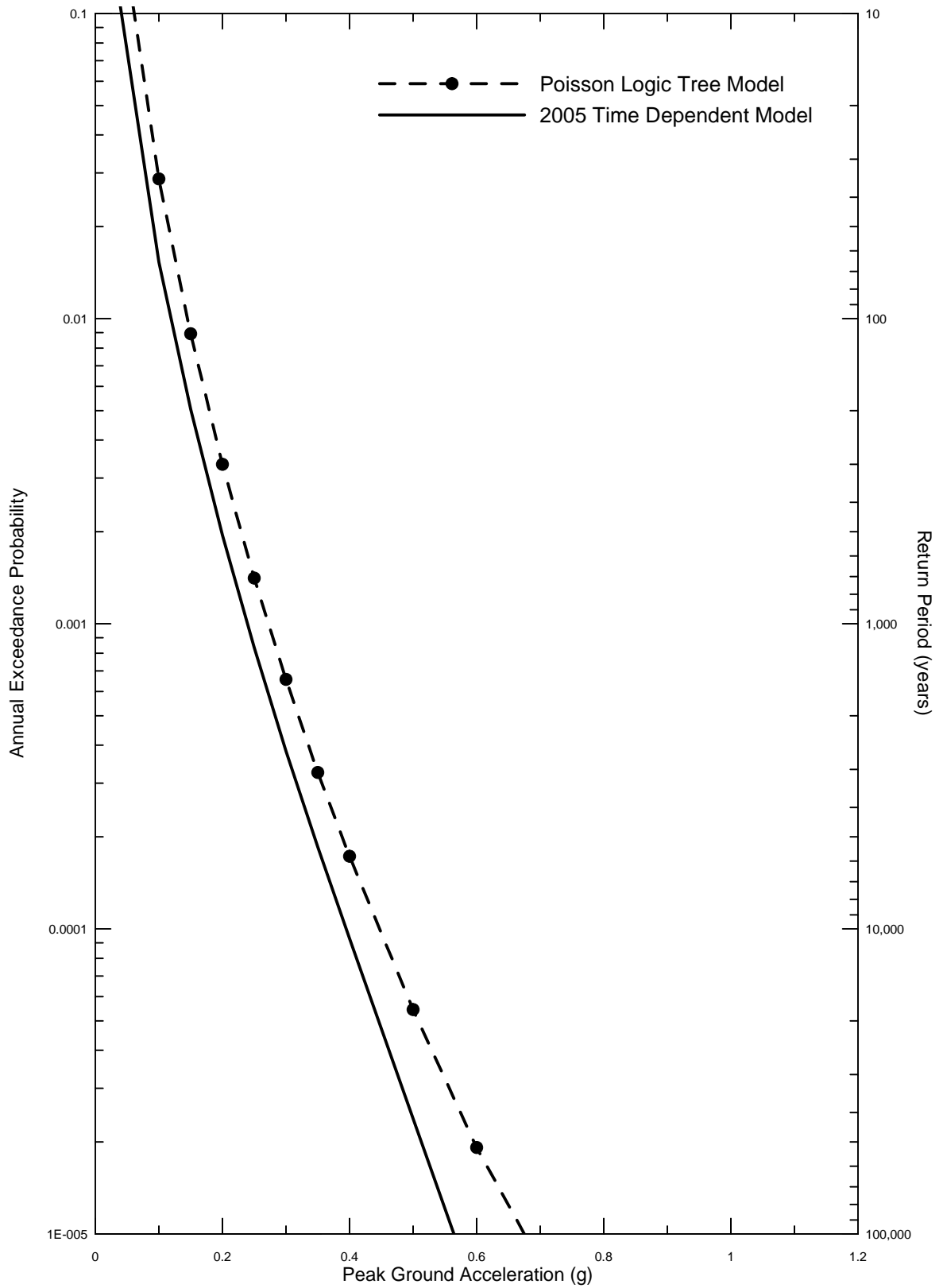


DELTA RISK
MANAGEMENT STRATEGY
California

Project No. 26815621

MEAN PEAK HORIZONTAL ACCELERATION
HAZARD TIME DEPENDENT AND POISSON MODELS
FOR MONTEZUMA SLOUGH FOR 2005

Figure
95



delta Risk\Figures\DR6-pga-TDvP.gif 6/1/07 11:16 AM

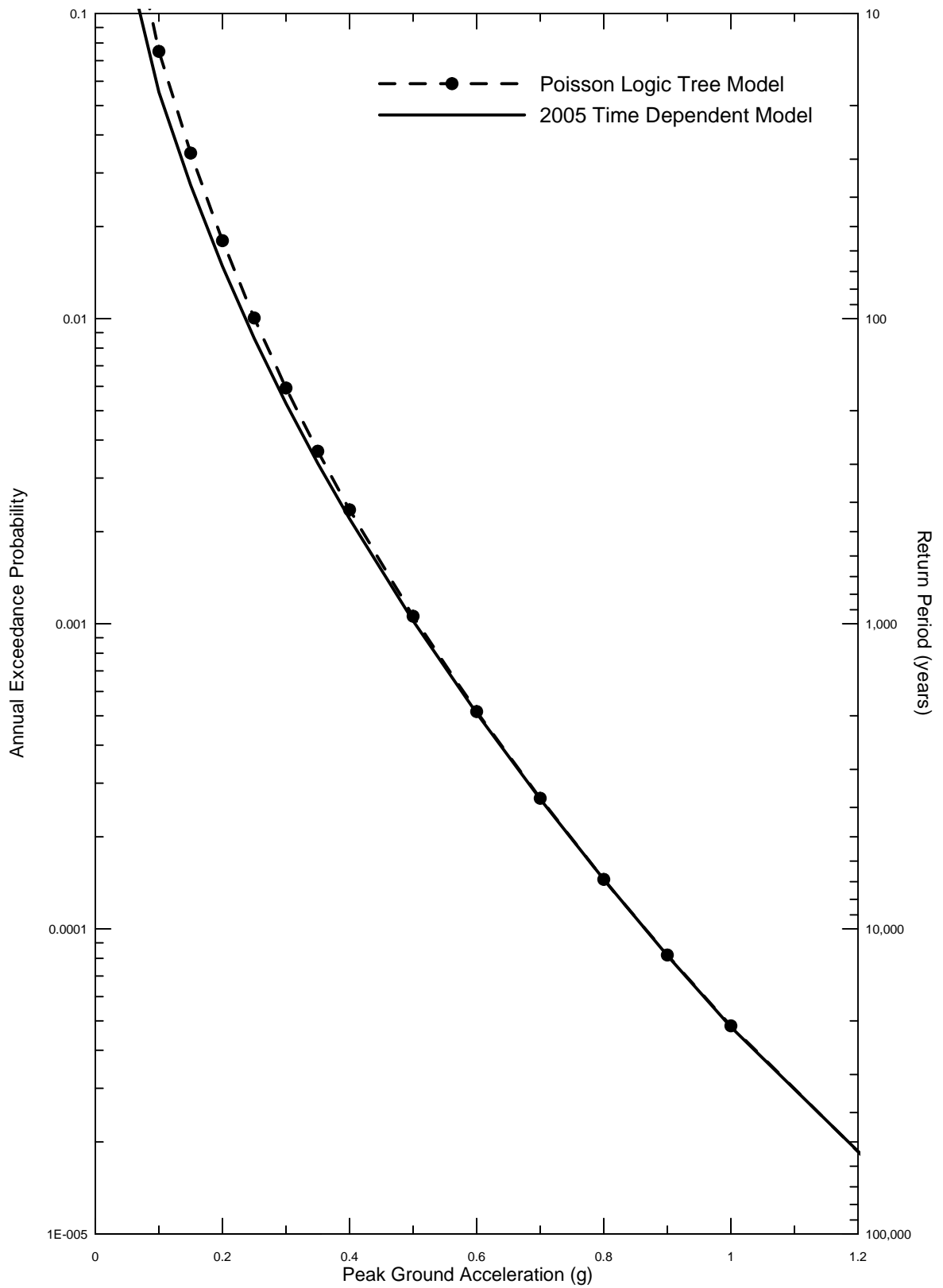


DELTA RISK
MANAGEMENT STRATEGY
California

Project No. 26815621

MEAN PEAK HORIZONTAL ACCELERATION
HAZARD TIME DEPENDENT AND POISSON MODELS
FOR SACRAMENTO FOR 2005

Figure
96



delta Risk\Figures\DR1-pga-TDvP.gif 6/1/07 11:19 AM

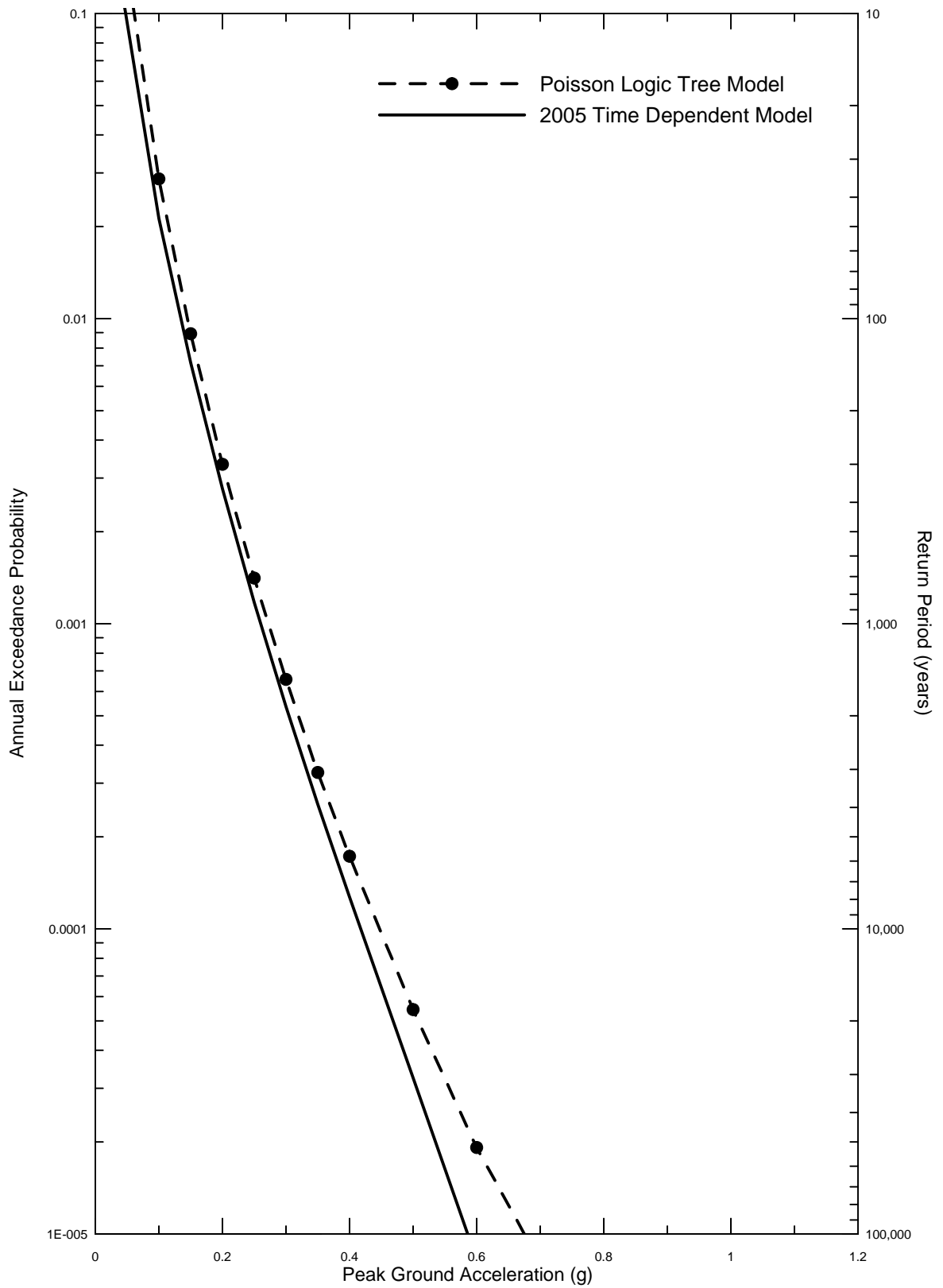


DELTA RISK
MANAGEMENT STRATEGY
California

Project No. 26815621

MEAN PEAK HORIZONTAL ACCELERATION
HAZARD TIME DEPENDENT AND POISSON MODELS
FOR SHERMAN ISLAND FOR 2005

Figure
97



delta Risk\Figures\DR5-pga-TDvP.gif 6/1/07 11:17 AM

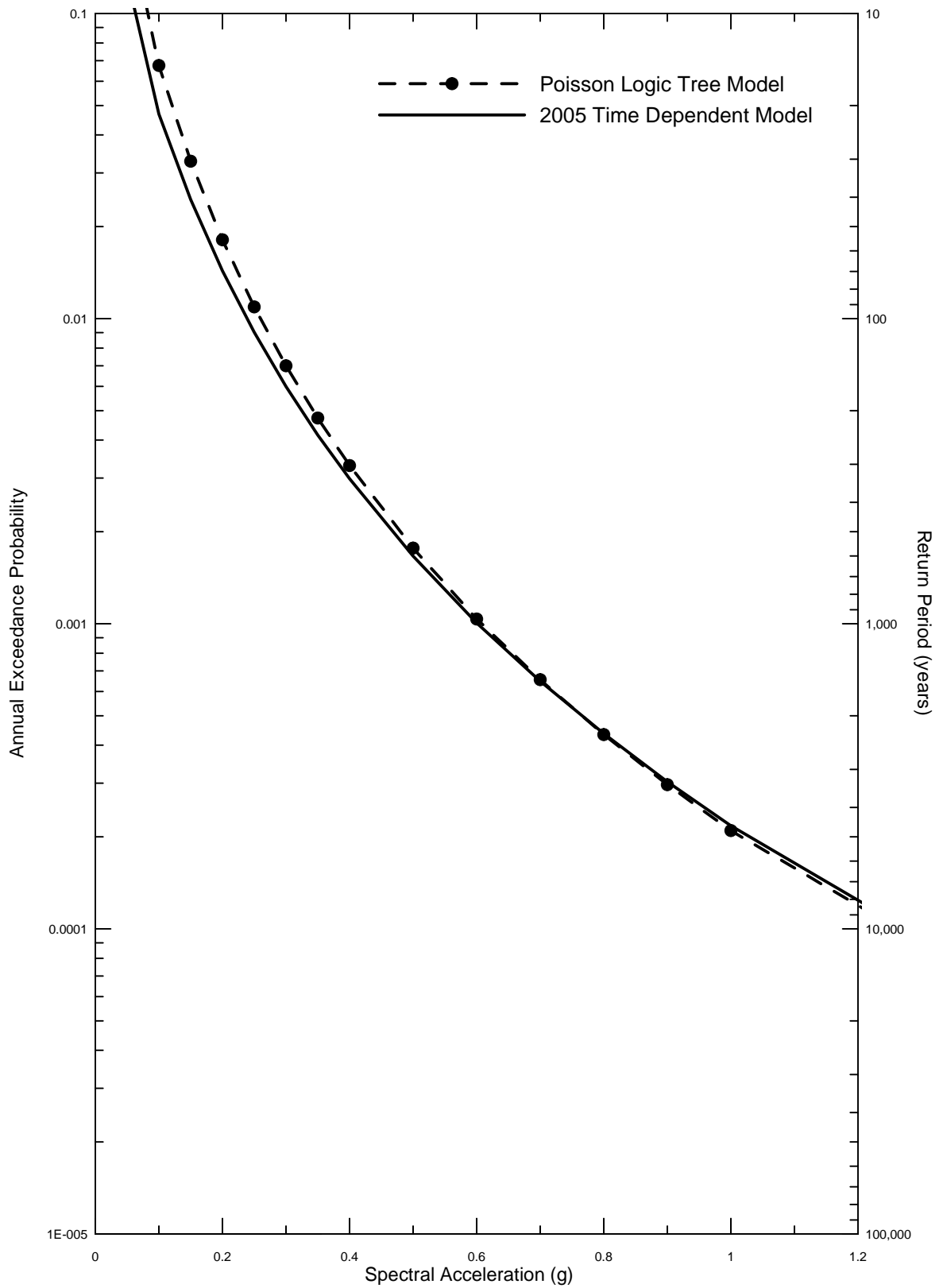


DELTA RISK
MANAGEMENT STRATEGY
California

Project No. 26815621

MEAN PEAK HORIZONTAL ACCELERATION
HAZARD TIME DEPENDENT AND POISSON MODELS
FOR STOCKTON FOR 2005

Figure
98



delta Risk\Figures\DR2-t1-TDVP.grf 6/1/07 11:14 AM

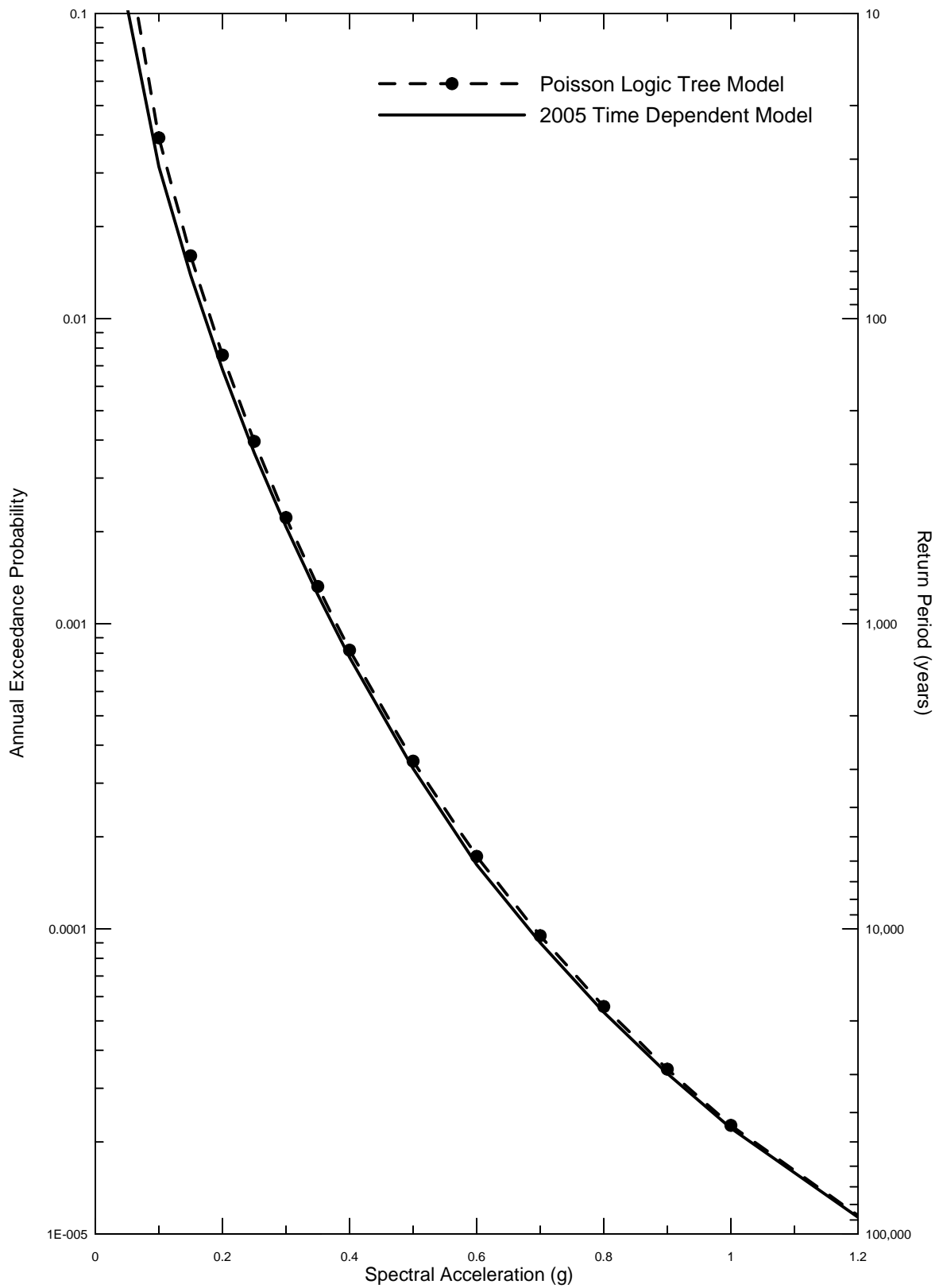


DELTA RISK
MANAGEMENT STRATEGY
California

Project No. 26815621

1.0 SEC HORIZONTAL SPECTRAL ACCELERATION
HAZARD TIME DEPENDENT AND POISSON MODELS
FOR CLIFTON COURT FOR 2005

Figure
99



delta Risk\Figures\DR4-t1-TDV.ppt 6/1/07 11:13 AM

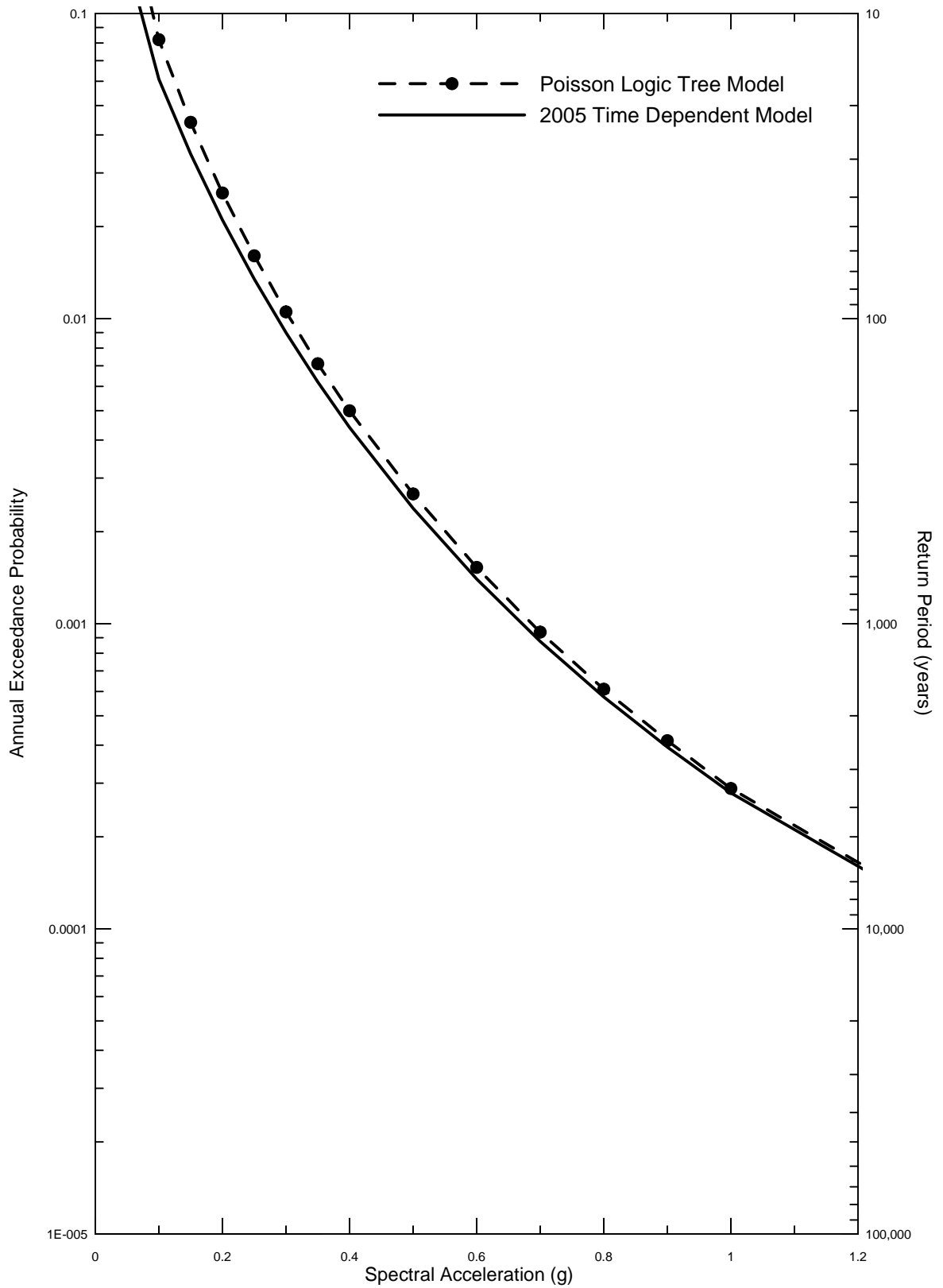


DELTA RISK
MANAGEMENT STRATEGY
California

Project No. 26815621

1.0 SEC HORIZONTAL SPECTRAL ACCELERATION
HAZARD TIME DEPENDENT AND POISSON MODELS
FOR DELTA CROSS CHANNEL FOR 2005

Figure
100



delta Risk\Figures\DR3-t1-TDV.ppt 6/1/07 11:13 AM

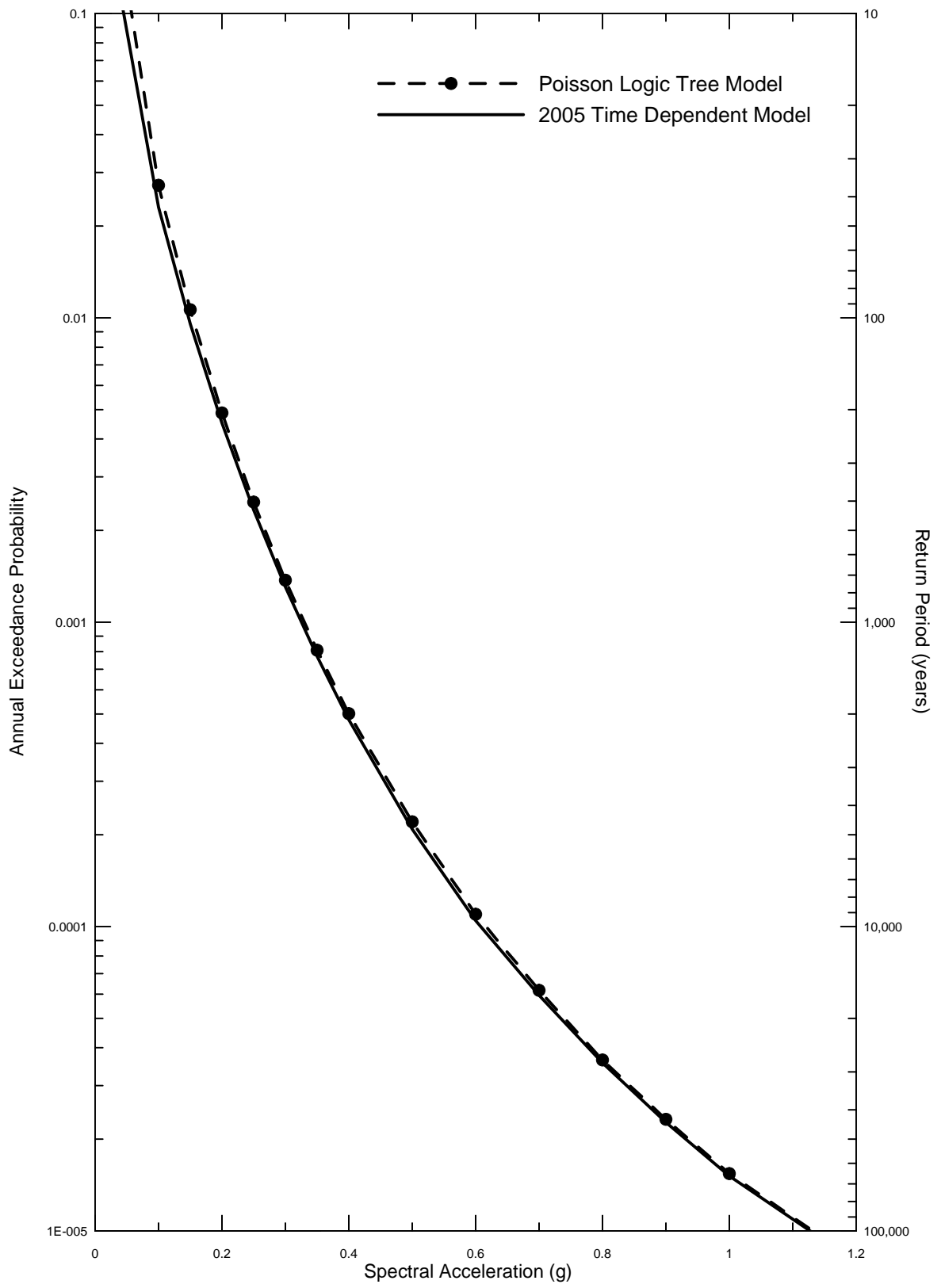


DELTA RISK
MANAGEMENT STRATEGY
California

1.0 SEC HORIZONTAL SPECTRAL ACCELERATION
HAZARD TIME DEPENDENT AND POISSON MODELS
FOR MONTEZUMA SLOUGH FOR 2005

Figure
101

Project No. 26815621



delta Risk\Figures\DR6-t1-TDV.ppt 6/1/07 11:10 AM

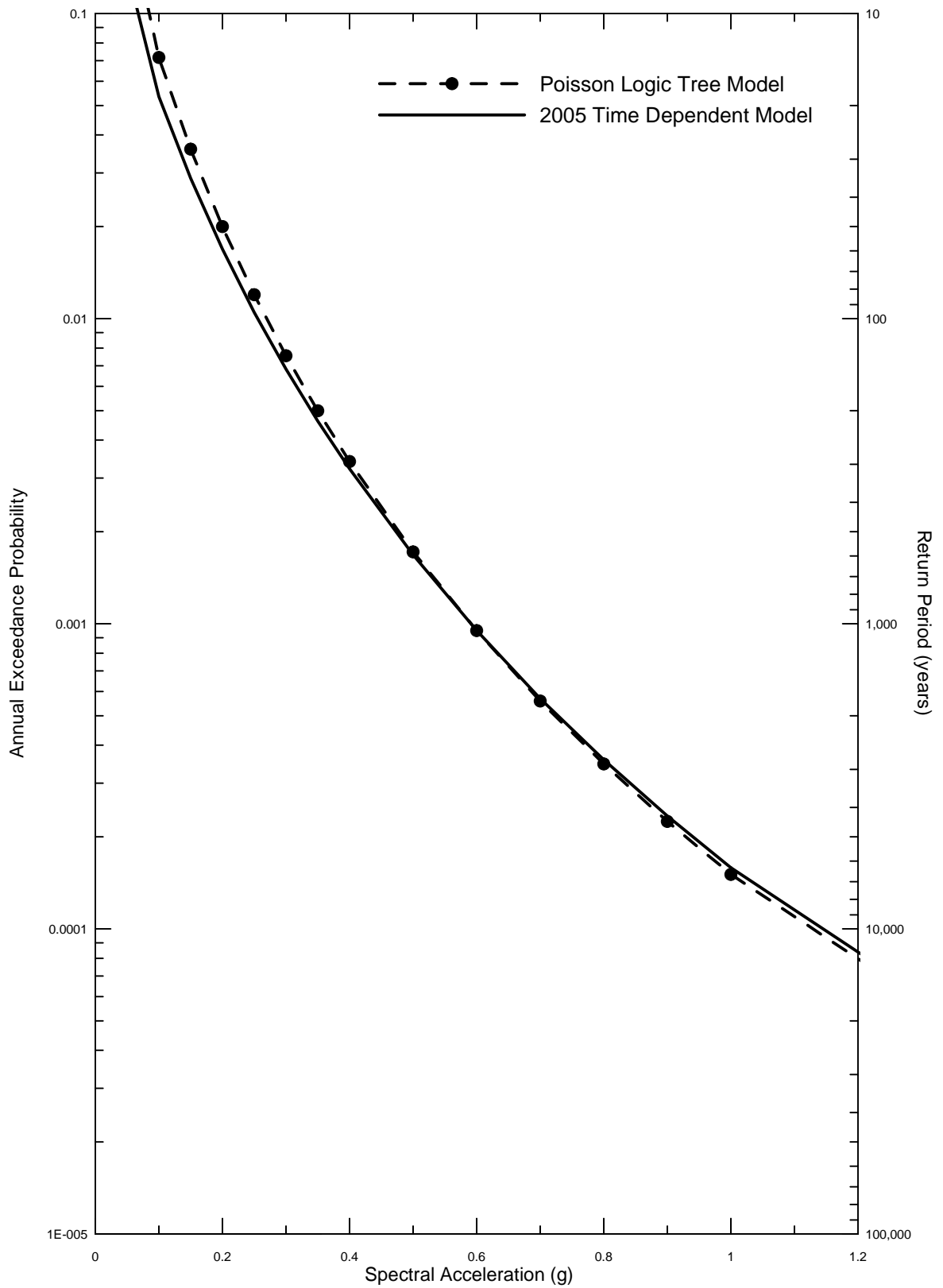


DELTA RISK
MANAGEMENT STRATEGY
California

Project No. 26815621

1.0 SEC HORIZONTALSPECTRAL ACCELERATION
HAZARD TIME DEPENDENT AND POISSON MODELS
FOR SACRAMENTO FOR 2005

Figure
102



delta Risk\Figures\DR1-11-TDV.ppt 6/1/07 11:15 AM

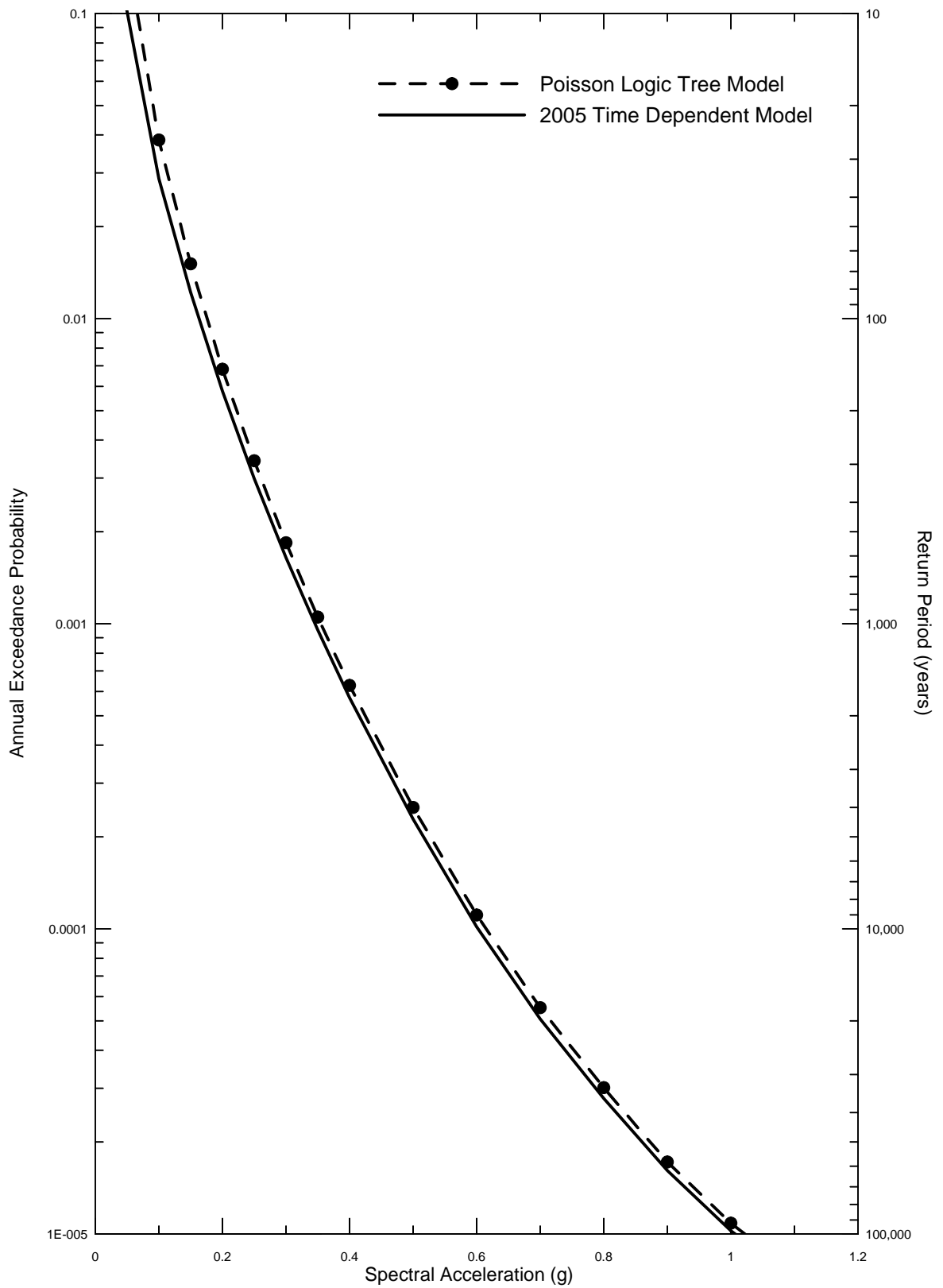


DELTA RISK
MANAGEMENT STRATEGY
California

Project No. 26815621

1.0 SEC HORIZONTAL SPECTRAL
ACCELERATION HAZARD FOR TIME-DEPENDENT
AND POISSON MODELS FOR
SHERMAN ISLAND FOR 2005

Figure
103



delta Risk\Figures\DRS-t1-TDV.ppt 6/1/07 11:11 AM

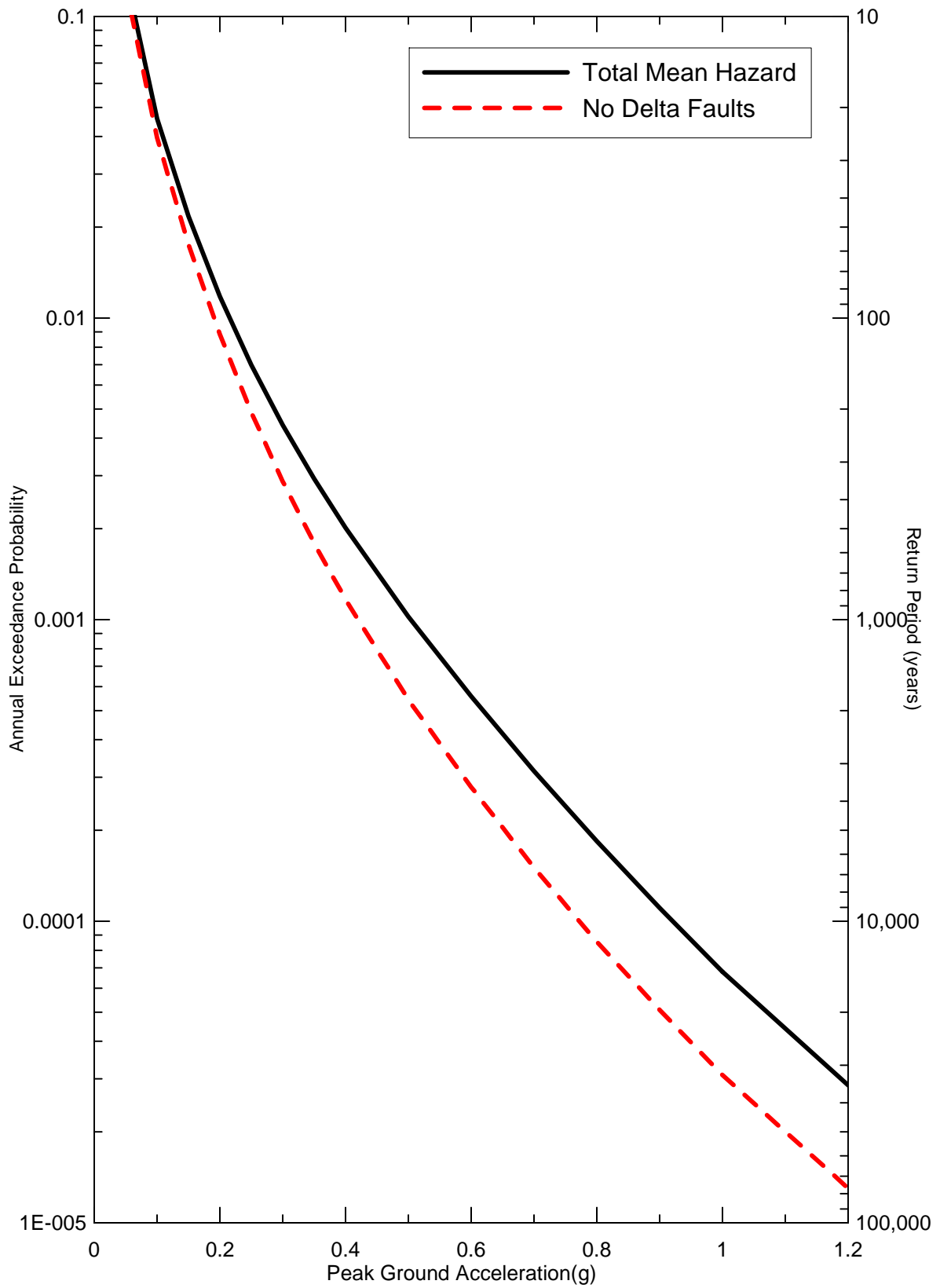


DELTA RISK
MANAGEMENT STRATEGY
California

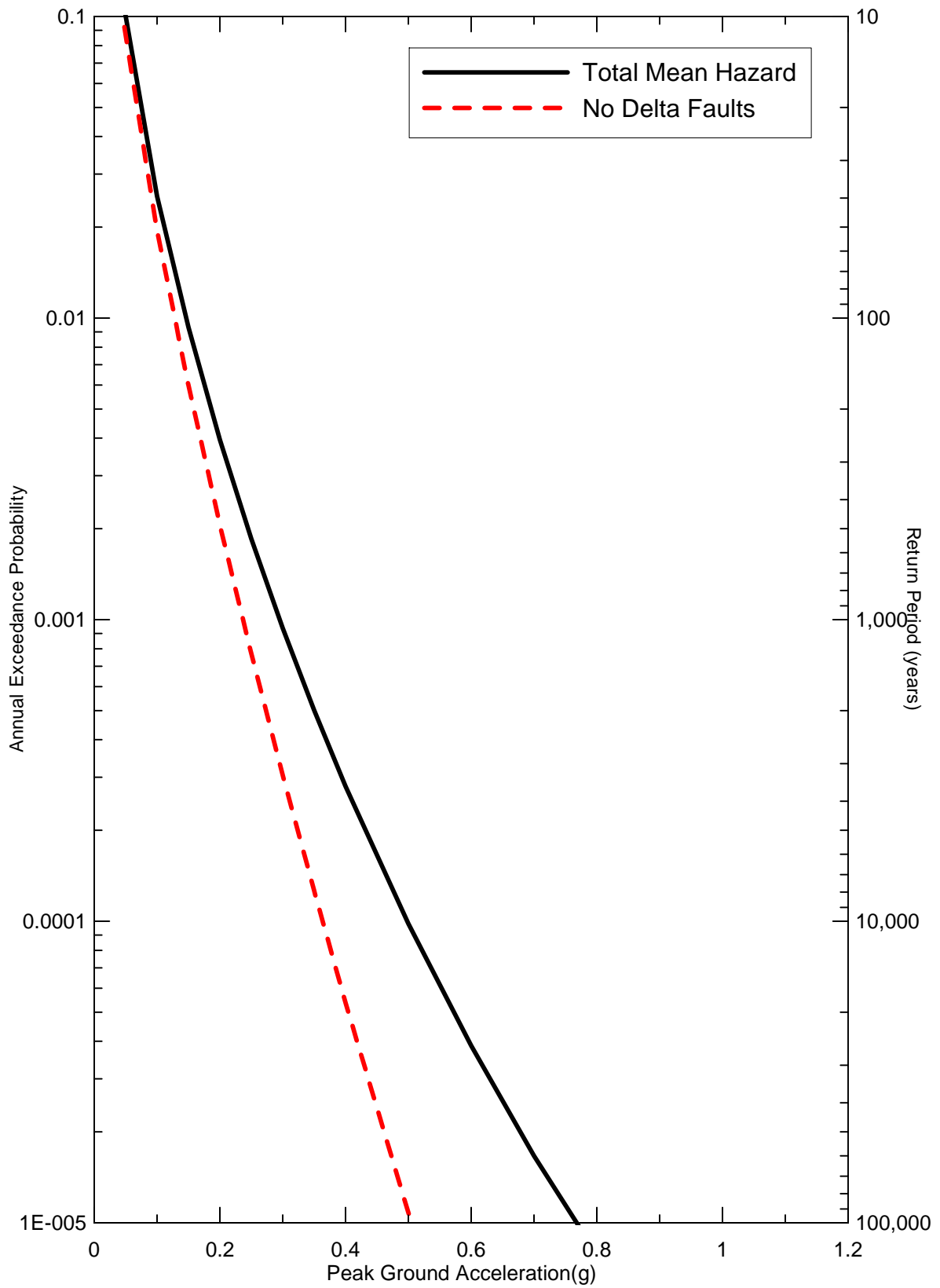
Project No. 26815621

1.0 SEC HORIZONTAL SPECTRAL ACCELERATION
HAZARD TIME DEPENDENT AND POISSON MODELS
FOR STOCKTON FOR 2005

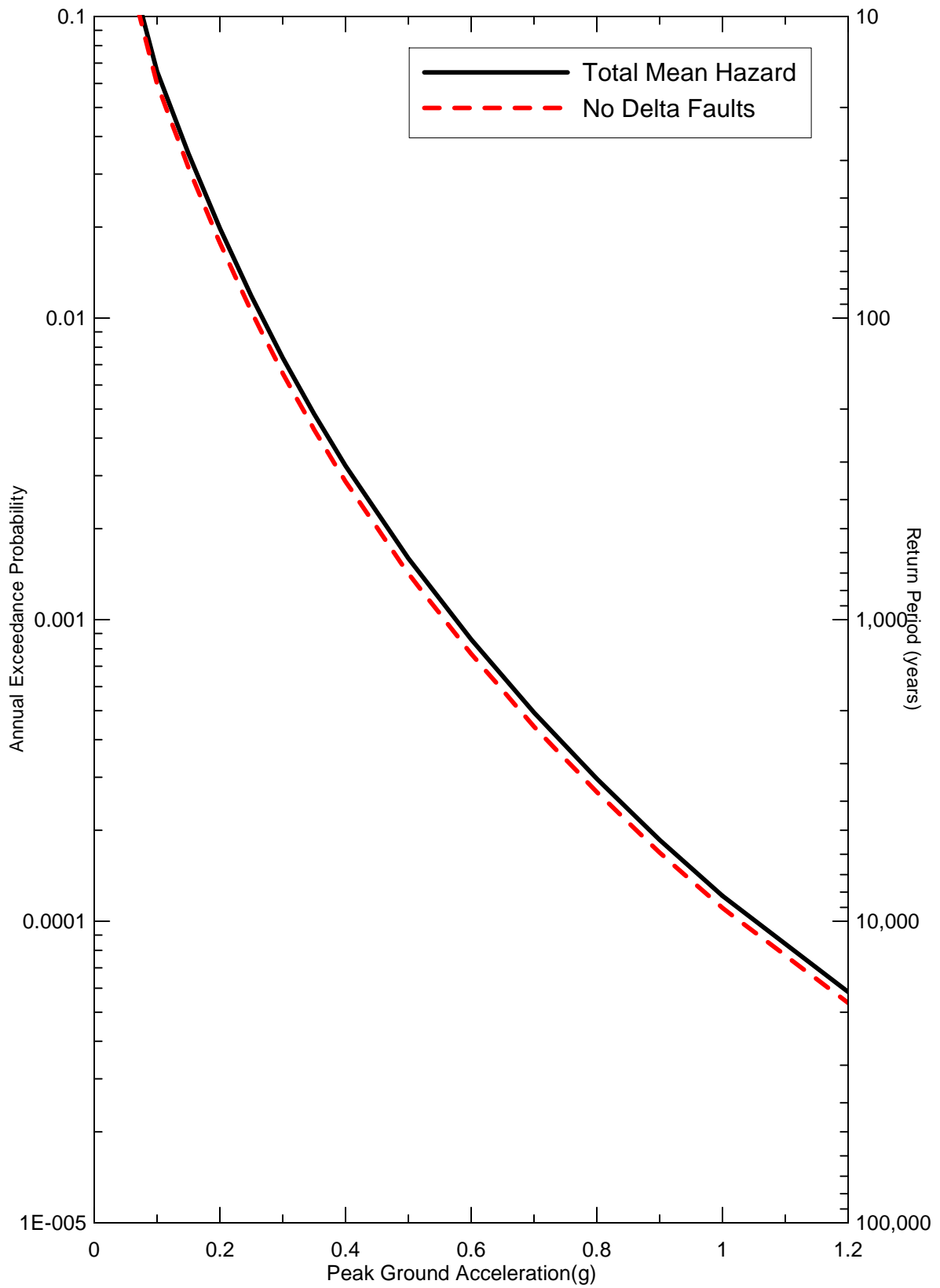
Figure
104



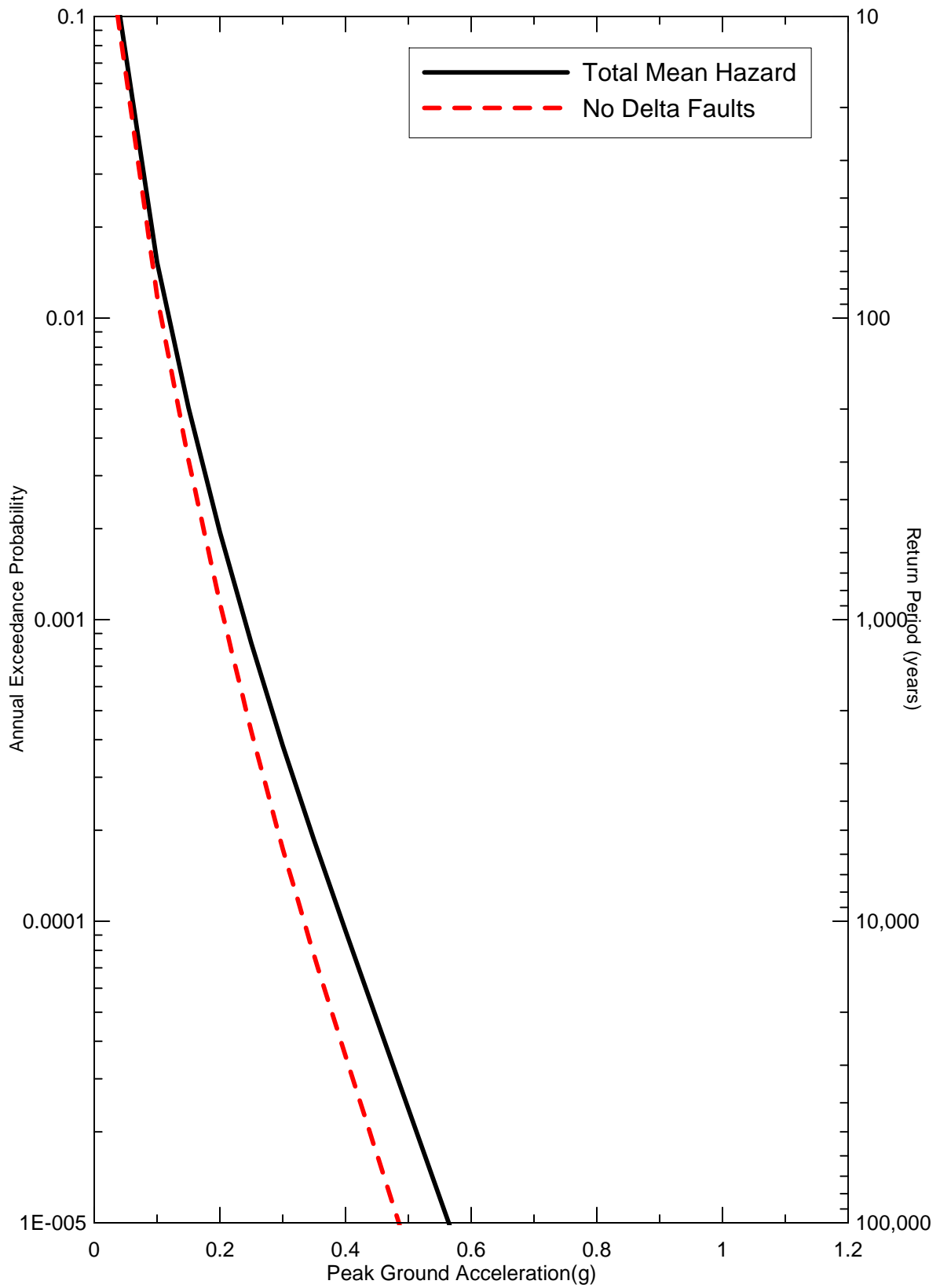
Delta Risk\figures\DR1-pga-2005.grf



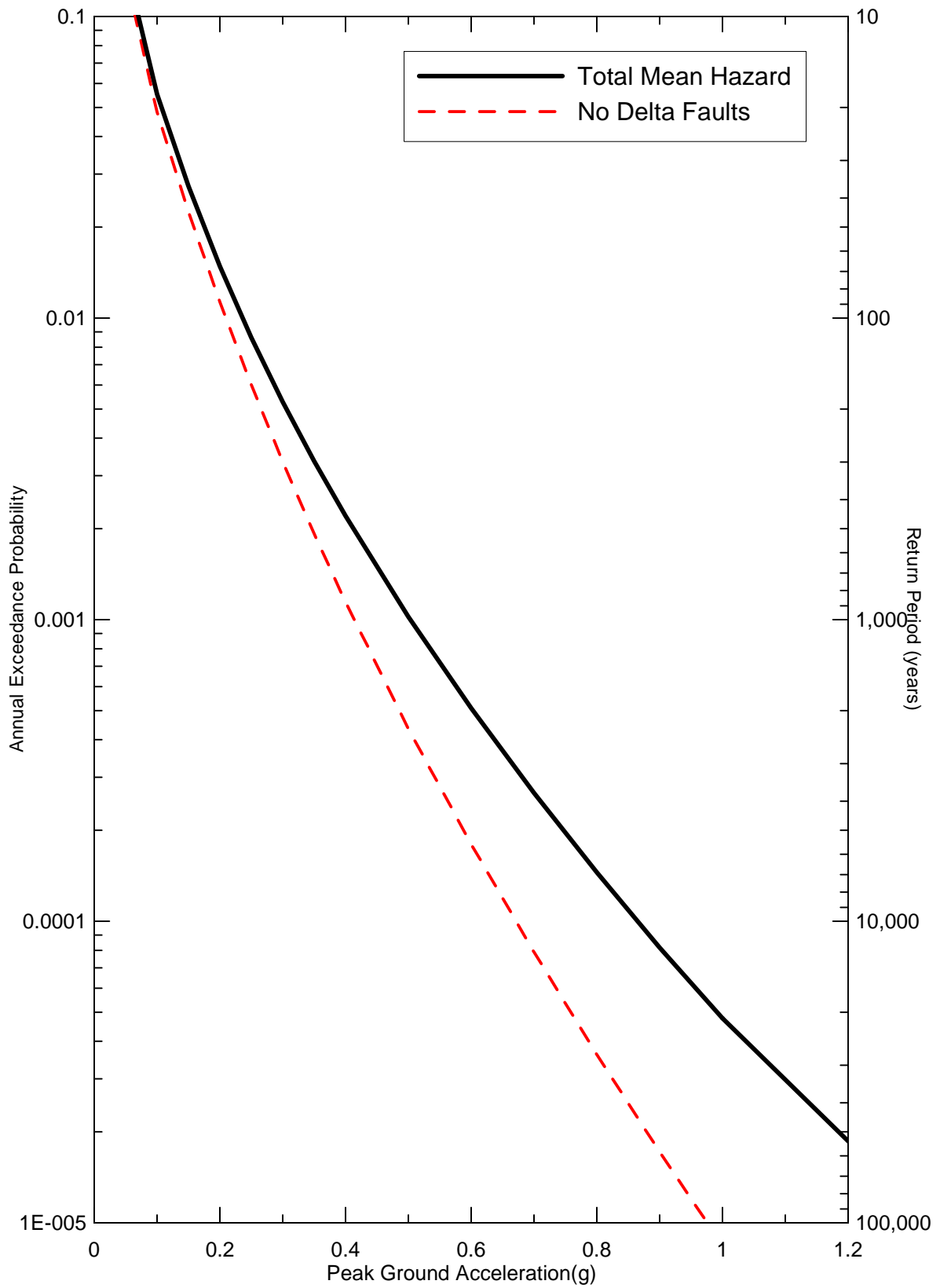
Delta Risk\figures\DR1-ppga-2005.grf



Delta Risk\figures\DR1-pga-2005.grf



Delta Risk\figures\DR1-pga-2005.grf

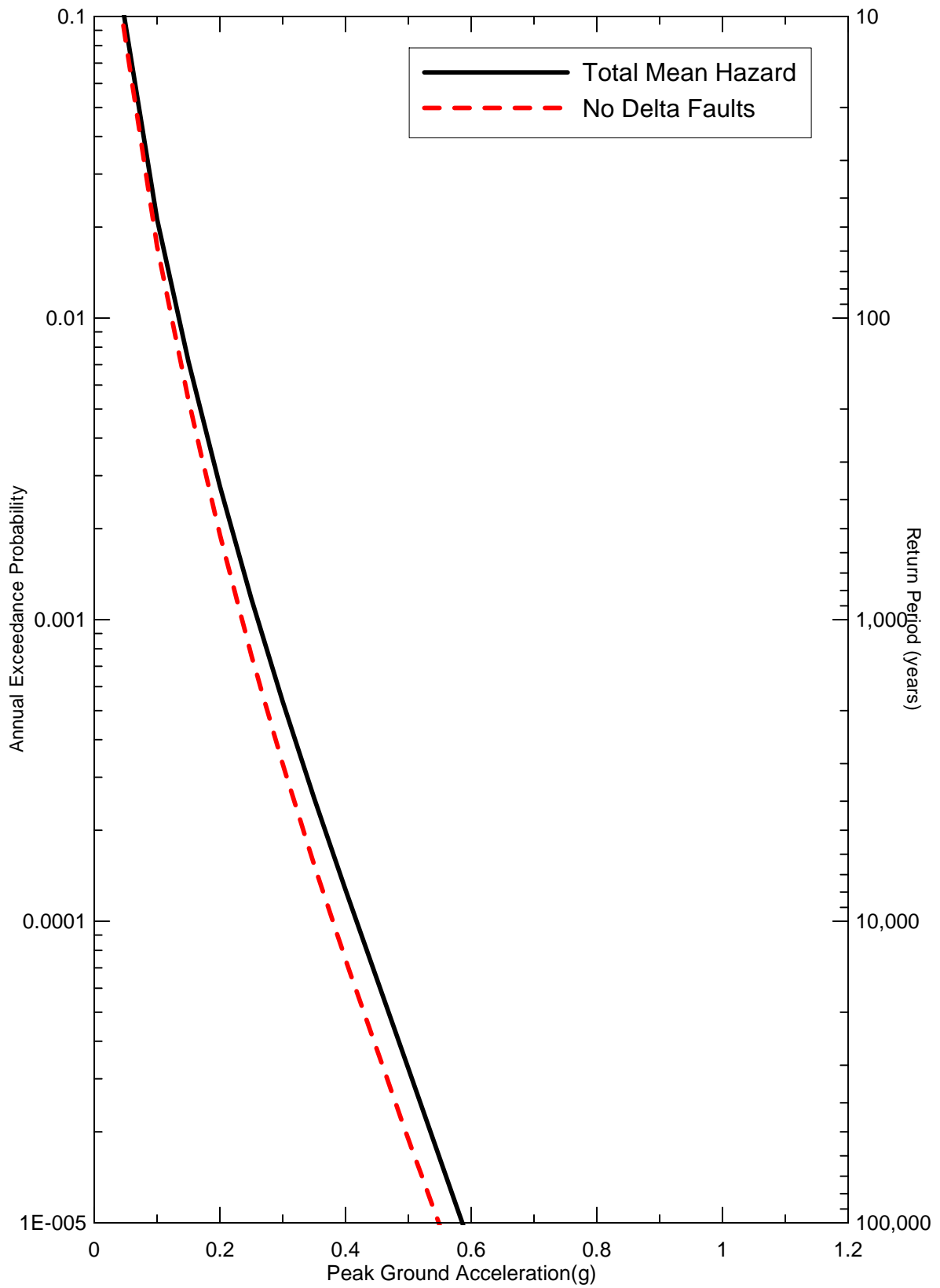


DELTA RISK
MANAGEMENT STRATEGY
CALIFORNIA

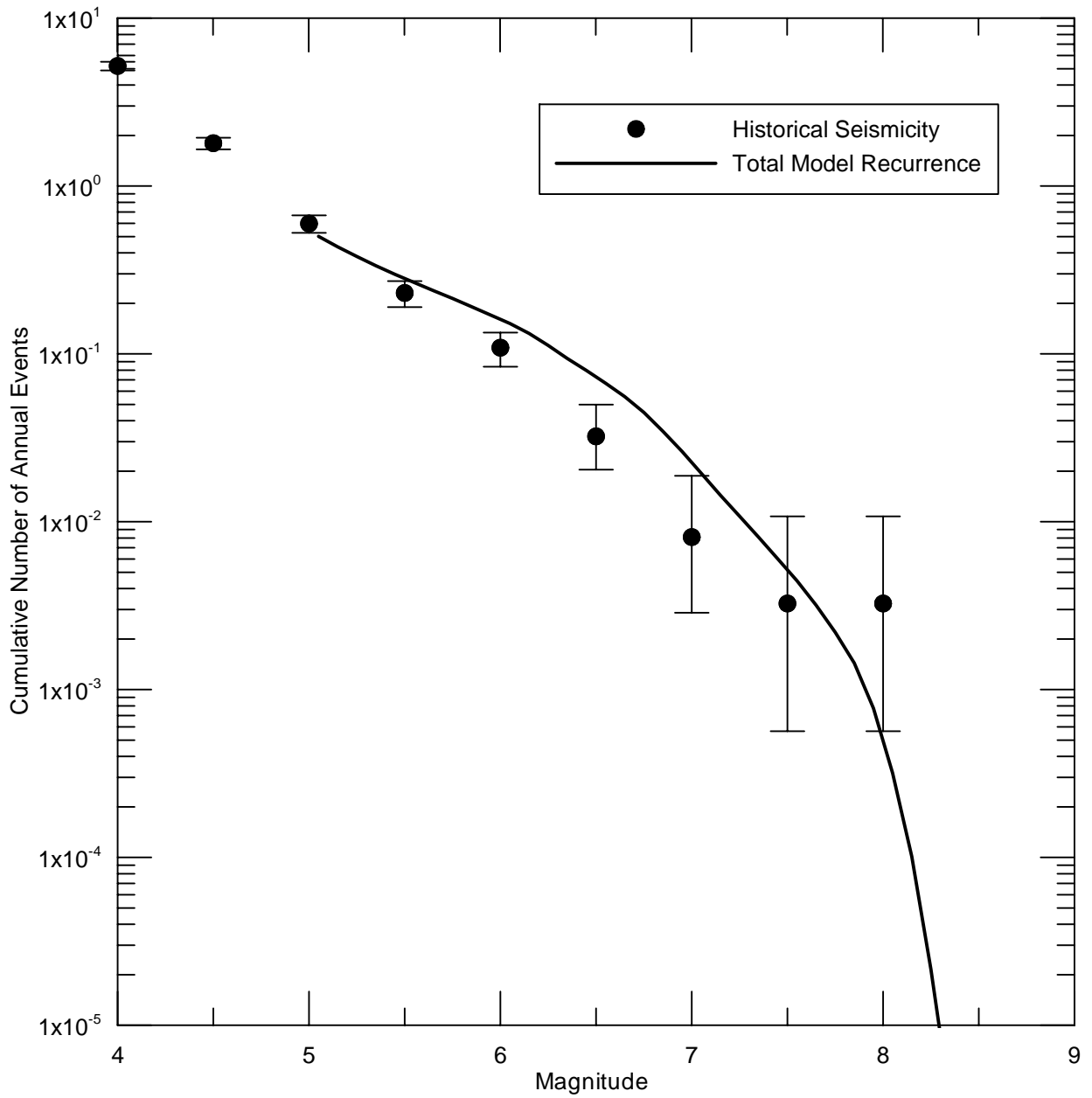
Project No. 26815900

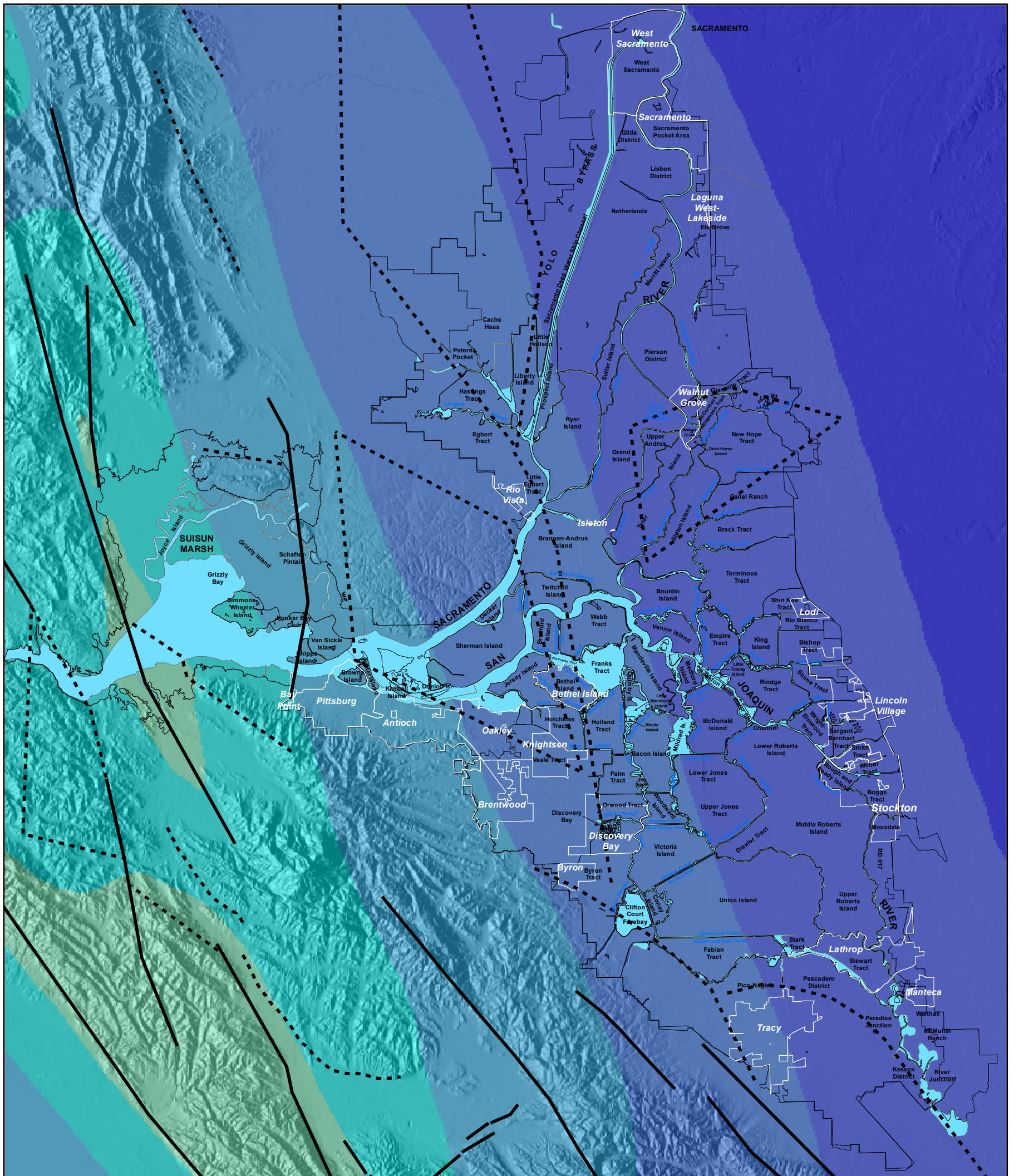
SENSITIVITY OF MEAN PEAK HORIZONTAL
ACCELERATION HAZARD TO DELTA FAULT
SOURCES FOR SHERMAN ISLAND FOR 2005

Figure
109



Delta Risk\figures\DR1-pga-2005.grf





Legend

Mapped Faults

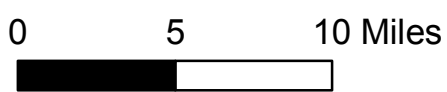
— Surficial faults used in the hazard analysis

Blind Faults

- - - - Blind faults used in the hazard analysis

□ Legal Delta and Suisun Marsh Boundary

PGA, 100 Year Return Period

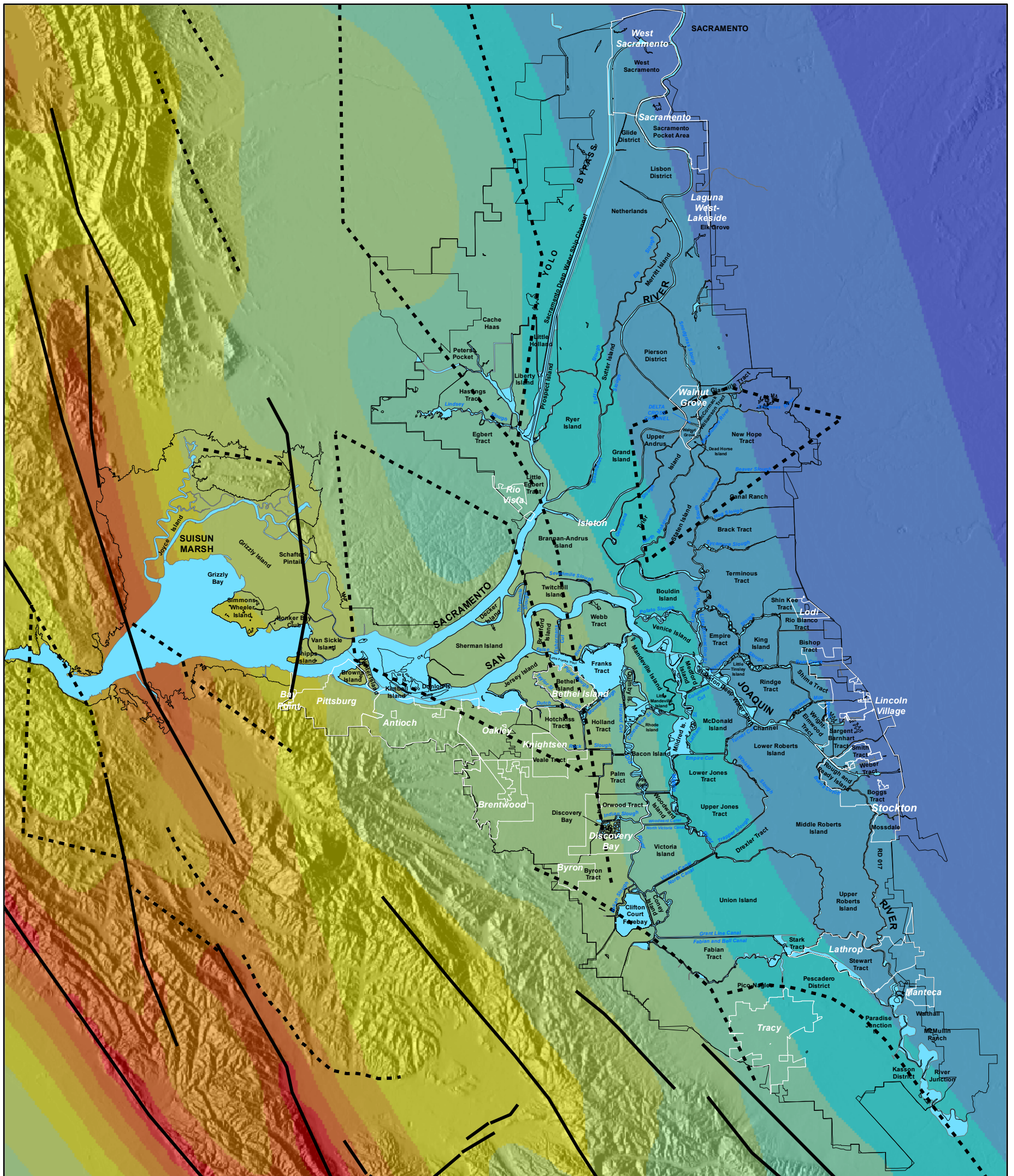


DRMS

26815431

PGA Hazard for a 100-Year Return Period

FIGURE 112



Legend

Mapped Faults

— Surficial faults used in the hazard analysis

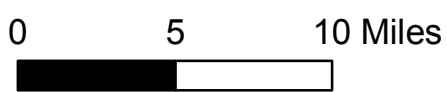
Blind Faults

- - - Blind faults used in the hazard analysis

□ Legal Delta and Suisun Marsh Boundary

PGA, 500 Year Return Period

0.00 - 0.10	0.36 - 0.40
0.11 - 0.15	0.41 - 0.45
0.16 - 0.20	0.46 - 0.50
0.21 - 0.25	0.51 - 0.55
0.26 - 0.30	0.56 - 0.60
0.31 - 0.35	0.61 - 0.65
	0.66 - 0.70

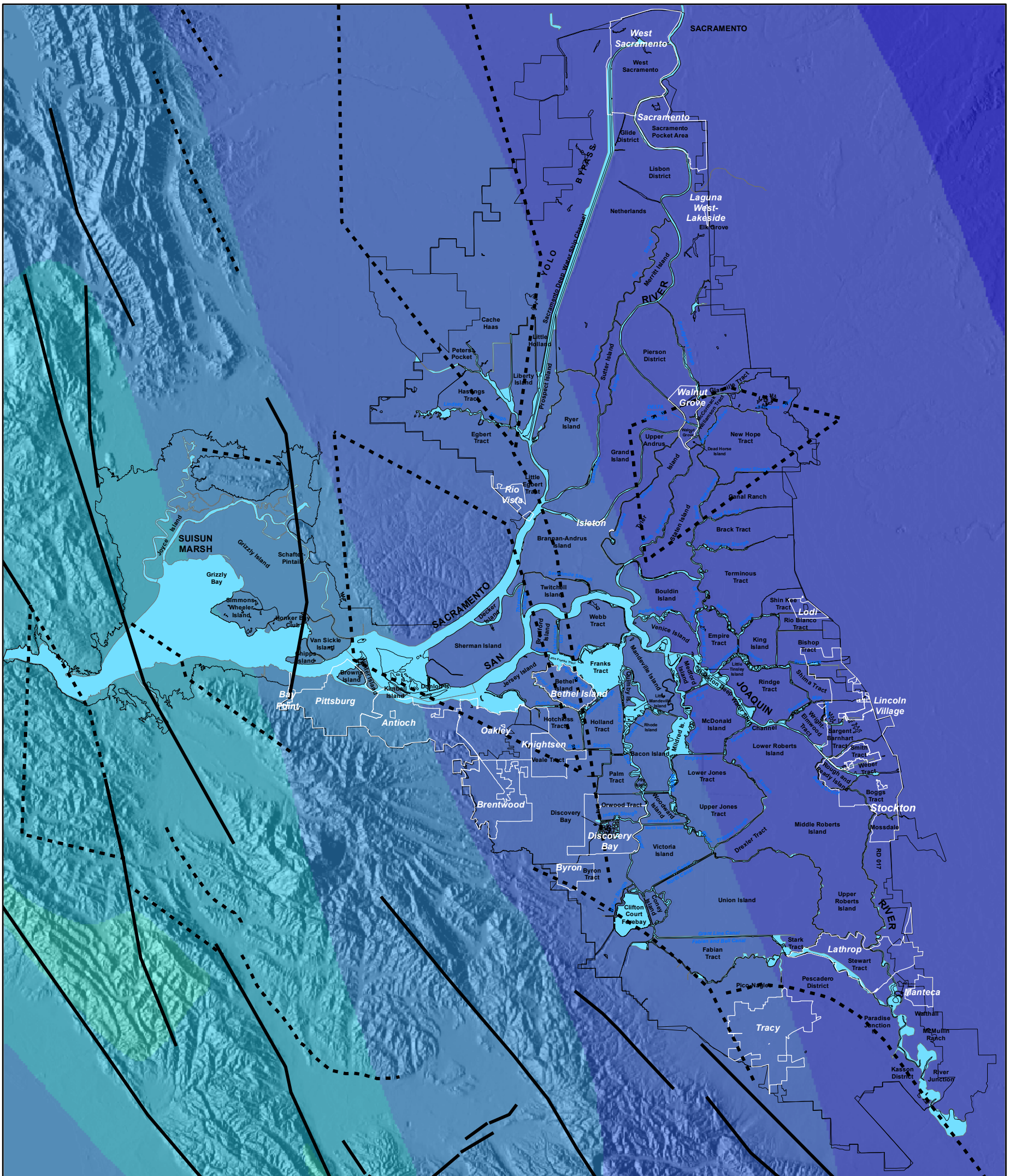


DRMS

26815431

PGA Hazard for a 500-Year Return Period

FIGURE 113



Legend

Mapped Faults

— Surficial faults used in the hazard analysis

Blind Faults

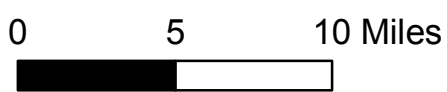
- - - - Blind faults used in the hazard analysis

□ Legal Delta and Suisun Marsh Boundary

One Second, 100 Year Return Period

- 0.00 - 0.10
- 0.11 - 0.15
- 0.16 - 0.20
- 0.21 - 0.25
- 0.26 - 0.30
- 0.31 - 0.35
- 0.36 - 0.40

- 0.41 - 0.45
- 0.46 - 0.50
- 0.51 - 0.55
- 0.56 - 0.60
- 0.61 - 0.65
- 0.66 - 0.70
- 0.71 - 0.75
- 0.76 - 0.80

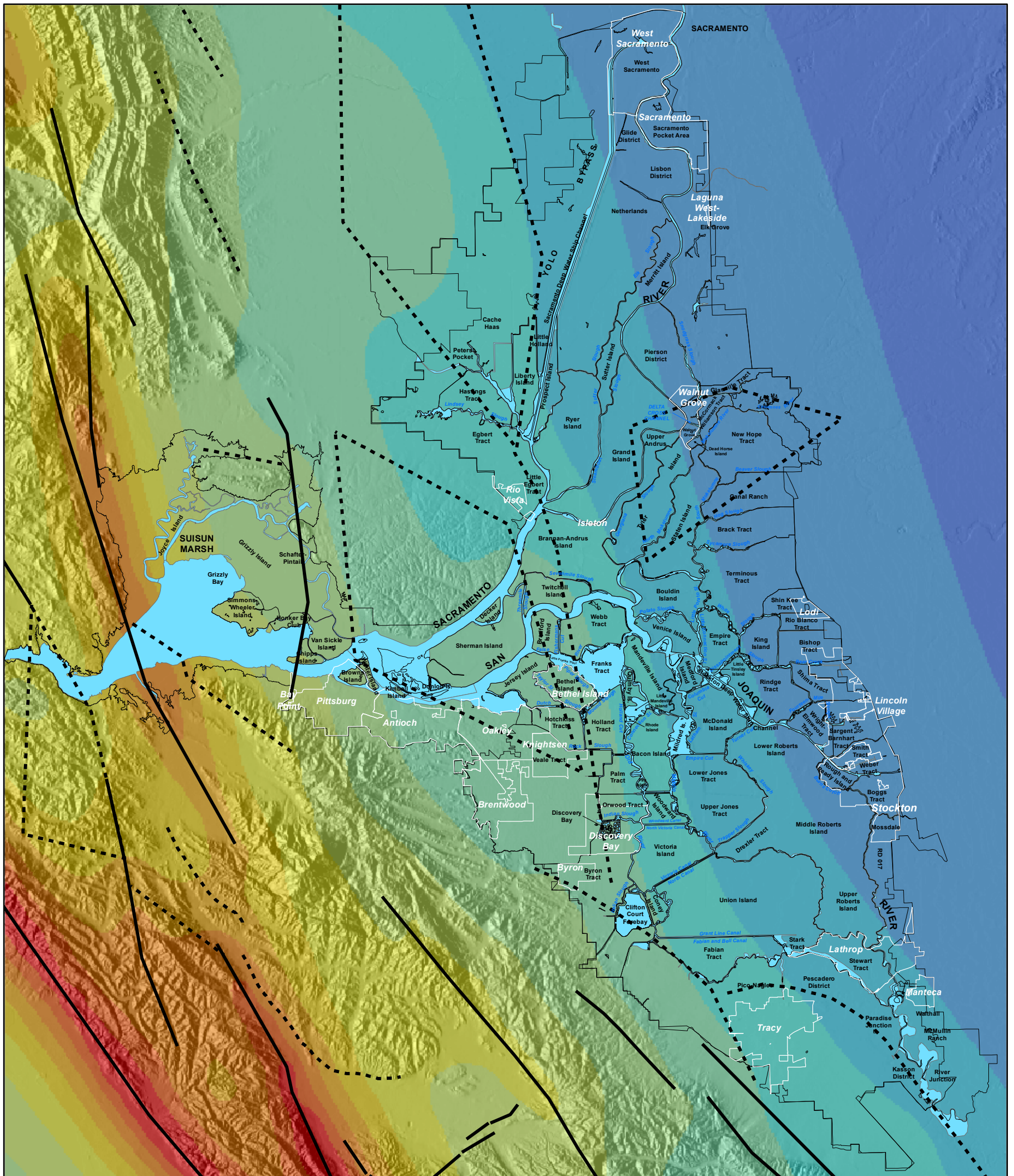


DRMS

26815431

1 Second Hazard for a 100-Year Return Period

FIGURE 114



Legend

Mapped Faults

— Surficial faults used in the hazard analysis

Blind Faults

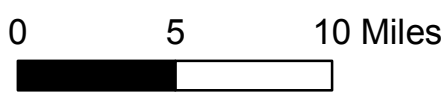
- - - Blind faults used in the hazard analysis

□ Legal Delta and Suisun Marsh Boundary

One Second, 500 Year Return Period

- 0.00 - 0.10
- 0.11 - 0.15
- 0.16 - 0.20
- 0.21 - 0.25
- 0.26 - 0.30
- 0.31 - 0.35
- 0.36 - 0.40

- 0.41 - 0.45
- 0.46 - 0.50
- 0.51 - 0.55
- 0.56 - 0.60
- 0.61 - 0.65
- 0.66 - 0.70
- 0.71 - 0.75
- 0.76 - 0.80



DRMS

26815431

1 Second Hazard for a 500-Year Return Period

FIGURE 115

Appendix A
Potential Deformation of the Base of Holocene Delta Peat by the Midland Fault

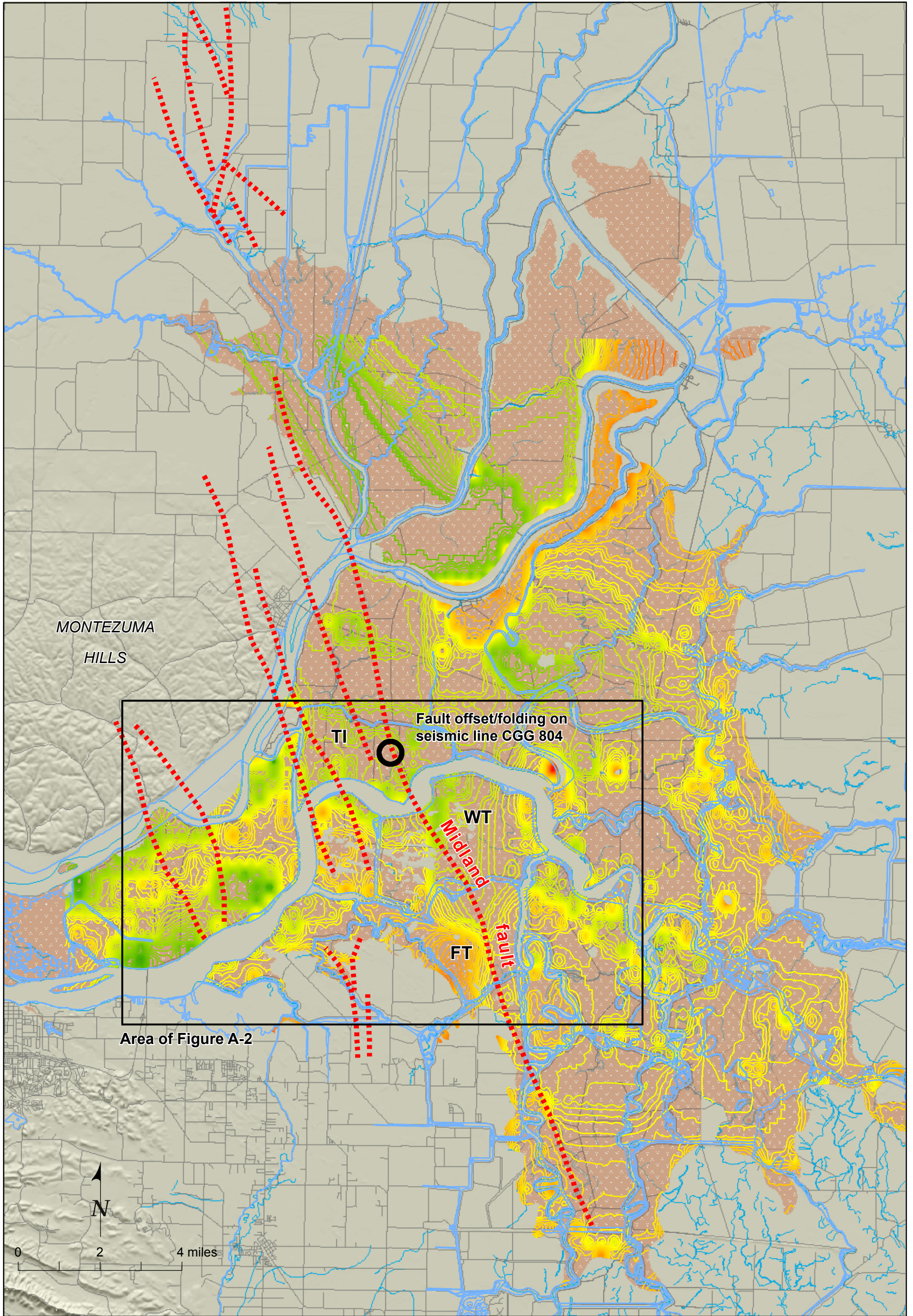
Potential Deformation of the Base of Holocene Delta Peat by the Midland Fault

We compared existing mapping of the Midland fault by the California Division of Oil and Gas (1982) with unpublished CDWR contour maps of the base of Holocene peat (Figure A-1). The mapping of the peat, which incorporates Atwater's (1980) surficial mapping of the extent of peat deposits with contours on base of peat identified in geotechnical borings, shows west-side-up relief on the base of peat through the central part of Franks Tract that is approximately coincident with the subsurface trace of the Midland fault (Figure A-1). Boring data acquired along the perimeters of Delta islands by the CDWR (1956) for the Salinity Control Barrier Investigations further document potentially anomalous relief on the base of peat across the Midland fault. Regional borehole transect A-A' across the Delta (Figures A-2 and A-3) was prepared by combining CDWR (1956) borehole data from Sherman Island, Twitchell Island, Andrus Island and Venice Island. There is a modest 2-3 m west-side-up step in the contact between the base of peat/top of sand across the subsurface trace of the Midland fault along transect A-A' (Figure A-3). Although this step in the base of the peat/top of sand is not unique on the transect (nor is it especially distinctive), it is located about 1.5 km south-southeast of and on trend with the east-facing monoclinical fold above the tip of the Midland fault imaged by CGG seismic line 804 (Figure A-2).

Anomalous relief on the base of peat/top of sand above the Midland fault is more pronounced and better defined in a transect of borings along the northern margin of Webb Tract (B'-B; Figures A-2 and A-4), directly across the San Joaquin River from transect A-A', where a west-up step is located above the fault between borings 49 and 50 and represents about 2-3 m of relief. Other CDWR (1956) transects that show potential west-up relief on the base of peat/top of sand across the Midland fault include borings along the southern margin of Webb Tract and the northern margin of Holland Tract (Figure A-2). These transects bracket the west-side-up relief on the base of peat above the reach of the Midland fault through inundated Franks Tract, shown by the structure contours in Figure A-1.

The contact between the top of sand/base of peat in the boring transects (Figures A-3 and A-4) may represent the Pleistocene-Holocene boundary. During low stands of sea level in late Pleistocene time, westerly winds likely carried glacial-age flood plain or river deposits into the Delta region, forming dune fields atop the exposed landscape. In the Delta area, intertidal peat began to accumulate about 6,000 to 7,000 years ago (Schlemon and Begg, 1973; Drexler et al., 2006). The Pleistocene landscape, mantled in part by eolian deposits and consisting largely of well consolidated sand, underlies the Holocene estuarine deposits. This abrupt contrast between Holocene and Pleistocene depositional environments (i.e., the top Pleistocene unconformity) is represented by the top of sand/base of peat contact (Atwater, 1980).

Recent age determination of the bottom of the peat column in the Webb tract by Drexler et al (2006) from radiocarbon dating indicates that basal peats formed between 6,200 and 6,700 cal years BP. Given the relief on the base of peat across the main strand of the Midland fault from our analysis of boring data (about 2 m to 4 m; Figure A-2), and the age of basal peat documented by Drexler et al. (2006), we estimate an approximate vertical separation rate of about 0.3 to 0.6 mm/yr, given the assumption that the relief is tectonic in origin. This estimate, based on potential deformation of a Holocene datum, is comparable to the long-term-average reverse slip rate of 0.1-0.5 mm/yr for the Midland fault estimated by Thrust Fault Subgroup (1999) from fold deformation of the 1.6 ± 1.0 Ma U1 unconformity.



Explanation

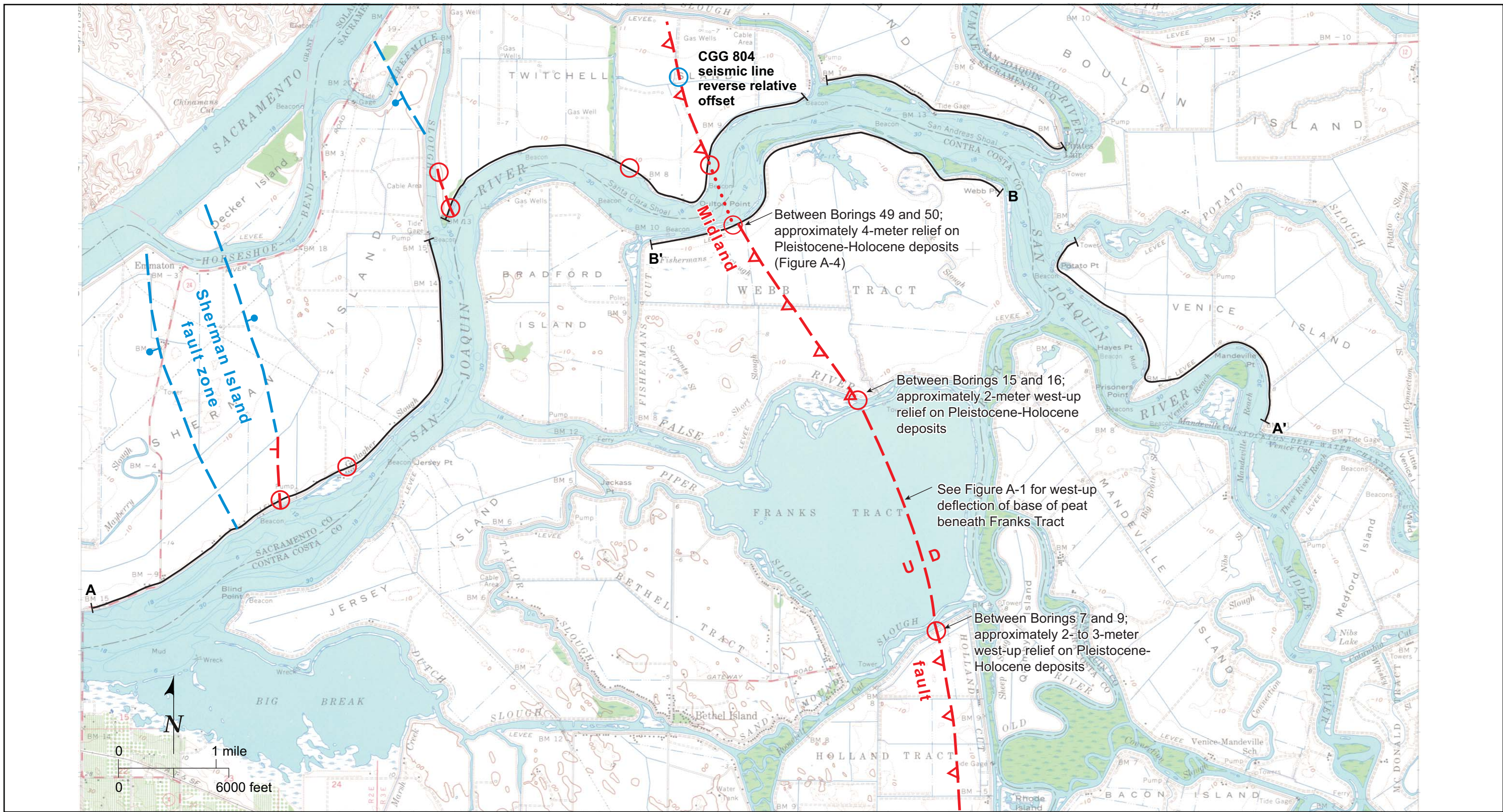
- - - Fault mapped in the subsurface by the California Division of Oil and Gas (1982)
- Peat (Qpm; Atwater, 1980)
- FT** Franks Tract
- WT** Webb Tract
- TI** Twitchell Island

Note: Contours of peat shown in warm (high) to low (green). Elevation from -58 feet to 33 feet relative to sea level.

DELTA RISK EVALUATION

Regional Map Showing Extent and Contoured Base of Peat

WLA **WILLIAM LETTIS & ASSOCIATES, INC.** Figure A-1



Base map: USGS Rio Vista 1:62,500-scale map, 1952

Explanation

- 

Possible fold scarp on base of peat, inferred from analysis or borehole data



Shallow folding observed on seismic line
- 

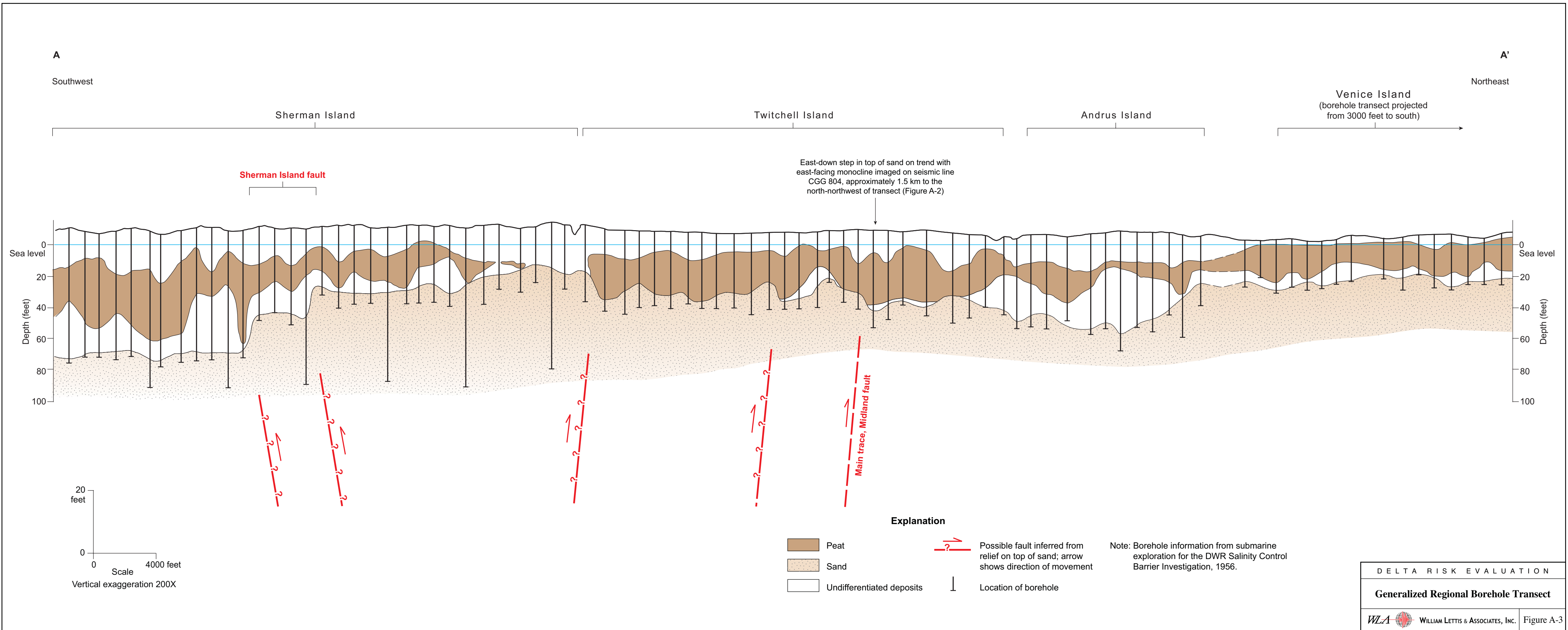
Inferred fault; barb on hanging wall where known; tick on downthrown side (California Division of Oil and Gas, 1982)



Fault compiled from subsurface mapping by the California Division of Oil and Gas (1982); ball on downthrown side
- 

Borehole transect (data from California Department of Water Resources)

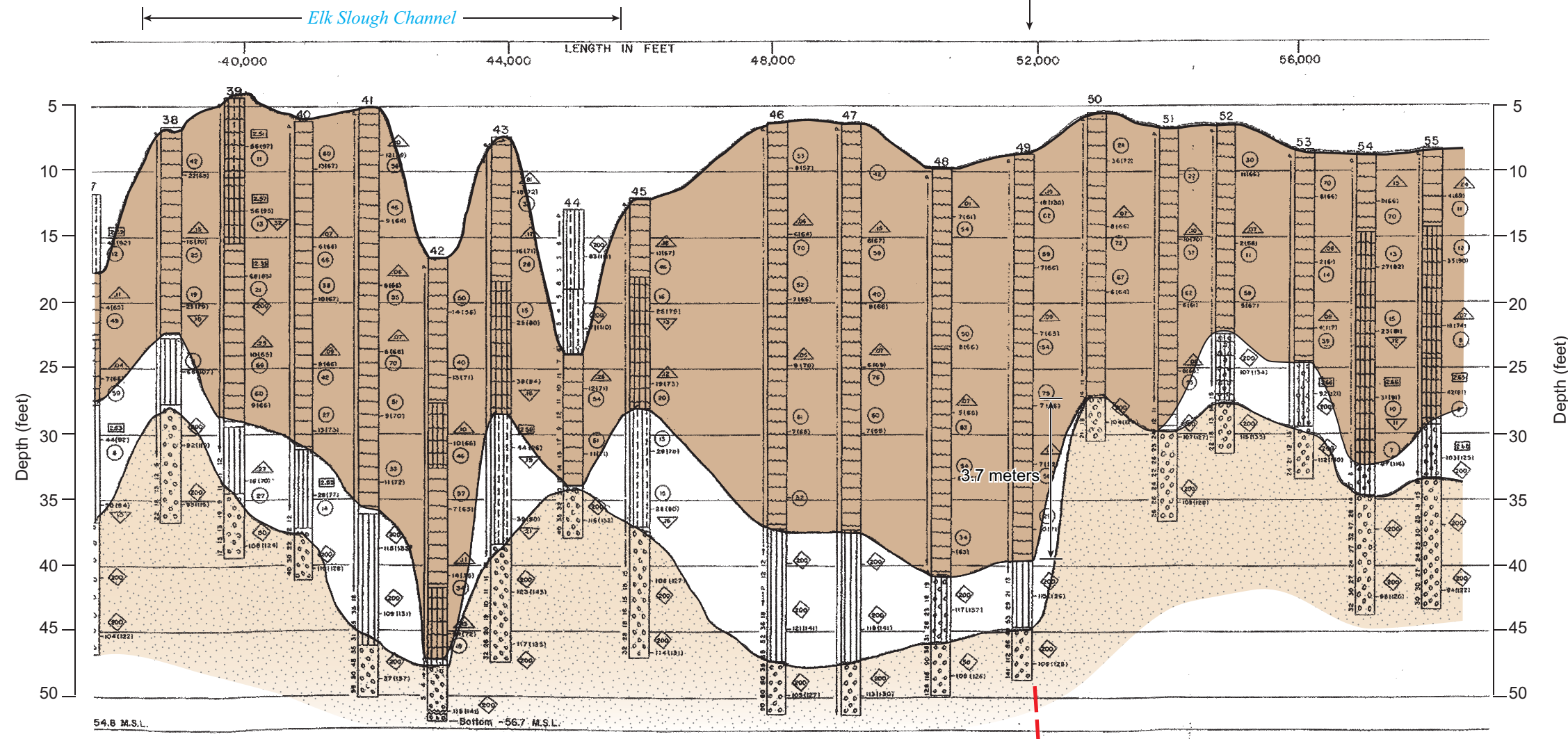
DELTA RISK EVALUATION	
Map of Inferred Faults and Borehole Transects	
	WILLIAM LETTIS & ASSOCIATES, INC. Figure A-2



B
East

West-side-up relief on top of sand/base of peat on trend with east-facing monocline imaged on seismic line CGG 804 on Twitchell Island, approximately 2.5 km to the north-northwest of transect

B'
West



Explanation

- Peat
- Sand
- Undifferentiated deposits
- Subsurface trace of the Midland fault (California Division of Oil and Gas, 1982)

Notes: 1. East and west directions are reversed in this cross section relative to Figures 1, 2, and 3.
 2. Base scan from DWR Salinity Control Barrier Investigation, Primary Subsurface Exploration on Webb Tract (drilling dates December 30, 1957 to June 19, 1958).

Vertical exaggeration 200X

DELTA RISK EVALUATION	
Geologic Transect along Webb Tract across the Midland Fault	
WILLIAM LETTIS & ASSOCIATES, INC.	Figure A-4